Development of Photoinduced Copper-Catalyzed Amination of Alkyl Electrophiles: Synthesis and Mechanism

Thesis by

Hyungdo Cho

In Partial Fulfillment of the Requirements for

the Degree of Doctor of Philosophy

CALIFORNIA INSTITUTE OF TECHNOLOGY

Pasadena, California

2025

(Defended June 27, 2024)

Hyungdo Cho
ORCID: 0000-0001-6109-5742

ACKNOWLEDGEMENTS

"Nobody who ever built something extraordinary did it on their own." These words resonate deeply with me as I reflect on the journey of completing this thesis. The path to this accomplishment has been paved with the guidance, support, and encouragement of many individuals. I would like to express my heartfelt gratitude to those who have generously shared their knowledge, time, and resources, contributing to the success of this work. This thesis is not just a reflection of my efforts, but a testament to the collective support and collaboration of a remarkable community.

Among the many people I should thank, I must first start with my research supervisor, Prof. Gregory Fu. His unwavering support for my ideas allowed me to explore a wide range of topics beyond organic chemistry. Under his mentorship, I have not only deepened my understanding of chemistry but also honed my skills in scientific presentation and laboratory management. Prof. Fu's encouragement of my goal to pursue an academic career was particularly impactful, providing me with opportunities to undergo various training sessions. These experiences have been invaluable, significantly shaping my professional development and preparing me for future challenges in academia.

I would also like to extend my gratitude to my thesis committee members, Prof. Sarah Reisman, Prof. Jonas Peters, and Prof. Theodore Agapie. Their invaluable insights, constructive feedback, and unwavering support have been crucial in refining my research. The guidance they offered was particularly instrumental in practicing my research proposal, a critical step in my academic career. Their efforts have not only improved my thesis but have also helped me to be better prepared for future endeavors in the academic field.

I am also deeply grateful to my undergraduate research and academic supervisors, Prof. Chulbom Lee, Prof. Eunsung Lee, Prof. Tae-Lim Choi, Prof. Yan Lee, and Prof. Seunghwan Cho. Their teaching and guidance during my undergraduate studies were instrumental in preparing me for graduate school. The laboratory experience and academic mentorship they provided were critical in shaping my research skills and scientific approach, laying a solid foundation for my subsequent studies.

Many of my most cherished memories and enriching experiences in graduate school stem from my interactions within the Fu Lab. Dr. Haohua Huo and Dr. Caiyou Chen, my

hood mates and mentors, were among the first people I met upon joining the group. Their exceptional work ethic and efficiency pushed the boundaries of productivity that I thought possible. I learned various techniques in organic chemistry from them, benefited from their insightful discussions, and remained motivated by their energetic presence. Dr. Dylan Freas, the lab manager when I joined, kindly helped me acclimate not only to the lab environment but also to the unfamiliar systems and culture of the US. Dr. Felix Schneck taught me extensively about mechanistic studies and set up the glovebox environment for air-sensitive experiments. Without his guidance, I would not have acquired the necessary skills to complete the mechanistic section of this thesis. Dr. Giuseppe Zuccarello, my second hood mate, was always kind and supportive. His invaluable advice helped me manage my stress and stay focused. I will always treasure our "Amigo times" on Fridays. I'd also like to thank Robert Anderson, the current group manager, for his efforts in improving the lab environment. Over the past five years, his contributions have significantly enhanced the lab's convenience and accessibility. Finally, I am grateful to Dr. Xiaoyu (Dan) Tong for being an excellent co-worker and friend, and for his help in completing my alkyl amination project.

Of course, they are not the only people in the Fu group to whom I feel grateful. Every member of the group has been exceptionally kind and helpful. I would like to thank Dr. Zhaobin Wang, Dr. Joe Ahn, Dr. Zepeng Yang, Dr. Jaika Dorfler, Dr. Haolin Yin, Dr. Hidehiro Suematsu, Dr. Carson Matier, Arianna Ayonon, James Lawniczak, Dr. Suzanne Batiste, Dr. Socrates Munoz, Dr. Robynne Neff, Dr. Wanji Zhang, Dr. Renhe Li, Dr. Feng Zhong, Dr. Asik Hossain, Matthew Wong, Zhuoyan Wang, Dr. Dong Liu, Dr. Arup Mondal, Dr. Shaoqian Yang, and Dr. Jason Rigus for their helpful discussions and contributions to the research.

Caltech boasts some of the most exceptional staff scientists. Many of the studies I conducted during my graduate studies required knowledge that extended beyond my initial training. Without the guidance and help of these outstanding scientists, I would not have been able to achieve a deeper level of mechanistic understanding in my research. Therefore, I would like to thank Dr. Paul Oyala, an EPR staff scientist, for teaching and sharing his expertise in basic to advanced EPR for paramagnetic copper species. I am grateful to Dr. Jay Winkler for the very productive discussions and experimental guidance in measuring the

photophysical properties of copper species. Dr. Scott Virgil provided excellent teaching and assistance with chiral chromatography, and Dr. David Vander Velde offered invaluable support with advanced NMR experiments. Additionally, I appreciate Dr. Mike Takase and Lawrence Henling for their training in X-ray crystallography, and Dr. Mona Shahgholi for her help with mass spectroscopy.

I would also like to acknowledge the members of other research groups at Caltech: the Peters group, Agapie group, Reisman group, Stoltz group, Robb group, Gray group, Goddard group, and Hadt group, who have provided technical assistance and helpful discussions throughout my research. In particular, I am thankful to Dr. Pablo Garrido Barros, Dr. Joseph Derosa, Christian M. Johansen, Dr. Linh Nguyen Vuong Le, Dr. David Cagan, Dr. Cooper Citek, Dr. Alexia Kim, Mengdi Li, Sasha Alabugin, Catherine Romero, Dr. Zachary Sercel, Dr. Jeff Kerkovious, and Dr. Tian Zeng. Their technical support and insights have been invaluable to my work.

I am also deeply grateful to the members of the Korean community, who helped me acclimate to life in the United States and provided friendship and support throughout my time here. Special thanks to Dr. Heejun Lee, Dr. Jeonghoon Ko, Dr. Sangjun Lee, Dr. Young Dae Yoon, Chungkeun Shin, Sanghyun Yi, Dongkwan Lee, and Dr. Jihong Min. Additionally, I want to thank my friends who were instrumental in preparing me for graduate studies: Dr. Youngsuk Kim, Dr. Jinyoung Seo, and Dr. Hayoung Song. Their guidance and assistance have made my experience both enriching and enjoyable.

I would also like to express my sincere gratitude to the Korea Foundation for Advanced Studies for their financial support throughout my research. Their funding has been instrumental in allowing me to focus on my studies and pursue my research goals. The opportunities provided by this support have significantly contributed to the progress and success of my work.

Finally, I want to extend my deepest thanks to my family. Their unwavering support and encouragement have been the foundation of my success. This achievement would not have been possible without their steadfast presence in my life.

ABSTRACT

The formation of carbon-nitrogen (C–N) bonds is crucial in organic chemistry due to the importance of nitrogen-containing functional groups. While traditional nucleophilic substitution reactions, such as S_N1, S_N2, and S_NAr, are limited in scope and efficiency, transition metal-catalyzed versions of these reactions, particularly involving copper, offer a more versatile approach by activating electrophiles and facilitating C–N bond formation via oxidative addition and reductive elimination.

Copper-catalyzed C–N couplings have been extensively developed but are primarily effective for aryl electrophiles rather than alkyl electrophiles due to the need for thermal activation, which often leads to undesired side reactions in alkyl electrophiles. The development of photoinduced copper-catalyzed reactions by Fu and Peters addresses these challenges, enabling the activation of alkyl electrophiles without thermal activation.

Over the past decade, the Fu group has focused on expanding the scope of this novel approach. The research detailed in this thesis focuses on developing photoinduced copper-catalyzed C–N coupling reactions for more challenging substrates, such as sterically hindered alkyl electrophiles and amines.

Chapter 2 discusses the photoinduced, enantio-convergent coupling of racemic tertiary alkyl electrophiles with aniline nucleophiles, catalyzed by bisphosphine-copper complexes. The mechanism of this reaction was elucidated using various tools, identifying key copper-based intermediates, including a chiral copper(II)–anilido complex that couples with a tertiary organic radical to form the C–N bond with good enantioselectivity.

Chapter 3 presents the photoinduced, copper-catalyzed coupling of secondary alkyl amines with secondary or tertiary alkyl bromides to synthesize N-tertiary alkyl amines under mild conditions. This novel reaction provides unique stereoselectivity and compatibility with strained electrophiles, contributing valuable methodologies to the synthesis of bioisosteres and other complex amine structures.

Overall, this work broadens the understanding and application of photoinduced copper-catalyzed reactions, offering new pathways for the synthesis of sterically hindered amines.

PUBLISHED CONTENT AND CONTRIBUTIONS

This dissertation contains materials adapted with permission from the following publications:

1. Cho, H.; Suematsu, H.; Oyala, P. H.; Peters, J. C.; Fu, G. C. Photoinduced, Copper-Catalyzed Enantioconvergent Alkylations of Anilines by Racemic Tertiary Electrophiles: Synthesis and Mechanism. *J. Am. Chem. Soc.* **2022**, *144*, 4550–4558. DOI: 10.1021/jacs.1c12749.

   H.C. optimized the reaction, explored the substrate scope, and performed mechanistic studies. H.C. participated in the writing of the manuscript.

2. Cho, H.; Tong, X.; Zuccarello, G.; Anderson, R. L.; Fu, G. C. Synthesis of Tertiary Alkyl Amines via Photoinduced, Copper-Catalyzed Nucleophilic Substitution of Unactivated Alkyl Halides by Secondary Alkyl Amines. *Submitted*.

   H.C. discovered and optimized the reaction, explored the substrate scope, and performed mechanistic studies. H.C. participated in the writing of the manuscript.

TABLE OF CONTENTS

LIST OF ABBREVIATIONS

^{1}H	proton
^{2}H	deuterium
^{13}C	carbon-13
^{14}N	nitrogen-14
^{15}N	nitrogen-15
^{19}F	fluorine-19
^{31}P	phosphorus-31
$^{63/65}Cu$	copper-63 and copper-65
$[\alpha]^{23}_{D}$	specific rotation at wavelength of sodium D line
A	hyperfine coupling constant
Å	Ångstrom
a_{iso}	isotropic hyperfine coupling constant
Ar	aryl group
BAr^{F}	tetrakis(3,5-bis(trifluoromethyl)phenyl)borate
Bn	benzyl
Boc	tert-butoxycarbonyl
Bpin	pinacol boryl
br	broad
BTMG	2-*tert*-Butyl-1,1,3,3-tetramethylguanidine
BTPP	Phosphazene base P1-*tert*-Butyl-tris(tetramethylene)
Bu	butyl
i-Bu	*iso*-butyl
n-Bu	butyl or *norm*-butyl
s-Bu	*sec*-butyl
t-Bu	*tert*-butyl
Bz	benzoyl
°C	degrees Celsius
calcd	calculated
Cbz	benzyloxycarbonyl
cm^{-1}	wavenumber
CV	cyclic voltammetry
CW	continuous-wave
Cy	cyclohexyl
d	doublet
DAST	diethylaminosulfur trifluoride
DFT	density functional theory
DMF	N,N-dimethylformamide

d.r.	diastereomeric ratio
e^-	electron
ε	extinction coefficient
E	trans (entgegen) olefin geometry
ee	enantiomeric excess
EFG	electron field gradient
e.g.	for example (Latin: exempli gratia)
EI	electron ionization mass spectroscopy
El	electrophile
ENDOR	electron-nuclear double resonance spectroscopy
EPR	electron paramagnetic resonance
ESI	electrospray ionization
ESEEM	electron spin echo envelope modulation
Et	ethyl
et al.	and others (Latin: et alii)
equiv	equivalent
eV	electron volt
EWG	electron withdrawing group
E^0	reduction or oxidation potential
$E_{1/2}$	half wave potential
E_P	peak potential of irreversible CV
Fc	ferrocene
FI	field ionization
FT-IR	fourier-transform infrared spectroscopy
G	Gauss
g	gram(s)
g	*g* value
GC	gas chromatography
GP	general procedure
GHz	gigahertz
h	hour(s)
n-Hex	hexyl or norm-hexyl group
HMDSO	hexamethyldisiloxane
hν	light irradiation
HOMO	highest-occupied molecular orbital
HPLC	high performance liquid chromatography
Hz	hertz
HYSCORE	hyperfine sub-level correlation
I	intensity
I	nuclear spin
I_0	initial intensity
i.e.	that is (Latin: id est)
IR	infrared spectroscopy
J	coupling constant
K	Kelvin

Kα	K (alpha) line of element
k_q	rate constant of quenching
kcal	kilocalorie(s)
kg	kilogram(s)
L	liter
λ	wavelength
λ_{max}	wavelength of local maximum intensity
λ_{probe}	wavelength detected
λ_{pump}	wavelength irradiated
LDA	lithium diisopropyl amide
LED	light-emitting diode
LUMO	lowest-unoccupied molecular orbital
m	multiplet or meter(s)
M	molar or molecular ion
m	meta
μ	micro
max	maximum
Me	methyl
mg	milligram(s)
MHz	megahertz
min	minutes
mL	milliliter(s)
MLCT	metal-to-ligand charge transfer
mM	millimolar
mm	millimeter
mmol	millimole
MO	molecular orbital
mol	mole(s)
MS	mass spectrometry
ms	milisecond
μs	microsecond
mT	militesla
mV	milivolt
MW	microwave
μW	microwatt
m/z	mass-to-charge ratio
N	normal or molar
NCS	N-chlorosuccinimide
nm	nanometer(s)
NMR	nuclear magnetic resonance
NQI	nuclear quadrupole interaction
ns	nanosecond
Nu	nucleophile
o	ortho
OD	optical density

OTf	trifluoromethanesulfonate
p	para
Ph	phenyl
ppm	parts per million
Pr	propyl
i-Pr	*iso*-propyl
n-Pr	propyl or *norm*-propyl
PTFE	polytetrafluoroethylene
q	quartet
R	alkyl group
ref	reference
RMS	root mean square
r.t.	room temperature
s	singlet or seconds
sat.	saturated
SCE	saturated calomel electrode
SET	single electron transfer
S_N1	unimolecular nucleophilic substitution
S_N2	bimolecular nucleophilic substitution
S_NAr	nucleophilic aromatic substitution
t	triplet
T	dipolar contribution of hyperfine tensor
τ	lifetime
TBA	tetrabutyl ammonium
TBS	*tert*-butyldimethylsilyl
TD	temperature-dependent
TFA	trifluoroacetic acid
THF	tetrahydrofuran
TLC	thin layer chromatography
TOF	time-of-flight
tol	tolyl
Ts	*para*-toluenesulfonyl (tosyl)
UV	ultraviolet
V	volt
vis	visible
W	watt
X	anionic ligand or halide
XRD	X-ray diffraction
Z	cis (zusammen) olefin geometry
*	excited state

Chapter 1

INTRODUCTION

1.1. Transition metal-catalyzed nucleophilic substitution for carbon–nitrogen bond formation.

Due to the ubiquity and significance of nitrogen-containing functional groups in a wide range of both naturally occurring and synthesized organic compounds, developing strategies to form carbon-nitrogen bonds has become a fundamental area of research in organic chemistry. Nucleophilic substitution, a reaction in which a leaving group attached to a carbon atom in an electrophile (C–X bond, X = the leaving group) is displaced by the attack of a nucleophile (e.g., amines), offers a straightforward and modular approach to constructing the desired C–N bonds (Figure 1.1a). However, classical nucleophilic substitution reactions, such as S_N1, S_N2, and S_NAr, are only effective for building a limited range of structures (**Figure 1.1b**).[1] For instance, in S_N1 reactions, the use of either a Brønsted or Lewis acid to promote carbocation formation often leads to the deactivation of the amine as a nucleophile. In S_N2 reactions, either the elimination of HX by a base or a nucleophile (with unreactive electrophiles) or excessive alkylation (with reactive electrophiles) frequently results in failure to efficiently deliver the desired product. Additionally, S_NAr reactions, which occur when the leaving group is attached to aromatic carbons (such as in benzenes), require strong electron-withdrawing groups on the aromatic ring to proceed effectively.[2]

Transition metal-catalyzed cross-coupling reactions offer a powerful strategy to overcome the limitations of classical nucleophilic substitution (**Figure 1.2**).[3] In these reactions, the electrophiles are "activated" by the catalyst, which facilitates the cleavage of the carbon-leaving group bond, generating alkyl-derived intermediates. This cleavage increases the formal oxidation state of the metal catalyst, a step known as oxidative addition.[4] Upon ligand exchange on the transition metal catalyst, a process called transmetalation, the C–N bond is formed between the alkyl intermediate and a nitrogen nucleophile by the catalyst, yielding the intended product. This bond formation step decreases the formal oxidation state of the metal catalyst, a process known as reductive elimination. The catalyst

lowers the activation energy of these processes, favoring the desired pathway over the side reactions typically encountered in classical nucleophilic substitutions.

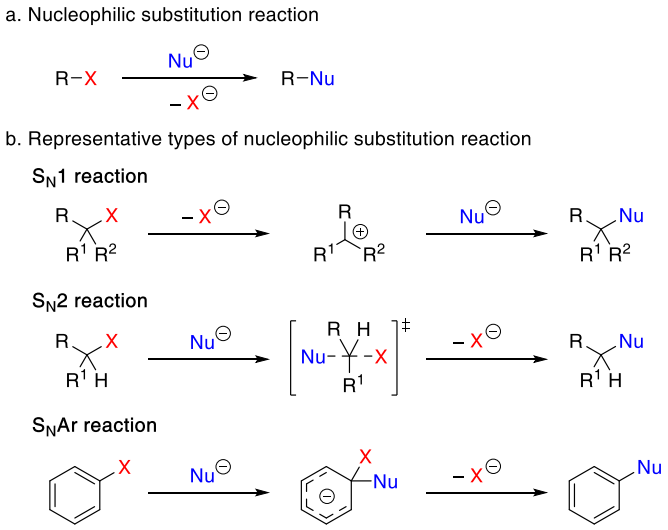

Figure 1.1. Classical nucleophilic substitution reactions.

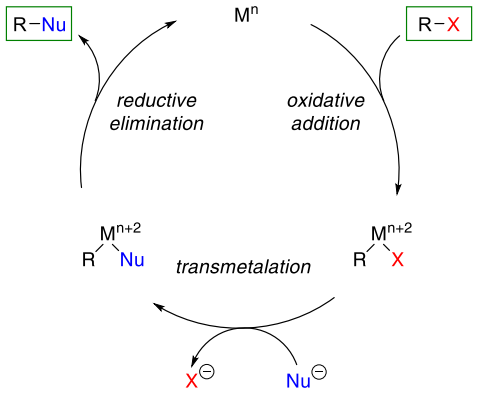

Figure 1.2. Transitional metal-catalyzed cross-coupling: representative mechanisms.

1.2. Thermally-induced copper-catalyzed cross-coupling reactions.

Among the transition metals frequently utilized for cross-coupling reactions, copper exhibits privileged reactivity toward C–N bond formation. Initially discovered by Ullmann and Goldberg in 1905, copper-catalyzed C–N couplings have been extensively developed over the past few decades.[5] Under these conditions, electrophiles and nitrogen nucleophiles typically undergo coupling reactions in the presence of a catalytic amount of copper salt/ligand and a stoichiometric amount of external base to absorb the proton equivalent from the N–H bond (**eq 1.1**). While the copper catalyst generally enables a facile C–N reductive

elimination, the oxidative addition of the C–X bond of the electrophile to copper is often sluggish, necessitating thermal activation to drive the transformation.[6]

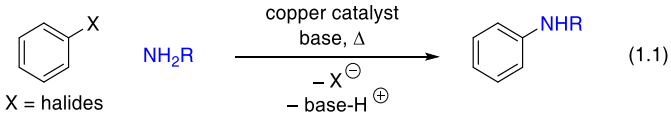

(1.1)

While the broad reactivity of coupling between aryl halides and various nitrogen-based nucleophiles (such as azoles, amides, and alkyl amines) has been demonstrated, effectively providing a wide range of aryl amines that classical S_NAr reactions cannot access, its application toward alkyl electrophiles to address the limitations of their S_N1 and S_N2 reactions had been unsuccessful for a prolonged period.[7] Unlike aryl halides, in the presence of a nucleophile and base, alkyl halides easily undergo undesired elimination of HX to form olefins, and the thermal activation required to facilitate oxidative addition also promotes these side reactions. Due to these challenges, no copper-catalyzed couplings between unactivated secondary and tertiary alkyl electrophiles and nitrogen nucleophiles were reported before 2013.

1.3. Photoinduced copper-catalyzed C–N bond formation.

Exploiting alternative pathways to activate alkyl electrophiles without the need for thermal input could circumvent this problem and broaden the potential of copper-catalyzed cross-coupling of alkyl electrophiles. In 2012, Fu and Peters reported a solution to this challenge, demonstrating copper-catalyzed C–N coupling under light irradiation (**Figure 1.3**).[8] In this system, copper(I) species decorated with phosphine and carbazolide ligands undergo photoinduced excitation. The excited copper species possessing a high-energy electron can undergo single electron transfer (SET) to the aryl halide, resulting in the formation of an aryl radical and copper(II) species. This aryl radical is proposed to recombine with the copper(II)-carbazolide complex to form an arylated carbazole through reductive elimination. Because this photoinduced activation process can occur at unusually low temperatures, where thermally induced side reactions are suppressed, applying it to the activation of alkyl electrophiles could enable efficient cross-coupling with nucleophiles.

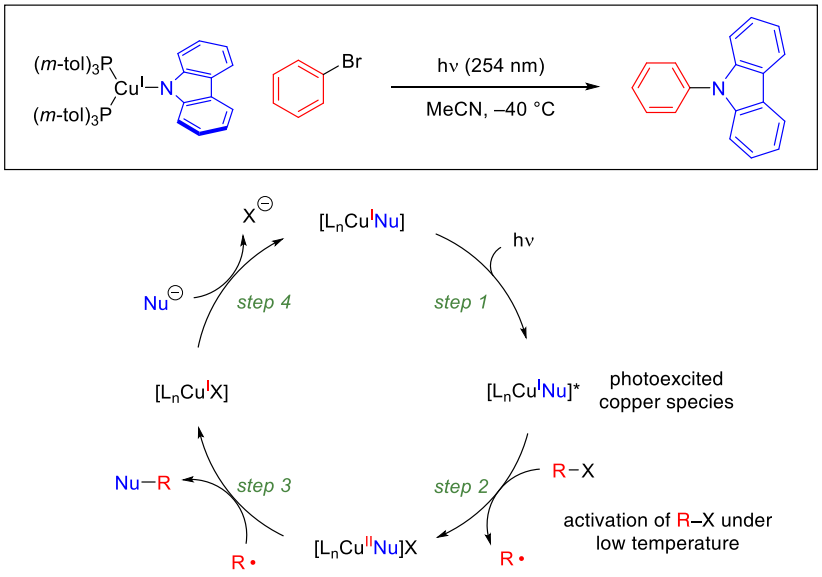

Figure 1.3. Photoinduced copper-catalyzed C–N bond formation: Fu and Peters' report and proposed mechanism.

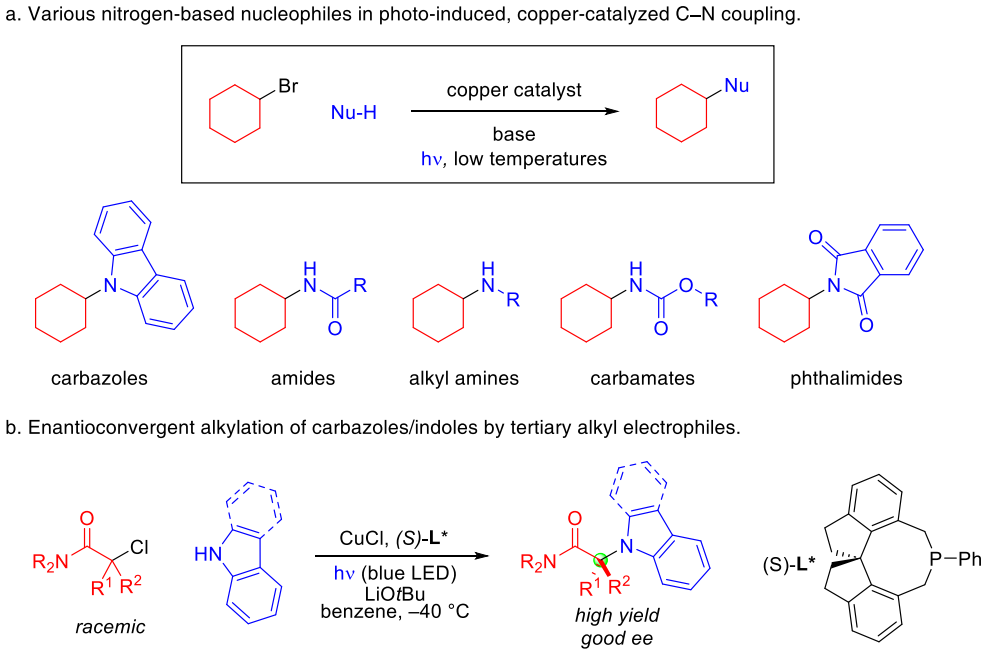

Figure 1.4. Expanding photoinduced copper-catalyzed C–N coupling to alkyl electrophiles.

It was soon found that this strategy is indeed effective for alkyl halides, leading to the development of a range of photoinduced, copper-catalyzed cross-coupling reactions between unactivated secondary alkyl halides and various nitrogen-based nucleophiles (**Figure 1.4a**).[9–13] Additionally, the photoinduced activation of copper allows both enantiomers of racemic

alkyl halides to be converted into a prochiral alkyl radical that asymmetrically couples with a nucleophile in a chiral environment, achieving enantio-convergent synthesis of chiral amines (**Figure 1.4b**).[14] In light of these earlier advancements, current research in the Fu group on copper catalysis focuses on developing: 1) various asymmetric C–N coupling reactions to deliver diverse chiral amine motifs, and 2) C–N coupling with more challenging substrates.

1.4. Mechanistic hypotheses and challenges in photoinduced, copper-catalyzed C–N bond formation.

Mechanistically, two key steps are hypothesized to contribute to the success of these reactions. First, the photoinduced excitation of copper species and subsequent activation of the alkyl electrophile should be efficient (**eq 1.2**). Earlier studies often relied on the reactivities of the copper-nucleophile complex without an additional ligand. The photochemical properties of these species are significantly influenced by the nucleophile and frequently required high-energy UV light to function. Developing a system that can robustly provide photochemical reactivity regardless of the type of nucleophile under milder light irradiation would be more desirable. Recently, the use of certain bisphosphine ligands or naphthol derived ligands has shown potential in this regard, enabling alkyl halides to couple with nucleophiles under blue light irradiation (**Figure 1.5**).[12,15,16] However, studies on the identification of the photo-reductants, origin of their photochemical reactivity, and the effect of substituents are lacking, resulting in a poor understanding of these species.

Photoinduced activation of alkyl electrophiles

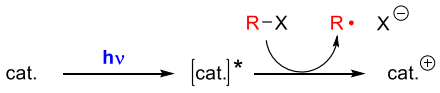

(1.2)

Radical capture and reductive C–N bond formation

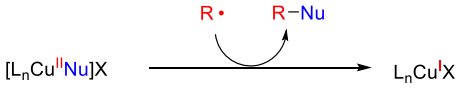

(1.3)

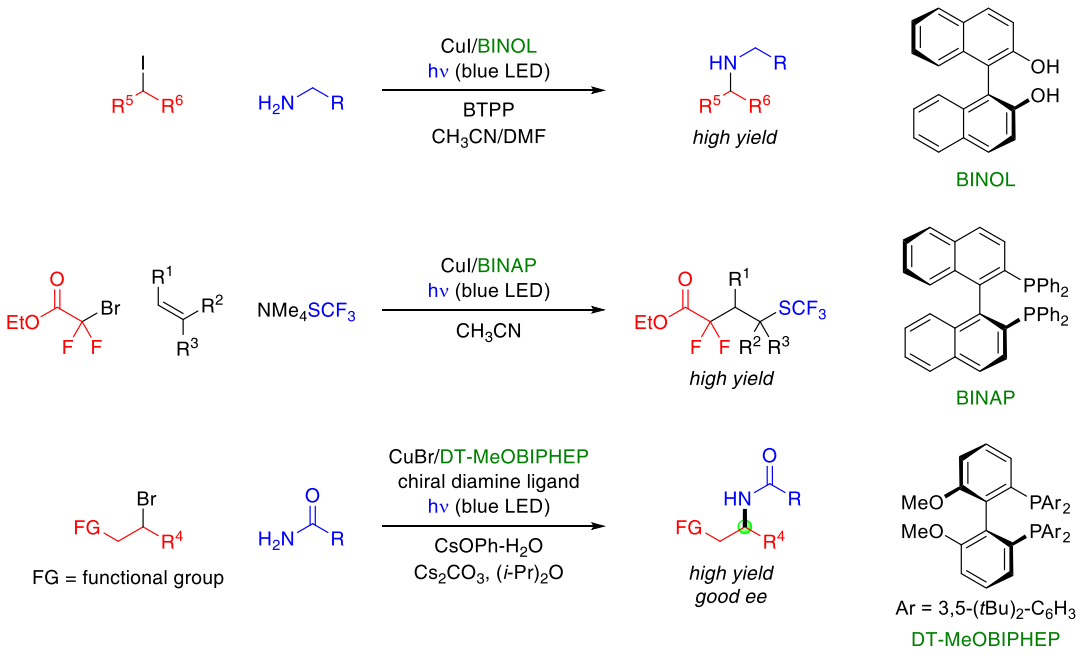

Figure 1.5. BINOL and BINAP derived ligands for photoinduced copper-catalyzed C–N couplings developed in Fu group.

Another important mechanistic step is the capture and coupling of alkyl radicals (**eq 1.3**). Although now considered key intermediates in many reactions,[17] alkyl radicals are highly unstable species with short lifetimes that were long regarded as intractable.[18] Failure to efficiently capture the alkyl radical by copper intermediates and subsequently form the C–N bond could result in an unsuccessful cross-coupling reaction. While many reported copper-catalyzed reactions propose alkyl radical intermediates, the unified character of the electronics and sterics of the copper intermediates that allow efficient capture of the alkyl radical, as well as the detailed mechanism of the alkyl radical capture processes, are still poorly understood. For example, few computational evaluations[19–21] and experimental model studies[22,23] have proposed two possible mechanisms of radical capture (**Figure 1.6a**). The first pathway involves direct addition of the alkyl radical to a copper(II) center, forming a copper alkyl (or aryl) species with a formal oxidation state of +3. Reductive elimination from the copper center results in C–N bond formation. The alternative pathway involves direct radical-radical coupling between the nitrogen of the nucleophile attached to copper and the alkyl radical. Due to the higher electronegativity of copper, the SOMO of the copper(II) metalloradical can have more ligand character (ligand field inversion),[24] rendering certain

copper(II)-nucleophile species be better viewed as copper(I)-nucleophile radicals that favor radical-radical coupling. The feasibility of both mechanisms has been demonstrated experimentally under designed model systems, but not within the context of photoinduced copper-catalyzed C–N coupling reactions (**Figure 1.6b**).

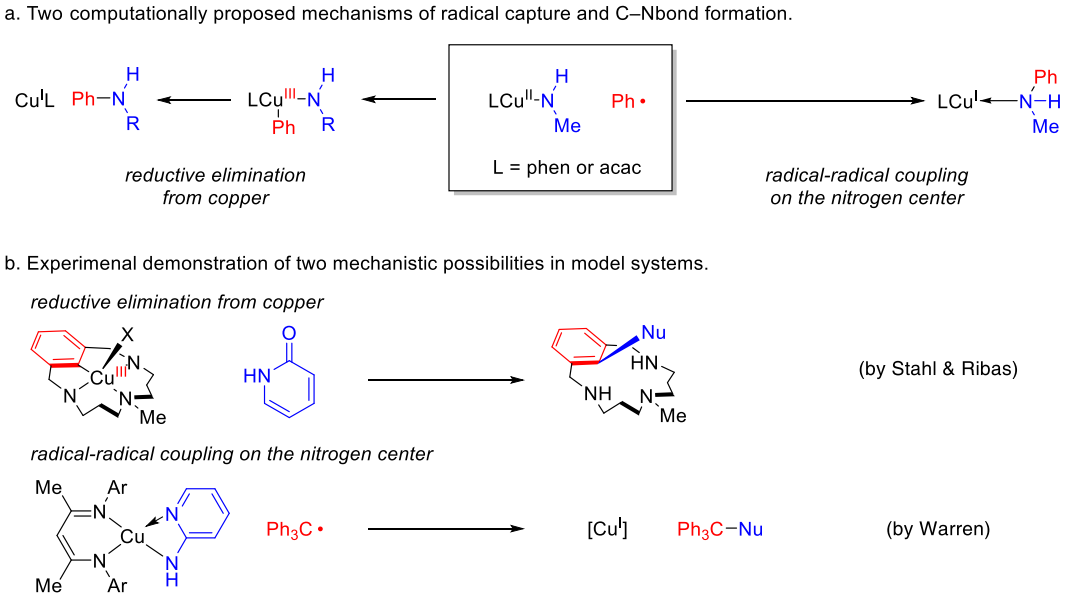

Figure 1.6. Proposed mechanisms for reductive elimination in copper-catalyzed C–N coupling.

1.5. Overview of individual chapters.

Building on these hypotheses and challenges, the goal of my research in the Fu group was to contribute to or achieve three specific objectives: 1) developing novel C–N coupling reactions that address current limitations in organic synthesis, 2) identifying the working photoreductants in the developed reactions and studying the mechanisms of their photoexcitation and alkyl electrophile activation processes, and 3) identifying the copper intermediates that capture alkyl radicals and broadening the understanding of alkyl radical capture and subsequent C–N bond formation by these copper species.

In Chapter 2, we describe photoinduced, enantio-convergent coupling of a variety of racemic tertiary alkyl electrophiles with aniline nucleophiles catalyzed by bisphosphine-copper complexes. The reaction can generate a new C–N bond with good ee at the fully

substituted stereocenter of the product (**Figure 1.7a**). The mechanism of this new reaction has been interrogated with the aid of a wide array of tools, including the independent synthesis of proposed intermediates and reactivity studies, spectroscopic investigations featuring photophysical and EPR data, and DFT calculations. These studies led to the identification of three copper-based intermediates in the proposed catalytic cycle, including a chiral three-coordinate formally copper(II)–anilido (DFT analysis points to its formulation as a copper(I)–anilidyl radical) complex that serves as a persistent radical that couples with a tertiary organic radical to generate the desired C–N bond with good enantioselectivity (**Figure 1.7b**).

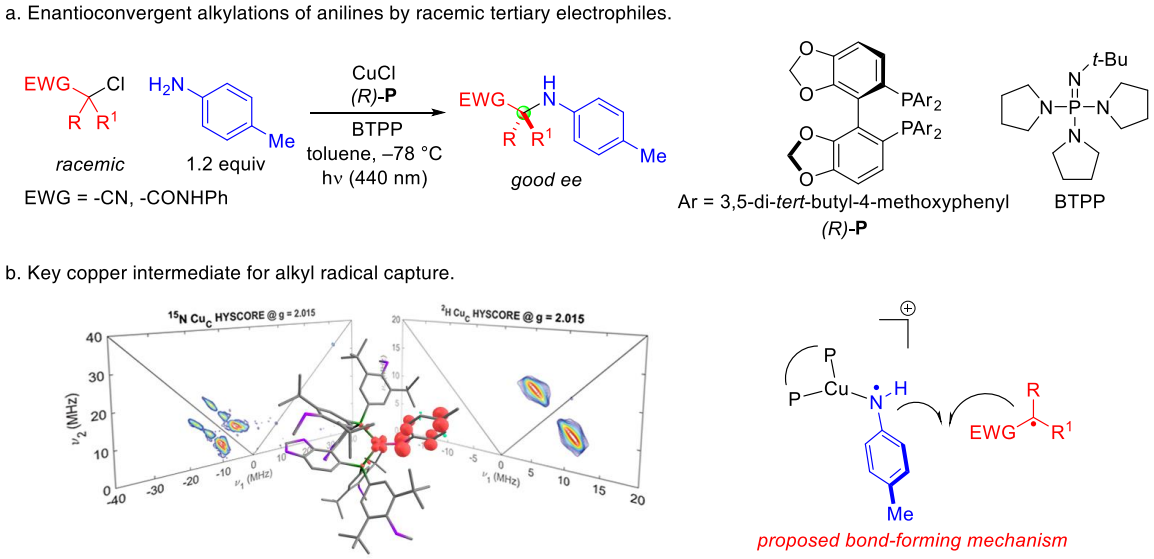

Figure 1.7. Overview of the key concepts and findings presented in chapter 2.

[Intentionally Redacted]

1.6. Notes and references.

1. Fu, G. C. Transition-Metal Catalysis of Nucleophilic Substitution Reactions: A Radical Alternative to SN1 and SN2 Processes. *ACS Cent. Sci.* **2017**, *3*, 692–700.
2. Bunnett, J. F.; Zahler, R. E. Aromatic Nucleophilic Substitution Reactions. *Chem. Rev.* **1951**, *49*, 273–412.
3. Campeau, L.-C.; Hazari, N. Cross-Coupling and Related Reactions: Connecting Past Success to the Development of New Reactions for the Future. *Organometallics* **2019**, *38*, 3–35.
4. Echavarren, A. M.; Homs, A. Mechanistic Aspects of Metal-catalyzed C,C- and C,X-bond Forming Reactions. *Metal-Catalyzed Cross-Coupling Reactions and More.* Wiley–VCH, 2014, pp 1–64.
5. Sambiagio, C.; Marsden, S. P.; Blacker, A. J.; McGowan, P. C. Copper Catalysed Ullmann Type Chemistry: From Mechanistic Aspects to Modern Development. *Chem. Soc. Rev.* **2014**, *43*, 3525–3550.
6. Le, C.; Chen, T. Q.; Liang, T.; Zhang, P.; MacMillan, D. W. C. A Radical Approach to the Copper Oxidative Addition Problem: Trifluoromethylation of Bromoarenes. *Science* **2018**, *360*, 1010–1014.
7. Cheng, L.-J.; Mankad, N. P. C–C and C–X Coupling Reactions of Unactivated Alkyl Electrophiles Using Copper Catalysis. *Chem. Soc. Rev.* **2020**, *49*, 8036–8064.
8. Creutz, S. E.; Lotito, K. J.; Fu, G. C.; Peters, J. C. Photoinduced Ullmann C–N Coupling: Demonstrating the Viability of a Radical Pathway. *Science* **2012**, *338*, 647–651.
9. Bissember, A. C.; Lundgren, R. J.; Creutz, S. E.; Peters, J. C.; Fu, G. C. Transition-metal-catalyzed Alkylations of Amines with Alkyl Halides: Photoinduced, Copper-catalyzed Couplings of Carbazoles. *Angew. Chem. Int. Ed.* **2013**, *52*, 5129–5133.
10. Do, H.-Q.; Bachman, S.; Bissember, A. C.; Peters, J. C.; Fu, G. C. Photoinduced, Copper-Catalyzed Alkylation of Amides with Unactivated Secondary Alkyl Halides at Room Temperature. *J. Am. Chem. Soc.* **2014**, *136*, 2162–2167.
11. Zhao, W.; Wurz, R. P.; Peters, J. C.; Fu, G. C. Photoinduced, Copper-Catalyzed Decarboxylative C–N Coupling to Generate Protected Amines: An Alternative to the Curtius Rearrangement. *J. Am. Chem. Soc.* **2017**, *139*, 12153–12156.

12. Matier, C. D.; Schwaben, J.; Peters, J. C.; Fu, G. C. Copper-Catalyzed Alkylation of Aliphatic Amines Induced by Visible Light. *J. Am. Chem. Soc.* **2017**, *139*, 17707–17710.
13. Ahn, J. M.; Peters, J. C.; Fu, G. C. Design of a Photoredox Catalyst That Enables the Direct Synthesis of Carbamate-Protected Primary Amines via Photoinduced, Copper-Catalyzed*N*-Alkylation Reactions of Unactivated Secondary Halides. *J. Am. Chem. Soc.* **2017**, *139*, 18101–18106.
14. Kainz, Q. M.; Matier, C. D.; Bartoszewicz, A.; Zultanski, S. L.; Peters, J. C.; Fu, G. C. Asymmetric Copper-Catalyzed C-N Cross-Couplings Induced by Visible Light. *Science* **2016**, *351*, 681–684.
15. He, J.; Chen, C.; Fu, G. C.; Peters, J. C. Visible-Light-Induced, Copper-Catalyzed Three-Component Coupling of Alkyl Halides, Olefins, and Trifluoromethylthiolate to Generate Trifluoromethyl Thioethers. *ACS Catal.* **2018**, *8*, 11741–11748.
16. Chen, C.; Peters, J. C.; Fu, G. C. Photoinduced Copper-Catalysed Asymmetric Amidation via Ligand Cooperativity. *Nature* **2021**, *596*, 250–256.
17. Crespi, S.; Fagnoni, M. Generation of Alkyl Radicals: From the Tyranny of Tin to the Photon Democracy. *Chem. Rev.* **2020**, *120*, 9790–9833.
18. Tsang, W. The Stability of Alkyl Radicals. *J. Am. Chem. Soc.* **1985**, *107*, 2872–2880.
19. Jones, G. O.; Liu, P.; Houk, K. N.; Buchwald, S. L. Computational Explorations of Mechanisms and Ligand-Directed Selectivities of Copper-Catalyzed Ullmann-Type Reactions. *J. Am. Chem. Soc.* **2010**, *132*, 6205–6213.
20. Yu, H.-Z.; Jiang, Y.-Y.; Fu, Y.; Liu, L. Alternative Mechanistic Explanation for Ligand-Dependent Selectivities in Copper-Catalyzed *N*- and *O*-Arylation Reactions. *J. Am. Chem. Soc.* **2010**, *132*, 18078–18091.
21. Sterling, A. J.; Ciccia, N. R.; Guo, Y.; Hartwig, J. F.; Head-Gordon, M. Mechanistic Insights into the Origins of Selectivity in a Cu-Catalyzed C–H Amidation Reaction. *J. Am. Chem. Soc.* **2024**, *146*, 6168–6177.
22. Casitas, A.; Ribas, X. The Role of Organometallic Copper(III) Complexes in Homogeneous Catalysis. *Chem. Sci.* **2013**, *4*, 2301–2318.
23. Jang, E. S.; McMullin, C. L.; Käß, M.; Meyer, K.; Cundari, T. R.; Warren, T. H. Copper(II) Anilides in sp^3 C–H Amination. *J. Am. Chem. Soc.* **2014**, *136*, 10930–10940.

24. Carsch, K. M. *Ligand Field Inversion in Sterically Confined Copper Architectures*, 2021, Doctoral dissertation, Harvard University Graduate School of Arts and Sciences.

C h a p t e r 2

PHOTOINDUCED, COPPER-CATALYZED ENANTIOCONVERGENT ALKYLATIONS OF ANILINES BY RACEMIC TERTIARY ELECTROPHILES: SYNTHESIS AND MECHANISM

Adapted in part with permission from:

Cho, H.; Suematsu, H.; Oyala, P. H.; Peters, J. C.; Fu, G. C. Photoinduced, Copper-Catalyzed Enantioconvergent Alkylations of Anilines by Racemic Tertiary Electrophiles: Synthesis and Mechanism. *J. Am. Chem. Soc.* **2022**, *144*, 4550–4558.

DOI: 10.1021/jacs.1c12749.

2.1. Introduction

Amines play an important role in a wide array of disciplines, including biology, materials science, organic chemistry, and pharmaceutical chemistry.[1–4] Although the nucleophilic substitution of an alkyl halide by an amine is an attractive approach to the synthesis of higher-order amines, traditional S_N2 reactions have limited applicability in the case of less reactive (e.g., hindered and unactivated) electrophiles, which instead engage in undesired side reactions, such as the elimination of H–X.[5,6] Furthermore, conventional substitution pathways almost never enable the control of stereochemistry at the carbon of the new C–N bond, starting with a readily available racemic electrophile.

To address these shortcomings with respect to reactivity and enantioselectivity, a number of laboratories have pursued the use of transition metals to catalyze substitution reactions of secondary and tertiary alkyl electrophiles by nitrogen nucleophiles.[7–13] To date, catalytic enantioconvergent substitutions have only been described for a few families of (mostly secondary) alkyl electrophiles, e.g., allylic electrophiles,[14] α-halocarbonyl compounds,[15–18] α-cyano-α-halocarbonyl compounds,[18,19] propargylic electrophiles,[18,20] benzylic electrophiles,[18] and unactivated alkyl halides that bear a directing group.[21]

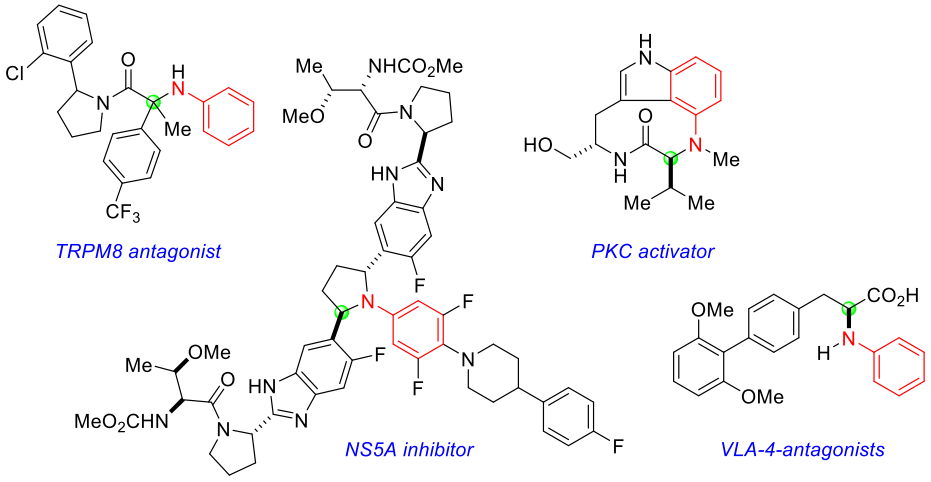

Figure 2.1. Examples of bioactive anilines with the nitrogen attached to a stereocenter.

Whereas a variety of bioactive molecules include as a subunit an arylamine (aniline) wherein the nitrogen is attached to a stereocenter (**Figure 2.1**),[22,23] to our knowledge there has been only one report of the synthesis of this motif via the enantioconvergent alkylation of an aniline by a racemic alkyl electrophile.[15,24,25] In the present study, we establish that, with the aid of a chiral copper catalyst and light, anilines can be coupled with a variety of racemic tertiary alkyl electrophiles to generate N-alkylanilines that bear a fully substituted stereocenter with good enantiomeric excess (**Figure 2.2**). Mechanistic studies are consistent with [**P**CuCl] acting as a photoreductant and with [**P**Cu(NHAr)]Cl serving as a key intermediate in the catalytic cycle.

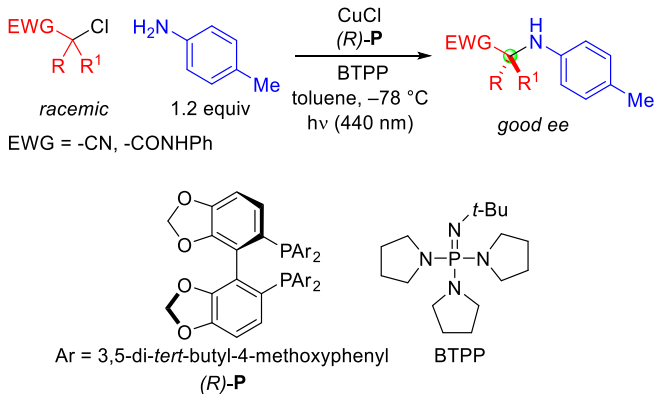

Figure 2.2. This study: photoinduced, copper-catalyzed enantioconvergent alkylations of anilines by racemic tertiary electrophiles.

2.2. Result and discussion

2.2.1. Reaction development

Seeking to expand the rather limited scope of enantioconvergent substitutions of alkyl electrophiles by nitrogen nucleophiles, we chose to explore reactions of α-halonitriles with anilines to generate α-aminonitriles. In particular, we decided to examine the use of tertiary α-halonitriles as electrophiles so as to produce α-disubstituted α-aminonitriles. Whereas catalytic enantioselective Strecker reactions of aldimines provide a versatile approach to the synthesis of enantioenriched α-monosubstituted α-aminonitrile families,[26,27] corresponding reactions of ketimines to afford α-disubstituted α-aminonitriles are less well-developed.[28–32]

Table 2.1. Effect of reaction parameters. All data are the average of two runs.

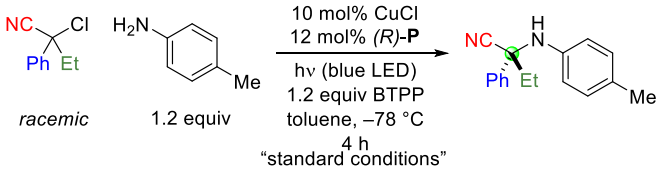

entry	variation from the "standard conditions"	yield (%)	ee (%)
1	none	77	92
2	no CuCl	<2	–
3	no **P**	<2	–
4	no BTPP	<2	–
5	no hν	<2	–
6	–10 °C instead of –78 °C	16	44
7	H_2O (5 equiv) added	78	92
8	air (5 mL) purged	68	92
9	2.0 mol% CuCl, 2.4 mol% **P**, 24 h	56	90
10	10 mol% ((*S*)-**P**)CuCl, instead of CuCl/**P**	76	92
11	no CuCl, no **P**, no hν, 80 °C	<2	–

Upon irradiation (blue LED) in the presence of CuCl and DTBM-SEGPHOS (**P**), a racemic tertiary α-chloronitrile undergoes substitution by *p*-toluidine (1.2 equiv) to furnish the desired α-disubstituted α-aminonitrile in good yield and ee (**Table 2.1**, entry 1: 77% yield, 92% ee; CuCl, **P**, and BTPP are all commercially available). Control experiments establish that CuCl, **P**, and light are critical for coupling under these conditions (entries 2–5; >95% recovery of the alkyl halide). At a higher reaction temperature (e.g., −10 °C), a lower yield and ee are observed (entry 6). The yield of the reaction is not particularly sensitive to small amounts of water or of air, which have no impact on enantioselectivity (entries 7 and 8). When a lower catalyst loading is employed (2.0 mol% copper), a turnover number greater

than 25 is observed (entry 9). A discrete, isolable bisphosphine copper(I) complex, [**P**CuCl] (**Cu**$_A$),[33,34] may be used in place of CuCl/**P** (entry 10). Whereas the photoinduced, copper-catalyzed coupling occurs in good yield at –78 °C, the corresponding S_N2 reaction does not proceed to a significant extent even at 80 °C (entry 11).

An array of racemic tertiary α-halonitriles serve as suitable electrophiles in these enantioconvergent N-alkylations. For example, consistently good enantioselectivity is observed as the R^1 group varies from Me to *i*-Bu (**Figure 2.3**, entry 1–3; on a gram scale of entry 2 (1.28 g of product), the coupling proceeds in 64% yield, 92% ee), although the yield is sensitive to the size of R^1. Functional groups such as an ester, olefin, unactivated alkyl chloride, aryl fluoride, aryl chloride, aryl bromide, amide, and phosphonate are compatible with the method (entry 5–12; also, an acetal, alcohol, alkylboronate ester, alkyl bromide, alkyl iodide, aryl iodide, aryl triflate, benzofuran, epoxide, ketone, sulfide, and tertiary amine: see the **Section 2.4.5**). Not only α-aryl-α-halonitriles (entry 1–10), but also α-acyl- and α-phosphonyl-substituted (entry 11 and 12; Br as the leaving group) α-halonitriles, serve as suitable coupling partners.

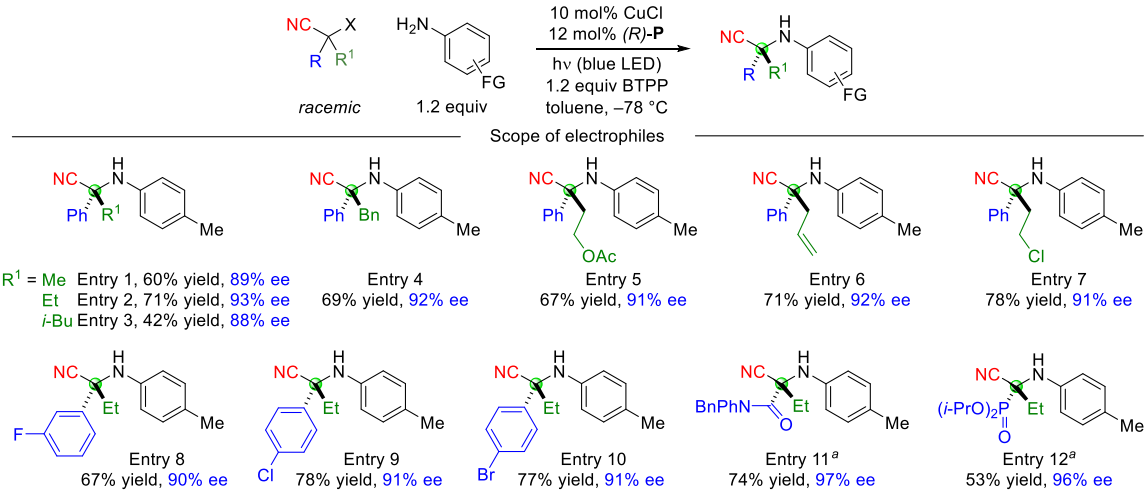

Figure 2.3. Photoinduced, copper-catalyzed enantioconvergent alkylations of anilines by racemic tertiary α-halonitrile: scope of electrophiles. Reactions were conducted on a 0.8-mmol scale, and yields are for purified compounds. All data are the average of two runs. X = Cl, unless otherwise noted. [a] X = Br.

The scope of this photoinduced, copper-catalyzed asymmetric N-alkylation is also reasonably broad with respect to the arylamine nucleophile. In the case of aniline itself, a substantial amount of addition of the electrophile to the para position is observed (C–C coupling: 24% yield, 27% ee; C–N coupling: 18% yield, 86% ee). However, if the para position bears a substituent, moderate-to-good yields and good enantioselectivities are obtained with either an electron-poor or an electron-rich aniline as the nucleophile (**Figure 2.4**, entry 13–18). Furthermore, meta substitution of the aniline can sufficiently impede addition to the para position such that the desired N-alkylation proceeds in fair yield as well as good enantioselectivity (entry 19–21).

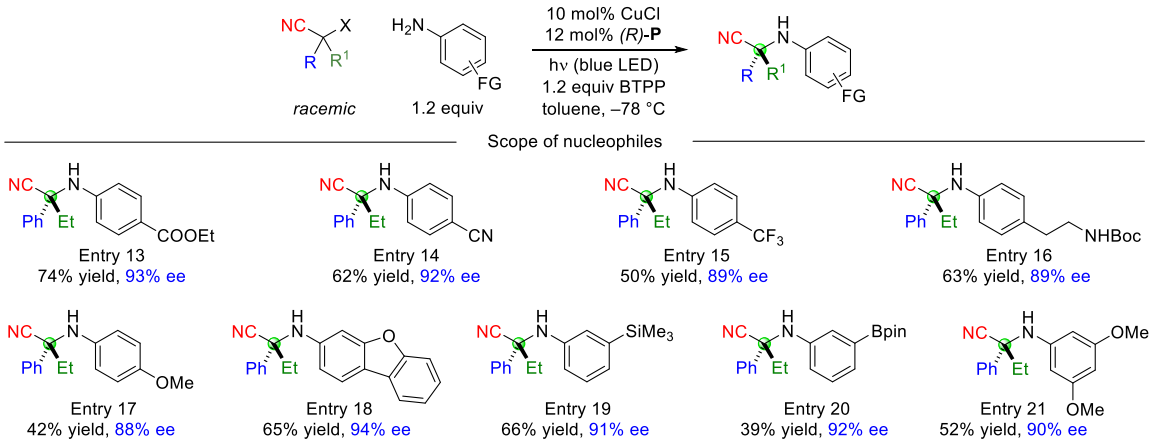

Figure 2.4. Photoinduced, copper-catalyzed enantioconvergent alkylations of anilines by racemic tertiary α-halonitrile: scope of nucleophiles. Reactions were conducted on a 0.8-mmol scale, and yields are for purified compounds. All data are the average of two runs. X = Cl, unless otherwise noted. Bpin, pinacolboryl.

It is noteworthy that enantioconvergent N-alkylation can be achieved with electrophiles that bear a leaving group other than chloride or bromide. In the case of a carbonate or a fluoride, although substitution does not occur in good yield and ee under the standard conditions, the addition of TBACl/$B(OMe)_3$ enables the desired C–N bond formation to proceed smoothly with good enantioselectivity (**eq 2.1**). To our knowledge, this is the first example of an alkyl fluoride serving as a suitable electrophile in a metal-catalyzed enantioconvergent substitution by a nitrogen nucleophile.

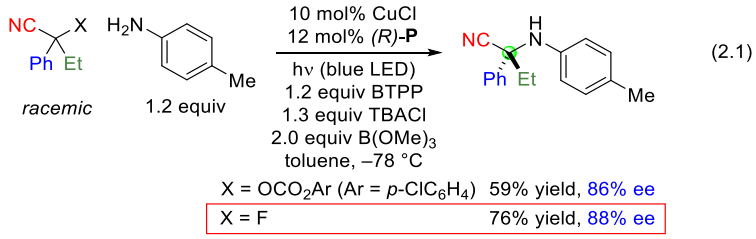

(2.1)

The standard reaction conditions can be applied to the enantioconvergent N-alkylation of anilines by racemic tertiary electrophiles that lack a cyano group. Thus, α-chloroamides are also suitable substrates, leading to coupling with good ee for both N-alkyl and N-aryl secondary amides (**Figure 2.5**, entry 22–26). Furthermore, the chiral catalyst can provide promising enantioselectivity when it is necessary to distinguish between two alkyl substituents on the electrophilic carbon, such as secondary vs. methyl (entry 25) or branched primary vs. methyl (entry 26).

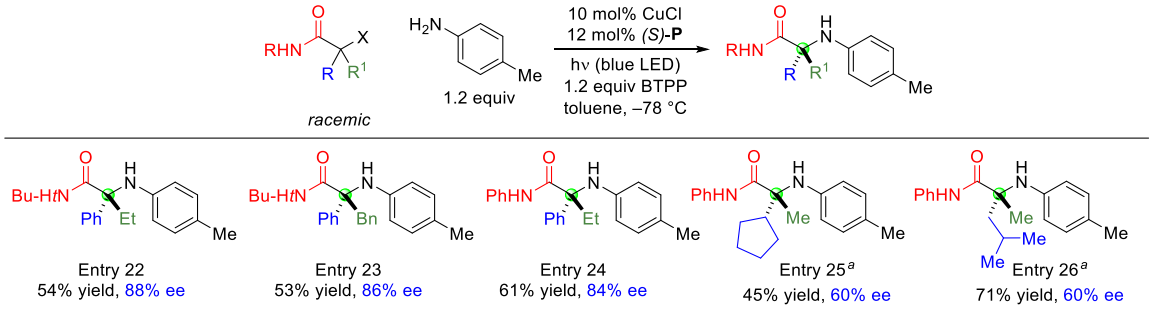

Figure 2.5. Photoinduced, copper-catalyzed enantioconvergent alkylations of anilines by tertiary *α*-haloamides as electrophiles. Reactions were conducted on a 0.8-mmol scale, and yields are for purified compounds. All data are the average of two runs. X= Cl, unless otherwise noted. [a] X = Br.

2.2.2. Mechanistic studies: overview

Our current working hypothesis is that these photoinduced, copper-catalyzed enantioconvergent C–N couplings may be proceeding through the pathway outlined in **Figure 2.6**. Thus, copper(I) complex **Cu$_A$**, which is a competent catalyst for the coupling (**Table 2.1**, entry 8; 10 mol% **Cu$_A$**, rather than 10 mol% CuCl/12 mol% **P**, was utilized in all catalyzed reactions for our mechanistic studies) undergoes excitation upon blue-LED irradiation to generate **Cu$_A$***, which reacts with electrophile R–Cl to afford organic radical

R• and copper(II) complex **Cu$_B$**. Complex **Cu$_B$** then undergoes base-induced substitution by the aniline to furnish copper complex **Cu$_C$**, which combines with R• to provide the coupling product and regenerate copper(I) complex **Cu$_A$**.

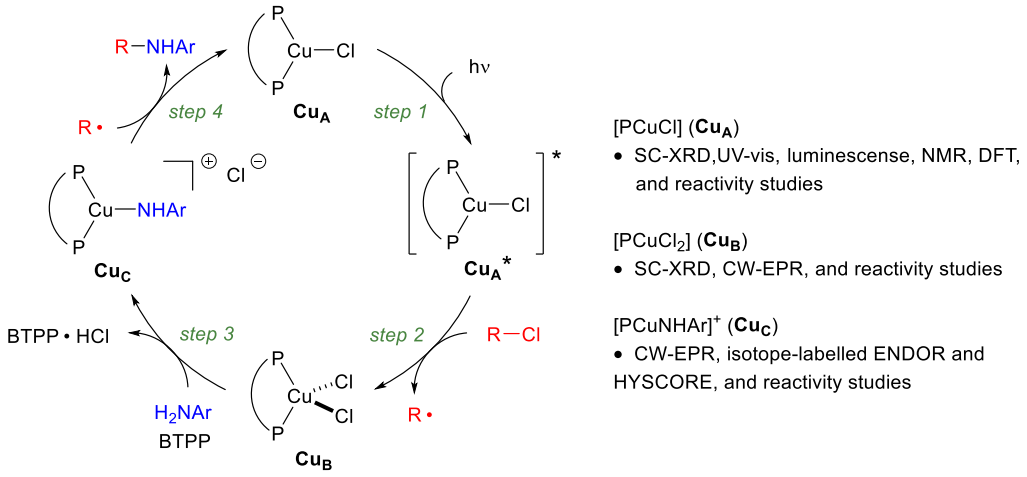

Figure 2.6. Outline of a possible mechanism for the photoinduced, copper-catalyzed enantioconvergent alkylation of anilines by racemic tertiary electrophiles. P⁀P = **P**.

2.2.3. Mechanistic studies: Cu$_A$

A solution of **Cu$_A$** in toluene at –78 °C shows a characteristic absorption at 376 nm (ε = 3890 M^{-1} cm^{-1}), as does the reaction mixture (the coupling depicted in Table 1) prior to irradiation (**Figure 2.7a**); because the concentrations of copper for the two UV–vis spectra are the same, virtually all of the copper in the reaction mixture appears to be present as **Cu$_A$** prior to irradiation (see the **Section 2.4.10.5**). As illustrated in **Figure 2.7b**, room-temperature ^{1}H and ^{31}P NMR spectroscopic analysis is consistent with this conclusion (>95%).[35] During a catalytic C–N coupling, the concentration of **Cu$_A$** decreases somewhat as the reaction progresses, to 54% of total copper at 64% conversion, according to ^{1}H NMR spectroscopy at –78 °C (see the **Section 2.4.10.5**).

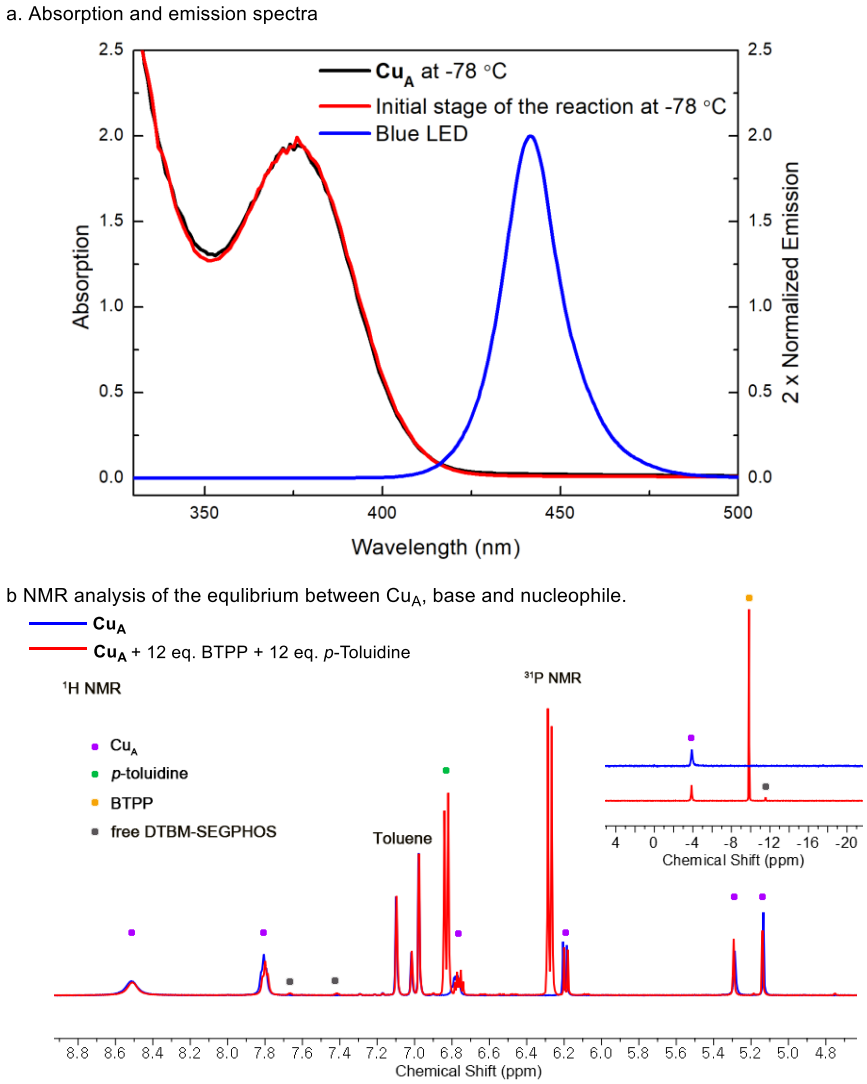

Figure 2.7. Cu$_A$ as a major component of the reaction mixture. a) Absorption and emission spectra of **Cu$_A$** (0.5 mM), reaction mixture ([**Cu$_A$**] = 0.5 mM, [2-chloro-2-phenylbutanenitrile] = 5 mM, [*p*-toluidine] = 6 mM, and [BTPP] = 6 mM), blue-LED lamp. b) ^{1}H NMR and ^{31}P NMR spectroscopy: comparison of a reaction mixture prior to irradiation versus **Cu$_A$**.

Having identified **Cu$_A$** as a major component of the reaction mixture, we carried out an investigation of its photophysical properties. The steady-state emission spectrum of **Cu$_A$*** shows a single emission band (λ_{max} = 480 nm) at temperatures ranging from 77 K to room temperature (see the **Section 2.4.10.6**). The luminescence decay of **Cu$_A$*** observed at 480

nm at room temperature shows two sets of decay curves, with lifetimes of 3.8 ns and 0.36 µs (**Figure 2.8**).

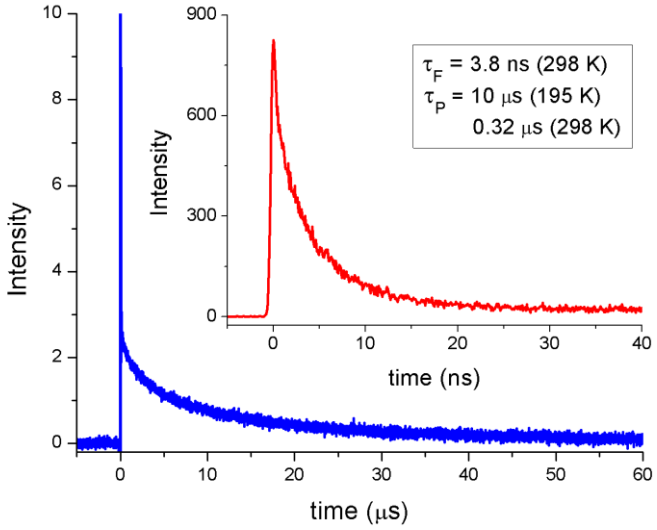

Figure 2.8. Luminescence lifetime of **Cu$_A$*** showing two sets of decay curves.

To avoid complications arising from the two luminescence-decay pathways, we measured the lifetime of a non-emissive excited state of **Cu$_A$** by transient absorption spectroscopy (λ_{pump} = 355 nm, λ_{probe} = 580 nm) as a function of electrophile concentration at room temperature (**Figure 2.9**). Addition of 2-chloro-2-phenylbutane-nitrile results in a decrease of the excited-state lifetime of **Cu$_A$*** that allows for the determination of the second-order rate constant, k_q = 3.7 x 10^8 M^{-1} s^{-1}, for the quenching process. The excited-state potential of **Cu$_A$*** is estimated to be $E_{1/2}$ ($Cu^{II/I*}$) ~ –2.6 V (vs Fc/Fc^+), based on E^{00} (3.0 eV) and $E_{1/2}$ ($Cu^{II/I}$; ~ 0.4 V vs Fc/Fc^+; irreversible), which are derived from emission spectroscopy and electrochemical characterization by cyclic voltammetry (CV); a CV of the model electrophile shows an irreversible feature at E_P ~ –2.2 V (see the **Section 2.4.10.8**).

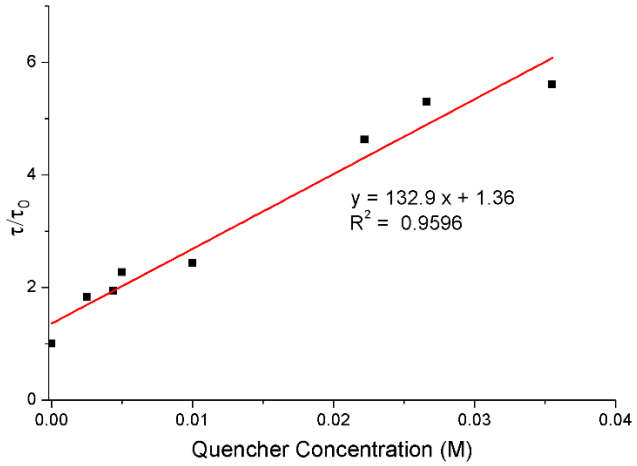

Figure 2.9. Stern-Volmer quenching of $\mathbf{Cu_A}$* by 2-chloro-2-phenylbutanenitrile (λ_{pump} = 355 nm, λ_{probe} = 580 nm).

2.2.4. Mechanistic studies: steps 1 and 2 of the catalytic cycle

No reaction between $\mathbf{Cu_A}$ and 2-chloro-2-phenylbutanenitrile occurs in toluene at –78 °C after 30 min in the dark, as determined by ^{1}H NMR spectroscopy. However, when this mixture is irradiated at –78 °C for 30 min, the initially colorless solution turns dark purple, and analysis by ^{1}H NMR spectroscopy shows that a C–C coupled dimer derived from the electrophile is formed (**Figure 2.10**: 43% yield based on $\mathbf{Cu_A}$; ~ 1:1 mixture of diastereomers). Formation of the dimer is readily accommodated by the reaction mechanism illustrated in **Figure 2.6**; specifically, excitation of $\mathbf{Cu_A}$ (step 1), followed by chlorine atom transfer, furnishes R• (step 2), which engages in radical–radical coupling in the absence of aniline (this R–R dimer is observed as a minor side product in the photoinduced, copper-catalyzed C–N coupling of this electrophile under the standard conditions; see **Section 2.4.10.2**).

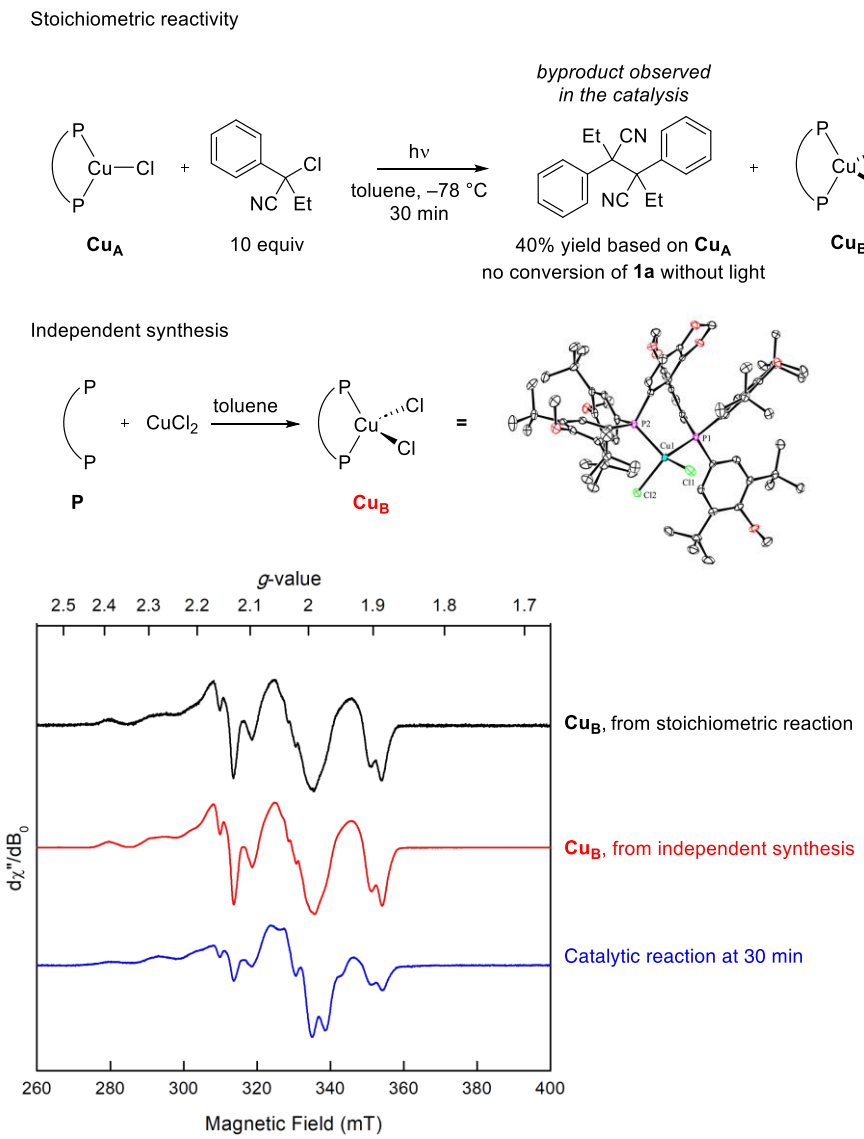

Figure 2.10. Steps 1 and 2 of the catalytic cycle: X-band CW-EPR spectra of **Cu$_B$** from a photoinduced reduction of 2-chloro-2-phenylbutanenitrile by **Cu$_A$** ([**Cu$_A$**] = 5 mM and [2-chloro-2-phenylbutanenitrile] = 50 mM; black), independent synthesis of **Cu$_B$** (red; X-ray crystal structure: thermal ellipsoids at 50% probability (solvents and hydrogen atoms are omitted for clarity)), and a catalyzed reaction after 30 min at –78 °C (blue); acquisition parameters: MW frequency = 9.37 GHz, MW power = 140 μW, modulation amplitude = 0.4 mT, conversion time = 5.02 ms, and temperature = 77 K.

2.2.5. Mechanistic studies: Cu_B

X-band continuous-wave (CW) EPR spectroscopy of the dark-purple solution obtained from this photoinduced reduction of 2-chloro-2-phenylbutanenitrile by $\mathbf{Cu_A}$ shows a signal characterized by large ^{31}P hyperfine couplings from two phosphorous atoms (**Figure 2.10**, black spectrum). We hypothesized that this paramagnet is **P**$CuCl_2$ ($\mathbf{Cu_B}$), which we then independently synthesized from **P** and $CuCl_2$ (toluene, r.t. to –78 °C) and crystallographically characterized (**Figure 2.10**; see the **Section 2.4.10.10**); the CW-EPR spectrum of this $\mathbf{Cu_B}$ at 77 K matches that of the photoinduced reduction of 2-chloro-2-phenylbutanen-itrile by $\mathbf{Cu_A}$ (**Figure 2.10**, black and red spectra). Upon monitoring the standard catalyzed C–N coupling reaction (**Table 2.1**), we determined that $\mathbf{Cu_B}$ is the predominant, but not the sole, paramagnetic species after 30 min of irradiation (**Figure 2.10**, blue spectrum; 82% conversion of the electrophile, 66% yield of the coupling product).

2.2.6. Mechanistic studies: Cu_C and step 3 of the catalytic cycle

X-band CW-EPR spectroscopic analysis of a catalytic reaction after 10 min of irradiation shows that a different copper(II) species is dominant at the beginning of the coupling process (**Figure 2.11**, red spectrum; 32% conversion of the electrophile, 22% yield of the coupling product; see the **Section 2.4.10.11**). We have determined that a matching EPR spectrum is observed upon treating $\mathbf{Cu_B}$ with *p*-toluidine in the presence of BTPP at –90 °C (**Figure 2.11**, black spectrum; if either *p*-toluidine or BTPP is absent, the black EPR spectrum is not observed). Under the same conditions, use of a different copper halide complex (Br instead of Cl) or a different base (2-*tert*-butyl-1,1,3,3-tetramethylguanidine (BTMG) instead of BTPP) leads to no noticeable change in the black EPR spectrum (including superhyperfine structures resolved in their second derivatives; see **Section 2.4.10.13**), consistent with the paramagnet being a copper(II) complex in which neither the halide nor the Brønsted base is bound. We therefore postulated that this complex might be three-coordinate [**P**Cu(NHAr)]X ($\mathbf{Cu_C}$), [**P**Cu=NAr], or four-coordinate [**P**$Cu(NHAr)_2$].

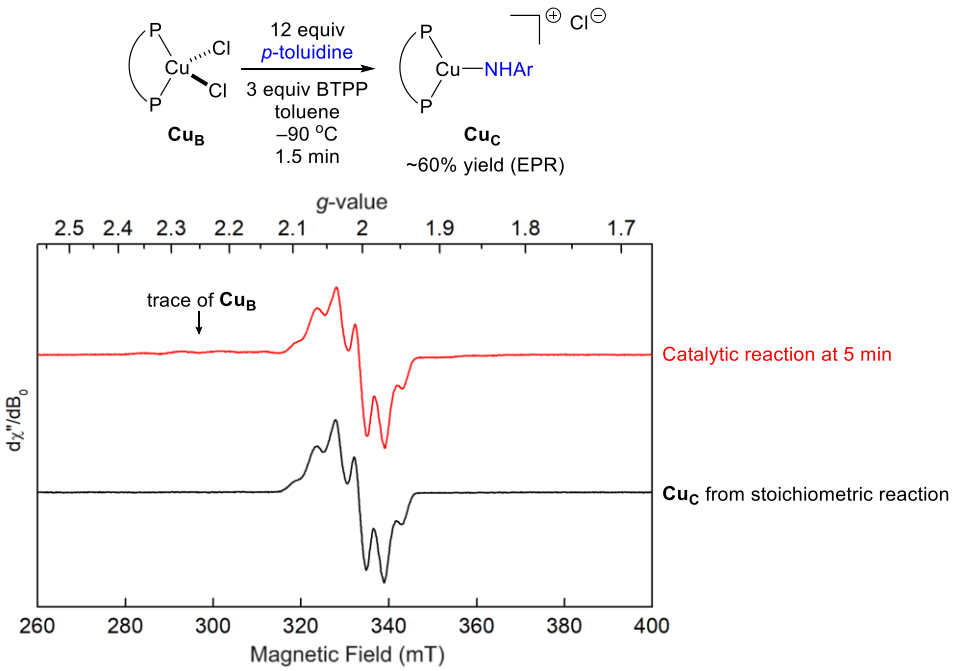

Figure 2.11. X-band CW-EPR spectra of a catalyzed reaction after 5 min at –78 °C (red) and of **Cu**$_{\mathbf{C}}$ prepared independently (black); acquisition parameters: MW frequency = 9.36 GHz, MW power = 140 μW, modulation amplitude = 0.4 mT, conversion time = 5.02 ms, and temperature = 77 K.

This paramagnetic copper complex (**Cu**$_{\mathbf{C}}$) is unstable at –78 °C, decomposing over 30 min (as observed by CW-EPR spectroscopy, see the **Section 2.4.10.12**) and forming (*E*)-1,2-di-*p*-tolyldiazene (this dimer is observed as a minor side product in photoinduced, copper-catalyzed N-alkylations of *p*-toluidine under the standard coupling conditions). Because the thermal instability of **Cu**$_{\mathbf{C}}$ frustrated our attempts at crystallographic characterization, we investigated its structure through EPR spectroscopy (**Figure 2.12**). The X-band EPR signal of **Cu**$_{\mathbf{C}}$ is dominated by hyperfine coupling to $^{63/65}$Cu (I = 3/2) and two inequivalent ^{31}P (I = 1/2) nuclei, without any additional hyperfine splitting being clearly resolved (see **Section 2.4.10.14**).

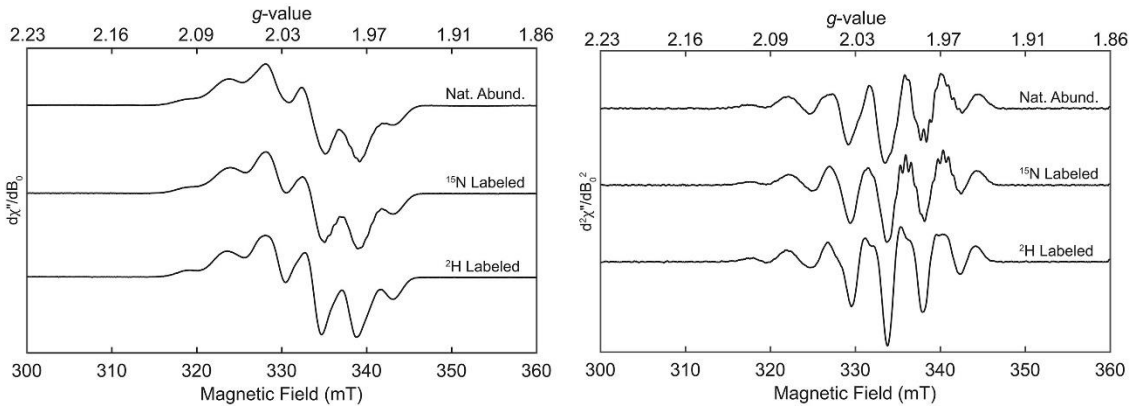

Figure 2.12. X-band CW-EPR spectra (left panel) and 2nd derivative (right panel) of **Cu**$_{\mathbf{C}}$ in toluene and isotopologues of *p*-toluidine; acquisition parameters: MW frequency = 9.372–9.374 GHz, MW power = 140 µW, modulation amplitude = 0.1 mT, conversion time = 5.3 ms, and temperature = 77 K.

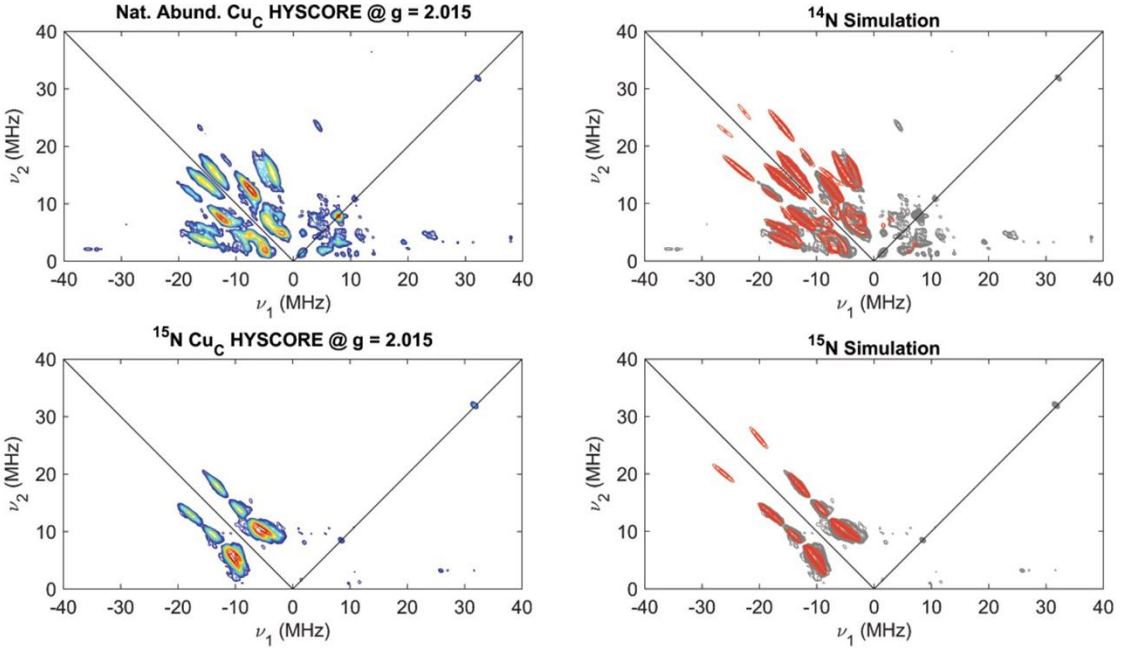

Figure 2.13. Q-band HYSCORE of **Cu**$_{\mathbf{C}}$ in toluene of isotopologues of *p*-toluidine (left) measured at 1206 mT (g = 2.015) with overlay of $^{14/15}$N simulation contours (right, red) with experimental contours (right, gray); experimental conditions: MW frequency = 34.005 GHz, τ = 128 ns, $t_1 = t_2$ = 100 ns, $\Delta t_1 = \Delta t_2$ = 12 ns, shot repetition time (srt) = 1.5 ms, and temperature = 30 K.

We investigated the incorporation of *p*-toluidine in the spin system using isotopically labeled *p*-toluidine (*p*-toluidine-^{15}N and *p*-toluidine-ND_2). The X-band CW-EPR spectra of these isotopologues show very subtle differences in the second-derivative plots (**Figure 2.12**, bottom panel). For quantitative determination of the natural abundance ^{14}N and introduced ^{2}H and ^{15}N couplings, we turned to pulsed EPR spectroscopy. Field-dependent Q-band hyperfine sublevel correlation (HYSCORE) spectra of ^{15}N labeled **Cu**C show a single set of elongated correlation ridges in the (–,+) quadrant, indicating that the coupling falls into the strongly coupled regime where $A > 2\nu_I$ (**Figure 2.13**, bottom panel).[36] These features are well simulated by a *single class* of highly anisotropic ^{15}N hyperfine tensor with $A(^{15}\text{N}) = \pm[6, 90, 6]$ MHz, $a_{iso}(^{15}\text{N}) = \pm 24.3$ MHz. The $^{\mathbf{14}}$N signals present in the analogous HYSCORE spectra of natural-abundance **Cu**C also fall into the strong-coupling regime but are additionally complicated by the influence of $^{\mathbf{14}}$N nuclear quadrupole interaction (**Figure 2.13**, top panel). These spectra are well simulated by scaling the ^{15}N hyperfine tensor determined from ^{15}N HYSCORE by the proportion of ^{15}N/^{14}N gyromagnetic ratios ($|\gamma^{15}\text{N}|/|\gamma^{14}\text{N}| = 1.403$), with further variation of the ^{14}N nuclear quadrupole parameters. The simulated $^{\mathbf{14}}$N quadrupole parameters are identical to those determined for the amide nitrogen of structurally relevant Ni(III)-amide and -anilido species using similar HYSCORE spectroscopic methods,[37] and they are consistent with the presence of a trisubstituted nitrogen with a lone pair oriented roughly orthogonal to the trigonal plane, as expected for a Cu–NHAr moiety. Q-band HYSCORE spectroscopy of ^{2}H-labeled **Cu**C shows a single set of intense cross-peaks in the (+,+) quadrant that thus fall into the weakly coupled regime where $A < 2\nu_I$ (**Figure 2.14**), which are well-simulated by a *single class* of relatively anisotropic ^{2}H hyperfine tensor with $A(^{2}\text{H}) = \pm[8.9, 4.3, 1.5]$ MHz, $a_{iso}(^{2}\text{H}) = \pm 4.9$ MHz.

The presence of multiple equivalent NHAr ligands could be ruled out by simulations that showed that the equivalent $^{\mathbf{14}/15}$N nuclei would generate combination peaks[38,39] that are absent in the observed spectra (see the **Section 2.4.10.14**). Additionally, multiple equivalent $^{\mathbf{1}}$H couplings of the class detected directly from the $^{\mathbf{2}}$H HYSCORE could not be accommodated by simulations of the X-band CW-EPR spectra. Collectively, the spectroscopic data are consistent with the presence of a single trisubstituted nitrogen with a single N–H, i.e., **Cu**C as [**P**Cu(NHAr)]Cl.

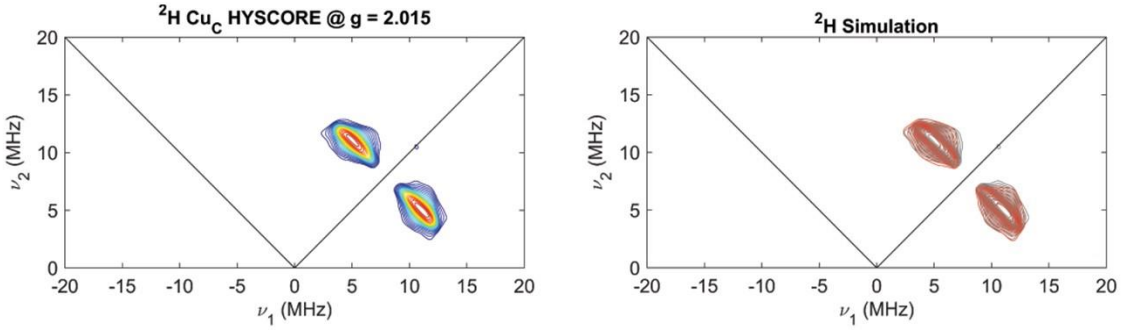

Figure 2.14. Q-band HYSCORE of **Cu**$_C$ in toluene of isotopologues of *p*-toluidine (left) measured at 1206 mT (g = 2.015) with overlay of ^{2}H simulation contours (right, red) with experimental contours (right, gray); experimental conditions: MW frequency = 34.005 GHz, τ = 128 ns, $t_1 = t_2$ = 100 ns, $\Delta t_1 = \Delta t_2$ = 12 ns, shot repetition time (srt) = 1.5 ms, and temperature = 30 K.

Further support for the proposed structure of **Cu**$_C$ has been obtained by comparing the experimentally derived CW-EPR parameters to values predicted by DFT calculations for the various possible structures. Only three-coordinate [**P**Cu(NHAr)]Cl is predicted to have EPR parameters similar to those observed (see the **Section 2.4.11**). Spin-density calculations of **Cu**$_C$ indicate that there is considerable spin density on the aniline ligand (0.33 e^- on NH, 0.32 e^- on the aromatic ring) and less spin density on copper (0.15 e^-) (**Figure 2.15**), indicating that **Cu**$_C$ is more accurately viewed as a copper(I)–(anilidyl radical) complex, rather than as its formal assignment as a copper(II)–anilido complex.[40]

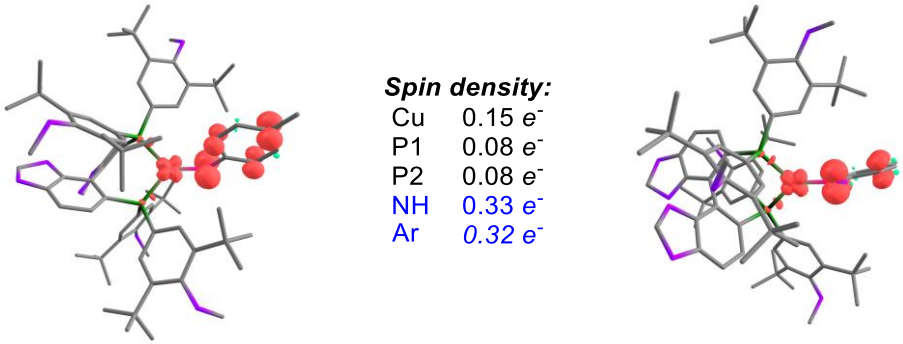

Figure 2.15. Calculated spin-density plot of **Cu**$_C$ viewed perpendicular to the NHAr plane and at a 45° angle (bp86 def2-TZVP; contour value = 0.005).

2.2.7. Mechanistic studies: step 4 of the catalytic cycle

We have shown that **Cu$_C$** can couple with an organic radical to afford a new C–N bond. Thus, generation of **Cu$_C$** at low temperature, followed by the addition of a persistent trityl-derived radical, leads to N-alkylation in 41% yield (**Figure 2.16a**). Based on the spin density at the nitrogen center and the sterically congested copper center of **Cu$_C$**, we propose that the tertiary alkyl radical derived from the electrophile undergoes C–N bond formation through direct radical-radical coupling between the carbon of the electrophile and the nitrogen of **Cu$_C$**, rather than through carbon-copper bond formation (**Figure 2.16b**). Similarly, the substantial spin density at the para carbon of the aniline (0.17 e–) aligns with our observation of significant C–C bond formation at that position when it is not blocked, through the radical-radical coupling.[41] The lower ee of the C−C coupling process (**section 2.2.1**) may be due to the greater distance of the site of bond formation from the chiral environment of the copper complex.

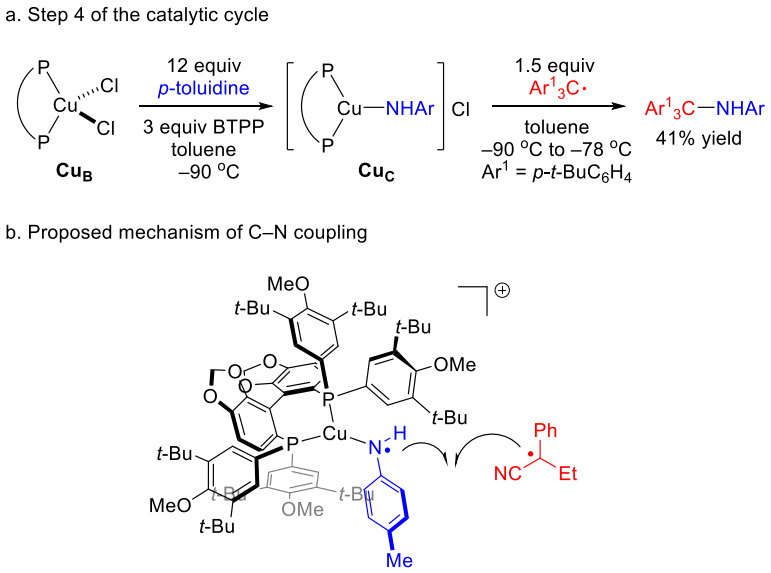

Figure 2.16. Step 4 of the catalytic cycle a) Stoichiometric reaction of **Cu$_C$** with persistent alkyl radical. b) Proposed mechanism of C–N bond formation.

2.3. Conclusions

We have developed a photoinduced, copper-catalyzed method for the enantio-convergent N-alkylation of anilines by an array of racemic tertiary alkyl electrophiles that generates fully-substituted stereocenters with good ee. The catalyst, composed of commercially available components, effects asymmetric C–N bond formation at –78 °C, whereas the corresponding uncatalyzed coupling does not proceed at a significant rate even at 80 °C. Although the use of alkyl chlorides as electrophiles is the primary focus of this study, examples have been presented of the use of other electrophiles, specifically, an alkyl fluoride and an alkyl carbonate, under similar conditions. Mechanistic studies have provided support for key intermediates and elementary steps in the proposed catalytic cycle. Future investigations will explore the development of other enantioselective bond-forming processes that employ catalysts based on earth-abundant copper.

2.4. Experimental section

2.4.1. General information

Chemicals. Unless otherwise noted, reagents purchased from commercial suppliers were used as received. CuCl, (*S*)-**P**, and (*R*)-**P** were purchased from Strem. BTPP was purchased from Sigma-Aldrich and stored inside a glovebox freezer (–30 °C); as needed, BTPP was filtered through a PTFE syringe filter (0.45 μm, InnoSep™) into a vial, the vial was capped with a PTFE-lined cap, and the vial was removed from the glovebox. Tetrabutylammonium chloride was purchased from Sigma Aldrich and gently ground under a nitrogen atmosphere before use. Unless otherwise noted, anilines purchased from commercial sources were purified by distillation or sublimation before use. Anhydrous toluene (99.8%) was purchased from Sigma-Aldrich, stored under nitrogen, and used with standard air-free techniques; other solvents were purified by passage through activated aluminum oxide in a solvent-purification system. All solvents for mechanistic studies were further degassed by freeze-pump-thaw cycles (five cycles) and stored over molecular sieves under a nitrogen atmosphere; the quality of the solvents was tested before use, using benzophenone-ketyl radical in THF. All manipulations of air-sensitive materials were carried out in oven-dried glassware under a nitrogen atmosphere using standard Schlenk or glovebox techniques. Flash column chromatography was performed using silica gel (SiliaFlash® P60, particle size 40-63 μm, Silicycle). Analytical thin-layer chromatography was conducted with glass TLC plates (silica gel 60 F254), and spots were visualized under UV light or after treatment with standard TLC stains.

NMR spectroscopy. NMR spectra were collected on a Bruker 400 MHz or a Varian 500 MHz spectrometer at ambient temperature; chemical shifts (δ) are reported in ppm downfield from tetramethylsilane, using the solvent resonance as an internal standard.

Other analyses. HPLC analyses were carried out on an Agilent 1100 series system with Daicel CHIRALPAK® or Daicel CHIRALCEL® columns (4.6 × 250 mm, particle size 5 μm). GC analyses were obtained on an Agilent 6890N GC. HRMS were acquired on an Agilent 1260 Infinity II HPLC-MS system in electrospray ionization (ESI+) mode or a JEOL AccuTOF GCx Plus system in field ionization (FI+) mode. FT-IR measurements were

carried out on a VERTEX 80 FT-IR purge spectrometer. Absorbance spectra were acquired on a Cary 50 UV-Vis spectrophotometer. Optical-rotation data were obtained with a Jasco P-2000 polarimeter at 589 nm, using a 100 mm pathlength cell in the solvent and at the concentration indicated. Elemental analyses were carried out in the Beckman Institute Crystallography Facility on a PerkinElmer 2400 Series II CHN Elemental Analyzer.

X-ray crystallography. X-ray crystallographic studies were carried out in the Beckman Institute Crystallography Facility on a Bruker APEX-II CCD diffractometer with filtered Cu-Kα radiation or Mo-Kα radiation. Suitable single crystals for X-ray structure determination were selected from the mother liquor and mounted in a nylon loop in immersion oil. The structures were solved and refined using APEX 3 software. Structure solution was performed using the SHELXT structure solution program using direct methods. Refinement was performed using the SHELXL refinement package using least squares minimization. All non-hydrogen atoms were refined with anisotropic displacement parameters. All C–H hydrogen atoms were refined isotropically on calculated positions by using a riding model with their U_{iso} values constrained to 1.5 U_{eq} of their pivot atoms for terminal sp^3 carbon atoms and 1.2 times for all other atoms.

Photoinduced reactions. Photoinduced reactions were performed using Kessil® PR160-440 nm lamps. The light source was placed approximately 5 cm above the sample, and the reaction mixture was stirred at 500 rpm using a magnetic stir bar. Temperature control was maintained with a methanol bath cooled by an SP Scientific cryostat. For reactions longer than 24 h, the methanol bath was replaced with a fresh bath after 24 h to prevent the accumulation of ice.

Photophysical measurements. Steady-state fluorimetry and time-resolved transient absorption and luminescence measurements were performed in the Beckman Institute Laser Research Center. Room-temperature samples for transient absorption and luminescence measurements were prepared with dry, degassed solvents inside a nitrogen-filled glovebox and transferred to a 1 cm pathlength fused quartz or glass cuvette (Starna Cells) which was sealed with a high-vacuum Teflon valve (Kontes) or a PTFE-lined open-top screw cap (Starna Cells). Samples for low-temperature measurements were prepared in a 4 mm EPR

tube (Wilmad or Norell) sealed with a rubber stopper. Steady-state emission spectra were collected on a Jobin S4 Yvon Spec Fluorolog-3-11 with a Hamamatsu R928P photomultiplier tube detector with photon counting.

For luminescence and transient absorption at the nanosecond to microsecond time scale, a Q-switched Nd:YAG laser (Spectra-Physics Quanta-Ray PRO-Series; 355 nm; pulse duration 8 ns, operating at 10 Hz) was used as the source of the excitation pulse, with laser power at 0.5 mJ/pulse. Probe light for transient absorption kinetics measurements was provided by a 75-W arc lamp (PTI Model A 1010) that was operated in continuous wave or pulsed modes. The laser light was aligned so as to be collinear with the arc lamp beam, and the scattered excitation light was rejected with appropriate long pass and short pass filters. Transmitted light from the sample was detected with a photomultiplier tube (Hamamatsu R928). All instruments and electronics in these systems were controlled by software written in LabVIEW (National Instruments).

Transient absorption difference spectra were collected using the same excitation source (λ_{ex} = 355 nm) and a white light flash lamp source with nanosecond durations. All instruments and electronics in these systems were controlled by software written in LabVIEW (National Instruments). Data processing was performed with MatlabR2018a and OriginPro 8.

Luminescence decay measurements at the picosecond time scale were performed as previously described.[42,43] A mode-locked Nd:YAG laser (Vanguard 2000-HM532; Spectra-Physics) provided 10 ps pulses that were regeneratively amplified (Continuum) and frequency tripled (355 nm excitation). Laser power was reduced to 0.5 mJ/pulse. Fluorescence from the sample was focused onto the entrance slit of a spectrograph (Acton Research Corp SpectraPro 275) through a 355 nm dielectric mirror to reject scattered excitation light. Fluorescence decays were obtained at a spectrograph center wavelength of 420 nm. Decays were collected using a streak camera (C5680; Hamamatsu Photonics) in photon counting mode over a 50 ns window.

CW EPR spectroscopy. 77 K X-band CW EPR spectra were obtained on a Bruker EMX spectrometer using a quartz liquid nitrogen immersion Dewar on solutions prepared as frozen glasses in toluene, unless otherwise noted.

Pulse EPR spectroscopy. All pulse EPR and electron nuclear double resonance (ENDOR) experiments were carried out using a Bruker ELEXSYS E580 pulse EPR spectrometer. All Q-band data was acquired using a Bruker D2 resonator. Temperature control was achieved using an ER 4118HV-CF5-L Flexline Cryogen-Free VT cryostat (ColdEdge) equipped with an Oxford Instruments Mercury ITC.

Pulse Q-band ENDOR was acquired using the Davies pulse sequence ($\pi - T_{RF} - \pi_{RF} - T_{RF} - \pi/2 - \tau - \pi -$ echo), where T_{RF} is the delay between MW pulses and RF pulses, π_{RF} is the length of the RF pulse, and the RF frequency is randomly sampled during each pulse sequence.

Q-band HYSCORE spectra were acquired using the 4-pulse sequence ($\pi/2 - \tau - \pi/2 - t_1 - \pi - t_2 - \pi/2 -$ echo), where τ is a fixed delay, while t_1 and t_2 are independently incremented by Δt_1 and Δt_2, respectively. The time domain data was baseline-corrected (third-order polynomial) to eliminate the exponential decay in the echo intensity, apodized with a Hamming window function, zero-filled to eight-fold points, and fast Fourier-transformed to yield the 2-dimensional frequency domain.

In general, the ENDOR spectrum for a given nucleus with spin I= ½ (^{1}H, ^{31}P) coupled to the S = ½ electron spin exhibits a doublet at frequencies (**eq. 2.2**)

$$\nu_{\pm} = \left|\frac{A}{2} \pm \nu_N\right| \tag{2.2}$$

where ν_N is the nuclear Larmor frequency and A is the hyperfine coupling. For nuclei with $I \geq 1$ (^{14}N, ^{2}H), an additional splitting of the $\nu_{\pm}$ manifolds is produced by the nuclear quadrupole interaction (P) (**eq. 2.3**)

$$\nu_{\pm,m_I} = \left|\nu_N \pm \frac{3P(2m_I - 1)}{2}\right| \tag{2.3}$$

In HYSCORE spectra, these signals manifest as cross-peaks or ridges in the 2-D frequency spectrum that are generally symmetric about the diagonal of a given quadrant. This technique allows hyperfine levels corresponding to the same electron-nuclear submanifold to be differentiated, as well as separating features from hyperfine couplings in the weak-coupling regime ($|A| < 2|\nu_I|$) in the (+,+) quadrant from those in the strong coupling regime ($|A| > 2|\nu_I|$) in the (−,+) quadrant. Because the (−,−) and (+,−) quadrants of these frequency spectra are symmetric to the (+,+) and (−,+) quadrants, only two of the quadrants are typically displayed in the literature.

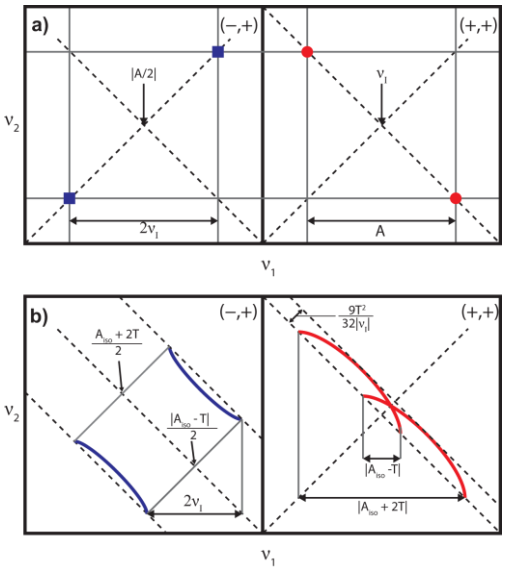

Figure 2.17. a) HYSCORE powder patterns for an S = ½, I = ½ spin system with an isotropic hyperfine tensor A. b) HYSCORE powder patterns for an S = ½, I = ½ spin system with an axial hyperfine tensor that contains isotropic (a_{iso}) and dipolar (T) contributions. Blue correlation ridges represent the strong coupling case; red correlation ridges represent the weak coupling case.

For systems with appreciable hyperfine anisotropy in frozen solutions or solids, HYSCORE spectra typically do not exhibit sharp cross peaks, but show ridges that represent the sum of cross peaks from selected orientations within the excitation bandwidth of the MW pulses at the magnetic field position at which the spectrum is collected. The length and curvature of these correlation ridges can allow for the separation and estimation of the magnitude of the isotropic and dipolar components of the hyperfine tensor (**Figure 2.17**).

EPR simulations. Simulations of all CW and pulse EPR data were achieved using the EasySpin[44] simulation toolbox (release 5.2.33) with Matlab 2020b using the following Hamiltonian (**eq. 2.4**):

$$\hat{H} = \mu_B \vec{B}_0 g \hat{S} + \mu_N g_N \vec{B}_0 \hat{I} + h\hat{S} \cdot \boldsymbol{A} \cdot \hat{I} + h\hat{I} \cdot \boldsymbol{P} \cdot \hat{I} \tag{2.4}$$

In this expression, the first term corresponds to the electron Zeeman interaction term where μ_B is the Bohr magneton, g is the electron spin g-value matrix with principal components g = [g_{xx} g_{yy} g_{zz}], and $\hat{S}$ is the electron spin operator; the second term corresponds to the nuclear Zeeman interaction term where μ_N is the nuclear magneton, g_N is the characteristic nuclear g-value for each nucleus (e.g. ^{1}H, ^{2}H, ^{31}P) and $\hat{I}$ is the nuclear spin operator; the third term corresponds to the electron-nuclear hyperfine term, where $\boldsymbol{A}$ is the hyperfine coupling tensor with principal components $\boldsymbol{A}$ = [A_{xx}, A_{yy}, A_{zz}]; and for nuclei with $I \geq 1$, the final term corresponds to the nuclear quadrupole (NQI) term which arises from the interaction of the nuclear quadrupole moment with the local electric field gradient (efg) at the nucleus, where $\boldsymbol{P}$ is the quadrupole coupling tensor. In the principal axis system (PAS), $\boldsymbol{P}$ is traceless and parametrized by the quadrupole coupling constant e^2Qq/h and the asymmetry parameter η such that (**eq. 2.5**):

$$\boldsymbol{P} = \begin{pmatrix} P_{xx} & 0 & 0 \\ 0 & P_{yy} & 0 \\ 0 & 0 & P_{zz} \end{pmatrix} = \frac{e^2Qq/h}{4I(2I-1)} \begin{pmatrix} -(1-\eta) & 0 & 0 \\ 0 & -(1+\eta) & 0 \\ 0 & 0 & 2 \end{pmatrix} \tag{2.5}$$

where $\frac{e^2Qq}{h} = 2I(2I-1)P_{zz}$ and $\eta = \frac{P_{xx}-P_{yy}}{P_{zz}}$. The asymmetry parameter may have values between 0 and 1, with 0 corresponding to an electric field gradient (EFG) with axial symmetry and 1 corresponding to a fully rhombic EFG.

The orientations between the hyperfine and NQI tensor principal axis systems and the g-matrix reference frame are defined by the Euler angles (α, β, γ), with rotations performed within the zyz convention where α rotates xyz counterclockwise about z-axis to give x'y'z', β rotates x'y'z counterclockwise about y'-axis to give x",y",z", and γ rotates xyz counterclockwise about z"-axis to give final frame orientation.

2.4.2. Preparation of electrophiles

The yields have not been optimized.

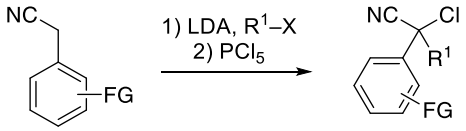

General Procedure 1 (GP-1): Preparation of *α*-chloronitriles. An oven-dried 250 mL round-bottom flask charged with a magnetic stir bar and capped with a rubber septum was placed under a nitrogen atmosphere by evacuating and backfilling the flask (three cycles). Anhydrous tetrahydrofuran (to form a 0.4 M solution of LDA) and anhydrous diisopropylamine (1 equiv) were added to the flask, and then the solution was cooled to –78 °C. Next, a solution of *n*-butyllithium (1 equiv; in hexane) was added into the flask over 1 min, and the resulting solution was stirred at –78 °C for 15 min. The substrate was added dropwise over 2 min, and then the reaction mixture stirred at –78 °C for an additional 40 min. Next, the alkyl bromide or iodide (1.1-1.2 equiv) was added dropwise into the reaction mixture over 5 min. The reaction mixture was slowly warmed to room temperature and stirred overnight. Then, the reaction mixture was acidified with 2 N aqueous HCl, and the organic layer was separated and dried over Na_2SO_4. The solid was removed via filtration, and the filtrate was concentrated in vacuo. The product was purified by flash column chromatography on silica gel (hexanes/dichloromethane = 10/1→5/1).

Next, an oven-dried 100 mL round-bottom flask was charged with the 2-alkyl-2-phenyl acetonitrile, PCl_5 (1.1-2.0 equiv), anhydrous 1,2-dichloroethane (1 equiv), and a magnetic stir bar. The flask was then equipped with a reflux condenser and a $CaCl_2$ drying tube. The reaction mixture was heated to 80 °C, and the reaction mixture was monitored by TLC. After the starting material had been consumed, the reaction mixture was cooled to room temperature and poured into ice (3 g/mmol of substrate). Dichloromethane (30 mL) was added, and then the organic layer was separated, dried over Na_2SO_4, filtered, and concentrated in vacuo. The residue was purified by flash column chromatography on silica gel (hexanes/dichloromethane = 10/1→5/1, unless otherwise noted).

2-Chloro-2-phenylpropanenitrile. The title compound was synthesized according to **GP-1** from 2-phenylpropanenitrile (3.28 g, 25.0 mmol), PCl_5 (6.25 g, 30.0 mmol), and 1,2-dichloroethane (2.0 mL, 25 mmol). The product was purified by flash column chromatography on silica gel. 1.81 g (10.9 mmol, 44% yield). Colorless oil.

^{1}H NMR (500 MHz, $CDCl_3$) δ 7.68 (d, *J* = 7.8 Hz, 2H), 7.49 – 7.39 (m, 3H), 2.29 (s, 3H).

^{13}C NMR (126 MHz, $CDCl_3$) δ 138.3, 129.9, 129.2, 125.5, 119.4, 57.1, 33.0.

FT-IR (film): 3065, 3039, 2994, 2937, 2243, 1492, 1452, 1380, 1229, 1145, 1074, 1038, 785, 745, 694, 650 cm^{-1}.

HRMS (FI+) *m/z* $[M]^+$ calcd for $C_9H_8ClN^+$: 165.0340, found: 165.0337.

2-Chloro-2-phenylbutanenitrile. The title compound was synthesized according to **GP-1** from 2-phenylbutanenitrile (9.73 g, 67.0 mmol), PCl_5 (14.6 g, 70.0 mmol), and 1,2-dichloroethane (5.3 mL, 67 mmol). The product was purified by flash column chromatography on silica gel. 7.69 g (42.8 mmol, 64% yield). Colorless oil.

^{1}H NMR (500 MHz, $CDCl_3$) δ 7.64 (d, *J* = 7.3 Hz, 2H), 7.47 – 7.38 (m, 3H), 2.47 (dq, *J* = 14.5, 7.3 Hz, 1H), 2.38 (dq, *J* = 14.4, 7.3 Hz, 1H), 1.16 (t, *J* = 7.3 Hz, 3H).

^{13}C NMR (126 MHz, $CDCl_3$) δ 137.3, 129.8, 129.1, 125.9, 118.3, 63.4, 39.0, 10.4.

FT-IR (film): 3064, 2982, 2941, 2881, 2242, 1492, 1450, 1207, 1080, 1002, 955, 908, 833, 751, 694 cm^{-1}.

HRMS (FI+) *m/z* $[M]^+$ calcd for $C_{10}H_{10}ClN^+$: 179.0496, found: 179.0494.

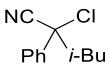

2-Chloro-4-methyl-2-phenylpentanenitrile. The title compound was synthesized according to **GP-1** from 2-phenylacetonitrile (5.86 g, 50.0 mmol), diisopropylamine (7.1 mL, 50 mmol), *n*-butyllithium (20.0 mL of 2.5 M solution, 50.0 mmol), 1-bromo-2-methylpropane (6.0 mL, 55 mmol), and THF (120 mL) for the first step, and from the

intermediate (53.1 mmol), PCl_5 (16.2 g, 78 mmol), and 1,2-dichloroethane (10 mL, 120 mmol) for the second step. The product was purified by flash column chromatography on silica gel. 3.86 g (18.6 mmol, 18% yield over 2 steps). Colorless oil.

^{1}H NMR (500 MHz, $CDCl_3$) δ 7.66 (d, *J* = 7.1 Hz, 2H), 7.48 – 7.37 (m, 3H), 2.39 (dd, *J* = 14.4, 6.2 Hz, 1H), 2.32 (dd, *J* = 14.4, 5.9 Hz, 1H), 1.91 – 1.78 (m, 1H), 1.05 (d, *J* = 6.7 Hz, 3H), 0.86 (d, *J* = 6.7 Hz, 3H).

^{13}C NMR (126 MHz, $CDCl_3$) δ 137.7, 129.8, 129.1, 126.0, 118.8, 61.6, 53.6, 26.6, 23.40, 23.37.

FT-IR (film): 3065, 2962, 2874, 2242, 1492, 1469, 1450, 1390, 1370, 1199, 754, 697 cm^{-1}.

HRMS (FI+) *m/z* $[M]^+$ calcd for $C_{12}H_{14}ClN^+$: 207.0809, found: 207.0808.

2-Chloro-2,3-diphenylpropanenitrile. The title compound was synthesized according to **GP-1** from 2-phenylacetonitrile (4.69 g, 40.0 mmol), diisopropylamine (5.7 mL, 40 mmol), *n*-butyllithium (16.0 mL of 2.5 M solution, 40.0 mmol), benzyl bromide (5.2 mL, 44 mmol), and THF (100 mL) for the first step, and from the intermediate (10.0 mmol), PCl_5 (3.33 g, 16.0 mmol), and 1,2-dichloroethane (2.0 mL, 24 mmol) for the second step. The product was purified by flash column chromatography on silica gel. 1.15 g (4.77 mmol, 38% yield over 2 steps). Pale-yellow solid.

^{1}H NMR (500 MHz, $CDCl_3$) δ 7.59 – 7.52 (m, 2H), 7.44 – 7.38 (m, 3H), 7.27 (dt, *J* = 14.4, 7.0 Hz, 3H), 7.06 (d, *J* = 7.2 Hz, 2H), 3.68 (d, *J* = 13.7 Hz, 1H), 3.58 (d, *J* = 13.7 Hz, 1H).

^{13}C NMR (126 MHz, $CDCl_3$) δ 136.7, 132.9, 130.9, 129.8, 128.9, 128.4, 128.3, 126.4, 118.0, 62.6, 51.7.

FT-IR (film): 3065, 3033, 2934, 2243, 1497, 1455, 1450, 1253, 1079, 1031, 764, 748, 699, 629 cm^{-1}.

HRMS (FI+) *m/z* $[M]^+$ calcd for $C_{15}H_{12}ClN^+$: 241.0653, found: 241.0626.

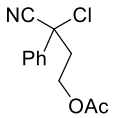

3-Chloro-3-cyano-3-phenylpropyl acetate. The title compound was synthesized according to **GP-1** from 3-cyano-3-phenylpropyl acetate[45] (2.04 g, 10.00 mmol), PCl_5 (2.28 g, 23.4 mmol), and 1,2-dichloroethane (6.0 mL, 72 mmol). The product was purified by flash column chromatography on silica gel (hexanes/EtOAc = 30/1→20/1). 721 mg (3.03 mmol, 30% yield). Pale-yellow oil.

^{1}H NMR (500 MHz, $CDCl_3$) δ 7.65 (d, *J* = 7.1 Hz, 2H), 7.45 (q, *J* = 8.5, 7.5 Hz, 3H), 4.31 (dt, *J* = 12.5, 6.4 Hz, 1H), 4.19 (dt, *J* = 12.0, 6.3 Hz, 1H), 2.80 (dt, *J* = 14.5, 6.2 Hz, 1H), 2.73 (dt, *J* = 14.7, 6.4 Hz, 1H), 2.00 (s, 3H).

^{13}C NMR (126 MHz, $CDCl_3$) δ 170.8, 136.6, 130.1, 129.3, 125.9, 117.9, 60.1, 59.5, 43.7, 20.7.

FT-IR (film): 3066, 2961, 2903, 2245, 1745, 1493, 1451, 1367, 1230, 1052, 830, 752, 696 cm^{-1}.

HRMS (FI+) *m/z* $[M]^+$ calcd for $C_{12}H_{12}ClNO_2^+$: 237.0551, found: 237.0539.

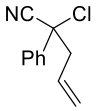

2-Chloro-2-phenylpent-4-enenitrile. The title compound was synthesized according to **GP-1** from 2-phenylacetonitrile (5.86 g, 50.0 mmol), diisopropylamine (7.1 mL, 50 mmol), *n*-butyllithium (20.0 mL of 2.5 M solution, 50.0 mmol), allyl bromide (4.8 mL, 55 mmol), and THF (120 mL) for the first step, and from the intermediate (19.1 mmol), PCl_5 (5.16 g, 24.8 mmol), and 1,2-dichloroethane (10 mL, 120 mmol) for the second step. The product was purified by flash column chromatography on silica gel. 1.00 g (5.22 mmol, 27% yield over 2 steps). Colorless oil.

^{1}H NMR (500 MHz, $CDCl_3$) δ 7.69 – 7.60 (m, 2H), 7.51 – 7.37 (m, 3H), 5.74 (ddt, *J* = 17.1, 10.3, 7.1 Hz, 1H), 5.35 – 5.23 (m, 2H), 3.15 (dd, *J* = 14.2, 7.3 Hz, 1H), 3.08 (dd, *J* = 14.2, 6.9 Hz, 1H).

^{13}C NMR (126 MHz, $CDCl_3$) δ 136.9, 129.94, 129.91, 129.1, 126.0, 122.3, 118.0, 61.5, 49.4.

FT-IR (film): 3085, 3067, 2985, 2918, 2244, 1491, 1450, 1290, 1265, 1191, 993, 933, 820, 758, 715, 694 cm^{-1}.

HRMS (FI+) *m/z* $[M]^+$ calcd for $C_{11}H_{10}ClN^+$: 191.0496, found: 191.0495.

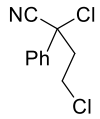

2,4-Dichloro-2-phenylbutanenitrile. The title compound was synthesized according to a modified **GP-1** from 4-hydroxy-2-phenylbutanenitrile[4] (1.00 g, 6.20 mmol), PCl_5 (2.71 g, 13.0 mmol), and 1,2-dichloroethane (4.0 mL, 76 mmol). An oven-dried 100 mL round-bottom flask (equipped with a reflux condenser with a $CaCl_2$-filled drying tube) was charged with 4-hydroxy-2-phenylbutanenitrile, PCl_5, anhydrous 1,2-dichloroethane, and a magnetic stir bar. The reaction mixture was stirred at room temperature for 30 min, and then it was heated to 80 °C. After full consumption of the starting material (monitored by TLC), the reaction mixture was cooled to room temperature and poured into ice (10 g). Dichloromethane (30 mL) was added, and then the organic layer was separated, dried over Na_2SO_4, filtered, and concentrated in vacuo. The residue was purified by flash column chromatography on silica gel (hexane/dichloromethane = 10/1→5/1). 821 mg (5.52 mmol, 62% yield). Colorless oil.

^{1}H NMR (500 MHz, $CDCl_3$) δ 7.65 (d, *J* = 7.3 Hz, 2H), 7.51 – 7.42 (m, 3H), 3.72 (td, *J* = 10.9, 5.2 Hz, 1H), 3.60 (td, *J* = 10.9, 5.1 Hz, 1H), 2.90 (ddd, *J* = 14.3, 10.8, 5.2 Hz, 1H), 2.79 (ddd, *J* = 14.4, 10.7, 5.1 Hz, 1H).

^{13}C NMR (126 MHz, $CDCl_3$) δ 136.2, 130.4, 129.5, 125.8, 117.4, 59.8, 47.4, 38.8.

FT-IR (film): 3065, 3040, 2967, 2245, 1491, 1450, 1339, 1261, 1182, 837, 758, 694, 672, 652 cm^{-1}.

HRMS (FI+) *m/z* $[M]^+$ calcd for $C_{10}H_9Cl_2N^+$: 213.0107, found: 213.0104.

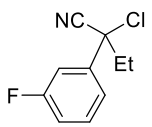

2-Chloro-2-(3-fluorophenyl)butanenitrile. The title compound was synthesized according to **GP-1** from 2-(3-fluorophenyl)acetonitrile (4.73 g, 35.0 mmol),

diisopropylamine (5.3 mL, 38 mmol), *n*-butyllithium (14.4 mL of 2.5 M solution, 36.0 mmol), iodoethane (3.1 mL, 38 mmol), and THF (70 mL) for the first step, and from the intermediate (9.20 mmol), PCl_5 (2.10 g, 10.1 mmol), and 1,2-dichloroethane (2.2 mL, 28 mmol) for the second step. The product was purified by flash column chromatography on silica gel. 842 mg (4.26 mmol, 25% yield over 2 steps). Colorless oil.

^{1}H NMR (500 MHz, $CDCl_3$) δ 7.47 – 7.38 (m, 2H), 7.35 (d, *J* = 9.8 Hz, 1H), 7.16 – 7.08 (m, 1H), 2.45 (dq, *J* = 14.5, 7.3 Hz, 1H), 2.36 (dq, *J* = 14.4, 7.2 Hz, 1H), 1.16 (t, *J* = 7.3 Hz, 3H).

^{13}C NMR (126 MHz, $CDCl_3$) δ 162.8 (d, *J* = 248.4 Hz), 139.6 (d, *J* = 7.3 Hz), 130.7 (d, *J* = 8.2 Hz), 121.6 (d, *J* = 3.1 Hz), 117.7, 116.8 (d, *J* = 21.1 Hz), 113.4 (d, *J* = 24.4 Hz), 62.4, 38.9, 10.2.

^{19}F NMR (376 MHz, $CDCl_3$) δ –110.7.

FT-IR (film): 3072, 2983, 2942, 2883, 2245, 1614, 1594, 1490, 1446, 1386, 1254, 1164, 859, 809, 785, 689 cm^{-1}.

HRMS (FI+) *m/z* $[M]^+$ calcd for $C_{10}H_9ClFN^+$: 197.0402, found: 197.0400.

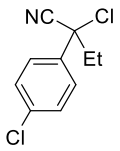

2-Chloro-2-(4-chlorophenyl)butanenitrile. The title compound was synthesized according to **GP-1** from 2-(4-chlorophenyl)acetonitrile (7.58 g, 50.0 mmol), diisopropylamine (7.1 mL, 50 mmol), *n*-butyllithium (31.3 mL of 1.6 M solution, 50.1 mmol), iodoethane (4.8 mL, 60 mmol), and THF (120 mL) for the first step, and from the intermediate (14.0 mmol), PCl_5 (4.35 g, 20.9 mmol), and 1,2-dichloroethane (2.4 mL, 30 mmol) for the second step. The product was purified by flash column chromatography on silica gel. 1.59 g (7.42 mmol, 37% yield over 2 steps). Colorless oil.

^{1}H NMR (500 MHz, $CDCl_3$) δ 7.57 (d, *J* = 8.6 Hz, 2H), 7.42 (d, *J* = 8.6 Hz, 2H), 2.45 (dq, *J* = 14.5, 7.3 Hz, 1H), 2.35 (dq, *J* = 14.4, 7.2 Hz, 1H), 1.15 (t, *J* = 7.3 Hz, 3H).

^{13}C NMR (126 MHz, $CDCl_3$) δ 135.95, 135.88, 129.4, 127.4, 117.9, 62.6, 39.0, 10.3.

FT-IR (film): 2982, 2941, 2882, 2242, 1596, 1493, 1457, 1403, 1208, 1097, 1015, 917, 848, 815, 764, 722 cm^{-1}.

HRMS (FI+) *m/z* $[M]^+$ calcd for $C_{10}H_9Cl_2N^+$: 213.0107, found: 213.0104.

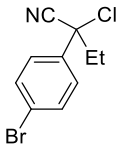

2-Chloro-2-(4-bromophenyl)butanenitrile. The title compound was synthesized according to **GP-1** from 2-(4-bromophenyl)acetonitrile (5.90 g, 30.0 mmol), diisopropylamine (5.1 mL, 36 mmol), *n*-butyllithium (13.2 mL of 2.5 M solution, 33.0 mmol), iodoethane (2.9 mL, 36 mmol), and THF (80 mL) for the first step, and from the intermediate (5.2 mmol), PCl_5 (4.35 g, 5.77 mmol), and 1,2-dichloroethane (2.5 mL, 30 mmol) for the second step. The product was purified by flash column chromatography on silica gel. 843 mg (3.26 mmol, 32% yield over 2 steps). Colorless oil.

^1H NMR (500 MHz, $CDCl_3$) δ 7.58 (d, *J* = 8.5 Hz, 2H), 7.50 (d, *J* = 8.6 Hz, 2H), 2.44 (dq, *J* = 14.5, 7.3 Hz, 1H), 2.34 (dq, *J* = 14.4, 7.2 Hz, 1H), 1.15 (t, *J* = 7.3 Hz, 3H).

^{13}C NMR (126 MHz, $CDCl_3$) δ 136.4, 132.3, 127.7, 124.1, 117.8, 62.7, 38.9, 10.3.

FT-IR (film): 2981, 2941, 2881, 2243, 1589, 1490, 1457, 1399, 1208, 1076, 1011, 916, 845, 813 cm^{-1}.

HRMS (FI+) *m/z* $[M]^+$ calcd for $C_{10}H_9BrClN^+$: 256.9601, found: 256.9591.

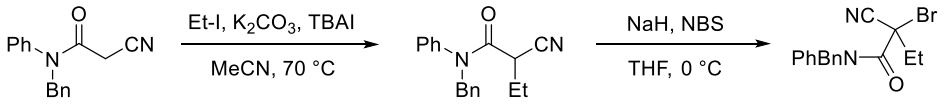

***N*-Benzyl-2-bromo-2-cyano-*N*-phenylbutanamide.** A 250 mL round-bottom flask charged with a magnetic stir bar, *N*-benzyl-2-cyano-*N*-phenylacetamide[46] (3.30 g, 13.2 mmol), K_2CO_3 (1.83 g, 13.2 mmol), tetrabutylammonium iodide (851 mg, 2.64 mmol), and acetonitrile (37 mL) was capped with a rubber septum. Iodoethane (1.2 mL, 15 mmol) was added, and a nitrogen-filled balloon was attached. The reaction mixture was heated to 70 °C and stirred for 24 h. Next, the solid was removed by filtration, and the filtrate was concentrated in vacuo. *N*-benzyl-2-cyano-*N*-phenylbutanamide was purified by flash

column chromatography on silica gel (10% EtOAc/hexane). 2.65 g (9.52 mmol, 72% yield). White solid.

Next, an oven-dried 100 mL round-bottom flask charged with *N*-benzyl-2-cyano-*N*-phenylbutanamide (1.05 g, 3.77 mmol) was capped with a rubber septum and placed under a nitrogen atmosphere by evacuating and backfilling the flask (three cycles). Anhydrous THF (18 mL) was added, and the resulting solution was cooled to 0 °C. Sodium hydride (158 mg, 3.96 mmol, 60% dispersion in mineral oil) was added under a gentle flow of nitrogen, and the reaction mixture was stirred for 30 min. *N*-Bromosuccinimide (805 mg, 4.15 mmol) was added, and the reaction mixture was stirred at 0 °C for 2 h. Then, the reaction was quenched by the addition of water (20 mL). Et_2O (20 mL) was added, and the organic layer was separated. The aqueous layer was extracted with Et_2O (20 mL), and the combined organic layer was dried over Na_2SO_4, filtered, and concentrated in vacuo. The residue was purified by flash column chromatography on silica gel (hexanes/EtOAc = 20/1→10/1). 1.08 g (3.02 mmol, 58% yield over 2 steps). White solid.

^{1}H NMR (500 MHz, $CDCl_3$) δ 7.44 (t, *J* = 7.0 Hz, 1H), 7.38 (s, 2H), 7.32 – 7.26 (m, 4H), 7.25 – 7.12 (m, 3H), 5.11 (d, *J* = 14.0 Hz, 1H), 4.75 (d, *J* = 14.0 Hz, 1H), 2.62 (dq, *J* = 14.2, 7.1 Hz, 1H), 2.39 (dq, *J* = 14.4, 7.3 Hz, 1H), 1.14 (t, *J* = 7.2 Hz, 3H).

^{13}C NMR (126 MHz, $CDCl_3$) δ 162.3, 139.6, 136.0, 130.1, 129.8, 129.4, 129.2, 128.7, 128.1, 115.5, 56.8, 43.6, 36.6, 11.0.

FT-IR (film): 3064, 3031, 2977, 2939, 2230, 1663, 1595, 1496, 1456, 1394, 1260, 1157, 1080, 1014, 690 cm^{-1}.

HRMS (ESI+) *m/z* $[M+H]^+$ calcd for $C_{18}H_{18}BrN_2O^+$: 357.0597, found: 357.0623.

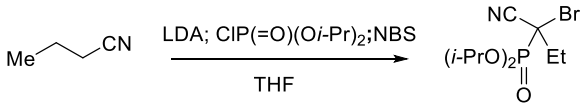

Diisopropyl (1-bromo-1-cyanopropyl)phosphonate. The title compound was synthesized according to a modified literature procedure.[47] An oven-dried 250 mL round-bottom flask charged with a magnetic stir bar and capped with a rubber septum was placed under a nitrogen atmosphere by evacuating and backfilling the flask (three cycles). Anhydrous THF (40 mL) and anhydrous diisopropylamine (6.7 mL, 48 mmol) were added,

and the mixture was cooled to –78 °C. A solution of *n*-butyllithium (18.3 mL, 45.8 mmol, 2.5 M solution in hexane) was slowly added into the flask, and then the reaction mixture was stirred at –78 °C for 15 min. Next, butyronitrile (1.44 g, 20.8 mmol) was added dropwise into the flask over 2 min, and the resulting mixture was stirred at –78 °C for 40 min. Then, a solution of diisopropyl chlorophosphate (4.81 g, 24.0 mmol) in 5 mL of THF was added over 2 min to the reaction mixture. The reaction mixture was stirred at –78 °C for 30 min, and then it was warmed to 0 °C. *N*-Bromosuccinimide (4.27 g, 24.0 mmol) was added, and the reaction mixture was stirred for 2 h. Next, the reaction was quenched with 20 mL of water. Et_2O (20 mL) was added to the mixture, and the organic layer was separated. The aqueous layer was extracted with Et_2O (20 mL), and the combined organic layer was dried over Na_2SO_4, filtered, and concentrated in vacuo. The residue was purified by flash column chromatography on silica gel (hexanes/EtOAc = 10/1). 4.37 g (14.0 mmol, 70% yield). Pale-brown oil.

^{1}H NMR (500 MHz, $CDCl_3$) δ 5.01 – 4.83 (m, 2H), 2.30 (dp, *J* = 14.2, 7.1 Hz, 1H), 2.17 (dp, *J* = 14.8, 7.4 Hz, 1H), 1.48 – 1.37 (m, 12H), 1.30 (t, *J* = 7.2 Hz, 3H).

^{13}C NMR (126 MHz, $CDCl_3$) δ 116.0 (d, *J* = 3.9 Hz), 75.6 (d, *J* = 7.4 Hz), 74.9 (d, *J* = 7.6 Hz), 43.3 (d, *J* = 159.7 Hz), 31.2 (d, *J* = 2.0 Hz), 24.4 (d, *J* = 2.8 Hz), 24.1 (d, *J* = 3.6 Hz), 23.8 (d, *J* = 5.5 Hz), 23.6 (d, *J* = 6.5 Hz), 10.7 (d, *J* = 9.1 Hz).

^{31}P NMR (162 MHz, $CDCl_3$) δ 9.31.

FT-IR (film): 2983, 2940, 2882, 2235, 1725, 1457, 1388, 1377, 1268, 1180, 1144, 1102, 988, 826, 766, 730 cm^{-1}.

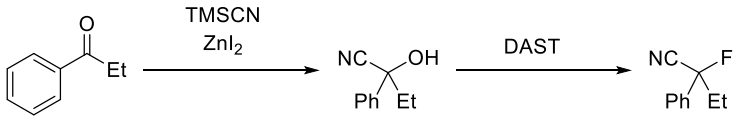

2-Fluoro-2-phenylbutanenitrile. An oven-dried 250 mL round-bottom flask charged with a magnetic stir bar and capped with a rubber septum was placed under a nitrogen atmosphere by evacuating and backfilling the flask (three cycles). ZnI_2 (3.86 g, 11.0 mmol) and anhydrous dichloromethane (50 mL) were added, and a nitrogen-filled balloon was attached. The reaction mixture was cooled to 0 °C, and propiophenone (1.46 mL, 11.0 mmol) was added. TMSCN (3.15 mL, 22.0 mmol) was carefully added dropwise, and the

reaction mixture was warmed to room temperature and stirred overnight. A saturated aqueous solution of $NaHCO_3$ (50 mL) was added, and the mixture was filtered through a short plug of Celite™, washing with dichloromethane (20 mL). The water layer was extracted with dichloromethane (2 x 25 mL), and the combined organic layer was dried over Na_2SO_4, filtered, and concentrated in vacuo. To the residue was added 30 mL of EtOH and 30 mL of 2 N HCl (aq), and the resulting mixture was stirred at room temperature for 3 h. Deionized water (50 mL) and dichloromethane (50 mL) were added, and then the aqueous layer was extracted with dichloromethane (2 x 30 mL). The combined organic layer was dried over Na_2SO_4, filtered, and concentrated in vacuo to afford the cyanohydrin, which was used without further purification. 1.57 g (9.74 mmol, 89% yield).

An oven-dried 50 mL round-bottom flask charged with a magnetic stir bar and capped with a rubber septum was placed under a nitrogen atmosphere by evacuating and backfilling the flask (three cycles). The cyanohydrin (967 mg, 6.00 mmol) and anhydrous dichloromethane (8 mL) were added, and a nitrogen-filled balloon was attached. The reaction mixture was cooled to 0 °C, and then DAST (910 μL, 6.9 mmol) was added dropwise over 2 min. The reaction mixture was stirred for 90 min, and then a saturated aqueous solution of $NaHCO_3$ (10 mL) was carefully added at 0 °C. The reaction mixture was diluted with water (10 mL), and the water layer was extracted with dichloromethane (2 x 10 mL). The combined organic layer was dried over Na_2SO_4, filtered, and concentrated in vacuo. The product was purified by column chromatography (hexanes/dichloromethane = 8/1). 825 mg (5.06 mmol, 84% yield). Colorless oil.

^{1}H NMR (500 MHz, $CDCl_3$) δ 7.54 – 7.48 (m, 2H), 7.48 – 7.41 (m, 3H), 2.36 – 2.14 (m, 2H), 1.14 (t, J = 7.4 Hz, 3H).

^{13}C NMR (126 MHz, $CDCl_3$) δ 136.2 (d, J = 22.9 Hz), 130.0 (d, J = 1.8 Hz), 129.0, 124.8 (d, J = 5.9 Hz), 117.4 (d, J = 34.1 Hz), 92.8 (d, J = 183.9 Hz), 35.2 (d, J = 25.9 Hz), 8.3 (d, J = 4.7 Hz).

^{19}F NMR (376 MHz, $CDCl_3$) δ –148.2.

FT-IR (film): 3067, 3037, 2982, 2944, 2886, 2247, 1494, 1452, 1300, 1229, 1068, 1008, 973, 760, 697 cm^{-1}.

HRMS (FI+) *m/z* $[M]^+$ calcd for $C_{10}H_{10}FN^+$: 163.0792, found: 163.0792.

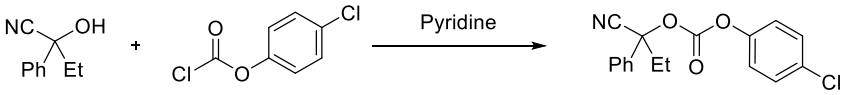

4-Chlorophenyl (1-cyano-1-phenylpropyl) carbonate. An oven-dried 50 mL round-bottom flask charged with a magnetic stir bar and capped with a rubber septum was placed under a nitrogen atmosphere by evacuating and backfilling the flask (three cycles). The cyanohydrin (1.61 g, 10.0 mmol) and dichloromethane 10 mL were added, and a nitrogen-filled balloon was attached. The reaction mixture was cooled to 0 °C, and 4-chlorophenyl chloroformate (2.87 g, 15.0 mmol) and pyridine (2.4 mL, 30 mmol) were sequentially added. The reaction mixture was warmed to room temperature and stirred overnight. Next, water was added (5 mL), and then the water layer was extracted with dichloromethane (5 mL x 2). The combined organic layer was dried over Na_2SO_4, filtered, and concentrated in vacuo. The product was purified by column chromatography (hexanes/EtOAc = 40/1). 2.90 g (9.18 mmol, 92% yield). Colorless oil.

^{1}H NMR (500 MHz, $CDCl_3$) δ 7.57 (d, *J* = 7.3 Hz, 2H), 7.49 – 7.38 (m, 3H), 7.30 (d, *J* = 8.8 Hz, 2H), 7.07 (d, *J* = 8.8 Hz, 2H), 2.43 (dq, *J* = 14.5, 7.3 Hz, 1H), 2.20 (dq, *J* = 14.7, 7.4 Hz, 1H), 1.12 (t, *J* = 7.4 Hz, 3H).

^{13}C NMR (126 MHz, $CDCl_3$) δ 150.6, 149.2, 136.1, 131.9, 129.8, 129.7, 129.2, 125.0, 122.2, 116.7, 81.5, 36.0, 8.7.

FT-IR (film): 3066, 2982, 2942, 2884, 2272, 1777, 1488, 1432, 1247, 1090, 1014, 829, 761, 698 cm^{-1}.

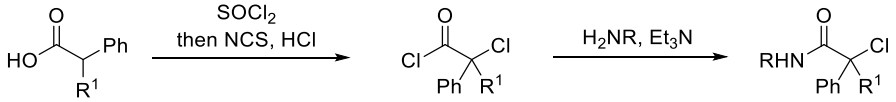

General Procedure 2 (GP-2): Preparation of α-chloroamides. A 100 mL three-neck round-bottom flask was charged with a magnetic stir bar, the carboxylic acid, and $SOCl_2$ (5-7 equiv), and then it was fitted with a reflux condenser to which a $CaCl_2$ drying tube was attached. The resulting solution was heated to reflux for 30 min with vigorous stirring, and then it was cooled to room temperature. *N*-Chlorosuccinimide (2.5 equiv), $SOCl_2$ (1 equiv), and HCl (35% in H_2O; 4 drops) were carefully added. The resulting mixture was heated to

reflux for 2.5 h, and then it was cooled to room temperature. Next, with vigorous stirring of the reaction mixture, 20 mL of anhydrous hexane/Et_2O (1:2) was slowly added, resulting in a black precipitate. The precipitate was removed by filtration, and the volatiles were removed by evaporation. The resulting brown liquid was purified by distillation or directly used without further purification.

Next, an oven-dried 100 mL round-bottom flask capped with a rubber septum was placed under a nitrogen atmosphere by evacuating and backfilling the flask (three cycles). The flask was charged with a magnetic stir bar, anhydrous dichloromethane (0.13-0.16 M), and the 2-alkyl-2-chloroalkanoyl chloride, and then it was cooled to 0 °C. The amine (1.05 equiv) and triethylamine (1.2 equiv) were sequentially added dropwise over 5 min. The reaction mixture was stirred at 0 °C for 2 h, and then it was warmed to room temperature. The reaction mixture was acidified with 50 mL of 0.2 N HCl, and the organic layer was separated. The aqueous layer was extracted with 20 mL of dichloromethane, and the combined organic layer was dried over Na_2SO_4, filtered, and concentrated in vacuo. The residue was purified by flash column chromatography on silica gel (hexanes/EtOAc = 40/1).

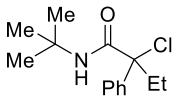

***N*-(*tert*-butyl)-2-chloro-2-phenylbutanamide.** The title compound was synthesized according to **GP-2** from 2-phenylbutanoic acid (16.4 g, 100 mmol), $SOCl_2$ (29 mL, 500 mmol), and NCS (33.4 g, 250 mmol) for the first step (18.2 g, 84% yield), and from the intermediate (1.09 g, 5.00 mmol), *t*-butyl amine (1.1 mL, 10 mmol), triethylamine (830 μL, 6.0 mmol), and dichloromethane (40 mL) for the second step. The product was purified by flash column chromatography on silica gel. 1.17 g (3.89 mmol, 57% yield over 2 steps). White solid.

^{1}H NMR (500 MHz, $CDCl_3$) δ 7.52 (d, *J* = 7.8 Hz, 2H), 7.35 (t, *J* = 7.5 Hz, 2H), 7.29 (t, *J* = 7.2 Hz, 1H), 6.74 (s, 1H), 2.59 (dq, *J* = 14.2, 7.1 Hz, 1H), 2.30 (dq, *J* = 14.3, 7.2 Hz, 1H), 1.39 (s, 9H), 1.06 (t, *J* = 7.1 Hz, 3H).

^{13}C NMR (126 MHz, $CDCl_3$) δ 168.9, 141.8, 128.5, 128.3, 126.4, 79.3, 52.0, 34.7, 28.5, 9.6.

FT-IR (film): 3423, 3061, 2972, 2938, 2882, 1678, 1514, 1455, 1393, 1366, 1269, 1226, 1085, 1034, 854, 826, 756, 736, 696 cm^{-1}.

HRMS (ESI+) *m/z* $[M+H]^+$ calcd for $C_{14}H_{21}ClNO^+$: 254.1306, found: 254.1328.

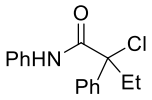

2-Chloro-*N*,2-diphenylbutanamide. The title compound was synthesized according to **GP-2** from 2-phenylbutanoic acid (16.4 g, 100 mmol), $SOCl_2$ (29 mL, 500 mmol), and NCS (33.4 g, 250 mmol) for the first step, and from the intermediate (5.40 g, 25 mmol), aniline (2.4 mL, 26 mmol), triethylamine (4.2 mL, 30 mmol), and dichloromethane (150 mL) for the second step. The product was purified by flash column chromatography on silica gel and further purified by recrystallization (hexanes/dichloromethane). 4.17 g (15.2 mmol, 51% yield over 2 steps). White solid.

^{1}H NMR (500 MHz, $CDCl_3$) δ 8.42 (s, 1H), 7.60 (d, *J* = 7.9 Hz, 2H), 7.54 (d, *J* = 8.1 Hz, 2H), 7.41 – 7.30 (m, 5H), 7.14 (t, *J* = 7.4 Hz, 1H), 2.67 (dq, *J* = 14.3, 7.1 Hz, 1H), 2.43 (dq, *J* = 14.4, 7.2 Hz, 1H), 1.08 (t, *J* = 7.1 Hz, 3H).

^{13}C NMR (126 MHz, $CDCl_3$) δ 168.1, 140.5, 137.3, 129.2, 128.7, 128.6, 126.5, 125.1, 120.1, 79.6, 35.1, 9.6.

FT-IR (film): 3399, 3341, 3060, 2978, 2938, 1685, 1600, 1526, 1442, 1314, 1240, 1078, 753, 691 cm^{-1}.

HRMS (ESI+) *m/z* $[M+H]^+$ calcd for $C_{16}H_{17}ClNO^+$: 274.0993, found: 274.1016.

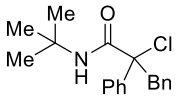

***N*-(*tert*-butyl)-2-chloro-2,3-diphenylpropanamide.** The title compound was synthesized according to a modified **GP-2**.[16] A 100 mL three-neck round-bottom flask was charged with a magnetic stir bar, 2,3-diphenylpropanoic acid (2.16 g, 9.54 mmol), and $SOCl_2$ (4.0 mL, 69 mmol), and then a reflux condenser with a $CaCl_2$ drying tube was

attached. The reaction mixture was heated to 76 °C for 30 min, and then it was cooled to room temperature. SO_2Cl_2 (7.7 mL, 95.4 mmol) was added, and the reaction mixture was heated to reflux for 24 h. The volatiles were distilled off, and the residue was transferred to an oven-dried 250 mL round-bottom flask charged with a magnetic stir bar and anhydrous dichloromethane (100 mL) under a nitrogen atmosphere. The mixture was cooled to 0 °C, and then *tert*-butyl amine (3.0 mL, 29 mmol) was added dropwise over 2 min. Next, the reaction mixture was stirred at 0 °C for 2 h. Then, the reaction mixture was acidified with 20 mL of 0.2 N HCl, and the organic layer was separated. The aqueous layer was extracted with 40 mL of dichloromethane, and the combined organic layer was dried over Na_2SO_4, filtered, and concentrated in vacuo. The residue was purified by flash column chromatography on silica gel (hexanes/dichloromethane = 3/1). The product was further purified by recrystallization (hexanes, 40 °C to 0 °C). 1.02 g (3.22 mmol, 34% yield over 2 steps). White solid.

^{1}H NMR (500 MHz, $CDCl_3$) δ 7.55 (d, *J* = 7.7 Hz, 2H), 7.36 (t, *J* = 7.3 Hz, 2H), 7.34 – 7.29 (m, 1H), 7.26 – 7.20 (m, 5H), 6.54 (s, 1H), 3.97 (d, *J* = 13.7 Hz, 1H), 3.47 (d, *J* = 13.7 Hz, 1H), 1.31 (s, 9H).

^{13}C NMR (126 MHz, $CDCl_3$) δ 168.3, 141.6, 135.7, 131.5, 128.5, 128.4, 127.8, 127.1, 126.7, 77.8, 52.0, 46.7, 28.4.

FT-IR (film): 3421, 3064, 3032, 2967, 2932, 1670, 1515, 1496, 1455, 1393, 1366, 1272, 1224, 700 cm^{-1}.

HRMS (ESI+) *m/z* $[M+H]^+$ calcd for $C_{19}H_{23}ClNO^+$: 316.1463, found: 316.1485.

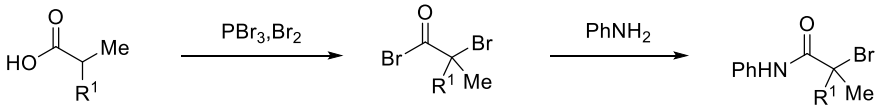

General Procedure 3 (GP-3): Preparation of α-bromoamides. The title compounds were synthesized according to a modified literature procedure.[48] A 100 mL two-neck round-bottom flask was charged with a magnetic stir bar, the carboxylic acid, and PBr_3 (0.4 equiv), and then one neck was capped with a rubber stopper and a reflux condenser with a $CaCl_2$ drying tube (connected to a Tygon® tube submerged in a saturated aqueous solution of sodium thiosulfate hydrate) was attached to the other neck. The reaction mixture was

warmed to 60 °C and stirred for 3 h or until all of the acid was consumed. The reaction mixture was cooled to room temperature, and bromine (1.4 equiv) was carefully added dropwise (vigorous gas evolution was observed). The heating bath was warmed to 100 °C for 3 h. Next, additional bromine (1.4 equiv) was added, and the reaction mixture was stirred for 2 h to complete the reaction. The reaction mixture was cooled to room temperature, and cyclohexene (2.5 equiv) was slowly added to quench the residual bromine. The volatiles were distilled off, and the residue was transferred to an oven-dried round-bottom flask charged with a magnetic stir bar and anhydrous dichloromethane (0.16 M, based on the carboxylic acid) under a nitrogen atmosphere. The mixture was cooled to 0 °C, and aniline (3 equiv) was added dropwise over 2 min. The reaction mixture was stirred at 0 °C for 2 h, and then it was acidified with 20 mL of 0.2 N HCl. The organic layer was separated, and the aqueous layer was extracted with 40 mL of dichloromethane. The combined organic layer was dried over Na_2SO_4, filtered, and concentrated in vacuo. The residue was purified by flash column chromatography on silica gel (hexanes/EtOAc = 100/1→50/1) or recrystallized from pentane/EtOAc.

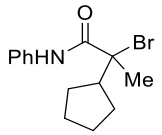

2-Bromo-2-cyclopentyl-*N*-phenylpropanamide. The title compound was synthesized according to **GP-3** from 2-cyclopentylpropanoic acid (960 mg, 6.80 mmol), PBr_3 (320 μL, 3.4 mmol), bromine (990 μL, 19 mmol), cyclohexene (1.7 mL, 17 mmol), aniline (1.9 mL, 20 mmol), and dichloromethane (45 mL). 1.13 g (3.81 mmol, 56% yield over 2 steps). Pale-brown solid.

^{1}H NMR (500 MHz, $CDCl_3$) δ 8.68 (s, 1H), 7.54 (d, *J* = 7.9 Hz, 2H), 7.35 (t, *J* = 7.9 Hz, 2H), 7.15 (t, *J* = 7.4 Hz, 1H), 2.51 (p, *J* = 8.4 Hz, 1H), 2.02 (s, 3H), 1.91 – 1.75 (m, 2H), 1.75 – 1.45 (m, 6H).

^{13}C NMR (126 MHz, $CDCl_3$) δ 169.8, 137.5, 129.2, 125.0, 120.2, 77.5, 50.4, 30.04, 30.01, 29.1, 25.7, 25.7.

FT-IR (film): 3386, 3349, 2956, 2868, 1673, 1598, 1529, 1499, 1442, 1314, 1242, 1163, 1074, 1029, 755, 690 cm^{-1}.

HRMS (ESI+) *m/z* $[M+H]^+$ calcd for $C_{14}H_{19}BrNO^+$: 296.0645/298.0625, found: 296.0670/298.0651.

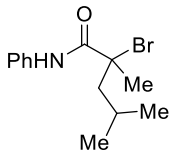

2-Bromo-2,4-dimethyl-*N*-phenylpentanamide. The title compound was synthesized according to **GP-3** from 2,4-dimethylpentanoic acid (5.20 g, 40.0 mmol), PBr_3 (1.5 mL, 16 mmol) bromine (2 x 2.9 mL, 112 mmol), cyclohexene (10.1 mL, 100 mmol), aniline (11.0 mL, 120 mmol), and dichloromethane (250 mL). The product was further purified by recrystallization (pentane/EtOAc). 7.56 g (26.6 mmol, 67% yield over 2 steps). White solid.

^{1}H NMR (500 MHz, $CDCl_3$) δ 8.64 (s, 1H), 7.54 (d, *J* = 8.0 Hz, 2H), 7.36 (t, *J* = 7.8 Hz, 2H), 7.16 (t, *J* = 7.4 Hz, 1H), 2.28 (dd, *J* = 14.3, 6.8 Hz, 1H), 2.05 (s, 3H), 2.00 (dd, *J* = 14.4, 4.5 Hz, 1H), 1.97 – 1.91 (m, 1H), 1.00 (d, *J* = 6.5 Hz, 3H), 0.94 (d, *J* = 6.5 Hz, 3H).

^{13}C NMR (126 MHz, $CDCl_3$) δ 169.6, 137.5, 129.2, 125.0, 120.1, 70.2, 52.3, 32.5, 27.3, 24.2, 22.9.

FT-IR (film): 3386, 3343, 2959, 2931, 2871, 1669, 1598, 1529, 1442, 1316, 1241, 1153, 854, 691 cm^{-1}.

HRMS (ESI+) *m/z* $[M+H]^+$ calcd for $C_{13}H_{19}BrNO^+$: 264.0958/266.0938, found: 264.0979/266.0959.

2.4.3. Enantioconvergent coupling reactions

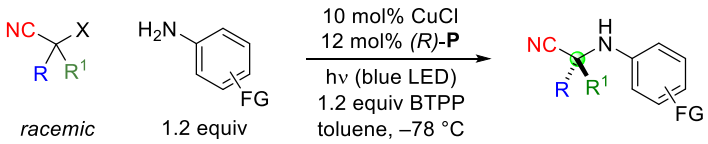

General Procedure 4 (GP-4). In the air, an oven-dried 20 mL vial equipped with a PTFE magnetic stir bar was charged with CuCl (8.0 mg, 0.080 mmol, white to off-white solid) and *(R)*-**P** (113 mg, 0.0960 mmol). The vial was capped with a PTFE-lined open top cap, and the joint was wrapped with electrical tape. The vial was evacuated/backfilled with nitrogen three times, using a 21G needle attached to a Schlenk line. Then, a nitrogen-filled balloon was attached, toluene (5 mL) and BTPP (290 μL, 0.960 mmol) were added using standard air-free technique by syringe, and the reaction mixture was stirred for 4 h (see **Note 1** below).

The aniline nucleophile (0.960 mmol) was weighed into an oven-dried 40 mL vial equipped with a PTFE magnetic stir bar. The vial was capped with a PTFE-lined open top cap, and the joint was wrapped with electrical tape. The vial was attached to a Schlenk line and evacuated/backfilled with nitrogen three times. A nitrogen-filled balloon was attached, and 5 mL of toluene was added. The catalyst solution was transferred to the vial containing the nucleophile. An additional 3 mL of toluene was used to wash the vial that had contained the catalyst, and the wash was added to the reaction vial. The reaction vial was submerged in a low-form hemispherical Dewar flask filled with pre-cooled methanol (–78 °C) and stirred for 10 min.

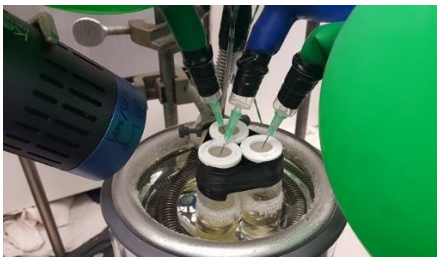

The electrophile (0.800 mmol) was weighed into a 4 mL vial, which was capped with a PTFE-lined open top cap. The vial was attached to a Schlenk line and evacuated/backfilled with nitrogen three times. A nitrogen-filled balloon was attached, and 1.5 mL of toluene was added. The resulting solution was transferred to the pre-cooled reaction vial. An

additional 1.5 mL of toluene was used to wash the vial that had contained the electrophile, and the wash was added to the reaction mixture. The reaction mixture was stirred for 5 min, the balloon was removed, and vacuum grease was applied to the PTFE cap to seal the needle puncture. Kessil® PR160-440 nm lamps (one lamp per reaction, 3-4 lamps per cooling bath) were installed 5 cm above the reaction vial, and the vial was irradiated for 12-48 h.

Work-up. The reaction was quenched by turning off the lamps. The reaction mixture was warmed to room temperature and opened to air. 2 mL of 30% NH_4OH (aq) and 2 mL of EtOAc were added, and the reaction mixture was vigorously stirred for 5 min, at which point the aqueous layer was blue (see **Note 2** below). The aqueous layer was extracted with EtOAc (2 x 3 mL), and the combined organic layer was passed through a short plug of silica gel with EtOAc washings (2 x 4 mL). The resulting filtrate was concentrated and purified by flash column chromatography.

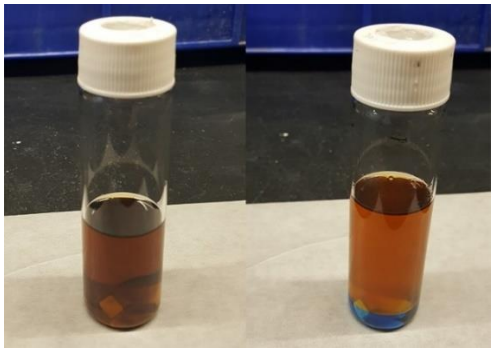

Left: immediately after irradiation and warming to room temperature.
Right: after the addition of NH_4OH and EtOAc and 5 min of stirring.

Note 1. In the presence of BTPP, we observe fast solubilization of CuCl in toluene, resulting in an apparently homogenous reaction mixture within 10 min. However, 4 h of stirring was necessary to obtain reproducible ee values with **GP-4**. If pre-made catalyst (**Cu$_A$**) is used (**GP-5** below), the 4 h of stirring can be omitted.

Note 2. The coupling products and **Cu$_A$** often have similar Rf values. Workup with NH_4OH results in the consumption of **Cu$_A$** and allows recovery of the ligand (if desired) and facile purification of the coupling product. This step is not required for the purification of substrates that have an Rf value significantly different from that of **Cu$_A$**.

General Procedure 5 (GP-5): Use of Cu$_A$ as a discrete catalyst. In the air, a 40 mL vial equipped with a PTFE stir bar was charged with **Cu$_A$** (synthesis: Section 2.4.10; 103 mg, 0.0800 mmol) and the nucleophile (0.960 mmol). The vial was capped with a PTFE-lined open top cap, and the joint was wrapped with electrical tape. The vial was evacuated/backfilled with nitrogen three times, using a 21G needle attached to a Schlenk line, and then a nitrogen-filled balloon was attached. Toluene (13 mL) and BTPP (290 μL, 0.960 mmol) were added, and the reaction mixture was stirred for 5 min. The remainder of the procedure is the same as **GP-4**.

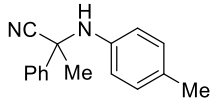

2-Phenyl-2-(*p*-tolylamino)propanenitrile. The title compound was prepared according to **GP-4** from 2-chloro-2-phenylpropanenitrile and *p*-toluidine with 12 h of reaction time. The product was purified by column chromatography on silica gel (hexanes/EtOAc/ dichloromethane = 25/1/1). Pale-yellow solid.

(R)-**P**: 112 mg, 59% yield, 89% ee; *(S)*-**P**: 113 mg, 60% yield, 88% ee.

HPLC analysis: The ee was determined via HPLC on a CHIRALPAK OD column (5% *i*-PrOH in hexane, 1 mL/min); retention times for compound obtained using *(R)*-**P**: 9.9 min (major), 14.6 min (minor).

^{1}H NMR (500 MHz, $CDCl_3$) δ 7.64 (d, *J* = 7.5 Hz, 2H), 7.41 (t, *J* = 7.4 Hz, 2H), 7.36 (t, *J* = 7.3 Hz, 1H), 6.94 (d, *J* = 8.3 Hz, 2H), 6.48 (d, *J* = 8.4 Hz, 2H), 4.19 (s, 1H), 2.22 (s, 3H), 1.94 (s, 3H).

^{13}C NMR (126 MHz, $CDCl_3$) δ 141.2, 140.2, 129.7, 129.5, 129.3, 128.7, 125.1, 116.2, 57.5, 33.4, 20.6.

FT-IR (film): 3383, 3026, 2989, 2917, 2865, 2230, 1618, 1518, 1448, 1303, 1258, 1219, 807, 759, 698 cm^{-1}.

HRMS (ESI+) *m/z* $[M+H]^+$ calcd for $C_{16}H_{17}N_2^+$: 237.1386, found: 237.1384.

$[\alpha]^{23}_D$ = –240 (*c* 1.0, $CHCl_3$); 89% ee, from *(R)*-**P**.

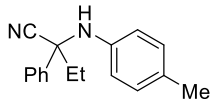

2-Phenyl-2-(*p*-tolylamino)butanenitrile. The title compound was prepared according to **GP-4** and **GP-5** from 2-chloro-2-phenylbutanenitrile and *p*-toluidine with 12 h of reaction time. The product was purified by column chromatography on silica gel (hexanes/EtOAc/ dichloromethane = 30/1/1). White solid.

From **GP-4**, *(R)*-**P**: 143 mg, 72% yield, 93% ee; *(S)*-**P**: 142 mg, 71% yield, 92% ee.

From **GP-5**, *(R)*-**P**: 143 mg, 72% yield, 93% ee.

HPLC analysis: The ee was determined via HPLC on a CHIRALPAK OD column (5% *i*-PrOH in hexane, 1 mL/min); retention times for compound obtained using *(R)*-**P**: 7.7 min (major), 11.3 min (minor).

^{1}H NMR (500 MHz, $CDCl_3$) δ 7.61 (d, *J* = 7.5 Hz, 2H), 7.41 (t, *J* = 7.4 Hz, 2H), 7.36 (t, *J* = 7.2 Hz, 1H), 6.92 (d, *J* = 8.4 Hz, 2H), 6.47 (d, *J* = 8.4 Hz, 2H), 4.22 (s, 1H), 2.24 – 2.16 (m, 4H), 2.09 (dq, *J* = 14.8, 7.4 Hz, 1H), 1.07 (t, *J* = 7.4 Hz, 3H).

^{13}C NMR (126 MHz, $CDCl_3$) δ 141.3, 138.6, 129.6, 129.3, 129.1, 128.6, 125.8, 120.2, 116.1, 62.5, 38.4, 20.5, 8.9.

FT-IR (film): 3387, 3026, 2975, 2924, 2231, 1620, 1522, 1449, 1318, 1305, 1254, 805, 757, 697 cm^{-1}.

HRMS (ESI+) *m/z* $[M+H]^+$ calcd for $C_{17}H_{19}N_2^+$: 251.1543, found: 251.1547.

$[\alpha]^{23}_D$ = –211 (*c* 1.0, $CHCl_3$); 93% ee, from *(R)*-**P**.

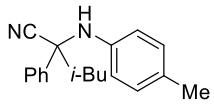

4-Methyl-2-phenyl-2-(*p*-tolylamino)pentanenitrile. The title compound was prepared according to **GP-4** from 2-chloro-4-methyl-2-phenylpentanenitrile and *p*-toluidine with 24 h of reaction time. The product was purified by column chromatography on silica gel (hexanes/EtOAc = 50/1). Pale-yellow solid.

(R)-**P**: 93 mg, 42% yield, 88% ee; *(S)*-**P**: 94 mg, 42% yield, 88% ee.

HPLC analysis: The ee was determined via HPLC on a CHIRALPAK OD column (5% *i*-PrOH in hexane, 1 mL/min); retention times for compound obtained using *(R)*-**P**: 5.8 min (major), 9.0 min (minor).

^{1}H NMR (500 MHz, $CDCl_3$) δ 7.62 (d, *J* = 7.9 Hz, 2H), 7.40 (t, *J* = 7.5 Hz, 2H), 7.35 (t, *J* = 7.2 Hz, 1H), 6.91 (d, *J* = 8.3 Hz, 2H), 6.44 (d, *J* = 8.3 Hz, 2H), 4.19 (s, 1H), 2.20 (s, 3H), 2.07 (dd, *J* = 13.9, 6.2 Hz, 1H), 2.00 (dd, *J* = 13.9, 5.8 Hz, 1H), 1.84 (dh, *J* = 12.9, 6.5 Hz, 1H), 1.07 (d, *J* = 6.7 Hz, 3H), 0.85 (d, *J* = 6.7 Hz, 3H).

^{13}C NMR (126 MHz, $CDCl_3$) δ 141.2, 139.3, 129.6, 129.4, 129.2, 128.6, 120.6, 116.3, 61.2, 53.5, 24.9, 23.9, 20.6.

FT-IR (film): 3373, 3022, 2956, 2927, 2873, 2244, 1617, 1521, 1448, 1304, 1252, 1189, 800, 754, 697 cm^{-1}.

HRMS (ESI+) *m/z* $[M+H]^+$ calcd for $C_{19}H_{23}N_2^+$: 279.1856, found: 279.1854.

$[\alpha]^{23}_D$ = –186 (*c* 1.0, $CHCl_3$); 88% ee, from *(R)*-**P**.

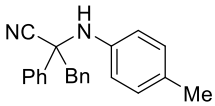

2,3-Diphenyl-2-(*p*-tolylamino)propanenitrile. The title compound was prepared according to **GP-4** from 2-chloro-2,3-diphenylpropanenitrile and *p*-toluidine with 14 h of reaction time. The product was purified by column chromatography on silica gel: column #1 (hexanes/EtOAc/dichloromethane = 35/1/3); column #2 (hexanes/toluene = 1/1). Pale-yellow solid.

(R)-**P**: 173 mg, 69% yield, 92% ee; *(S)*-**P**: 171 mg, 68% yield, 91% ee.

HPLC analysis: The ee was determined via HPLC on a CHIRALPAK OD column (5% *i*-PrOH in hexane, 1 mL/min); retention times for compound obtained using *(R)*-**P**: 9.7 min (major), 14.0 min (minor).

^{1}H NMR (500 MHz, $CDCl_3$) δ 7.58 (d, *J* = 7.4 Hz, 2H), 7.41 – 7.33 (m, 6H), 7.29 – 7.22 (m, 2H), 6.38 (d, *J* = 8.3 Hz, 2H), 4.28 (s, 1H), 3.35 (d, *J* = 13.5 Hz, 1H), 3.23 (d, *J* = 13.5 Hz, 1H), 2.18 (s, 3H).

^{13}C NMR (126 MHz, $CDCl_3$) δ 141.1, 138.9, 133.1, 130.7, 129.63, 129.57, 129.2, 129.0, 128.8, 128.4, 125.8, 119.9, 116.5, 62.1, 51.2, 20.6.

FT-IR (film): 3380, 3031, 2920, 2858, 2234, 1620, 1522, 1449, 1303, 1256, 805, 758, 702 cm^{-1}.

HRMS (ESI+) *m/z* $[M+H]^+$ calcd for $C_{22}H_{21}N_2^+$: 313.1699, found: 313.1708.

$[\alpha]^{23}_D$ = +224 (*c* 1.0, $CHCl_3$); 91% ee, from *(S)*-**P**.

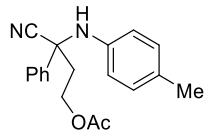

3-Cyano-3-phenyl-3-(*p*-tolylamino)propyl acetate. The title compound was prepared according to **GP-4** from 3-chloro-3-cyano-3-phenylpropyl acetate and *p*-toluidine with 24 h of reaction time. The product was purified by column chromatography on silica gel (hexanes/EtOAc = 10/1→5/1). Pale-yellow solid.

(R)-**P**: 167 mg, 67% yield, 91% ee; *(S)*-**P**: 163 mg, 66% yield, 91% ee.

HPLC analysis: The ee was determined via HPLC on a CHIRALPAK OD column (10% *i*-PrOH in hexane, 1 mL/min); retention times for compound obtained using *(R)*-**P**: 10.1 min (major), 14.1 min (minor).

^{1}H NMR (500 MHz, $CDCl_3$) δ 7.61 (d, *J* = 7.5 Hz, 2H), 7.41 (t, *J* = 7.3 Hz, 2H), 7.38 – 7.34 (m, 1H), 6.92 (d, *J* = 8.1 Hz, 2H), 6.44 (d, *J* = 8.4 Hz, 2H), 4.75 (s, 1H), 4.35 (dt, *J* = 11.4, 5.5 Hz, 1H), 4.25 (ddd, *J* = 12.4, 8.0, 5.0 Hz, 1H), 2.49 (ddd, *J* = 14.7, 8.0, 5.3 Hz, 1H), 2.37 (dt, *J* = 14.7, 5.4 Hz, 1H), 2.21 (s, 3H), 2.10 (s, 3H).

^{13}C NMR (126 MHz, $CDCl_3$) δ 170.6, 141.0, 138.4, 129.71, 129.69, 129.4, 129.0, 125.6, 119.6, 116.3, 60.8, 60.6, 43.2, 21.0, 20.6.

FT-IR (film): 3366, 3027, 2962, 2919, 2865, 2229, 1740, 1617, 1521, 1448, 1366, 1232, 1049, 809, 769, 701 cm^{-1}.

HRMS (ESI+) *m/z* $[M+H]^+$ calcd for $C_{19}H_{21}N_2O_2^+$: 309.1598, found: 309.1610.

$[\alpha]^{23}_D$ = +202 (*c* 1.0, $CHCl_3$); 91% ee, from *(S)*-**P**.

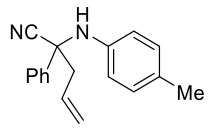

2-Phenyl-2-(*p*-tolylamino)pent-4-enenitrile. The title compound was prepared according to **GP-4** from 2-chloro-2-phenylpent-4-enenitrile and *p*-toluidine with 18 h of reaction time. The product was purified by column chromatography on silica gel (hexanes/EtOAc = 45/1). Pale-yellow solid.

(R)-**P**: 149 mg, 71% yield, 91% ee; *(S)*-**P**: 147 mg, 70% yield, 92% ee.

HPLC analysis: The ee was determined via HPLC on a CHIRALPAK OD column (5% *i*-PrOH in hexane, 1 mL/min); retention times for compound obtained using *(R)*-**P**: 6.4 min (major), 8.8 min (minor).

^{1}H NMR (500 MHz, $CDCl_3$) δ 7.62 (d, *J* = 7.7 Hz, 2H), 7.41 (t, *J* = 7.4 Hz, 2H), 7.36 (t, *J* = 7.2 Hz, 1H), 6.91 (d, *J* = 8.2 Hz, 2H), 6.43 (d, *J* = 8.2 Hz, 2H), 5.95 (dtd, *J* = 19.4, 9.7, 5.3 Hz, 1H), 5.45 – 5.34 (m, 2H), 4.32 (s, 1H), 2.89 (dd, *J* = 13.7, 5.1 Hz, 1H), 2.66 (dd, *J* = 13.9, 9.4 Hz, 1H), 2.20 (s, 3H).

^{13}C NMR (126 MHz, $CDCl_3$) δ 141.1, 139.0, 131.0, 129.7, 129.5, 129.3, 128.8, 125.6, 122.8, 119.9, 116.1, 60.3, 49.9, 20.6.

FT-IR (film): 3370, 3078, 3026, 2981, 2918, 2864, 2230, 1617, 1558, 1519, 1448, 1301, 995, 931, 808, 772, 700 cm^{-1}.

HRMS (ESI+) *m/z* $[M+H]^+$ calcd for $C_{18}H_{19}N_2^+$: 263.1543, found: 263.1545.

$[\alpha]^{23}_D$ = –245 (*c* 1.0, $CHCl_3$); 91% ee, from *(R)*-**P**.

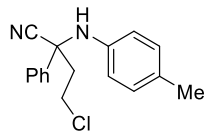

4-Chloro-2-phenyl-2-(*p*-tolylamino)butanenitrile. The title compound was prepared according to **GP-4** from 2,4-dichloro-2-phenylbutanenitrile and *p*-toluidine with 20 h of reaction time. The product was purified by column chromatography on silica gel (hexanes/EtOAc = 40/1). Pale-yellow solid.

(R)-**P**: 178 mg, 78% yield, 90% ee; *(S)*-**P**: 177 mg, 77% yield, 91% ee.

HPLC analysis: The ee was determined via HPLC on a CHIRALPAK OD column (5% *i*-PrOH in hexane, 1 mL/min); retention times for compound obtained using *(R)*-**P**: 11.6 min (major), 18.2 min (minor).

^{1}H NMR (500 MHz, $CDCl_3$) δ 7.60 (d, *J* = 7.5 Hz, 2H), 7.43 (t, *J* = 7.4 Hz, 2H), 7.39 (t, *J* = 7.1 Hz, 1H), 6.93 (d, *J* = 8.3 Hz, 2H), 6.46 (d, *J* = 8.3 Hz, 2H), 4.53 (s, 1H), 3.72 (ddd, *J* = 11.2, 8.7, 6.8 Hz, 1H), 3.50 (ddd, *J* = 11.3, 8.7, 5.4 Hz, 1H), 2.64 (ddd, *J* = 15.1, 8.5, 6.8 Hz, 1H), 2.55 (ddd, *J* = 14.1, 8.8, 5.5 Hz, 1H), 2.21 (s, 3H).

^{13}C NMR (126 MHz, $CDCl_3$) δ 140.7, 137.7, 130.1, 129.7, 129.5, 129.3, 125.6, 119.4, 116.6, 61.4, 46.6, 39.1, 20.6.

FT-IR (film): 3362, 3061, 3026, 2962, 2919, 2864, 2231, 1617, 1518, 1490, 1448, 1301, 1249, 809, 770, 699 cm^{-1}.

HRMS (ESI+) *m/z* $[M+H]^+$ calcd for $C_{17}H_{18}ClN_2^+$: 285.1154, found: 285.1150.

$[\alpha]^{23}_D$ = –173 (*c* 1.0, $CHCl_3$); 89% ee, from *(R)*-**P**.

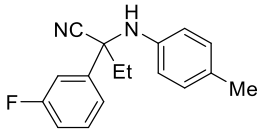

2-(3-Fluorophenyl)-2-(*p*-tolylamino)butanenitrile. The title compound was prepared according to **GP-4** from 2-chloro-2-(3-fluorophenyl)butanenitrile and *p*-toluidine with 18 h of reaction time. The product was purified by column chromatography on silica gel (hexanes/EtOAc/dichloromethane = 25/1/1). Pale-yellow solid.

(R)-**P**: 141 mg, 66% yield, 90% ee; *(S)*-**P**: 143 mg, 67% yield, 90% ee.

HPLC analysis: The ee was determined via HPLC on a CHIRALPAK OD column (5% *i*-PrOH in hexane, 1 mL/min); retention times for compound obtained using *(R)*-**P**: 8.4 min (major), 13.1 min (minor).

^{1}H NMR (500 MHz, $CDCl_3$) δ 7.44 – 7.35 (m, 2H), 7.31 (dt, *J* = 9.9, 2.0 Hz, 1H), 7.08 – 7.02 (m, 1H), 6.93 (d, *J* = 8.4 Hz, 2H), 6.46 (d, *J* = 8.4 Hz, 2H), 4.20 (s, 1H), 2.24 – 2.13 (m, 4H), 2.08 (dq, *J* = 14.9, 7.4 Hz, 1H), 1.08 (t, *J* = 7.4 Hz, 3H).

^{13}C NMR (126 MHz, $CDCl_3$) δ 163.3 (d, *J* = 247.2 Hz), 141.5 (d, *J* = 6.9 Hz), 141.0, 130.7 (d, *J* = 8.2 Hz), 129.71, 129.67, 121.6 (d, *J* = 2.9 Hz), 119.7, 116.1, 115.8 (d, *J* = 21.2 Hz), 113.0 (d, *J* = 23.6 Hz), 62.2 (d, *J* = 2.2 Hz), 38.3, 20.5, 8.9.

^{19}F NMR (376 MHz, $CDCl_3$) δ –111.4.

FT-IR (film): 3370, 3027, 2976, 2939, 2922, 2882, 2865, 2229, 1617, 1592, 1521, 1484, 1457, 1443, 1302, 1175, 1159, 974, 848, 808, 789, 694 cm^{-1}.

HRMS (ESI+) *m/z* $[M+H]^+$ calcd for $C_{17}H_{18}FN_2^+$: 269.1449, found: 269.1458.

$[\alpha]^{23}_D$ = –217 (*c* 1.0, $CHCl_3$); 90% ee, from *(R)*-**P**.

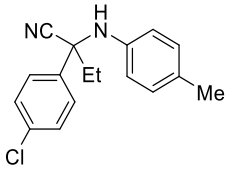

2-(4-Chlorophenyl)-2-(*p*-tolylamino)butanenitrile. The title compound was prepared according to **GP-4** from 2-chloro-2-(4-chlorophenyl)butanenitrile and *p*-toluidine with 14 h of reaction time. The product was purified by column chromatography on silica gel (hexanes/EtOAc/dichloromethane = 20/1/1). White solid.

(R)-**P**: 177 mg, 78% yield, 91% ee; *(S)*-**P**: 177 mg, 78% yield, 91% ee.

HPLC analysis: The ee was determined via HPLC on a CHIRALPAK OD column (5% *i*-PrOH in hexane, 1 mL/min); retention times for compound obtained using *(R)*-**P**: 9.1 min (major), 13.4 min (minor).

^{1}H NMR (500 MHz, $CDCl_3$) δ 7.54 (d, *J* = 8.6 Hz, 2H), 7.38 (d, *J* = 8.6 Hz, 2H), 6.93 (d, *J* = 8.3 Hz, 2H), 6.45 (d, *J* = 8.4 Hz, 2H), 4.20 (s, 1H), 2.26 – 2.13 (m, 4H), 2.06 (dq, *J* = 14.9, 7.4 Hz, 1H), 1.07 (t, *J* = 7.4 Hz, 3H).

^{13}C NMR (126 MHz, $CDCl_3$) δ 141.0, 137.3, 134.5, 129.70, 129.65, 129.3, 127.3, 119.8, 116.1, 62.0, 38.3, 20.5, 8.9.

FT-IR (film): 3372, 3028, 2976, 2921, 2880, 2230, 1614, 1518, 1488, 1401, 1303, 1251, 1094, 1013, 920, 808, 751 cm^{-1}.

HRMS (ESI+) *m/z*$[M+H]^+$ calcd for $C_{17}H_{17}ClN_2$: 285.1154, found: 285.1158.

$[\alpha]^{23}_D$ = –187 (*c* 1.0, $CHCl_3$); 91% ee, from *(R)*-**P**.

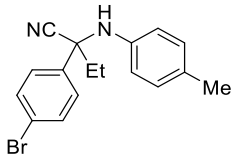

2-(4-Bromophenyl)-2-(*p*-tolylamino)butanenitrile. The title compound was prepared according to **GP-4** from 2-chloro-2-(4-bromophenyl)butanenitrile and *p*-toluidine with 16 h of reaction time. The product was purified by column chromatography on silica gel (hexanes/EtOAc/dichloromethane = 25/1/1). White solid.

(R)-**P**: 200 mg, 76% yield, 91% ee; *(S)*-**P**: 203 mg, 77% yield, 91% ee.

HPLC analysis: The ee was determined via HPLC on a CHIRALPAK OD column (5% *i*-PrOH in hexane, 1 mL/min); retention times for compound obtained using *(R)*-**P**: 9.4 min (major), 13.5 min (minor).

^{1}H NMR (500 MHz, $CDCl_3$) δ 7.53 (d, *J* = 8.6 Hz, 2H), 7.47 (d, *J* = 8.7 Hz, 2H), 6.93 (d, *J* = 8.4 Hz, 2H), 6.45 (d, *J* = 8.4 Hz, 2H), 4.20 (s, 1H), 2.25 – 2.13 (m, 4H), 2.05 (dq, *J* = 14.8, 7.4 Hz, 1H), 1.06 (t, *J* = 7.4 Hz, 3H).

^{13}C NMR (126 MHz, $CDCl_3$) δ 141.0, 137.9, 132.3, 129.70, 129.67, 127.6, 122.7, 119.7, 116.1, 62.1, 38.3, 20.5, 8.9.

FT-IR (film): 3369, 3024, 2976, 2938, 2921, 2880, 2864, 2229, 1617, 1518, 1486, 1396, 1303, 1251, 1219, 1073, 1009, 920, 808, 772 cm^{-1}.

HRMS (ESI+) *m/z* $[M+H]^+$ calcd for $C_{17}H_{18}BrN_2^+$: 329.0648, found: 329.0642.

$[\alpha]^{23}_D$ = –154 (*c* 1.0, $CHCl_3$); 91% ee, from *(R)*-**P**.

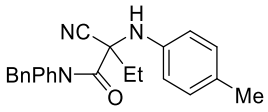

***N*-Benzyl-2-cyano-*N*-phenyl-2-(*p*-tolylamino)butanamide.** The title compound was prepared according to **GP-4** from *N*-benzyl-2-bromo-2-cyano-*N*-phenylbutanamide and *p*-toluidine with 18 h of reaction time. The product was purified by column chromatography on silica gel (hexanes/EtOAc = 10/1→7/1). Pale-brown solid.

(R)-**P**: 223 mg, 73% yield, 97% ee; *(S)*-**P**: 226 mg, 74% yield, 97% ee.

HPLC analysis: The ee was determined via HPLC on a CHIRALPAK AD column (10% *i*-PrOH in hexane, 1 mL/min); retention times for compound obtained using *(R)*-**P**: 12.9 min (major), 17.1 min (minor).

^{1}H NMR (500 MHz, $CDCl_3$) δ 7.32 – 7.17 (m, 5H), 7.11 (d, *J* = 6.8 Hz, 3H), 7.03 (d, *J* = 8.2 Hz, 2H), 6.77 (s, 1H), 6.50 (d, *J* = 8.0 Hz, 2H), 6.42 (s, 1H), 4.93 (d, *J* = 13.8 Hz, 1H), 4.66 (d, *J* = 13.8 Hz, 1H), 3.40 (s, 1H), 2.29 (s, 3H), 2.05 (q, *J* = 7.2 Hz, 2H), 1.22 (t, *J* = 7.4 Hz, 3H).

^{13}C NMR (126 MHz, $CDCl_3$) δ 166.5, 140.5, 139.9, 136.4, 129.9, 129.4, 129.3, 129.0, 128.8, 128.7, 128.4, 128.2, 127.9, 118.1, 114.9, 66.2, 56.9, 32.7, 20.6, 9.0.

FT-IR (film): 3369, 3064, 3030, 2982, 2939, 2921, 2236, 1646, 1593, 1522, 1496, 1457, 1395, 1320, 1252, 809, 753, 701 cm^{-1}.

HRMS (ESI+) *m/z* $[M+H]^+$ calcd for $C_{25}H_{26}N_3O^+$: 384.2070, found: 384.2078.

$[\alpha]^{23}_D$ = +17.6 (*c* 1.0, $CHCl_3$); 97% ee, from *(R)*-**P**.

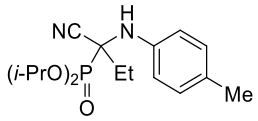

Diisopropyl (1-cyano-1-(*p*-tolylamino)propyl)phosphonate. The title compound was prepared according to **GP-4** from diisopropyl (1-bromo-1-cyanopropyl)phosphonate and *p*-toluidine with 24 h of reaction time. The product was purified by column chromatography on silica gel (hexanes/EtOAc = 3/1). Pale-brown solid.

(R)-**P**: 144 mg, 53% yield, 95% ee; *(S)*-**P**: 145 mg, 53% yield, 96% ee.

HPLC analysis: The ee was determined via HPLC on a CHIRALPAK AD column (10% *i*-PrOH in hexane, 1 mL/min); retention times for compound obtained using *(R)*-**P**: 7.7 min (major), 10.8 min (minor).

^{1}H NMR (500 MHz, $CDCl_3$) δ 7.06 (d, *J* = 8.3 Hz, 2H), 6.98 (d, *J* = 8.4 Hz, 2H), 4.88 (hept, *J* = 6.2 Hz, 2H), 3.94 (d, *J* = 7.9 Hz, 1H), 2.28 (s, 3H), 2.28 – 2.14 (m, 1H), 2.15 – 2.01 (m, 1H), 1.42 – 1.36 (m, 12H), 1.13 (t, *J* = 7.4 Hz, 3H).

^{13}C NMR (126 MHz, $CDCl_3$) δ 141.0 (d, *J* = 11.2 Hz), 131.8, 129.9, 120.0, 117.9 (d, *J* = 4.5 Hz), 74.3 (d, *J* = 7.3 Hz), 74.0 (d, *J* = 7.8 Hz), 57.6 (d, *J* = 157.8 Hz), 27.9 (d, *J* =

2.7 Hz), 24.4 (d, *J* = 3.0 Hz), 24.1 (d, *J* = 3.8 Hz), 24.0 (d, *J* = 5.2 Hz), 23.7 (d, *J* = 5.9 Hz), 20.7, 9.0 (d, *J* = 4.1 Hz).

^{31}P NMR (162 MHz, $CDCl_3$) δ 15.0.

FT-IR (film): 3306, 3026, 2982, 2938, 2884, 2873, 2237, 1617, 1515, 1453, 1387, 1377, 1243, 1178, 1143, 1192, 995, 811, 768, 582 cm^{-1}.

HRMS (ESI+) *m/z* $[M+H]^+$ calcd for $C_{17}H_{28}N_2O_3P^+$: 339.1833, found: 339.1835.

$[\alpha]^{23}_D$ = +60.7 (*c* 1.0, $CHCl_3$); 95% ee, from *(R)*-**P**.

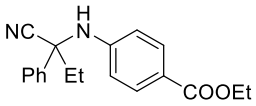

Ethyl 4-((1-cyano-1-phenylpropyl)amino)benzoate. The title compound was prepared according to **GP-4** from 2-chloro-2-phenylbutanenitrile and ethyl 4-aminobenzoate with 24 h of reaction time. The product was purified by column chromatography on silica gel (hexanes/EtOAc/dichloromethane = 8/1/1). Pale-yellow solid.

(R)-**P**: 186 mg, 75% yield, 93% ee; *(S)*-**P**: 181 mg, 73% yield, 93% ee.

HPLC analysis: The ee was determined via HPLC on a CHIRALPAK AD column (10% *i*-PrOH in hexane, 1 mL/min); retention times for compound obtained using *(R)*-**P**: 9.4 min (major), 10.3 min (minor).

^{1}H NMR (500 MHz, $CDCl_3$) δ 7.80 (d, *J* = 8.7 Hz, 2H), 7.54 (d, *J* = 7.5 Hz, 2H), 7.39 (t, *J* = 7.4 Hz, 2H), 7.35 (t, *J* = 7.2 Hz, 1H), 6.54 (d, *J* = 8.7 Hz, 2H), 4.86 (s, 1H), 4.28 (q, *J* = 7.1 Hz, 2H), 2.24 (dq, *J* = 14.5, 7.3 Hz, 1H), 2.10 (dq, *J* = 14.8, 7.4 Hz, 1H), 1.32 (t, *J* = 7.1 Hz, 3H), 1.08 (t, *J* = 7.4 Hz, 3H).

^{13}C NMR (126 MHz, $CDCl_3$) δ 166.6, 147.5, 137.7, 131.1, 129.3, 128.9, 125.6, 121.4, 119.4, 114.6, 61.7, 60.5, 38.3, 14.5, 8.9.

FT-IR (film): 3364, 3063, 3029, 2979, 2938, 2903, 2881, 2233, 1689, 1608, 1521, 1490, 1449, 1367, 1315, 1279, 1180, 1108, 1025, 925, 841, 771, 699 cm^{-1}.

HRMS (ESI+) *m/z* $[M+H]^+$ calcd for $C_{19}H_{21}N_2O_2^+$: 309.1598, found: 309.1612.

$[\alpha]^{23}_D$ = –238 (*c* 1.0, $CHCl_3$); 93% ee, from *(R)*-**P**.

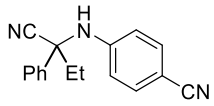

4-((1-Cyano-1-phenylpropyl)amino)benzonitrile. The title compound was prepared according to **GP-4** from 2-chloro-2-phenylbutanenitrile and 4-aminobenzonitrile with 24 h of reaction time. The product was purified by column chromatography on silica gel (hexanes/EtOAc = 15/1). Pale-yellow solid.

(R)-**P**: 132 mg, 63% yield, 92% ee; *(S)*-**P**: 128 mg, 61% yield, 92% ee.

HPLC analysis: The ee was determined via HPLC on a CHIRALPAK OD column (10% *i*-PrOH in hexane, 1 mL/min); retention times for compound obtained using *(R)*-**P**: 13.2 min (major), 17.2 min (minor).

^{1}H NMR (500 MHz, $CDCl_3$) δ 7.51 (d, *J* = 7.5 Hz, 2H), 7.44 – 7.33 (m, 5H), 6.56 (d, *J* = 8.7 Hz, 2H), 4.97 (s, 1H), 2.25 (dq, *J* = 14.5, 7.3 Hz, 1H), 2.11 (dq, *J* = 14.8, 7.4 Hz, 1H), 1.08 (t, *J* = 7.4 Hz, 3H).

^{13}C NMR (126 MHz, $CDCl_3$) δ 147.3, 137.1, 133.5, 129.4, 129.2, 125.5, 119.8, 119.1, 115.3, 101.9, 61.6, 38.2, 8.9.

FT-IR (film): 3351, 2977, 2939, 2881, 2218, 1608, 1521, 1449, 1328, 1265, 1177, 925, 827, 760, 700 cm^{-1}.

HRMS (ESI+) *m/z* $[M+H]^+$ calcd for $C_{17}H_{16}N_3^+$: 262.1339, found: 262.1356.

$[\alpha]^{23}_D$ = +267 (*c* 1.0, $CHCl_3$); 92% ee, from *(S)*-**P**.

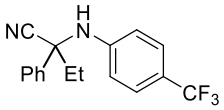

2-Phenyl-2-((4-(trifluoromethyl)phenyl)amino)butanenitrile. The title compound was prepared according to **GP-4** from 2-chloro-2-phenylbutanenitrile and 4-trifluoromethylaniline with 24 h of reaction time. The product was purified by column chromatography on silica gel (hexanes/EtOAc = 20/1). Pale-yellow solid.

(R)-**P**: 120 mg, 49% yield, 89% ee; *(S)*-**P**: 123 mg, 51% yield, 89% ee.

HPLC analysis: The ee was determined via HPLC on a CHIRALPAK OD column (10% *i*-PrOH in hexane, 1 mL/min); retention times for compound obtained using *(R)*-**P**: 6.5 min (major), 7.6 min (minor).

^{1}H NMR (500 MHz, $CDCl_3$) δ 7.55 (d, *J* = 7.6 Hz, 2H), 7.46 – 7.36 (m, 3H), 7.34 (d, *J* = 8.4 Hz, 2H), 6.57 (d, *J* = 8.4 Hz, 2H), 4.61 (s, 1H), 2.24 (dq, *J* = 14.7, 7.3 Hz, 1H), 2.12 (dq, *J* = 14.7, 7.4 Hz, 1H), 1.09 (t, *J* = 7.4 Hz, 3H).

^{13}C NMR (126 MHz, $CDCl_3$) 146.3, 137.6, 129.4, 129.1, 126.5 (q, *J* = 3.8 Hz), 125.6, 124.6 (q, *J* = 270.5 Hz), 121.8, 121.5, 119.4, 61.8, 38.4, 8.9.

^{19}F NMR (376 MHz, $CDCl_3$) δ –61.6.

FT-IR (film): 3350, 3027, 2982, 2947, 2925, 2248, 1617, 1536, 1449, 1327, 1162, 1117, 1072, 834, 815, 755, 700 cm^{-1}.

HRMS (ESI+) *m/z* $[M+H]^+$ calcd for $C_{17}H_{16}F_3N_2^+$: 305.1260, found: 305.1286.

$[\alpha]^{23}_D$ = –204 (*c* 1.0, $CHCl_3$); 89% ee, from *(R)*-**P**.

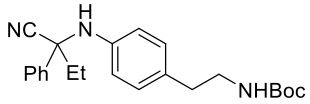

***tert*-Butyl (4-((1-cyano-1-phenylpropyl)amino)phenethyl)carbamate.** The title compound was prepared according to **GP-4** from 2-chloro-2-phenylbutanenitrile and *tert*-butyl (4-aminophenethyl)carbamate with 24 h of reaction time. The product was purified by column chromatography on silica gel (hexanes/EtOAc = 8/1→5/1). White solid.

(R)-**P**: 201 mg, 66% yield, 89% ee; *(S)*-**P**: 180 mg, 59% yield, 89% ee.

HPLC analysis: The ee was determined via HPLC on a CHIRALPAK OD column (15% *i*-PrOH in hexane, 1 mL/min); retention times for compound obtained using *(R)*-**P**: 7.8 min (major), 10.7 min (minor).

^{1}H NMR (500 MHz, $CDCl_3$) δ 7.58 (d, *J* = 7.7 Hz, 2H), 7.40 (t, *J* = 7.5 Hz, 2H), 7.35 (t, *J* = 7.2 Hz, 1H), 6.91 (d, *J* = 8.2 Hz, 2H), 6.48 (d, *J* = 8.3 Hz, 2H), 4.52 (s, 1H), 4.32 (s, 1H), 3.28 (t, *J* = 6.9 Hz, 2H), 2.63 (t, *J* = 6.5 Hz, 2H), 2.20 (dq, *J* = 14.5, 7.3 Hz, 1H), 2.08 (dq, *J* = 14.3, 7.4 Hz, 1H), 1.43 (s, 9H), 1.06 (t, *J* = 7.4 Hz, 3H).

^{13}C NMR (126 MHz, $CDCl_3$) δ 156.0, 142.2, 138.5, 130.3, 129.4, 129.1, 128.7, 125.7, 120.1, 116.0, 79.2, 62.3, 41.8, 38.4, 35.3, 28.5, 8.9.

FT-IR (film): 3366, 2977, 2930, 2229, 1696, 1616, 1521, 1456, 1251, 1168, 1053, 924, 824, 759, 700 cm^{-1}.

HRMS (ESI+) *m/z* $[M+H]^+$ calcd for $C_{23}H_{30}N_3O_2^+$: 380.2333, found: 380.2348.

$[\alpha]^{23}_D$ = +133 (*c* 1.0, $CHCl_3$); 89% ee, from (*S*)-**P**.

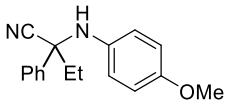

2-((4-Methoxyphenyl)amino)-2-phenylbutanenitrile. The title compound was prepared according to **GP-4** from 2-chloro-2-phenylbutanenitrile and 4-methoxyaniline with 24 h of reaction time. The product was purified by column chromatography on silica gel (hexanes/EtOAc/dichloromethane = 15/1/1). Pale-brown solid.

(R)-**P**: 90 mg, 42% yield, 88% ee; *(S)*-**P**: 90 mg, 42% yield, 88% ee.

HPLC analysis: The ee was determined via HPLC on a CHIRALPAK OD column (10% *i*-PrOH in hexane, 1 mL/min); retention times for compound obtained using *(R)*-**P**: 8.2 min (major), 15.1 min (minor).

^{1}H NMR (500 MHz, $CDCl_3$) δ 7.60 (d, *J* = 7.5 Hz, 2H), 7.40 (t, *J* = 7.5 Hz, 2H), 7.35 (t, *J* = 7.2 Hz, 1H), 6.68 (d, *J* = 8.9 Hz, 2H), 6.53 (d, *J* = 8.9 Hz, 2H), 4.04 (s, 1H), 3.70 (s, 3H), 2.18 (dq, *J* = 14.7, 7.3 Hz, 1H), 2.09 (dq, *J* = 13.6, 7.3 Hz, 1H), 1.04 (t, *J* = 7.4 Hz, 3H).

^{13}C NMR (126 MHz, $CDCl_3$) δ 154.0, 138.6, 137.4, 129.1, 128.7, 126.0, 120.3, 118.2, 114.6, 63.3, 55.6, 38.2, 9.0.

FT-IR (film): 3370, 3031, 2975, 2937, 2839, 2229, 1617, 1601, 1457, 1205, 1153, 1069, 925, 816, 761, 700 cm^{-1}.

HRMS (ESI+) *m/z* $[M+H]^+$ calcd for $C_{17}H_{19}N_2O$: 267.1492, found: 267.1507.

$[\alpha]^{23}_D$ = –161 (*c* 1.0, $CHCl_3$); 88% ee, from (*R)*-**P**.

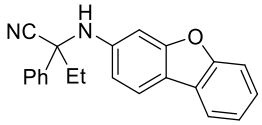

2-(Dibenzo[*b,d*]furan-3-ylamino)-2-phenylbutanenitrile. The title compound was prepared according to **GP-4** from 2-chloro-2-phenylbutanenitrile and 3-(4,4,5-trimethyl-1,3,2-dioxaborolan-2-yl)aniline with 24 h of reaction time. The product was purified by column chromatography on silica gel: column #1 (hexanes/EtOAc/dichloromethane =

10/1/1→4/1/1); column #2 (toluene). The reaction mixture was dry-loaded on the silica due to the poor solubility of the title compound. Pale-brown solid.

(R)-**P**: 175 mg, 67% yield, 94% ee; *(S)*-**P**: 161 mg, 62% yield, 94% ee.

HPLC analysis: The ee was determined via HPLC on a CHIRALPAK OD column (5% *i*-PrOH in hexane, 1 mL/min); retention times for compound obtained using *(R)*-**P**: 22.0 min (major), 24.9 min (minor).

^{1}H NMR (500 MHz, $CDCl_3$) δ 7.76 (d, *J* = 7.6 Hz, 1H), 7.66 (d, *J* = 9.0 Hz, 1H), 7.63 (d, *J* = 7.5 Hz, 2H), 7.42 (t, *J* = 7.3 Hz, 3H), 7.37 (t, *J* = 7.3 Hz, 1H), 7.30 (t, *J* = 7.7 Hz, 1H), 7.28 – 7.21 (m, 1H), 6.67 – 6.59 (m, 2H), 4.55 (s, 1H), 2.26 (dq, *J* = 14.6, 7.3 Hz, 1H), 2.14 (dq, *J* = 14.8, 7.4 Hz, 1H), 1.10 (t, *J* = 7.4 Hz, 3H).

^{13}C NMR (126 MHz, $CDCl_3$) δ 157.4, 156.1, 143.8, 138.1, 129.3, 128.9, 125.8, 125.7, 124.6, 122.7, 121.1, 119.8, 119.7, 116.8, 112.2, 111.3, 98.6, 62.5, 38.6, 9.0.

FT-IR (film): 3381, 3062, 2976, 2925, 2230, 1636, 1606, 1506, 1457, 1260, 1165, 1130, 747, 721, 699 cm^{-1}.

HRMS (ESI+) *m/z* $[M+H]^+$ calcd for $C_{22}H_{19}N_2O^+$: 327.1492, found: 327.1509.

$[\alpha]^{23}_D$ = +199 (*c* 1.0, $CHCl_3$); 94% ee, from (*S*)-**P**.

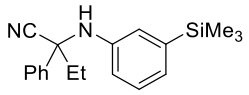

2-Phenyl-2-((3-(trimethylsilyl)phenyl)amino)butanenitrile. The title compound was prepared according to **GP-4** from 2-chloro-2-phenylbutanenitrile and 3-(trimethylsilyl)aniline[49] with 24 h of reaction time. The product was purified by column chromatography on silica gel (hexanes/EtOAc = 45/1). Pale-yellow solid.

(R)-**P**: 167 mg, 68% yield, 91% ee; *(S)*-**P**: 158 mg, 64% yield, 92% ee.

HPLC analysis: The ee was determined via HPLC on a CHIRALPAK OD column (5% *i*-PrOH in hexane, 1 mL/min); retention times for compound obtained using *(R)*-**P**: 5.7 min (major), 6.2 min (minor).

^{1}H NMR (500 MHz, $CDCl_3$) δ 7.61 (d, *J* = 7.6 Hz, 2H), 7.41 (t, *J* = 7.5 Hz, 2H), 7.35 (t, *J* = 7.3 Hz, 1H), 7.09 (t, *J* = 7.6 Hz, 1H), 6.94 (d, *J* = 7.2 Hz, 1H), 6.70 (d, *J* = 2.3 Hz,

1H), 6.51 (ddd, *J* = 8.1, 2.7, 1.0 Hz, 1H), 4.33 (s, 1H), 2.23 (dq, *J* = 14.7, 7.3 Hz, 1H), 2.12 (dq, *J* = 14.9, 7.4 Hz, 1H), 1.09 (t, *J* = 7.4 Hz, 3H), 0.16 (s, 9H).

^{13}C NMR (126 MHz, $CDCl_3$) δ 142.9, 141.3, 138.6, 129.1, 128.6, 128.5, 125.8, 124.8, 120.9, 120.0, 116.1, 62.3, 38.4, 9.0, –1.2.

FT-IR (film): 3370, 3033, 2953, 2230, 1594, 1576, 1399, 1304, 1248, 1123, 936, 754, 699 cm^{-1}.

HRMS (ESI+) *m/z* $[M+H]^+$ calcd for $C_{19}H_{25}N_2Si^+$: 309.1782, found: 309.1797.

$[\alpha]^{23}_D$ = +199 (*c* 1.0, $CHCl_3$); 92% ee, from (*S*)-**P**.

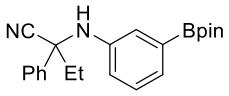

2-Phenyl-2-((3-(4,4,5,5-tetramethyl-1,3,2-dioxaborolan-2-yl)phenyl)amino)butanenitrile. The title compound was prepared according to **GP-4** from 2-chloro-2-phenylbutanenitrile and 3-(4,4,5-trimethyl-1,3,2-dioxaborolan-2-yl)aniline with 24 h of reaction time. The product was purified by column chromatography on silica gel (hexanes/EtOAc = 8/1→5/1). Pale-yellow solid.

(R)-**P**: 110 mg, 38% yield, 93% ee; *(S)*-**P**: 116 mg, 40% yield, 93% ee.

HPLC analysis: The ee was determined via HPLC on a CHIRALPAK OD column (2% *i*-PrOH in hexane, 1 mL/min); retention times for compound obtained using *(R)*-**P**: 7.9 min (major), 9.8 min (minor).

^{1}H NMR (500 MHz, $CDCl_3$) δ 7.57 (d, *J* = 7.5 Hz, 2H), 7.38 (t, *J* = 7.3 Hz, 2H), 7.34 (t, *J* = 7.2 Hz, 1H), 7.22 (d, *J* = 7.3 Hz, 1H), 7.19 (d, *J* = 2.1 Hz, 1H), 7.04 (t, *J* = 7.7 Hz, 1H), 6.44 (dd, *J* = 8.1, 1.9 Hz, 1H), 4.32 (s, 1H), 2.17 (dq, *J* = 14.5, 7.3 Hz, 1H), 2.08 (dq, *J* = 14.4, 7.4 Hz, 1H), 1.33 (d, *J* = 3.1 Hz, 12H), 1.07 (t, *J* = 7.4 Hz, 3H).

^{13}C NMR (126 MHz, $CDCl_3$) δ 143.1, 138.5, 129.2, 128.7, 128.6, 126.1, 125.8, 123.2, 119.9, 117.5, 83.9, 62.1, 38.5, 25.02, 24.98, 9.0.

^{11}B NMR (128 MHz, $CDCl_3$) δ 31.2.

FT-IR (film): 3384, 2978, 2929, 2229, 1576, 1361, 1319, 1144, 995, 854, 760, 702 cm^{-1}.

HRMS (ESI+) *m/z* $[M+H]^+$ calcd for $C_{22}H_{28}BN_2O_2^+$: 363.2238, found: 363.2261.

$[\alpha]^{23}_D$ = +174 (*c* 1.0, $CHCl_3$); 93% ee, from (*S*)-**P**.

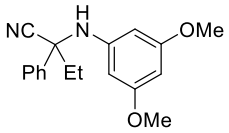

2-((3,5-Dimethoxyphenyl)amino)-2-phenylbutanenitrile. The title compound was prepared according to **GP-4** from 2-chloro-2-phenylbutanenitrile and 3,5-dimethoxyaniline with 24 h of reaction time. The product was purified by column chromatography on silica gel (hexanes/EtOAc/dichloromethane = 10/1/2). Yellow solid.

(R)-**P**: 127 mg, 54% yield, 90% ee; *(S)*-**P**: 116 mg, 49% yield, 89% ee.

HPLC analysis: The ee was determined via HPLC on a CHIRALPAK OD column (10% *i*-PrOH in hexane, 1 mL/min); retention times for compound obtained using *(R)*-**P**: 12.3 min (major), 19.4 min (minor).

^{1}H NMR (500 MHz, $CDCl_3$) δ 7.58 (d, *J* = 7.6 Hz, 2H), 7.40 (t, *J* = 7.5 Hz, 2H), 7.34 (t, *J* = 7.3 Hz, 1H), 5.93 (t, *J* = 2.0 Hz, 1H), 5.71 (d, *J* = 2.0 Hz, 2H), 4.33 (s, 1H), 3.61 (s, 6H), 2.19 (dq, *J* = 14.5, 7.3 Hz, 1H), 2.08 (dq, *J* = 14.8, 7.5 Hz, 1H), 1.06 (t, *J* = 7.4 Hz, 3H).

^{13}C NMR (126 MHz, $CDCl_3$) δ 161.3, 145.6, 138.6, 129.2, 128.7, 125.7, 119.9, 94.7, 92.4, 62.3, 55.2, 38.4, 8.9.

FT-IR (film): 3370, 2972, 2937, 2839, 2229, 1617, 1601, 1457, 1205, 1153, 1069, 925, 816, 761, 700 cm^{-1}.

HRMS (ESI+) *m/z* $[M+H]^+$ calcd for $C_{18}H_{21}N_2O_2^+$: 297.1598, found: 297.1615.

$[\alpha]^{23}_D$ = –176 (*c* 1.0, $CHCl_3$); 90% ee, from *(R)*-**P**.

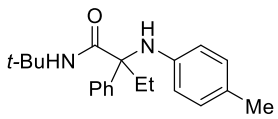

***N*-(*tert*-butyl)-2-phenyl-2-(*p*-tolylamino)butanamide.** The title compound was prepared according to **GP-4** from *N*-(*tert*-butyl)-2-chloro-2-phenylbutanamide and *p*-toluidine with 48 h of reaction time. The product was purified by column chromatography on silica gel (hexanes/EtOAc/dichloromethane = 30/1/1). Pale-yellow solid.

(R)-**P**: 128 mg, 49% yield, 88% ee; *(S)*-**P**: 146 mg, 59% yield, 88% ee.

HPLC analysis: The ee was determined via HPLC on a CHIRALPAK OD column (3% *i*-PrOH in hexane, 1 mL/min); retention times for compound obtained using *(R)*-**P**: 4.4 min (major), 4.8 min (minor).

^{1}H NMR (500 MHz, $CDCl_3$) δ 7.60 (d, *J* = 7.9 Hz, 2H), 7.38 (t, *J* = 7.7 Hz, 2H), 7.29 (t, *J* = 7.3 Hz, 1H), 6.87 (d, *J* = 8.4 Hz, 2H), 6.41 (d, *J* = 8.4 Hz, 2H), 5.87 (s, 1H), 5.08 (s, 1H), 2.54 (dq, *J* = 14.6, 7.4 Hz, 1H), 2.28 (dq, *J* = 14.3, 7.2 Hz, 1H), 2.20 (s, 3H), 1.23 (s, 9H), 0.77 (t, *J* = 7.3 Hz, 3H).

^{13}C NMR (126 MHz, $CDCl_3$) δ 172.5, 142.7, 142.2, 129.5, 129.0, 127.5, 127.2, 126.3, 115.7, 66.5, 51.2, 28.5, 26.0, 20.5, 7.9.

FT-IR (film): 3379, 3055, 3021, 2967, 2934, 2877, 1669, 1617, 1517, 1394, 1364, 1296, 1227, 1034, 812, 757, 700 cm^{-1}.

HRMS (ESI+) *m/z* $[M+H]^+$ calcd for $C_{21}H_{29}N_2O^+$: 325.2274, found: 325.2296.

$[\alpha]^{23}_D$ = +24.3 (*c* 1.0, $CHCl_3$); 88% ee, from *(R)*-**P**.

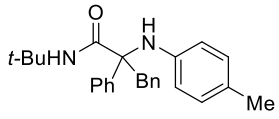

***N*-(*tert*-Butyl)-2,3-diphenyl-2-(*p*-tolylamino)propenamide.** The title compound was prepared according to **GP-4** from *N*-(*tert*-butyl)-2-chloro-2,3-diphenylpropanamide and *p*-toluidine with 48 h of reaction time. The product was purified by column chromatography on silica gel (hexanes/EtOAc/dichloromethane = 50/1/1). Pale-yellow solid.

(R)-**P**: 165 mg, 53% yield, 85% ee; *(S)*-**P**: 162 mg, 52% yield, 87% ee.

HPLC analysis: The ee was determined via HPLC on a CHIRALPAK IC column (5% *i*-PrOH in hexane, 1 mL/min); retention times for compound obtained using *(R)*-**P**: 6.5 min (major), 5.5 min (minor).

^{1}H NMR (500 MHz, $CDCl_3$) δ 7.51 (d, *J* = 7.6 Hz, 2H), 7.33 (t, *J* = 7.5 Hz, 2H), 7.28 (d, *J* = 7.2 Hz, 1H), 7.13 (t, *J* = 7.2 Hz, 1H), 7.08 (t, *J* = 7.4 Hz, 2H), 6.94 (d, *J* = 8.0 Hz, 2H), 6.73 (d, *J* = 7.5 Hz, 2H), 6.44 (d, *J* = 8.1 Hz, 2H), 6.20 (s, 1H), 4.57 (s, 1H), 3.72 (d, *J* = 13.7 Hz, 1H), 3.60 (d, *J* = 13.6 Hz, 1H), 2.24 (s, 3H), 1.22 (s, 9H).

^{13}C NMR (126 MHz, $CDCl_3$) δ 171.9, 142.0, 141.6, 136.3, 130.8, 129.7, 128.7, 127.8, 127.7, 127.5, 126.7, 126.2, 116.1, 67.1, 51.2, 40.2, 28.4, 20.6.

FT-IR (film): 3386, 3062, 3029, 2965, 2919, 2864, 1675, 1617, 1517, 1453, 1365, 1226, 1033, 809, 757, 701 cm^{-1}.

HRMS (ESI+) *m/z* $[M+H]^+$ calcd for $C_{26}H_{31}N_2O^+$: 387.2431, found: 387.2468.

$[\alpha]^{23}_D$ = –28.5 (*c* 1.0, $CHCl_3$); 85% ee, from *(R)*-**P**.

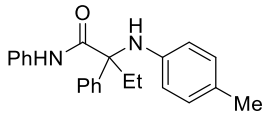

***N*,2-Diphenyl-2-(*p*-tolylamino)butanamide.** The title compound was prepared according to **GP-4** from 2-chloro-*N*,2-diphenylbutanamide and *p*-toluidine with 48 h of reaction time. The product was purified by column chromatography on silica gel (hexanes/EtOAc = 30/1). Pale-yellow solid.

(R)-**P**: 168 mg, 61% yield, 84% ee; *(S)*-**P**: 168 mg, 61% yield, 84% ee.

HPLC analysis: The ee was determined via HPLC on a CHIRALPAK OD column (3% *i*-PrOH in hexane, 1 mL/min); retention times for compound obtained using *(R)*-**P**: 10.1 min (major), 14.3 min (minor).

^{1}H NMR (500 MHz, $CDCl_3$) δ 8.33 (s, 1H), 7.70 (d, *J* = 8.0 Hz, 2H), 7.41 (t, *J* = 8.0 Hz, 4H), 7.31 (t, *J* = 7.3 Hz, 1H), 7.26 (t, *J* = 7.7 Hz, 2H), 7.06 (t, *J* = 7.4 Hz, 1H), 6.94 (d, *J* = 8.3 Hz, 2H), 6.55 (d, *J* = 8.4 Hz, 2H), 4.82 (s, 1H), 2.64 (dq, *J* = 14.7, 7.4 Hz, 1H), 2.44 (dq, *J* = 14.5, 7.3 Hz, 1H), 2.22 (s, 3H), 0.74 (t, *J* = 7.3 Hz, 3H).

^{13}C NMR (126 MHz, $CDCl_3$) δ 171.8, 141.8, 141.1, 137.8, 129.8, 129.2, 129.0, 128.6, 127.9, 126.2, 124.4, 119.9, 116.4, 67.5, 25.7, 20.5, 7.8.

FT-IR (film): 3351, 3055, 3023, 2975, 2934, 2876, 1675, 1617, 1599, 1517, 1439, 1312, 1245, 1185, 812, 753, 693 cm^{-1}.

HRMS (ESI+) *m/z* $[M+H]^+$ calcd for $C_{23}H_{25}N_2O^+$: 345.1961, found: 345.1978.

$[\alpha]^{23}_D$ = +4.5 (*c* 1.0, $CHCl_3$); 84% ee, from *(S)*-**P**.

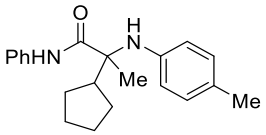

2-Cyclopentyl-*N*-phenyl-2-(*p*-tolylamino)propenamide. The title compound was prepared according to **GP-4** from 2-bromo-2-cyclopentyl-*N*-phenylpropanamide and *p*-toluidine with 48 h of reaction time. The product was purified by column chromatography on silica gel (hexanes/EtOAc = 30/1). Pale-yellow solid.

(R)-**P**: 118 mg, 46% yield, 60% ee; *(S)*-**P**: 117 mg, 45% yield, 60% ee.

HPLC analysis: The ee was determined via HPLC on a CHIRALPAK IC column (10% *i*-PrOH in hexane, 1 mL/min); retention times for compound obtained using *(R)*-**P**: 6.5 min (minor), 7.0 min (major).

^{1}H NMR (500 MHz, $CDCl_3$) δ 9.04 (s, 1H), 7.52 (d, *J* = 8.1 Hz, 2H), 7.31 (t, *J* = 7.9 Hz, 2H), 7.09 (t, *J* = 7.4 Hz, 1H), 6.99 (d, *J* = 8.2 Hz, 2H), 6.59 (d, *J* = 8.3 Hz, 2H), 3.77 (s, 1H), 2.36 (p, *J* = 9.3 Hz, 1H), 2.25 (s, 3H), 1.91 – 1.73 (m, 2H), 1.73 – 1.50 (m, 6H), 1.45 (s, 3H).

^{13}C NMR (126 MHz, $CDCl_3$) δ 173.8, 142.3, 138.0, 129.9, 129.3, 129.1, 124.2, 119.9, 117.0, 63.7, 50.3, 27.4, 27.0, 25.54, 25.49, 20.6, 17.8.

FT-IR (film): 3386, 3349, 2956, 2868, 1673, 1598, 1529, 1499, 1442, 1314, 1242, 1163, 1074, 1029, 755, 690 cm^{-1}.

HRMS (ESI+) *m/z* $[M+H]^+$ calcd for $C_{26}H_{31}N_2O^+$: 387.2431, found: 387.2468.

$[\alpha]^{23}_D$ = +44.1 (*c* 1.0, $CHCl_3$); 60% ee, from *(S)*-**P**.

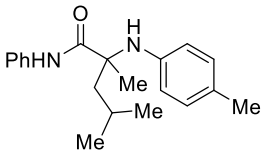

2,4-Dimethyl-*N*-phenyl-2-(*p*-tolylamino)pentanamide. The title compound was prepared according to **GP-4** from 2-bromo-2,4-dimethyl-*N*-phenylpentanamide and *p*-toluidine with 48 h of reaction time. The product was purified by column chromatography on silica gel (hexanes/EtOAc = 40/1). Pale-orange solid.

(R)-**P**: 182 mg, 73% yield, 61% ee; *(S)*-**P**: 170 mg, 68% yield, 59% ee.

HPLC analysis: The ee was determined via HPLC on a CHIRALPAK IC column (2% *i*-PrOH in hexane, 1 mL/min); retention times for compound obtained using *(R)*-**P**: 9.3 min (major), 8.7 min (minor).

^{1}H NMR (500 MHz, $CDCl_3$) δ 9.04 (s, 1H), 7.50 (d, *J* = 7.9 Hz, 2H), 7.30 (t, *J* = 7.9 Hz, 2H), 7.09 (t, *J* = 7.4 Hz, 1H), 6.97 (d, *J* = 8.0 Hz, 2H), 6.55 (d, *J* = 8.2 Hz, 2H), 3.76 (s, 1H), 2.24 (s, 3H), 1.94 – 1.85 (m, 1H), 1.85 – 1.79 (m, 2H), 1.50 (s, 3H), 0.99 (d, *J* = 6.4 Hz, 3H), 0.92 (d, *J* = 6.5 Hz, 3H).

^{13}C NMR (126 MHz, $CDCl_3$) δ 174.0, 142.0, 138.0, 129.9, 129.2, 129.1, 124.3, 119.9, 116.9, 62.2, 48.9, 25.0, 24.5, 24.1, 21.7, 20.6.

FT-IR (film): 3344, 2956, 2927, 2868, 1675, 1617, 1601, 1512, 1439, 1311, 1250, 812, 754, 693 cm^{-1}.

HRMS (ESI+) *m/z* $[M+H]^+$ calcd for $C_{20}H_{27}N_2O^+$: 311.2118, found: 311.2145.

$[\alpha]^{21}_D$ = +21.2 (*c* 1.0, $CHCl_3$); 61% ee, from *(S)*-**P**.

2.4.4. Effect of reaction parameters

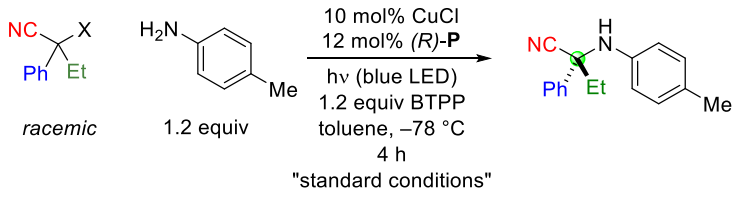

General Procedure 6 (GP-6). In a nitrogen-filled glovebox, a 4 mL vial was charged with a PTFE stir bar, CuCl (1.0 mg, 0.010 mmol), **P** (14 mg, 0.012 mmol), toluene (1 mL), and BTPP (38 μL, 0.12 mmol). The resulting mixture was stirred for 4 h. A separate 4 mL vial was charged with a PTFE stir bar, *p*-toluidine (13 mg, 0.12 mmol), 2-chloro-2-phenylbutanenitrile (18 mg, 0.10 mmol), and toluene (0.5 mL). This mixture was stirred for 1 min, and then the solution of the catalyst was added; additional toluene (0.5 mL) was used to wash the vial that had contained the catalyst, and the washing was added to the reaction mixture. The reaction vial was capped with a PTFE-lined cap, removed from the glovebox, submerged in a low-form hemispherical Dewar flask filled with pre-cooled methanol (–78 °C), and stirred for 5 min. Two Kessil® PR160-440nm lamps were installed 5 cm above the vial, and the vial was irradiated for 4 h.

Work-up. The reaction was quenched by turning off the lamps. The reaction mixture was opened to air and passed through a 2 cm plug of silica gel loaded in a pipet, with EtOAc washings (3 x 4 mL). The filtrate was concentrated in vacuo, 1,3,5-trimethoxybenzene (internal standard; 17 mg, 0.10 mmol) was added, and the mixture was dissolved in $CDCl_3$ (0.6 mL). The yield was determined via ^1H NMR spectroscopy. Part of the solution in $CDCl_3$ was purified by preparative TLC (hexane/EtOAc 5:1 eluent) and analyzed via chiral HPLC analysis to determine the enantiomeric excess.

Note. The model electrophile, 2-chloro-2-phenylbutanenitrile, was stable for at least 10 min under the reaction conditions in the absence of irradiation.

Table 2.2. Effect of the Reaction Parameters.

entry	variation from the "standard conditions"	yield (%)	ee (%)	entry	variation from the "standard conditions"	yield (%)	ee (%)
1	none	77	92	21[b]	BTMG, instead of BTPP	75	92
2[a]	no CuCl	<2	-	22[b]	DBU, instead of BTPP	14	52
3	no **P**	<2	-	23	CsOPh-H_2O, instead of BTPP	16	86
4	no BTPP	<2	-	24	Et_2O, instead of Toluene	72	92
5	no hν	<2	-	25	EtOAc, instead of Toluene	68	94
6	no hν, room temperature	<5	-	26	–60 °C, instead of –78 °C	49	81
7	no hν, no **P**	<5	-	27	–10 °C, instead of –78 °C	16	44
8	no hν, 80 °C	14	13	28	5 mol% **P**	60	76
9	no hν, no CuCl, no **P**, 80 °C	<5	-	29	20 mol% **P**	79	92
10[b]	CuBr instead of CuCl	77	92	30	2 mol% CuCl, 2.4 mol% **P**	38(56[c])	90(90[c])
11[b]	$CuCl_2$ instead of CuCl	68	87	31	5 mol% CuCl, 6 mol% **P**	70(73[c])	92(92[c])
12[b]	$(MeCN)_4CuBF_4$ instead of CuCl	71	92	32	1.1 equiv *p*-Toluidine	73	92
13[c]	**L1**, instead of **P**	33	41	33	1.5 equiv *p*-Toluidine	77	92
14[c]	**L2**, instead of **P**	5	7	34	0.1 M, instead of 0.05 M	75	92
15[c]	**L3**, instead of **P**	<2	-	35	1 lamp	78	92
16[c]	**L4**, instead of **P**	21	20	36	3 lamps	78	93
17[c]	**L5**, instead of **P**	8	4	37	2 h, instead of 4 h	72	92
18[c]	**L6**, instead of **P**	<2	-	38	5 equiv H_2O	78	92
19[c]	**L7**, instead of **P**	12	2	39	air (5 mL) purged	68	92
20[c]	**L8**, instead of **P**	6	*rac*	40[d]	HPLC grade toluene without degassing	76	92
				41[d]	10 mol% $\mathbf{Cu_A}$	76	92

All data are the average of two or more runs. [a] Conversion of the electrophile: <1%. [b] To ensure reproducibility, stirring time during catalyst preparation: 6 h. [c] Reaction time: 24 h. [d] The reaction was set up outside of the glovebox, using standard air-free techniques.

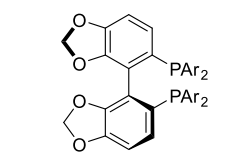

Ar = 3,5-(*t*-Bu)$_2$-4-MeO-C_6H_2

P

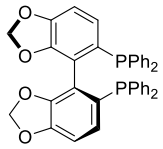

L1

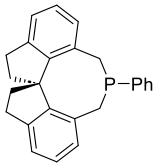

L2

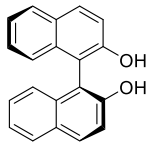

L3

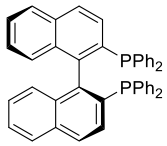

L4

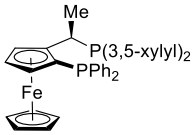

L5

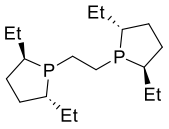

L6

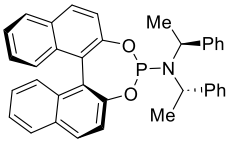

L7

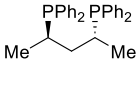

L8

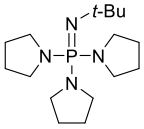

BTPP

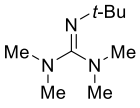

BTMG

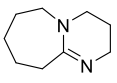

DBU

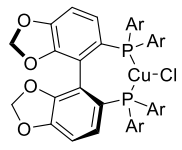

Ar = 3,5-(*t*-Bu)$_2$-4-MeO-C_6H_2

$\mathbf{Cu_A}$

2.4.5. Functional-group compatibility

2-Chloro-2-phenylbutanenitrile was reacted with *p*-toluidine according to modified **GP-6** in the presence of 1.0 equiv of each of the additives shown below. The additive was added before the addition of the catalyst solution. The yield and the recovery of the additive was determined by GC analysis using dodecane as an internal standard, and the ee was determined by chiral HPLC.

Table 2.3. Functional-Group Compatibility.

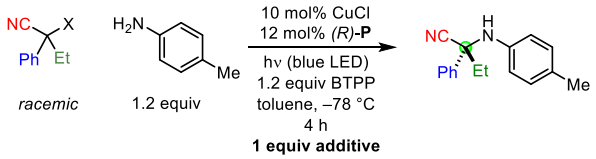

A. Additives with good compatibility.

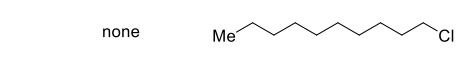

76% yield[a], 92% ee[b]

77% yield, 91% ee
95% recovered[a]

77% yield, 92% ee
>95% recovered

79% yield, 92% ee
95% recovered

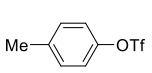

76% yield, 91% ee
94% recovered

74% yield, 92% ee
>95% recovered

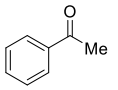

73% yield, 92% ee
>95% recovered

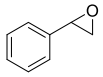

77% yield, 88% ee
92% recovered

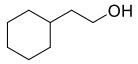

77% yield, 91% ee
92% recovered

77% yield, 92% ee
92% recovered

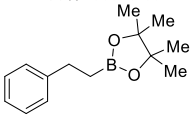

76% yield, 92% ee
>95% recovered

80% yield, 91% ee
>95% recovered

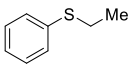

76% yield, 92% ee
>95% recovered

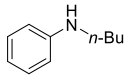

76% yield, 91% ee
>95% recovered

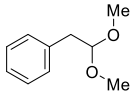

75% yield, 92% ee
>95% recovered

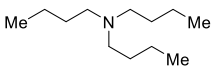

81% yield, 91% ee
94% recovered

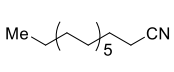

77% yield, 91% ee
>95% recovered

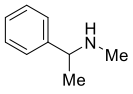

81% yield, 92% ee
>95% recovered

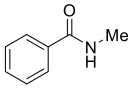

84% yield, 93% ee
>95% recovered

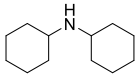

81% yield, 92% ee
>95% recovered

B. Additives with modest to low compatibility.

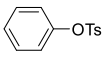

70% yield, 93% ee
77% recovered

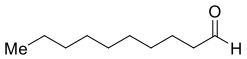

78% yield, 92% ee
75% recovered

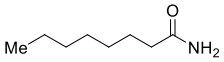

75% yield, 91% ee
82% recovered

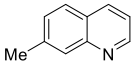

67% yield[c], 91% ee
68% recovered

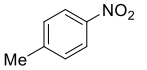

42% yield[c], 92% ee
>95% recovered

46% yield, 92% ee
>95% recovered

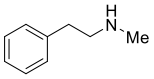

27% yield, 91% ee
71% recovered

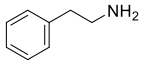

6% yield
<10% recovered

All data are the average of two or more runs. [a] Reaction time: 24 h.

2.4.6. Gram-scale coupling

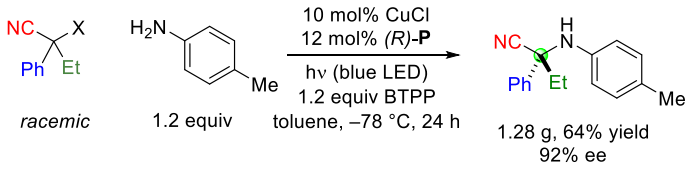

In the air, an oven-dried 250 mL round-bottom flask equipped with a PTFE stir bar was charged with CuCl (80 mg, 0.80 mmol) and *(R)*-**P** (1.13 g, 0.960 mmol). The flask was sealed with a rubber stopper, and the joint was wrapped with electrical tape. The flask was evacuated/backfilled with nitrogen three times, using a 20G needle attached to a Schlenk line. Then, a nitrogen-filled balloon was attached, and toluene (50 mL) and BTPP (2.90 mL, 9.60 mmol) were added via syringe. The mixture was stirred for 4 h, and then additional toluene (80 mL) was added. *p*-Toluidine (1.03 g, 9.60 mmol) was weighed into an oven-dried 40 mL vial equipped with a PTFE stir bar. The vial was capped with a PTFE-lined open top cap, and the joint was wrapped with electrical tape. The vial was attached to a Schlenk line and evacuated/backfilled with nitrogen three times. A nitrogen-filled balloon was attached, and 15 mL of toluene was added. This solution of *p*-toluidine was transferred to the round-bottom flask containing the catalyst solution. An additional 15 mL of toluene was used to wash the vial, and the washing was added to the flask. The flask was submerged in a low-form hemispherical Dewar flask filled with pre-cooled methanol (–78 °C), and the reaction mixture was stirred for 10 min. 2-Chloro-2-phenylbutanenitrile (1.43 g, 8.00 mmol) was weighed into a syringe and transferred to the pre-cooled reaction mixture. The reaction mixture was stirred for 5 min, and then four Kessil® PR160-440 nm lamps were installed 5 cm above the reaction mixture, and the mixture was irradiated for 24 h under a positive pressure of nitrogen from the nitrogen-filled balloon.

Work-up. The reaction was quenched by turning off the lamps. The reaction mixture was warmed to room temperature, opened to air, and concentrated in vacuo. 30% aq NH_4OH (20 mL) and EtOAc (30 mL) were added, and the reaction mixture was vigorously stirred for 15 min, at which point the aqueous layer was blue (see **Note 2** in **GP-4**). The aqueous layer was extracted with EtOAc (3 x 10 mL), and the combined organic layer was dried over Na_2SO_4 and then passed through a plug of silica gel (2 cm) with an EtOAc washing (50 mL). The organic layer was concentrated in vacuo and purified by flash

column chromatography on silica gel (hexanes/EtOAc/dichloromethane = 40/1/1) to afford a pale-yellow solid (1.28 g, 64% yield). The ee was determined via HPLC analysis to be 92%.

2.4.7. Ligand recovery

2-Chloro-2-phenylbutanenitrile was reacted with *p*-toluidine (Run 1) and 4-methoxyaniline (Run 2) according to **GP-4**. Fractions containing the ligand were collected via column chromatography during the purification of the coupling product. The ligand was further purified by column chromatography on silica gel: column #1 (hexanes/EtOAc = 100/1); column #2 (hexanes/toluene = 1/1).

Run 1: recovered *(S)*-**P**: 92 mg (82% of the initial loading). Run 2: recovered *(R)*-**P**: 91 mg (81% of the initial loading).

Recovered *(R)*-**P** and *(S)*-**P** were used in a copper-catalyzed coupling between 2-chloro-2-phenylbutanenitrile and *p*-toluidine, following **GP-6**. Recovered *(R)*-**P**: 75% yield and 92% ee. Recovered *(S)*-**P**, 75% yield and 92% ee.

2.4.8. Couplings of an alkyl carbonate and an alkyl fluoride

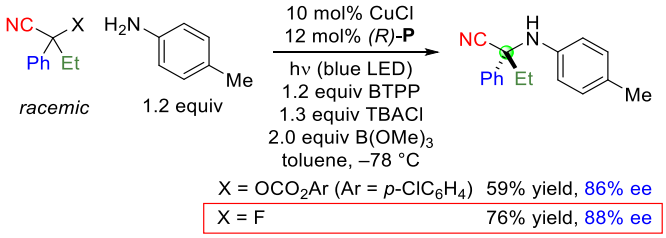

Procedure. In a nitrogen-filled glovebox, a 40 mL vial equipped with a PTFE magnetic stir bar was charged with CuCl (8.0 mg, 0.080 mmol), **P** (113 mg, 0.096 mmol), toluene (5 mL), and BTPP (290 μL, 0.960 mmol). The reaction mixture was stirred for 4 h. Next, *p*-toluidine (103 mg, 0.960 mmol), tetrabutylammonium chloride (289 mg, 1.04 mmol), and toluene (8 mL) were added, and the mixture was stirred for 5 min. The vial was capped with a PTFE-lined open top cap, and the joint was wrapped with electrical tape. The vial was removed from the glovebox, and a nitrogen-filled balloon was attached. The vial was

submerged in a low-form hemispherical Dewar flask filled with pre-cooled methanol (–78 °C), and the reaction mixture was stirred for 5 min. The electrophile (0.800 mmol) was weighed into a 4 mL vial, and the vial was capped with a PTFE-lined open top cap. The vial was attached to a Schlenk line and evacuated/backfilled with nitrogen three times. A nitrogen-filled balloon was attached, and 1.5 mL of toluene was added. The resulting solution was transferred to the pre-cooled reaction mixture; additional toluene (1.5 mL) was used to wash the vial, and the washing was added to the reaction mixture. $B(OMe)_3$ (180 μL, 1.6 mmol) was added via syringe, and the resulting mixture was stirred for 5 min. The balloon was removed, and vacuum grease was applied to the PTFE cap to seal the needle puncture. Kessil® PR160-440 nm lamps (one per reaction) were installed 5 cm above the reaction, and the vial was irradiated for 48 h.

Work-up. Same as **GP-4.**

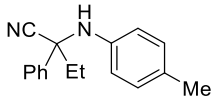

2-Phenyl-2-(*p*-tolylamino)butanenitrile. The title compound was prepared according to the above procedure from *p*-toluidine and the two electrophiles indicated below, with 48 h of reaction time. The product was purified by column chromatography on silica gel (hexanes/EtOAc/dichloromethane = 30/1/1). Pale-yellow solid.

From 2-fluoro-2-phenylbutanenitrile: *(R)*-**P**: 152 mg, 76% yield, 88% ee; *(S)*-**P**: 147 mg, 73% yield, 88% ee.

From 4-chlorophenyl (1-cyano-1-phenylpropyl) carbonate: *(R)*-**P**: 113 mg, 57% yield, 87% ee; *(S)*-**P**: 121 mg, 60% yield, 86% ee.

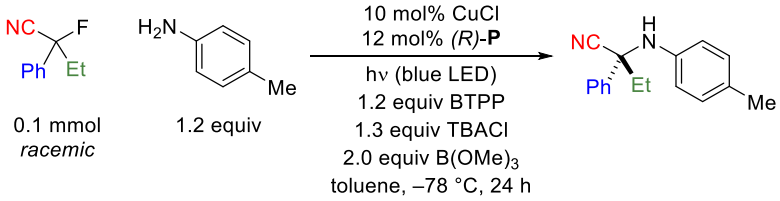

Variations	conv.	yield	ee
-	**93%**	**83%**	**90%**
TBACl only	56%	41%	75%
$B(OMe)_3$ only	51%	37%	35%
no TBACl and $B(OMe)_3$	44%	33%	35%
no light irradiation	<1%	-	-

Control Experiments. 2-Fluoro-2-phenylbutanenitrile was reacted with *p*-toluidine according to modified **GP-6** in the presence of 1.0 equiv the additives. The yield of the product and the conversion of the electrophile were determined by ^{1}H NMR analysis using 1,3,5-trimethoxybenzene as an internal standard, and the ee was determined by chiral HPLC.

2.4.9. Assignments of absolute configuration

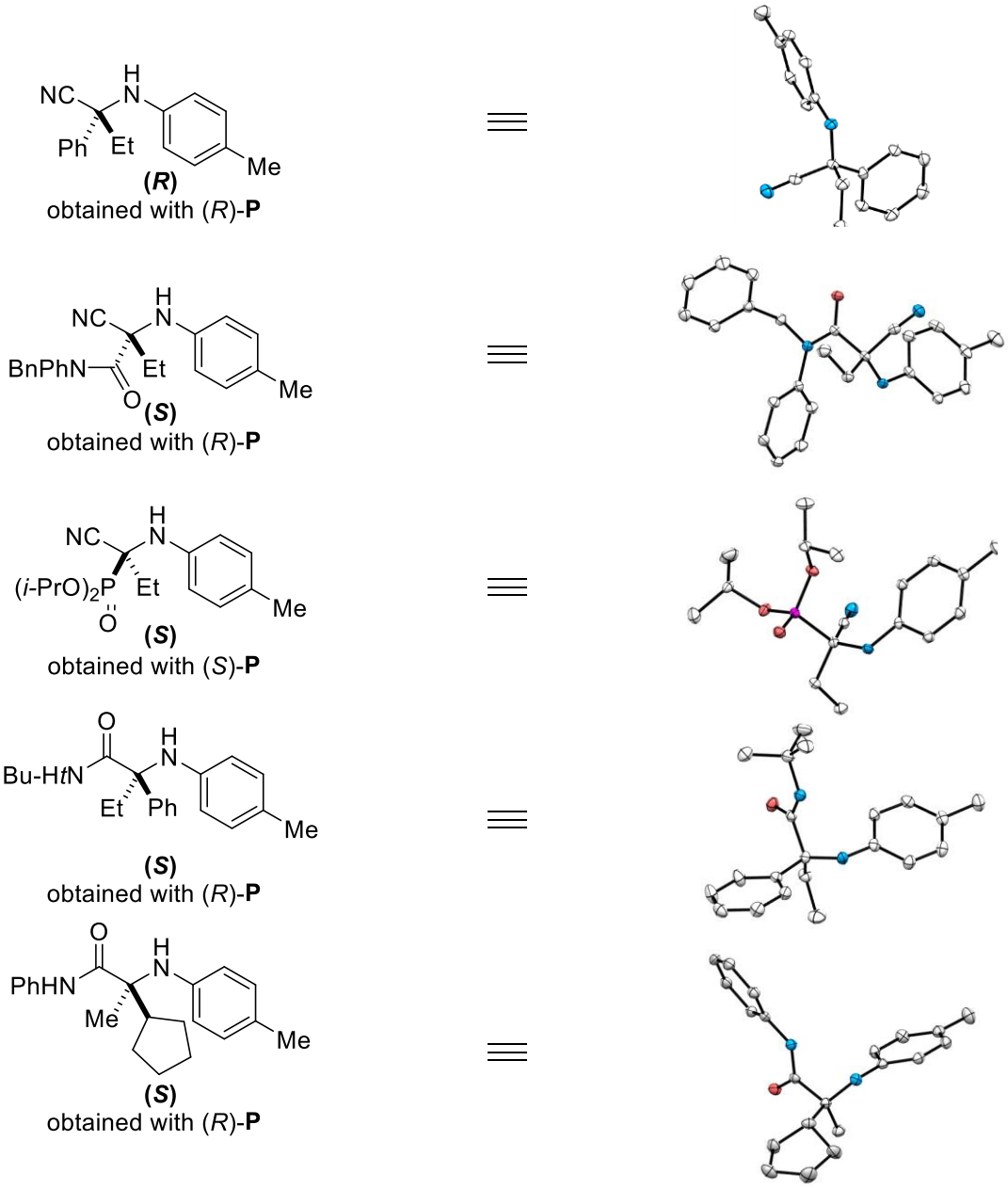

Overview of the X-ray crystal structures of the coupling products, with thermal ellipsoids at 50% probability level.

All other absolute configurations are assigned by analogy.

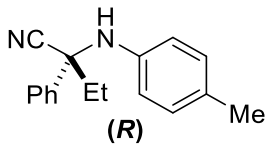

(*R*)
obtained with (*R*)-**P**
CCDC 2098019

≡

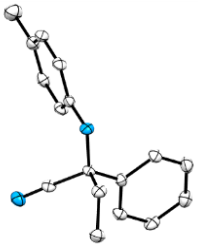

Thermal ellipsoid plot at 50% probability level. For clarity, the hydrogen atoms are not shown. The N–H hydrogen atom was found in the residual density map and refined isotropically.

A colorless needle-like specimen of $C_{17}H_{18}N_2$ was used for the X-ray crystallographic analysis. The X-ray intensity data were measured (λ = 1.54178 Å). The total exposure time was 21.48 h. The frames were integrated with the Bruker SAINT software package using a narrow-frame algorithm. The integration of the data using an orthorhombic unit cell yielded a total of 16065 reflections to a maximum θ angle of 70.05° (0.82 Å resolution), of which 2665 were independent (average redundancy 6.028, completeness = 100.0%, R_{int} = 7.28%, R_{sig} = 4.40%) and 2477 (92.95%) were greater than $2\sigma(F^2)$. The final cell constants of a = 5.8710(6) Å, b = 9.1726(9) Å, c = 25.984(4) Å, volume = 1399.3(3) $Å^3$, are based upon the refinement of the XYZ-centroids of 8448 reflections above 20 σ(I) with 6.803° < 2θ < 144.9°. Data were corrected for absorption effects using the Multi-Scan method (SADABS). The ratio of minimum to maximum apparent transmission was 0.765.

The structure was solved and refined using the Bruker SHELXTL Software Package, using the space group P 21 21 21, with Z = 4 for the formula unit, $C_{17}H_{18}N_2$. The final anisotropic full-matrix least-squares refinement on F^2 with 178 variables converged at R1 = 3.81%, for the observed data and wR2 = 8.87% for all data. The goodness-of-fit was 1.101. The largest peak in the final difference electron density synthesis was 0.191 $e^-/Å^3$, and the largest hole was -0.156 $e^-/Å^3$ with an RMS deviation of 0.038 $e^-/Å^3$. On the basis of the final model, the calculated density was 1.188 g/cm^3 and F(000), 536 e^-.

Sample and crystal data

Identification code	V21210_1	
Chemical formula	$C_{17}H_{18}N_2$	
Formula weight	250.33 g/mol	
Temperature	100(2) K	
Wavelength	1.54178 Å	
Crystal system	orthorhombic	
Space group	P 21 21 21	
Unit cell dimensions	a = 5.8710(6) Å	α = 90°
	b = 9.1726(9) Å	β = 90°
	c = 25.984(4) Å	γ = 90°
Volume	1399.3(3) $Å^3$	
Z	4	
Density (calculated)	1.188 g/cm^3	
Absorption coefficient	0.539 mm^{-1}	
F(000)	536	

Data collection and structural refinement

Theta range for data collection	3.40 to 70.05°
Index ranges	-7<=h<=7, -11<=k<=11, -31<=l<=31
Reflections collected	16065
Independent reflections	2665 [R(int) = 0.0728]
Coverage of independent reflections	100.0%
Absorption correction	Multi-Scan
Structure solution technique	direct methods
Structure solution program	SHELXT 2018/2 (Sheldrick, 2018)
Refinement method	Full-matrix least-squares on F^2
Refinement program	SHELXL-2018/3 (Sheldrick, 2018)

Function minimized	$\Sigma\, w(F_o^2 - F_c^2)^2$	
Data / restraints / parameters	2665 / 0 / 178	
Goodness-of-fit on F^2	1.101	
Final R indices	2477 data; $I>2\sigma(I)$	R1 = 0.0381, wR2 = 0.0870
	all data	R1 = 0.0431, wR2 = 0.0887
Weighting scheme	$w=1/[\sigma^2(F_o^2)+(0.0158P)^2+0.5513P]$ where $P=(F_o^2+2F_c^2)/3$	
Absolute structure parameter	0.0(3)	
Largest diff. peak and hole	0.191 and -0.156 eÅ^{-3}	
R.M.S. deviation from mean	0.038 eÅ^{-3}	

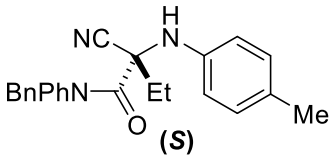

obtained with (*R*)-**P**

CCDC 2098016

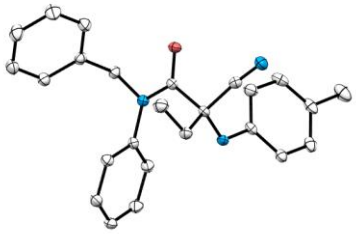

Thermal ellipsoid plot at 50% probability level. For clarity, the hydrogen atoms are not shown. The N–H hydrogen atom was found in the residual density map and refined isotropically.

A colorless needle-like specimen of $C_{25}H_{25}N_3O$, approximate dimensions 0.050 mm x 0.050 mm x 0.200 mm, was used for the X-ray crystallographic analysis. The X-ray intensity data were measured (λ = 1.54178 Å). The integration of the data using an orthorhombic unit cell yielded a total of 24918 reflections to a maximum θ angle of 70.07° (0.82 Å resolution), of which 4074 were independent (average redundancy 6.116, completeness = 100.0%, R_{int} = 4.91%, R_{sig} = 2.65%) and 3848 (94.45%) were greater than $2\sigma(F^2)$. The final cell constants of a = 10.1183(4) Å, b = 13.4557(5) Å, c = 15.7406(6) Å, volume = 2143.06(14) $Å^3$, are based upon the refinement of the XYZ-centroids of 9977 reflections above 20 σ(I) with 8.645° < 2θ < 144.7°. The calculated minimum and maximum transmission coefficients (based on crystal size) are 0.8930 and 0.9720.

The structure was solved and refined using the Bruker SHELXTL Software Package, using the space group P 21 21 21, with Z = 4 for the formula unit, $C_{25}H_{25}N_3O$. The final anisotropic full-matrix least-squares refinement on F^2 with 268 variables converged at R1 = 3.06%, for the observed data and wR2 = 7.66% for all data. The goodness-of-fit was 1.085. The largest peak in the final difference electron density synthesis was 0.138 $e^-/Å^3$, and the largest hole was -0.186 $e^-/Å^3$ with an RMS deviation of 0.035 $e^-/Å^3$. On the basis of the final model, the calculated density was 1.189 g/cm^3 and F(000), 816 e^-.

Sample and crystal data

Identification code	V21193	
Chemical formula	$C_{25}H_{25}N_3O$	
Formula weight	383.48 g/mol	
Temperature	100(2) K	
Wavelength	1.54178 Å	
Crystal size	0.050 x 0.050 x 0.200 mm	
Crystal habit	colorless needle	
Crystal system	orthorhombic	
Space group	P 21 21 21	
Unit cell dimensions	a = 10.1183(4) Å	α = 90°
	b = 13.4557(5) Å	β = 90°
	c = 15.7406(6) Å	γ = 90°
Volume	2143.06(14) $Å^3$	
Z	4	
Density (calculated)	1.189 g/cm^3	
Absorption coefficient	0.576 mm^{-1}	
F(000)	816	

Data collection and structural refinement

Theta range for data collection	4.32 to 70.07°
Index ranges	-12<=h<=12, -16<=k<=16, -19<=l<=19
Reflections collected	24918
Independent reflections	4074 [R(int) = 0.0491]
Coverage of independent reflections	100.0%
Max. and min. transmission	0.9720 and 0.8930
Structure solution technique	direct methods
Structure solution program	SHELXT 2014/5 (Sheldrick, 2014)

Refinement method	Full-matrix least-squares on F^2	
Refinement program	SHELXL-2018/3 (Sheldrick, 2018)	
Function minimized	$\Sigma\, w(F_o^2 - F_c^2)^2$	
Data / restraints / parameters	4074 / 0 / 268	
Goodness-of-fit on F^2	1.085	
Final R indices	3848 data; $I>2\sigma(I)$	R1 = 0.0306, wR2 = 0.0740
	all data	R1 = 0.0337, wR2 = 0.0766
Weighting scheme	$w=1/[\sigma^2(F_o^2)+(0.0372P)^2+0.3289P]$ where $P=(F_o^2+2F_c^2)/3$	
Absolute structure parameter	0.12(11)	
Largest diff. peak and hole	0.138 and -0.186 eÅ^{-3}	
R.M.S. deviation from mean	0.035 eÅ^{-3}	

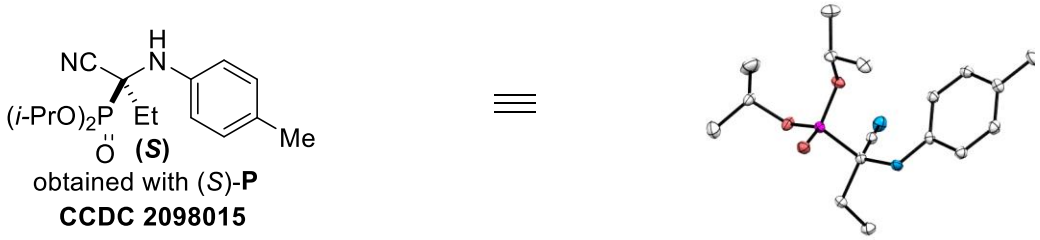

Thermal ellipsoid plot at 50% probability level. For clarity, the hydrogen atoms are not shown. The N–H hydrogen atom was found in the residual density map and refined isotropically.

A clear colorless block-like specimen of $C_{17}H_{27}N_2O_3P$, approximate dimensions 0.100 mm x 0.150 mm x 0.300 mm, was used for the X-ray crystallographic analysis. The X-ray intensity data were measured (λ = 1.54178 Å). The total exposure time was 2.67 h. The frames were integrated with the Bruker SAINT software package using a narrow-frame algorithm. The integration of the data using a monoclinic unit cell yielded a total of 18004 reflections to a maximum θ angle of 70.04° (0.82 Å resolution), of which 3476 were independent (average redundancy 5.180, completeness = 100.0%, R_{int} = 3.31%, R_{sig} = 2.68%) and 3405 (97.96%) were greater than $2\sigma(F^2)$. The final cell constants of a = 9.7328(3) Å, b = 7.5268(2) Å, c = 12.9041(4) Å, β = 100.3380(10)°, volume = 929.97(5) $Å^3$, are based upon the refinement of the XYZ-centroids of 9861 reflections above 20 σ(I) with 6.963° < 2θ < 144.8°. Data were corrected for absorption effects using the Multi-Scan method (SADABS). The ratio of minimum to maximum apparent transmission was 0.871.

The structure was solved and refined using the Bruker SHELXTL Software Package, using the space group P 1 21 1, with Z = 2 for the formula unit, $C_{17}H_{27}N_2O_3P$. The final anisotropic full-matrix least-squares refinement on F^2 with 218 variables converged at R1 = 2.41%, for the observed data and wR2 = 6.31% for all data. The goodness-of-fit was 1.056. The largest peak in the final difference electron density synthesis was 0.230 $e^-/Å^3$, and the largest hole was -0.235 $e^-/Å^3$ with an RMS deviation of 0.037 $e^-/Å^3$. On the basis of the final model, the calculated density was 1.208 g/cm^3 and F(000), 364 e^-.

Sample and crystal data

Identification code	V21188
Chemical formula	$C_{17}H_{27}N_2O_3P$
Formula weight	338.37 g/mol
Temperature	100(2) K
Wavelength	1.54178 Å
Crystal size	0.100 x 0.150 x 0.300 mm
Crystal habit	clear colorless block
Crystal system	monoclinic
Space group	P 1 21 1
Unit cell dimensions	a = 9.7328(3) Å α = 90°
	b = 7.5268(2) Å β = 100.3380(10)°
	c = 12.9041(4) Å γ = 90°
Volume	929.97(5) $Å^3$
Z	2
Density (calculated)	1.208 g/cm^3
Absorption coefficient	1.437 mm^{-1}
F(000)	364

Data collection and structural refinement

Theta range for data collection	3.48 to 70.04°
Index ranges	-11<=h<=11, -9<=k<=9, -15<=l<=15
Reflections collected	18004
Independent reflections	3476 [R(int) = 0.0331]
Coverage of independent reflections	100.0%
Absorption correction	Multi-Scan
Structure solution technique	direct methods
Structure solution program	SHELXT 2014/5 (Sheldrick, 2014)
Refinement method	Full-matrix least-squares on F^2

Refinement program	SHELXL-2018/3 (Sheldrick, 2018)	
Function minimized	$\Sigma\, w(F_o^2 - F_c^2)^2$	
Data / restraints / parameters	3476 / 1 / 218	
Goodness-of-fit on F^2	1.056	
Final R indices	3405 data; $I>2\sigma(I)$	R1 = 0.0241, wR2 = 0.0627
	all data	R1 = 0.0247, wR2 = 0.0631
Weighting scheme	$w=1/[\sigma^2(F_o^2)+(0.0363P)^2+0.1270P]$ where $P=(F_o^2+2F_c^2)/3$	
Absolute structure parameter	0.037(6)	
Largest diff. peak and hole	0.230 and -0.235 $eÅ^{-3}$	
R.M.S. deviation from mean	0.037 $eÅ^{-3}$	

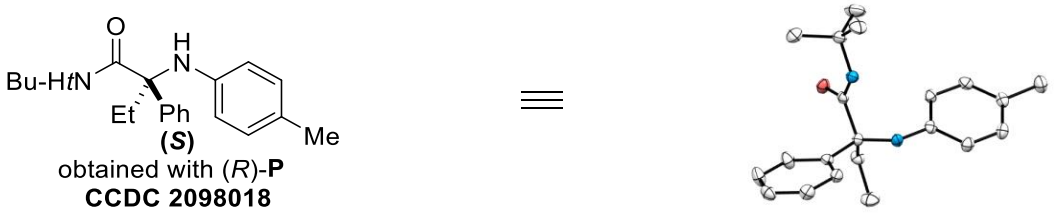

Thermal ellipsoid plot at 50% probability level. For clarity, the hydrogen atoms are not shown. The N–H hydrogen atom was found in the residual density map and refined isotropically.

A specimen of $C_{21}H_{28}N_2O$ was used for the X-ray crystallographic analysis. The X-ray intensity data were measured (λ = 1.54178 Å). The total exposure time was 10.53 h. The frames were integrated with the Bruker SAINT software package using a narrow-frame algorithm. The integration of the data using an orthorhombic unit cell yielded a total of 22825 reflections to a maximum θ angle of 70.10° (0.82 Å resolution), of which 3758 were independent (average redundancy 6.074, completeness = 100.0%, R_{int} = 6.46%, R_{sig} = 3.78%) and 3540 (94.20%) were greater than $2\sigma(F^2)$. The final cell constants of a = 6.3131(14) Å, b = 16.797(4) Å, c = 18.605(3) Å, volume = 1972.9(7) $Å^3$, are based upon the refinement of the XYZ-centroids of 9931 reflections above 20 σ(I) with 7.088° < 2θ < 144.7°. Data were corrected for absorption effects using the Multi-Scan method (SADABS). The ratio of minimum to maximum apparent transmission was 0.883.

The structure was solved and refined using the Bruker SHELXTL Software Package, using the space group P 21 21 21, with Z = 4 for the formula unit, $C_{21}H_{28}N_2O$. The final anisotropic full-matrix least-squares refinement on F^2 with 230 variables converged at R1 = 3.22%, for the observed data and wR2 = 7.79% for all data. The goodness-of-fit was 1.039. The largest peak in the final difference electron density synthesis was 0.165 $e^-/Å^3$, and the largest hole was -0.154 $e^-/Å^3$ with an RMS deviation of 0.032 $e^-/Å^3$. On the basis of the final model, the calculated density was 1.092 g/cm^3 and F(000), 704 e^-.

Sample and crystal data

Identification code	V21199	
Chemical formula	$C_{21}H_{28}N_2O$	
Formula weight	324.45 g/mol	
Temperature	100(2) K	
Wavelength	1.54178 Å	
Crystal size	0.200 x 0.100 x 0.050 mm	
Crystal habit	clear colorless needle	
Crystal system	orthorhombic	
Space group	P 21 21 21	
Unit cell dimensions	a = 6.3131(14) Å	α = 90°
	b = 16.797(4) Å	β = 90°
	c = 18.605(3) Å	γ = 90°
Volume	1972.9(7) $Å^3$	
Z	4	
Density (calculated)	1.092 g/cm^3	
Absorption coefficient	0.518 mm^{-1}	
F(000)	704	

Data collection and structural refinement

Theta range for data collection	3.54 to 70.10°
Index ranges	-7<=h<=7, -20<=k<=20, -22<=l<=22
Reflections collected	22825
Independent reflections	3758 [R(int) = 0.0646]
Coverage of independent reflections	100.0%
Absorption correction	Multi-Scan
Structure solution technique	direct methods
Structure solution program	SHELXT 2014/5 (Sheldrick, 2014)
Refinement method	Full-matrix least-squares on F^2
Refinement program	SHELXL-2018/3 (Sheldrick, 2018)

Function minimized	$\Sigma\, w(F_o^2 - F_c^2)^2$	
Data / restraints / parameters	3758 / 0 / 230	
Goodness-of-fit on F^2	1.039	
Final R indices	3540 data; $I>2\sigma(I)$	R1 = 0.0322, wR2 = 0.0763
	all data	R1 = 0.0374, wR2 = 0.0779
Weighting scheme	$w=1/[\sigma^2(F_o^2)+(0.0396P)^2+0.2154P]$ where $P=(F_o^2+2F_c^2)/3$	
Absolute structure parameter	0.21(11)	
Largest diff. peak and hole	0.165 and -0.154 $eÅ^{-3}$	
R.M.S. deviation from mean	0.032 $eÅ^{-3}$	

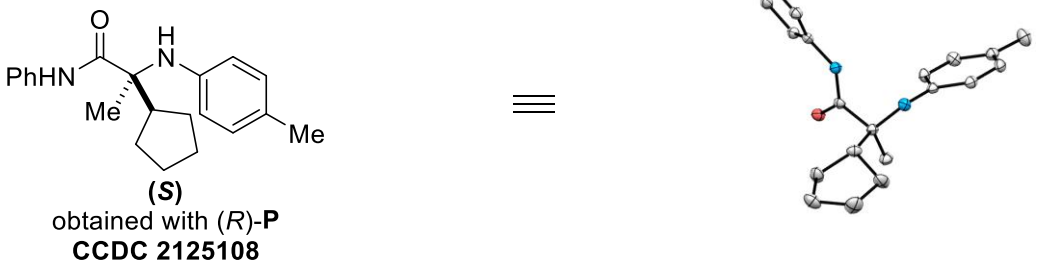

Thermal ellipsoid plot at 50% probability level. For clarity, the hydrogen atoms are not shown. The N–H hydrogen atom was found in the residual density map and refined isotropically.

A clear white needle-like specimen of $C_{21}H_{26}N_2O$ was used for the X-ray crystallographic analysis. The X-ray intensity data were measured (λ = 1.54178 Å). The total exposure time was 4.67 hours. The frames were integrated with the Bruker SAINT software package using a narrow-frame algorithm. The integration of the data using a monoclinic unit cell yielded a total of 15223 reflections to a maximum θ angle of 74.68° (0.80 Å resolution), of which 3600 were independent (average redundancy 4.229, completeness = 99.4%, R_{int} = 3.42%, R_{sig} = 2.54%) and 3506 (97.39%) were greater than $2\sigma(F^2)$. The final cell constants of a = 11.3104(15) Å, b = 6.3399(4) Å, c = 13.0915(13) Å, β = 108.923(9)°, volume = 888.02(16) $Å^3$, are based upon the refinement of the XYZ-centroids of 9981 reflections above 20 σ(I) with 7.138° < 2θ < 144.4°. Data were corrected for absorption effects using the Multi-Scan method (SADABS). The ratio of minimum to maximum apparent transmission was 0.895.

The structure was solved and refined using the Bruker SHELXTL Software Package, using the space group P2(1), with Z = 2 for the formula unit, $C_{21}H_{26}N_2O$. The final anisotropic full-matrix least-squares refinement on F^2 with 231 variables converged at R1 = 2.99%, for the observed data and wR2 = 7.80% for all data. The goodness-of-fit was 1.040. The largest peak in the final difference electron density synthesis was 0.186 $e^-/Å^3$, and the largest hole was -0.156 $e^-/Å^3$ with an RMS deviation of 0.031 $e^-/Å^3$. On the basis of the final model, the calculated density was 1.206 g/cm^3 and F(000), 348 e^-.

Sample and crystal data

Identification code	V21353	
Chemical formula	$C_{21}H_{26}N_2O$	
Formula weight	322.44 g/mol	
Temperature	100(2) K	
Wavelength	1.54178 Å	
Crystal habit	clear white needle	
Crystal system	monoclinic	
Space group	P2(1)	
Unit cell dimensions	a = 11.3104(15) Å	α = 90°
	b = 6.3399(4) Å	β = 108.923(9)°
	c = 13.0915(13) Å	γ = 90°
Volume	888.02(16) $Å^3$	
Z	2	
Density (calculated)	1.206 g/cm^3	
Absorption coefficient	0.575 mm^{-1}	
F(000)	348	

Data collection and structure refinement

Theta range for data collection	3.57 to 74.68°
Index ranges	-12<=h<=14, -7<=k<=7, -16<=l<=16
Reflections collected	15223
Independent reflections	3600 [R(int) = 0.0342]
Coverage of independent reflections	99.4%
Absorption correction	Multi-Scan
Structure solution technique	direct methods
Structure solution program	SHELXT 2018/2 (Sheldrick, 2018)
Refinement method	Full-matrix least-squares on F^2
Refinement program	SHELXL-2018/3 (Sheldrick, 2018)
Function minimized	$\Sigma\, w(F_o^2 - F_c^2)^2$
Data / restraints / parameters	3600 / 1 / 231
Goodness-of-fit on F^2	1.040

Final R indices	3506 data; $I>2\sigma(I)$	R1 = 0.0299, wR2 = 0.0772
	all data	R1 = 0.0306, wR2 = 0.0780
Weighting scheme	$w=1/[\sigma^2(F_o^2)+(0.0419P)^2+0.1765P]$ where $P=(F_o^2+2F_c^2)/3$	
Absolute structure parameter	-0.04(8)	
Largest diff. peak and hole	0.186 and -0.156 eÅ^{-3}	
R.M.S. deviation from mean		0.031 eÅ^{-3}

2.4.10. Mechanistic studies

2.4.10.1. Preparation of *(S)*-DTBM-SEGPHOS-CuCl (Cu_A)

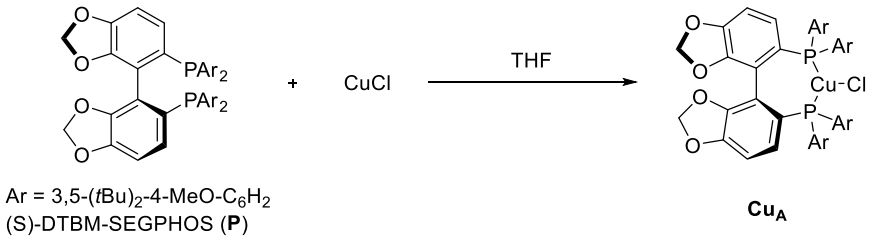

***(S)*-DTBM-SEGPHOS-CuCl (Cu_A).** The title compound was synthesized via a slight modification of a literature procedure.[10,11] An oven-dried 20 mL vial was charged with CuCl (104 mg, 1.05 mmol), (*S*)-**P** (1.18 g, 1.00 mmol), and a magnetic stir bar. THF (4 mL) was added, and the vial was capped and covered with aluminum foil. The reaction mixture was stirred for 6 h, and then it was filtered through Grade GF/D Glass Microfiber (Whatman products, Cytiva) tightly fixed in an oven-dried glass pipette. The solvent was removed in vacuo, and the resulting solid was triturated with pentane (2 mL) three times to afford a white solid (1.27 g, 99% yield). Spectroscopic data match those reported in the literature.[34,50] The title compound was stored in a glovebox (–35 °C).

^{1}H NMR (400 MHz, toluene-d_8) δ 8.51 (br, 4H), 7.80 (t, J = 5.8 Hz, 4H), 6.77 (dt, J = 9.1, 4.8 Hz, 2H), 6.19 (d, J = 8.0 Hz, 2H), 5.28 (s, 2H), 5.13 (s, 2H), 3.32 (s, 6H), 3.22 (s, 6H), 1.58 (s, 36H), 1.31 (s, 36H).

^{31}P NMR (162 MHz, toluene-d_8) δ –4.8.

2.4.10.2. Representative side products from a coupling reaction

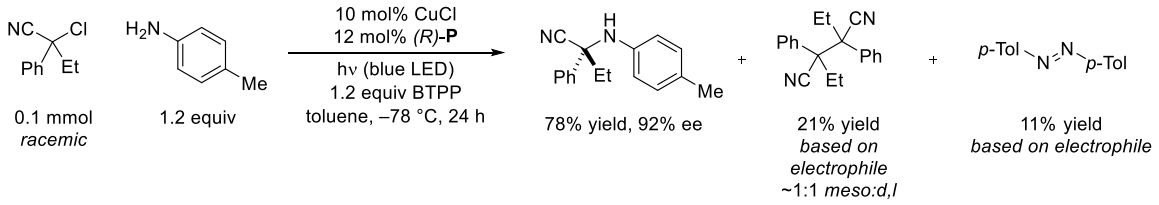

2-Chloro-2-phenylbutanenitrile was reacted with *p*-toluidine according to **GP-6**. The yields of 2-phenyl-2-(*p*-tolylamino)butanenitrile, 2,3-diethyl-2,3-diphenylsuccinonitrile, and (*E*)-1,2-di-*p*-tolyldiazene were analyzed via ^{1}H NMR spectroscopy with 1,3,5-trimethoxybenzene (17 mg, 0.10 mmol) as an internal standard.

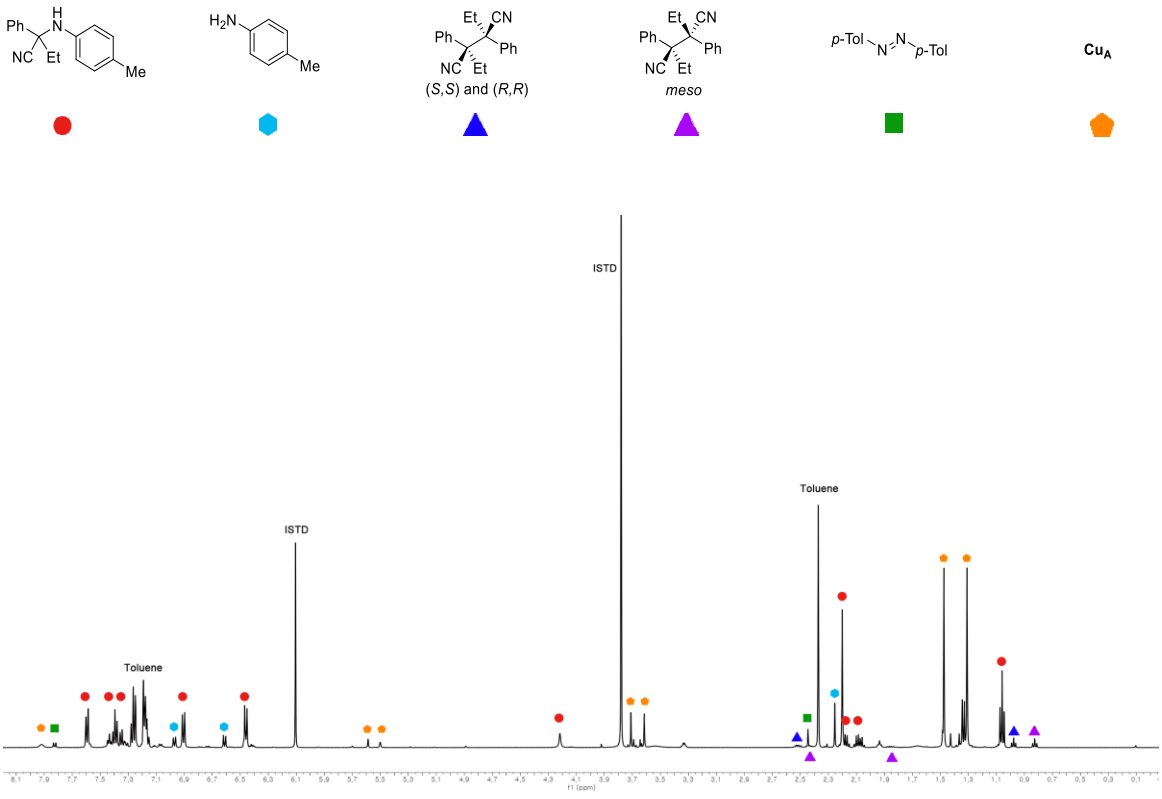

Figure 2.18. Representative ^{1}H NMR spectrum ($CDCl_3$, 500 MHz) of an unpurified reaction mixture showing a 78% yield of the C–N coupling product (calibrated using 1,3,5-trimethoxybenzene).

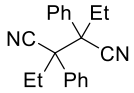

2,3-Diethyl-2,3-diphenylsuccinonitrile. The title compound was isolated via preparative TLC (hexanes/EtOAc = 10/1) as a mixture of two diastereomers. Spectroscopic data match those reported in the literature.[51]

Meso: ^{1}H NMR (500 MHz, $CDCl_3$) δ 7.57 (d, *J* = 7.1 Hz, 4H), 7.44 (d, *J* = 7.0 Hz, 6H), 2.43 (dq, *J* = 14.3, 7.3 Hz, 2H), 1.84 (dq, *J* = 14.4, 7.3 Hz, 2H), 0.81 (t, *J* = 7.2 Hz, 6H).

(*S,S*) and (*R,R*): ^{1}H NMR (500 MHz, $CDCl_3$) δ 7.24 (d, *J* = 7.2 Hz, 2H), 7.18 (t, *J* = 7.5 Hz, 4H), 7.06 (d, *J* = 7.7 Hz, 4H), 2.52 (qd, *J* = 7.1, 2.4 Hz, 4H), 0.97 (t, *J* = 7.2 Hz, 6H).

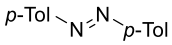

***(E)*-1,2-di-*p*-tolyldiazene.** The title compound was purified via preparative TLC (hexanes/EtOAc = 10/1). Spectroscopic data match those reported in the literature.[52]

^{1}H NMR (500 MHz, $CDCl_3$) δ 7.81 (d, *J* = 8.1 Hz, 4H), 7.31 (d, *J* = 8.0 Hz, 4H), 2.44 (s, 6H).

2.4.10.3. Coupling with aniline ($PhNH_2$) as the nucleophile

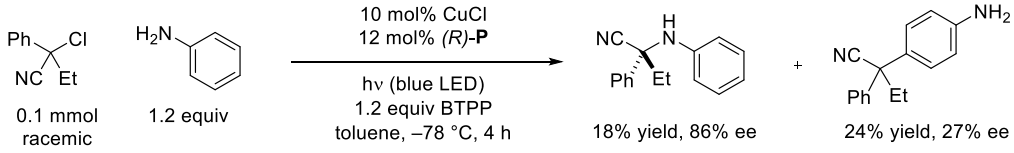

2-Chloro-2-phenylbutanenitrile was reacted with aniline according to **GP-6**. The yields of 2-phenyl-2-(phenylamino)butanenitrile and 2-(4-aminophenyl)-2-phenylbutanenitrile were analyzed via ^{1}H NMR spectroscopy with 1,3,5-trimethoxybenzene (17 mg, 0.10 mmol) as an internal standard. Samples of pure products were obtained via preparative TLC (hexanes/EtOAc = 5/1) for chiral HPLC analysis.

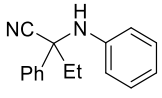

2-Phenyl-2-(phenylamino)butanenitrile. Yellow solid.

(R)-**P**: 17% yield, 83% ee; *(S)*-**P**: 18% yield, 84% ee

HPLC analysis: The ee was determined via HPLC on a CHIRALCEL OD-H column (10% *i*-PrOH in hexane, 1 mL/min); retention times for compound obtained using *(R)*-**P**: 6.6 min (major), 8.2 min (minor).

^{1}H NMR (500 MHz, $CDCl_3$) δ 7.59 (d, *J* = 7.7 Hz, 2H), 7.40 (t, *J* = 7.4 Hz, 2H), 7.35 (t, *J* = 7.2 Hz, 1H), 7.10 (t, *J* = 7.8 Hz, 2H), 6.78 (t, *J* = 7.3 Hz, 1H), 6.54 (d, *J* = 8.2 Hz, 2H), 4.30 (s, 1H), 2.21 (dq, *J* = 14.5, 7.3 Hz, 1H), 2.10 (dq, *J* = 14.5, 7.5 Hz, 1H), 1.07 (t, *J* = 7.4 Hz, 3H).

^{13}C NMR (126 MHz, $CDCl_3$) δ 143.7, 138.5, 129.2, 129.1, 128.7, 125.8, 120.0, 119.9, 115.8, 62.2, 38.5, 9.0.

FT-IR (film): 3382, 3057, 3027, 2973, 2851, 2232, 1604, 1518, 1499, 1449, 1318, 1258, 1204, 1181, 1078, 1038, 919, 872, 747, 697, 691 cm^{-1}.

HRMS (ESI+) *m/z* $[M+H]^+$ calcd for $C_{16}H_{17}N_2^+$: 237.1386, found: 237.1398.

$[\alpha]^{23}_D$ = –154 (*c* 1.0, $CHCl_3$); 83% ee, from (*R)*-**P**.

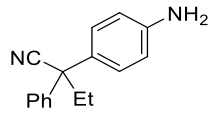

2-(4-Aminophenyl)-2-phenylbutanenitrile. Brown solid.

(R)-**P**: 22% yield, 23% ee; *(S)*-**P**: 26% yield, 24% ee.

HPLC analysis: The ee was determined via HPLC on a CHIRALPAK IC column (30% *i*-PrOH in hexane, 1 mL/min); retention times for compound obtained using *(R)*-**P**: 9.2 min (major), 7.7 min (minor).

^{1}H NMR (500 MHz, $CDCl_3$) δ 7.40 – 7.29 (m, 4H), 7.27 (t, *J* = 7.3 Hz, 1H), 7.14 (d, *J* = 8.5 Hz, 2H), 6.64 (d, *J* = 8.5 Hz, 2H), 3.72 (s, 2H), 2.47 – 2.27 (m, *J* = 7.0 Hz, 2H), 1.05 (t, *J* = 7.3 Hz, 3H).

^{13}C NMR (126 MHz, $CDCl_3$) δ 146.0, 140.9, 130.0, 128.8, 128.2, 127.7, 127.0, 122.8, 115.2, 51.9, 33.0, 10.3.

FT-IR (film): 3370, 3031, 2973, 2937, 2879, 2232, 1624, 1515, 1448, 1291, 1187, 1139, 824, 756, 699 cm^{-1}.

HRMS (ESI+) *m/z* $[M+H]^+$ calcd for $C_{16}H_{17}N_2^+$: 237.1386, found: 237.1400.

$[\alpha]^{23}_D$ = +13.5 (*c* 1.0, $CHCl_3$); 23% ee, from (R*)*-**P**.

2.4.10.4. Time-course profile of the standard coupling reaction

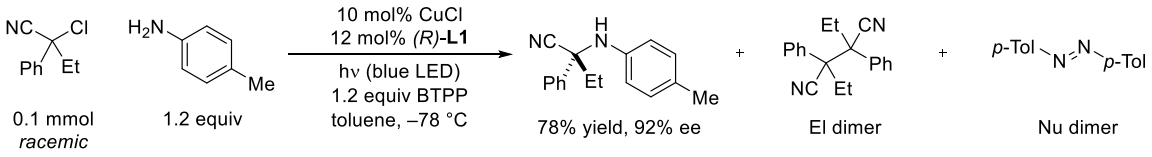

2-Chloro-2-phenylbutanenitrile and *p*-toluidine were reacted and analyzed (**GP-6**).

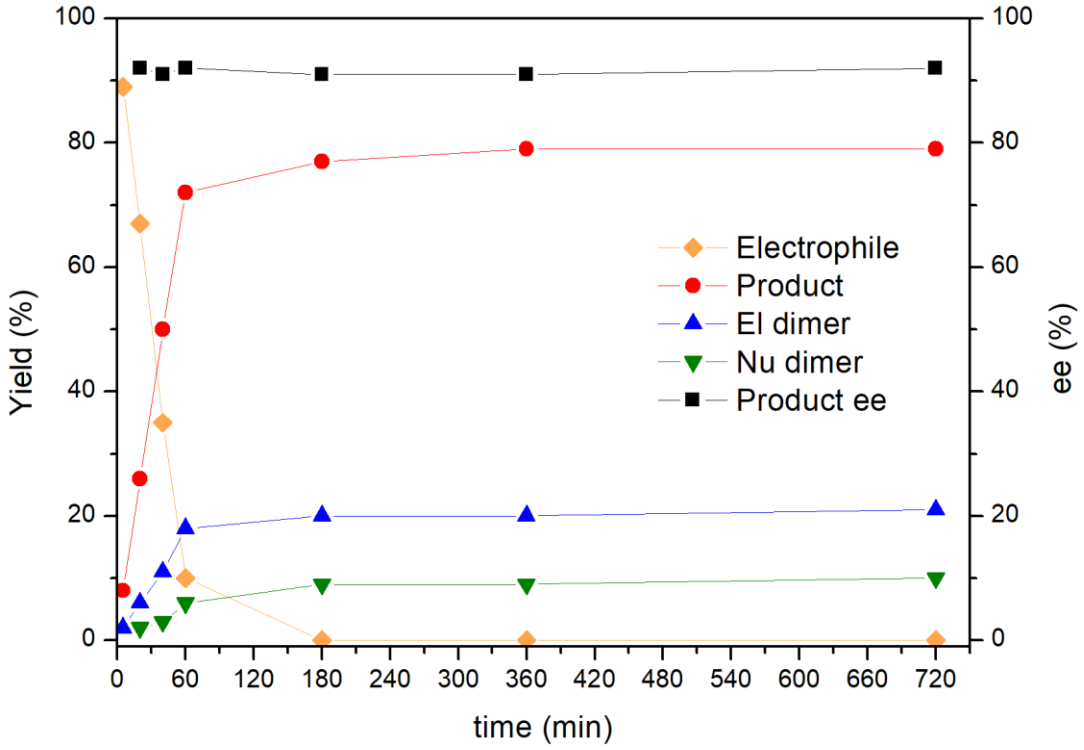

Figure 2.19. Time-course profile of the standard coupling reaction, analyzed via ^{1}H NMR spectroscopy to determine the conversion of the electrophile and the yield of the desired product and byproducts, and analyzed via chiral HPLC to determine the ee of the desired product. "time" = time of irradiation. Yields of the byproducts are based on the electrophile and yields of the "El dimer" are the sum of the two diastereomers.

2.4.10.5. Cu_A as the dominant Cu(I) species during catalysis

UV-vis analysis of the initial stage of the reaction at –78 °C. A solution of **Cu_A** (0.5 mM) was prepared by dissolving 6.4 mg (5.0 μmol) of **Cu_A** in 10 mL of toluene. A solution of **Cu_A** (0.5 mM), BTPP (6.0 mM), *p*-toluidine (6.0 mM), and 2-chloro-2-phenylbutanenitrile (5.0 mM) was prepared by dissolving 6.4 mg (5.0 μmol) of **Cu_A,** 18.8 mg (60 μmol) of BTPP, 6.4 mg of *p*-toluidine (60 μmol), and 9.0 mg of 2-chloro-2-phenylbutanenitrile (50 μmol) in 10 mL of toluene. Each solution was pipetted into a 1 cm path length cuvette, which was sealed with a high-vacuum Teflon valve (Kontes). The absorption spectra were acquired at –78 °C (**Figure 2.7a**). The absorption of **Cu_A** has λ_{max} = 376 nm with $\varepsilon = 3890\ M^{-1}\ cm^{-1}$.

The UV-vis absorption of each reagent in the catalytic reaction was measured to ensure that there is no significant overlap between **Cu_A** and the other reagents (**Figure 2.20**). Time-course UV-vis monitoring of **Cu_A** during catalysis could not be achieved due to overlap of the absorption peak of **Cu_A** with peaks that emerge upon irradiation.

The emission spectrum of a Kessil® PR160-440 nm lamp was measured at the Beckman Institute Molecular Materials Resource Center (MMRC) using a StellarNet BlackComet Spectroradiometer.

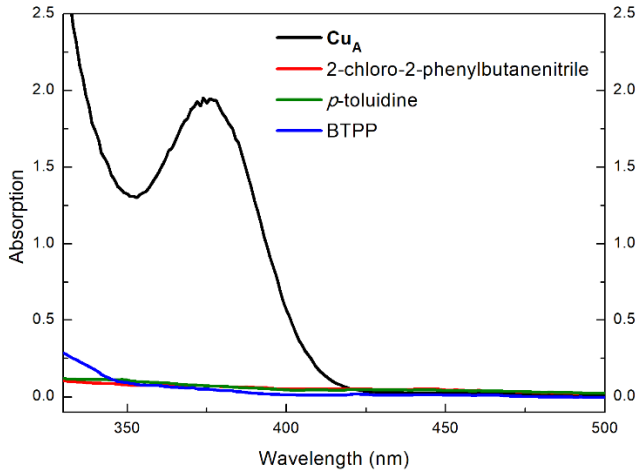

Figure 2.20. UV-vis absorption of **Cu_A** (0.5 mM, black), 2-chloro-2-phenylbutanenitrile (5 mM, red), *p*-toluidine (6 mM, green), and BTPP (6 mM, blue) in toluene at –78 °C.

NMR analysis at room temperature. A solution of **Cu$_A$** (12.8 mg, 5.0 mM), BTPP (37.5 mg, 60 mM), and *p*-toluidine(12.9 mg, 60 mM) in toluene-d_8 (2 mL), as well as a solution of **Cu$_A$** (12.8 mg, 5.0 mM) in toluene-d_8 (2 mL), were prepared, and 500 μL of each solution was loaded into a J. Young NMR tube. The samples were analyzed via ^{1}H NMR (400 MHz) and ^{31}P NMR (162 MHz) spectroscopy at room temperature (**Figure 2.21**). ~3% free **P** is observed in the three-component mixture.

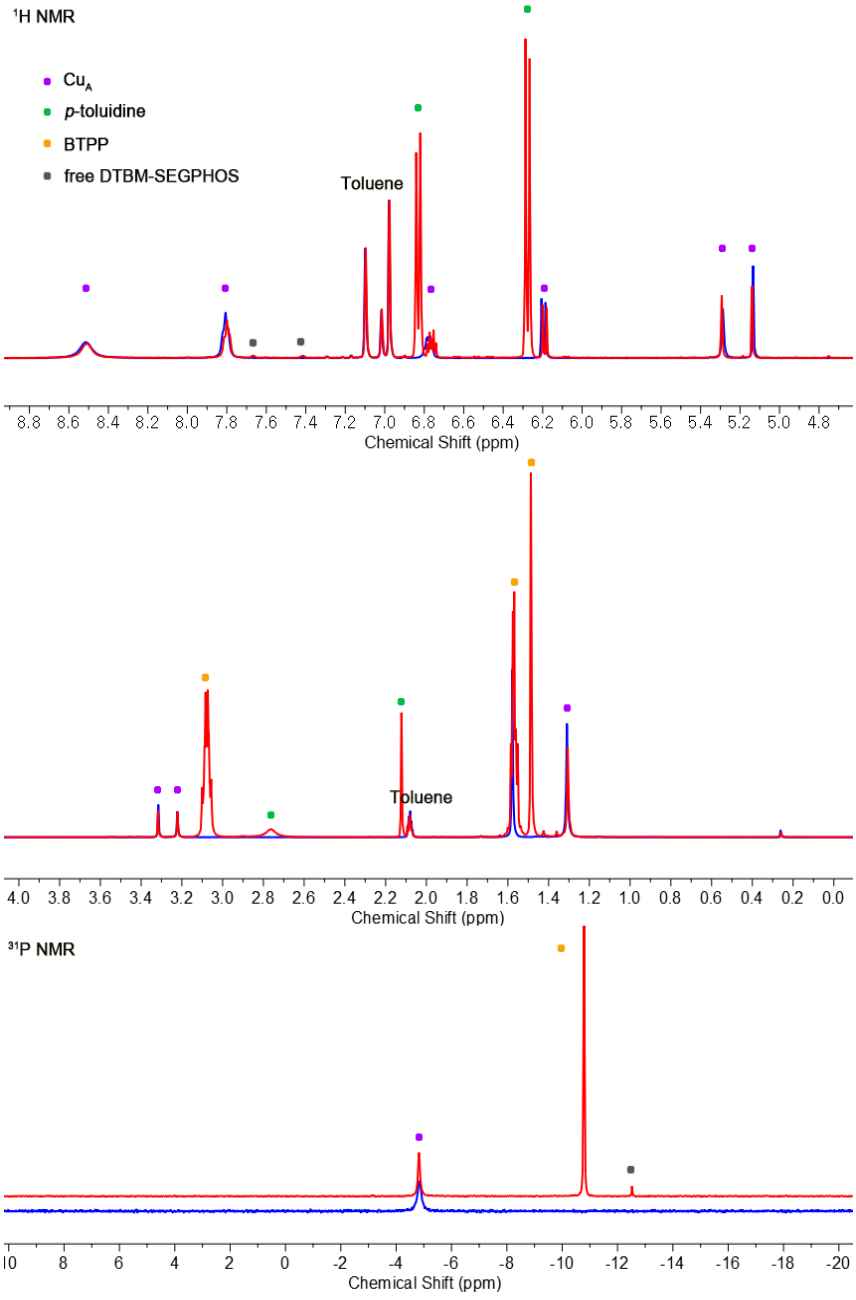

Figure 2.21. Blue: **Cu$_A$** only in toluene-d_8. Red: **Cu$_A$**, *p*-toluidine, and BTPP in toluene-d_8.

Temperature-dependent ^{1}H NMR spectra NMR spectra of Cu$_A$. A solution of **Cu$_A$** (3.2 mg, 5.0 mM) in toluene-d_8 (500 μL) was analyzed via ^{1}H NMR (400 MHz) and ^{31}P NMR (162 MHz) spectroscopy at different temperatures (**Figures 2.22** and **2.23**).

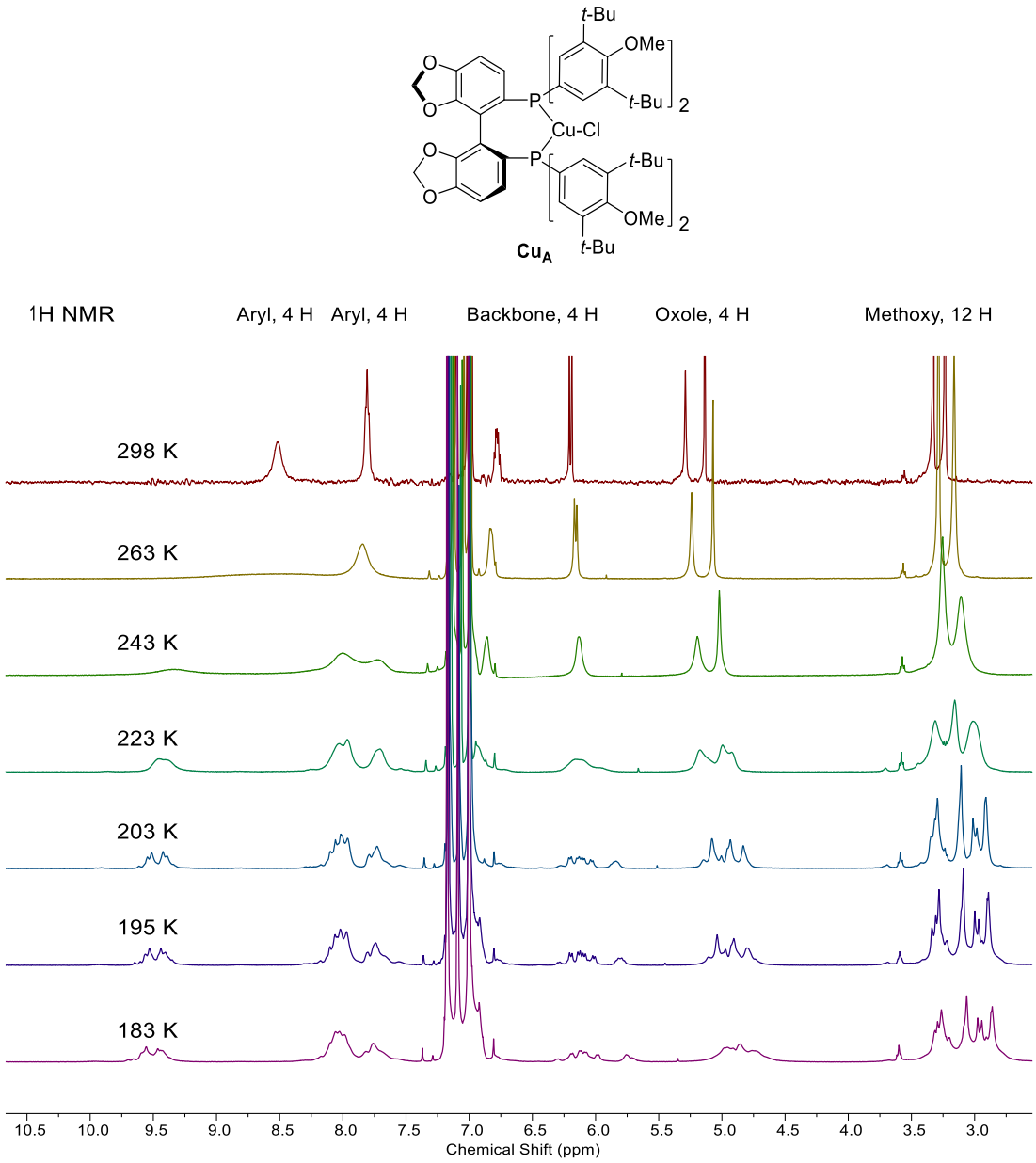

Figure 2.22. Temperature-dependent ^{1}H NMR spectra (400 MHz) of **Cu$_A$**.

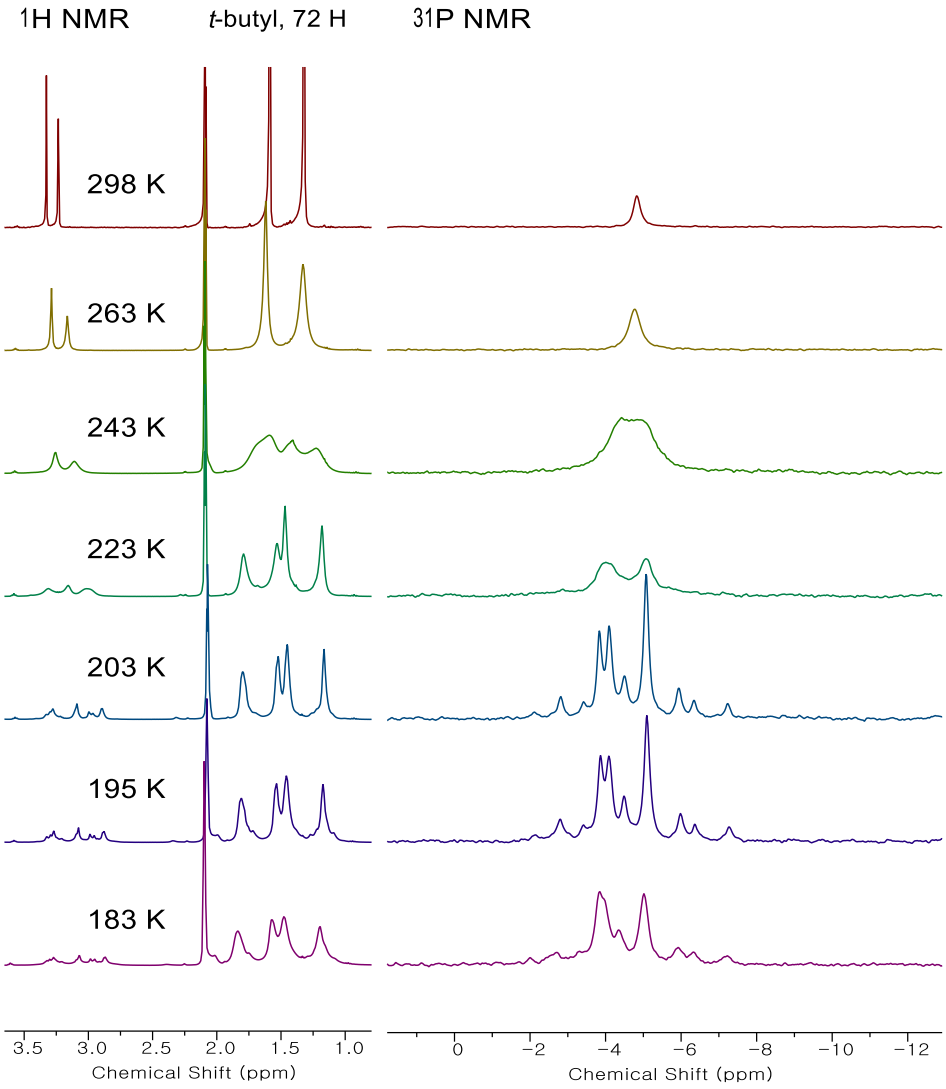

Figure 2.23. Temperature-dependent ^{1}H NMR (400 MHz) and ^{31}P NMR (162 MHz) spectra of **Cu$_A$**.

The complexity of the ^{31}P NMR spectra at lower temperature is presumably due to hindered rotation of the 4-methoxy groups of DTBM-SEGPHOS (**P**) at low temperature.[34]

^{1}H NMR (–78 °C, 400 MHz, toluene-d_8) δ 9.72 – 9.13 (m, 2H), 8.30 – 7.84 (m, 4H), 7.84 – 7.48 (m, 2H), 6.97 – 6.82 (m, 2H), 6.33 – 5.66 (m, 2H), 5.24 – 4.55 (m, 4H), 3.50 – 2.71 (m, 12H), 1.82 (s, 18H), 1.55 (s, 18H), 1.47 (s, 18H), 1.18 (s, 18H).

^{31}P NMR (–78 °C, 162 MHz, toluene-d_8) δ –2.16, –2.81, –3.42, –3.87, –4.11, –4.50, –5.11, –6.00, –6.38, –7.28.

Low-temperature monitoring of a catalyzed reaction via NMR spectroscopy.

Control reaction: 2-Chloro-2-phenylbutanenitrile was reacted with *p*-toluidine according to modified **GP-6** (in the presence of 1.0 equiv (17 mg, 0.10 mmol) of 1,3,5-trimethoxybenzene). The yield (80%, analyzed by GC using dodecane as an internal standard; average of two runs) and the ee (92%) of the coupling product were essentially identical to a reaction run in the absence of 1,3,5-trimethoxybenzene (77% yield and 92% ee), and 1,3,5-trimethoxybenzene was fully recovered from the reaction mixture (analyzed by GC). On the basis of these data, we conclude that the presence of 1,3,5-trimethoxybenzene does not interfere with the reaction of interest.

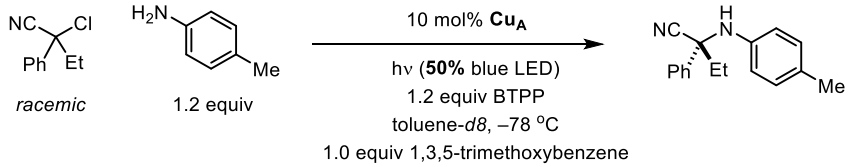

In a nitrogen-filled glovebox, a 4 mL vial equipped with a PTFE stir bar was sequentially charged with **Cu$_A$** (13 mg, 0.010 mmol), toluene-d_8 (2 mL), *p*-toluidine (13 mg, 0.12 mmol), BTPP (38 μL, 0.12 mmol), 1,3,5-trimethoxybenzene (17 mg, 0.10 mmol), and 2-chloro-2-phenylbutanenitrile (18 mg, 0.10 mmol). The mixture was stirred for 3 min, and then the resulting homogenous solution was transferred to three J. Young NMR tubes (500 μL each). The tubes were sealed, removed from the glovebox, and cooled for 5 min in a low-form hemispherical Dewar flask filled with pre-cooled methanol (–78 °C). Two Kessil® PR160-440 nm lamps were set at 50% intensity and placed 5 cm above the reaction mixtures. The mixtures were irradiated for the indicated times and then immediately frozen in a –116 °C bath (frozen ethanol). The tubes were quickly placed in a pre-cooled (–78 °C) Bruker 400 MHz NMR spectrometer and analyzed via ^{1}H NMR spectroscopy (**Figures 2.24** and **2.25**). The concentration of **Cu$_A$** was determined based on calibration of the resonance of **Cu$_A$** (δ 9.72 – 9.13 ppm, 2H) and the resonance of the internal standard (**Table 2.4**). The NMR tubes were warmed to room temperature and again analyzed via ^{1}H NMR spectroscopy to determine the yield and the conversion based on the internal standard. Overlap of the phosphorus chemical shifts of BTPP and **Cu$_A$** at –78°C prevented the reaction from being analyzed by ^{31}P NMR spectroscopy at –78°C.

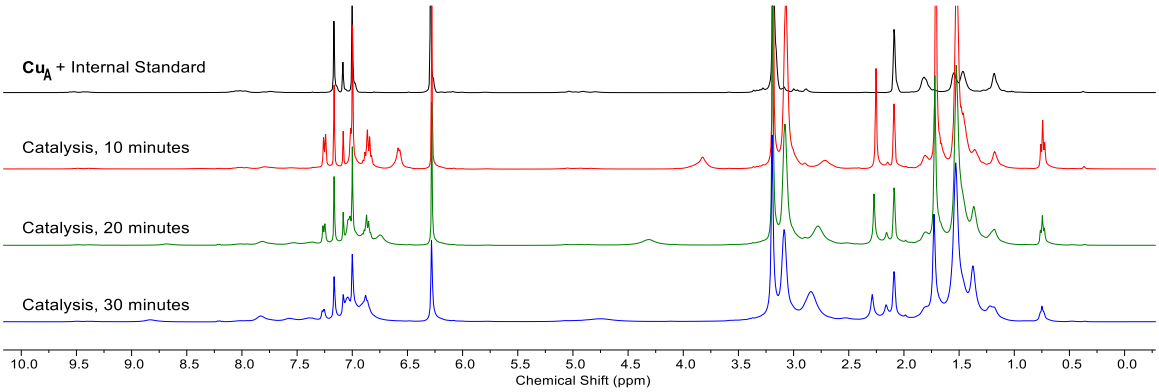

Figure 2.24. Monitoring **Cu$_A$** at low temperature during a coupling reaction.

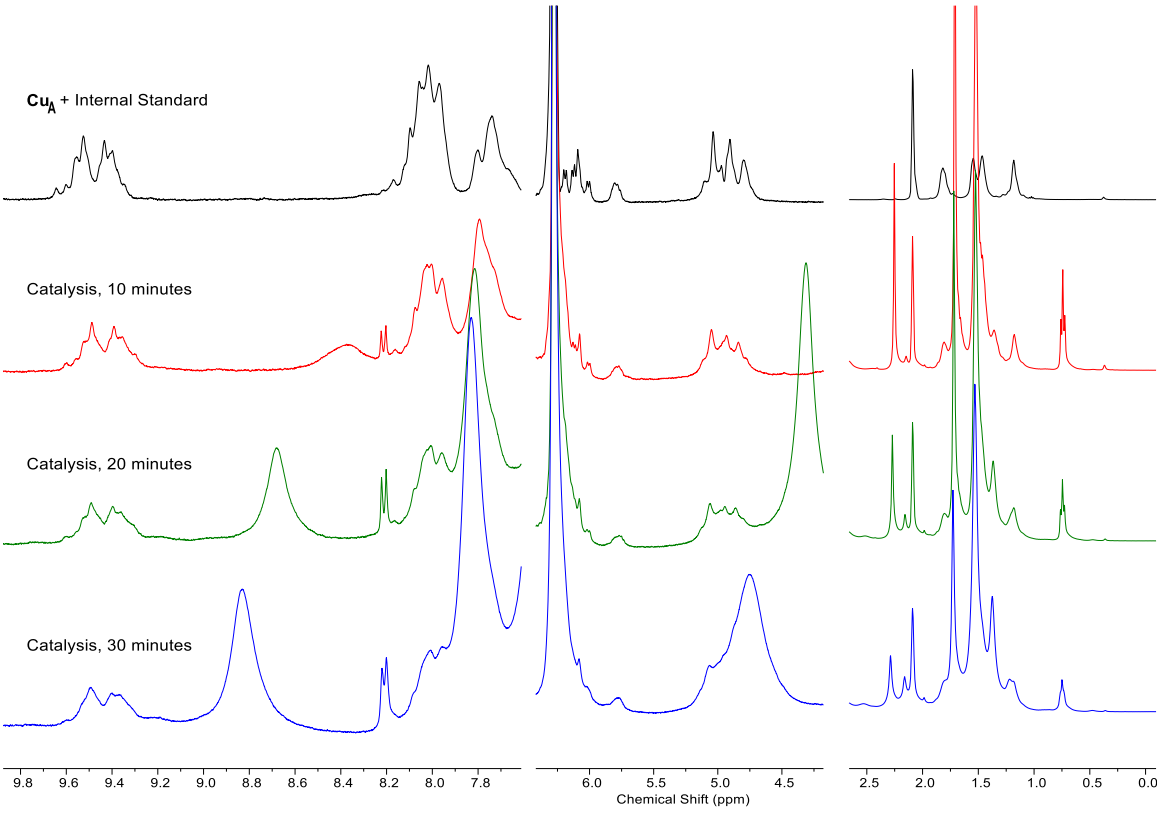

Figure 2.25. Characteristic resonances of **Cu$_A$** are maintained during a coupling reaction monitored at low temperature.

Table 2.4. Concentration of **Cu$_A$**, conversion of the electrophile, and yield of the coupling product according to NMR spectroscopy.

Reaction time	[Cu$_A$]/[Cu$_A$]$_0$	Conversion (%)	Product Yield (%)
10 min	93%	19	16
20 min	79%	42	36
30 min	54%	64	55

Note: The rate of these NMR-tube reactions was faster than that of the standard 0.10-mmol reaction (**GP-6**). The intensity of the light for the NMR-tube reactions was accordingly decreased so that the reactions have a similar rate (see the **Section 2.4.10.4**).

2.4.10.6. Steady-state and time-resolved emission spectroscopy of Cu$_A$

Steady-state emission spectra of Cu$_A$. Steady-state emission measurements at room temperature were performed with a 1 cm fluorescence cuvette containing a solution of **Cu$_A$** in toluene (0.50 mM). Steady-state emission measurements at 195 K and 77 K were performed by immersing EPR tubes containing solutions or glassed samples of **Cu$_A$** in toluene (0.5 mM) in a glass Dewar filled with dry ice/acetone or liquid nitrogen (**Figure 2.26**).

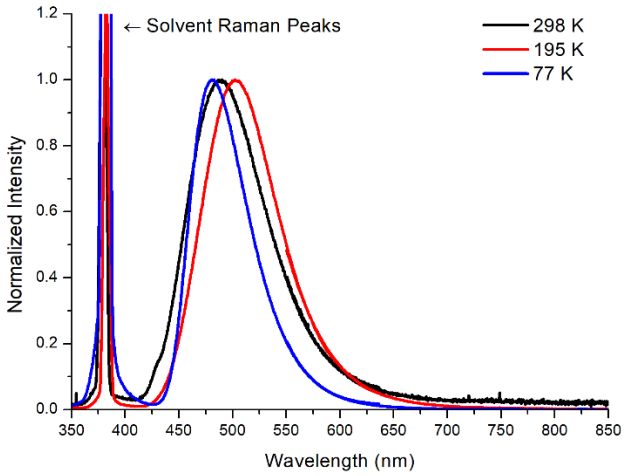

Figure 2.26. Steady-state emission of **Cu$_A$** in toluene at different temperatures ($\lambda_{excitation}$ = 355 nm).

Luminescence decay of Cu_A (298 K). Nanosecond ~ microsecond time scale luminescence decay measurements were performed with a 1 cm fluorescence cuvette containing a solution of **Cu_A** in toluene (5 mM, λ_{pump} = 355 nm, λ_{probe} = 480 nm). Two sets of decay were observed (long-lived, microsecond scale and short-lived, nanosecond scale). The lifetime of the long-lived luminescence of **Cu_A** was determined by the default exponential fitting tool provided in OriginPro 8 (**Figure 2.27**).

The lifetime of the short-lived luminescence of **Cu_A** was independently measured with a 1 cm fluorescence cuvette containing a solution of **Cu_A** in toluene (5 mM, λ_{pump} = 255 nm, λ_{probe} = 480 nm). The lifetime of the short-lived luminescence of **Cu_A** was determined by the default exponential fitting tool provided in OriginPro 8 (**Figure 2.28**).

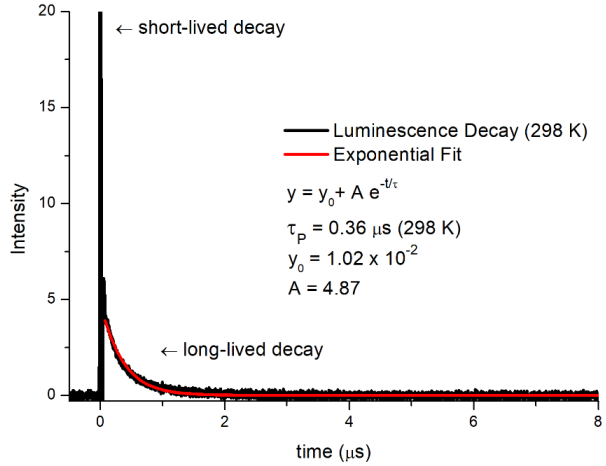

Figure 2.27. Long-lived luminescence decay for **Cu_A** measured at 298 K.

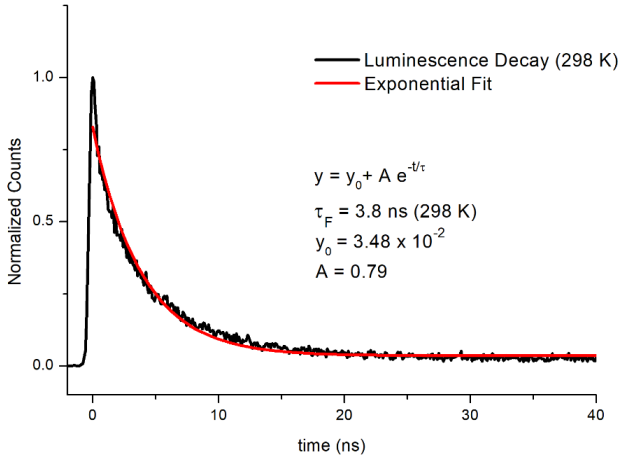

Figure 2.28. Short-lived luminescence decay for **Cu_A** measured at 298 K.

Excitation nature of Cu_A. Two sets of luminescence decay at the same observation wavelength are frequently observed for thermally activated delayed fluorescence (TADF) materials.[53] While these materials typically have a red shift of the emission at lower temperature due to the diminished delayed fluorescence (larger contribution of the phosphorescence),[54] emission of **Cu_A** at 77 K shows a blue shift compared to that measured at 195 K. The luminescence decay measured at this temperature performed by immersing EPR tubes containing solutions or glassed samples of **Cu_A** in toluene (5 mM) in a glass Dewar filled with dry ice/acetone (195 K, **Figure 2.29**, left) or liquid nitrogen (77 K, **Figure 2.29**, right) shows that the observed slow-decay process still contributes significantly. We therefore attribute the two sets of the decay directly to the fluorescence and phosphorescence of **Cu_A**. Based on their lifetimes, we propose the phosphorescence to be the dominant process of **Cu_A** for the photoinduced reduction of the electrophiles. MO visualization of the ground and triplet excited states of **Cu_A** suggests ^{3}MLCT from the copper *d* orbital to the ligand backbone (see the **Section 2.4.11**; DFT calculations).

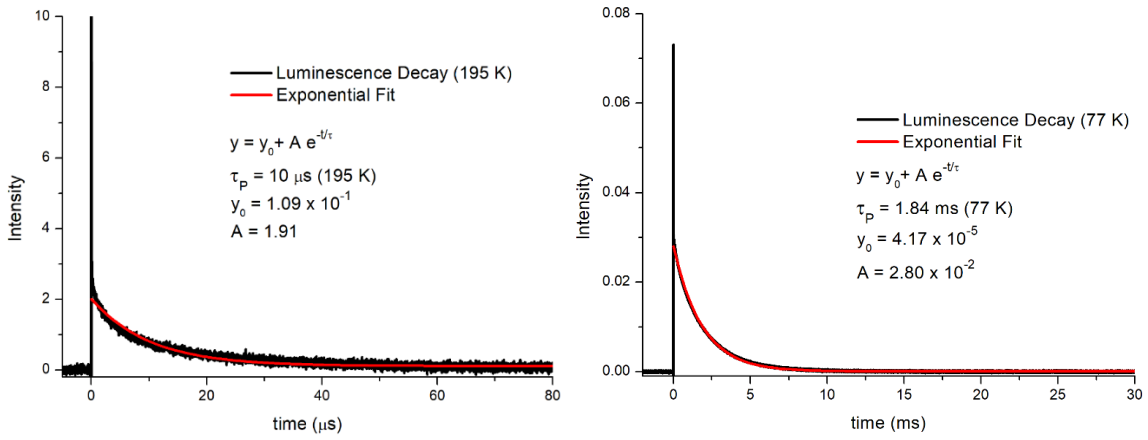

Figure 2.29. Long-lived luminescence decay for **Cu_A** measured at 195 K (left) and 77 K (right).

2.4.10.7. Stern-Volmer quenching of Cu_A

In a glovebox, **Cu_A** was dissolved in toluene to provide a 0.010 M solution. In a 4 mL vial with a PTFE-lined open-top screw cap, 2-chloro-2-phenylbutanenitrile was dissolved in toluene to make 0.0050, 0.010, 0.020, 0.044, 0.054, 0.072 M solutions. 1.5 mL of the solutions containing **Cu_A** was charged into 1 cm fluorescence cuvettes with a magnetic stir bar and PTFE-lined open-top screw cap (Starna Cells), and the cuvettes were sealed. The sealed cuvettes and vials were removed from the glovebox. Before the measurement, 1.5 mL of the solutions containing the electrophile were added to the cuvettes by syringe using air-free technique, and the solutions were vigorously stirred for 1 min and immediately subjected to the measurement. The lifetime of a non-emissive excited state of **Cu_A** as a function of electrophile concentration was measured at room temperature by transient absorption spectroscopy (λ_{pump} = 355 nm, λ_{probe} = 580 nm) (**Figure 2.30**). Data were analyzed using OriginPro 8 with the default exponential curve fitting function. The rate of quenching was determined to be k_q = 3.7 x 10^8 M^{-1} s^{-1} (**Figure 2.9**).

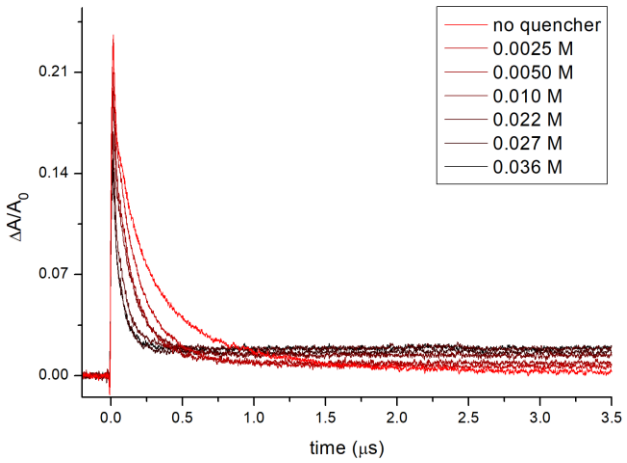

Figure 2.30. Transient absorbance decays for **Cu_A** with varying electrophile concentrations.

2.4.10.8. Electrochemistry

Electrochemical measurements were carried out using a CD instrument 600B electrochemical analyzer (**Figure 2.31** and **2.32**). A freshly polished glassy carbon electrode was used as the working electrode, and a graphite rod was used as the auxiliary electrode. An Ag/AgOTf reference electrode was employed, and solutions (THF) of electrolyte (0.1 M $TBAPF_6$) and analyte (1 mM) were used for each measurement. All redox potentials in the present work are reported versus the Fc/Fc^+ couple (+0.115 V versus our Ag/AgOTf reference electrode).

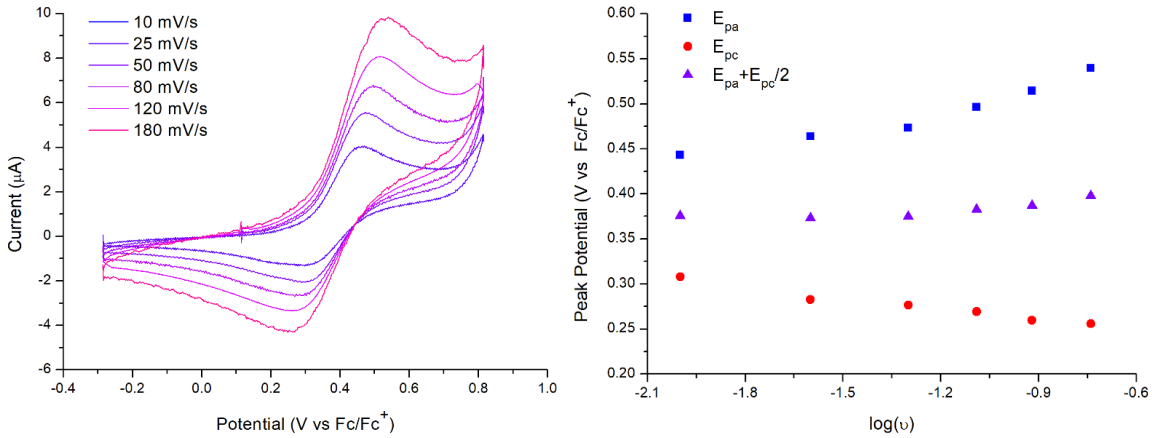

Figure 2.31. Cyclic voltammogram of **Cu_A** with scan rates ranging from 10 mV/s to 180 mV/s (left) and plot of the peak potentials vs the log of the scan rate (right), showing quasi-reversible features at $E_{1/2}$ = ~ 0.4 V (versus Fc/Fc^+).

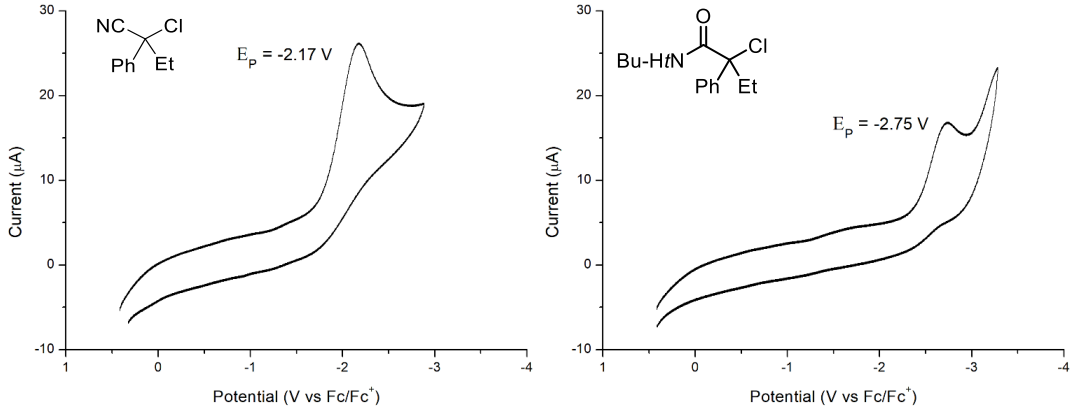

Figure 2.32. Cyclic voltammograms of representative electrophiles, showing irreversible features at E_P = –2.17 V and –2.75 V (versus Fc/Fc^+), respectively. Scan rate = 50 mV/s.

2.4.10.9. Estimated excited-state oxidation potential of Cu_A in THF

Steady-state emission spectra of Cu_A. Steady-state emission spectra were collected with a 1 cm fluorescence cuvette containing a solution of **Cu_A** in THF (0.5 mM). When light with $\lambda < 360$ nm was used, decomposition of **Cu_A** in THF generated a new emission band at ~400 nm and prevented the emission spectrum from being accurately measured. Therefore, the emission spectrum measured at $\lambda_{excitation} = 370$ nm was extrapolated using the default GaussAmp fitting function in OriginPro 8. The intensity plot of the emission of **Cu_A** at different excitation wavelengths was measured using $\lambda_{probe} = 480$ nm (**Figure 2.33**). E^{00} is estimated from the crossing point of the two plots (410 nm, ~ 3.0 eV). From the cyclic voltammogram of **Cu_A** (**Figure 2.31**), the excited-state oxidation potential of **Cu_A** is estimated to be $E_{1/2}(Cu^{II/I*}) \sim -2.6$ V (versus Fc/Fc^{+}).

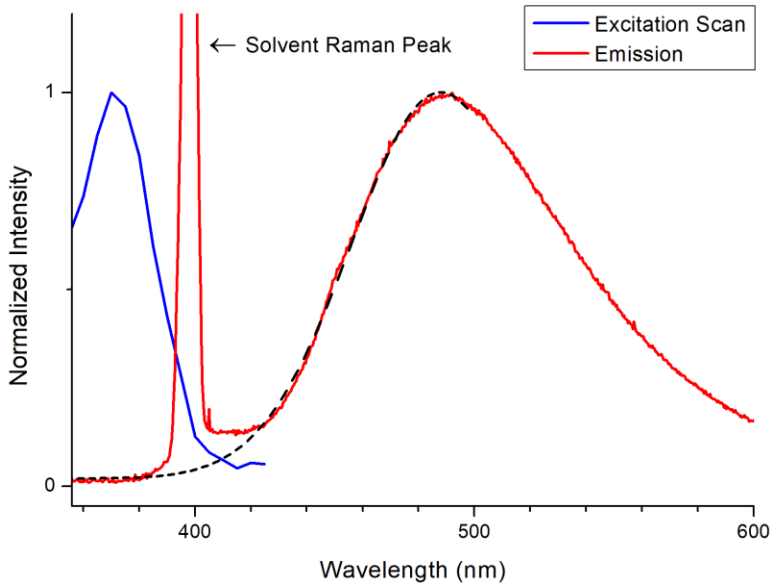

Figure 2.33. Steady-state emission of **Cu_A** in THF at room temperature ($\lambda_{excitation} = 370$ nm) and excitation scan of **Cu_A** in THF ($\lambda_{probe} = 480$ nm).

2.4.10.10. Reaction of Cu_A to form Cu_B; independent preparation of Cu_B

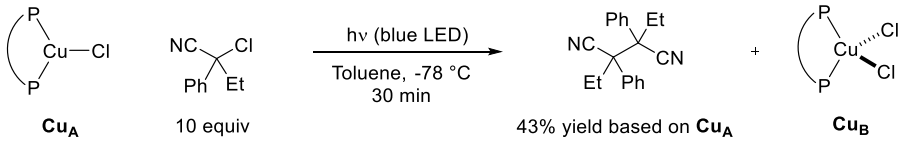

Photoinduced reduction of the electrophile by Cu_A: Quantification of the formation of the C–C coupled dimer of the electrophile. In a glovebox, a 4 mL vial equipped with a PTFE stir bar was sequentially charged with **Cu_A** (13 mg, 0.010 mmol), toluene (2 mL), and 2-chloro-2-phenylbutanenitrile (18 mg, 0.10 mmol). The vial was capped with a PTFE-lined cap and removed from the glovebox. The vial was cooled for 5 min in a low-form hemispherical Dewar flask filled with pre-cooled methanol (–78 °C). Two Kessil® PR160-440 nm lamps were installed 5 cm above the vials, and the vials were irradiated for 30 min, during which time the solution turned dark purple. The reaction mixture was warmed to room temperature, and 30% aqueous NH_4OH (0.5 mL) and EtOAc (0.5 mL) were added. The mixture was stirred for 1 min, and then the aqueous layer was extracted with 2 mL of EtOAc. The organic layer was dried over Na_2SO_4 and passed through a 2 cm plug of silica gel loaded in a pipet (the Na_2SO_4 was washed with EtOAc (2 x 2 mL), and the washings were passed through the silica gel). The combined organic filtrate was concentrated in vacuo, and an internal standard (1,3,5-trimethoxybenzene, 17 mg, 0.10 mmol) was added. The residue was dissolved in $CDCl_3$ and analyzed by ^1H NMR spectroscopy. The yield of the dimer was 43% based on **Cu_A** (average of two runs).

For control reactions, an analogous procedure was followed, using a vial covered with aluminum foil to block the light. The reaction mixture remained colorless, and the electrophile remained intact according to ^1H NMR spectroscopy.

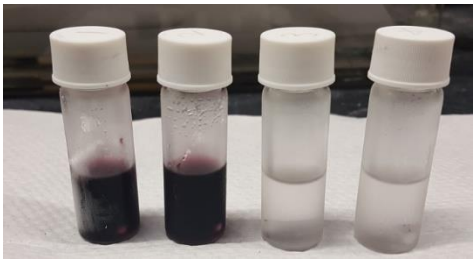

Stoichiometric reactions with irradiation (left two) and control reactions (right two).

Photoinduced reduction of the electrophile by Cu_A to form Cu_B (X-band EPR, 77 K). In a glovebox, a 4 mL vial equipped with a PTFE stir bar was sequentially charged with **Cu_A** (13 mg, 0.010 mmol), toluene (2 mL), and 2-chloro-2-phenylbutanenitrile (18 mg, 0.10 mmol). The resulting solution (300 µL) was loaded into an X-band EPR tube. The tube was sealed with a rubber stopper and removed from the glovebox. A nitrogen-filled balloon was quickly attached, and the reaction mixture was cooled for 5 min in a low-form hemispherical Dewar flask filled with pre-cooled methanol (–78 °C). Two Kessil® PR160-440 nm lamps were installed 5 cm above the tube, and the tube was irradiated for 40 min. The solution was frozen at 77 K and analyzed by X-band EPR spectroscopy (**Figure 2.34**).

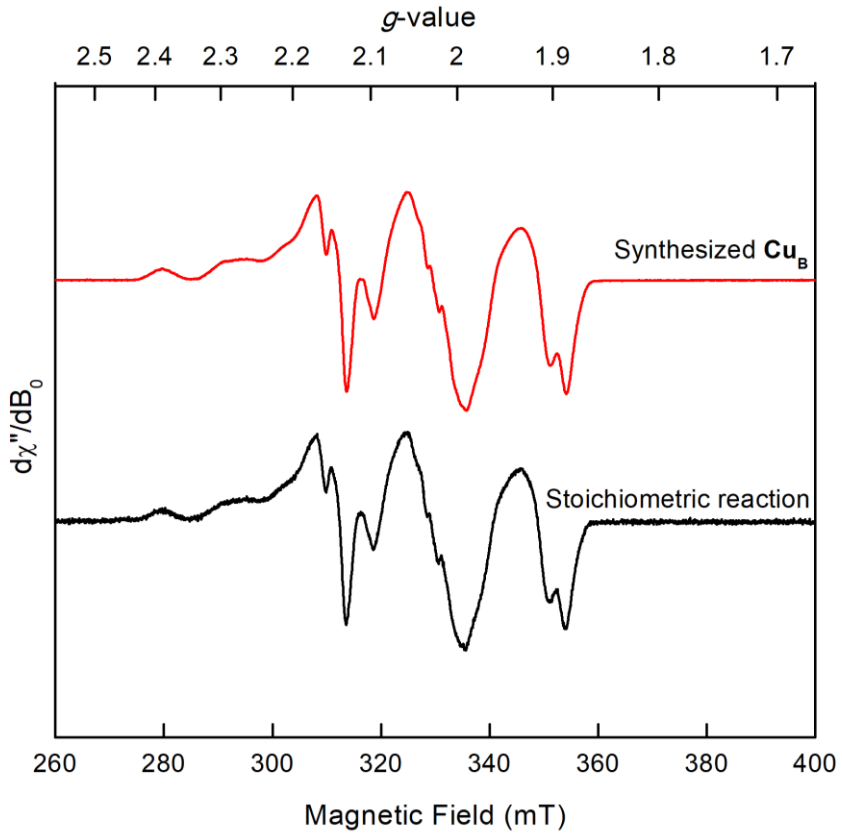

Figure 2.34. Normalized X-band EPR spectra of **Cu_B** (red trace) and a photoinduced stoichiometric reaction between **Cu_A** and 2-chloro-2-phenylbutanenitrile (black trace). Acquisition parameters: MW frequency = 9.372-9.374 GHz; temperature = 77 K; MW power = 140 µW; modulation amplitude = 0.4 mT; conversion time = 5.0 ms.

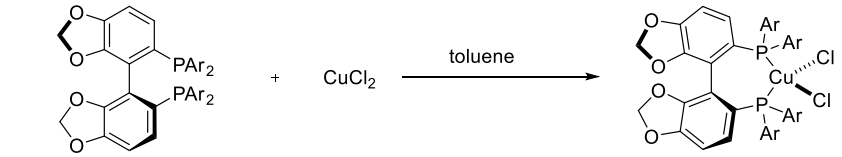

Ar = 3,5-(*t*Bu)$_2$-4-MeO-C$_6$H$_2$
(S)-DTBM-SEGPHOS (**P**)

Cu$_B$

Independent Synthesis of DTBM-SEGPHOS-CuCl$_2$ (Cu$_B$).

In-situ preparation (GP-8). In a glovebox, a 4 mL vial equipped with a PTFE stir bar was sequentially charged with $CuCl_2$ (1.6 mg, 0.012mmol), *(R)*-**P** (12 mg, 0.010 mmol), and toluene (1 mL). The reaction mixture was vigorously stirred for 30 min. The resulting dark-purple solution was filtered through a PTFE syringe filter (0.45 μm, InnoSep™). The yield of **Cu$_B$** was determined to be >95% by quantitative X- band EPR spectroscopy, using a solution of $CuSO_4$•$5H_2O$ in deionized water/glycerol (4:1, v/v) as an external standard. The dark-purple solution lost its color over 24 h at room temperature. Due to the instability of **Cu$_B$**, this solution was used immediately for further transformations. The identity of **Cu$_B$** was determined by its isolation (below).

Isolation. In a glovebox, a 20 mL vial equipped with a PTFE stir bar was sequentially charged with $CuCl_2$ (8.1 mg, 0.060 mmol), *(R)*-**P** (59 mg, 0.05 mmol), and 5 mL of toluene. The reaction mixture was vigorously stirred for 40 min. The resulting dark-purple solution was filtered through a PTFE syringe filter (0.45 μm, InnoSep™). The solution was cooled to –78 °C (glovebox cold well) for 5 min, and pre-chilled pentane (–78 °C, 12 mL) was layered onto the solution. The vial was capped and allowed to stand at –78 °C for 48 h. The resulting dark-purple solids were washed with pre-chilled pentane (–78 °C, 2 mL) two times and placed under vacuum to remove residual solvent. The purified material was obtained as DTBMSEGPHOS-$CuCl_2$(toluene)$_2$(pentane), as determined by X-ray crystallography and elemental analysis (40.9 mg, 54% yield). The isolated compound dissolved in toluene showed an identical X-band EPR spectrum to the solution prepared in situ (**Figure 2.34**).

Elemental analysis. Calcd for $C_{88}H_{116}O_8P_2Cl_2Cu$: C, 70.55; H, 7.80; Cl, 4.73; Cu, 4.24; O, 8.54; P, 4.13. Found: C, 70.11; H, 7.52.

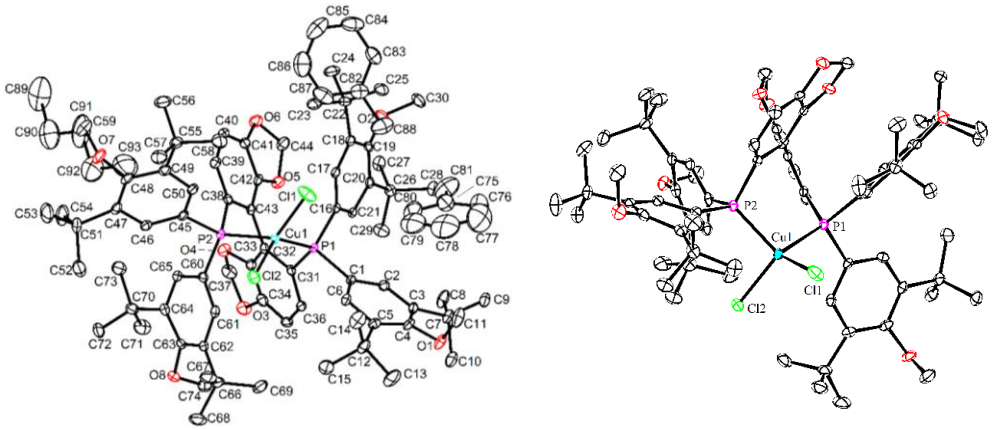

CCDC 2098022

Thermal ellipsoid plot of **Cu$_B$** at 50% probability level. For clarity, the hydrogen atoms are not shown. The asymmetric unit contains two molecules of toluene and one molecule of pentane (left), which are omitted on the right.

X-ray analysis. A brown needle-like specimen of $C_{93}H_{128}Cl_2CuO_8P_2$, approximate dimensions 0.100 mm x 0.100 mm x 0.250 mm, was used for the X-ray crystallographic analysis. The X-ray intensity data were measured (λ = 0.71073 Å). The total exposure time was 12.22 h. The frames were integrated with the Bruker SAINT software package using a narrow-frame algorithm. The integration of the data using an orthorhombic unit cell yielded a total of 61680 reflections to a maximum θ angle of 26.48° (0.80 Å resolution), of which 18034 were independent (average redundancy 3.420, completeness = 99.6%, R_{int} = 4.42%, R_{sig} = 5.08%) and 15750 (87.34%) were greater than $2\sigma(F^2)$. The final cell constants of a = 15.959(7) Å, b = 21.778(6) Å, c = 25.211(13) Å, volume = 8762.(6) $Å^3$, are based upon the refinement of the XYZ-centroids of 9095 reflections above 20 σ(I) with 4.519° < 2θ < 52.82°. Data were corrected for absorption effects using the Multi-Scan method (SADABS). The ratio of minimum to maximum apparent transmission was 0.880. The calculated minimum and maximum transmission coefficients (based on crystal size) are 0.9070 and 0.9610.

The structure was solved and refined using the Bruker SHELXTL Software Package, using the space group P 21 21 21, with Z = 4 for the formula unit, $C_{93}H_{128}Cl_2CuO_8P_2$. The final anisotropic full-matrix least-squares refinement on

F^2 with 987 variables converged at R1 = 3.95%, for the observed data and wR2 = 8.71% for all data. The goodness-of-fit was 1.020. The largest peak in the final difference electron density synthesis was 0.568 $e^-/Å^3$, and the largest hole was -0.390 $e^-/Å^3$ with an RMS deviation of 0.056 $e^-/Å^3$. On the basis of the final model, the calculated density was 1.190 g/cm^3 and F(000), 3372 e^-.

Sample and crystal data of $Cu_B(toluene)_2(pentane)$

Identification code	D21005	
Chemical formula	$C_{93}H_{128}Cl_2CuO_8P_2$	
Formula weight	1570.33 g/mol	
Temperature	100(2) K	
Wavelength	0.71073 Å	
Crystal size	0.100 x 0.100 x 0.250 mm	
Crystal habit	brown needle	
Crystal system	orthorhombic	
Space group	P 21 21 21	
Unit cell dimensions	a = 15.959(7) Å	α = 90°
	b = 21.778(6) Å	β = 90°
	c = 25.211(13) Å	γ = 90°
Volume	8762.(6) $Å^3$	
Z	4	
Density (calculated)	1.190 g/cm^3	
Absorption coefficient	0.400 mm^{-1}	
F(000)	3372	

Data collection and structural refinement for $Cu_B(toluene)_2(pentane)$

Theta range for data collection	1.24 to 26.48°
Index ranges	-20<=h<=19, -23<=k<=27, -31<=l<=31
Reflections collected	61680
Independent reflections	18034 [R(int) = 0.0442]

Coverage of independent reflections	99.6%	
Absorption correction	Multi-Scan	
Max. and min. transmission	0.9610 and 0.9070	
Structure solution technique	direct methods	
Structure solution program	SHELXT 2018/2 (Sheldrick, 2018)	
Refinement method	Full-matrix least-squares on F^2	
Refinement program	SHELXL-2018/3 (Sheldrick, 2018)	
Function minimized	$\Sigma\, w(F_o^2 - F_c^2)^2$	
Data / restraints / parameters	18034 / 15 / 987	
Goodness-of-fit on F^2	1.020	
Δ/σ_{max}	0.002	
Final R indices	15750 data; $I>2\sigma(I)$	R1 = 0.0395, wR2 = 0.0833
	all data	R1 = 0.0507, wR2 = 0.0871
Weighting scheme	$w=1/[\sigma^2(F_o^2)+(0.0374P)^2+3.8840P]$ where $P=(F_o^2+2F_c^2)/3$	
Absolute structure parameter	0.002(4)	
Largest diff. peak and hole	0.568 and -0.390 eÅ^{-3}	
R.M.S. deviation from mean	0.56 $^{-3}$	

2.4.10.11. Monitoring the standard coupling reaction by EPR spectroscopy

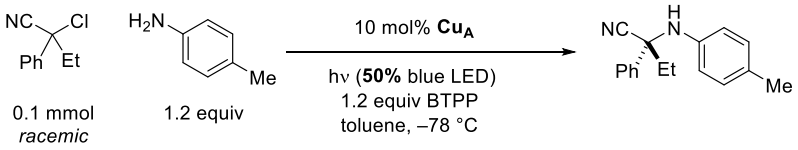

Under a nitrogen atmosphere, a 4 mL vial equipped with a PTFE stir bar was sequentially charged with **Cu$_A$** (13 mg, 0.010 mmol), toluene (2 mL), *p*-toluidine (13 mg, 0.12 mmol), BTPP (38 μL, 0.12 mmol), and 2-chloro-2-phenylbutanenitrile (18 mg, 0.10 mmol) and then stirred for 3 min. The resulting homogenous solution was transferred to EPR tubes (300 μL per tube). The tubes were sealed with a rubber stopper and removed from the glovebox, and a nitrogen-filled balloon was attached. The tubes were cooled for 5 min in a low-form hemispherical Dewar flask filled with pre-cooled methanol (–78 °C). Two Kessil® PR160-440 nm lamps were set to have 50% intensity by adjusting the dial and placed 5 cm above the reactions. The reaction mixtures were irradiated for the given times and then immediately frozen at 77 K. The stoppers and the balloons were removed, and the samples were analyzed by X-band EPR spectroscopy (**Figure 2.35**). The concentrations of the paramagnet were determined using a solution of $CuSO_4 \bullet 5H_2O$ in deionized water/glycerol (4:1, v/v) as an external standard. Selected samples were carefully warmed, and an aliquot was recovered with the aid of dichloromethane. The volatiles were removed, and the residue was re-dissolved in $CDCl_3$. The reactions were analyzed via ^{1}H NMR spectroscopy to determine the conversion and the yield, assuming that the sum of the remaining electrophile, the C–N coupling product, and the electrophile dimers gives 100% of the initially loaded electrophile (see section **B** of the mechanistic section: the sum of the C–N coupling product and the electrophile dimers gave 99% of the initially loaded electrophile) (**Table 2.5**).

Note. The rate of these EPR-tube reactions was faster than that of the standard 0.10-mmol reaction (**GP-6)**. The intensity of the light for the EPR-tube reactions was accordingly decreased so that the reactions have a similar rate of conversion.

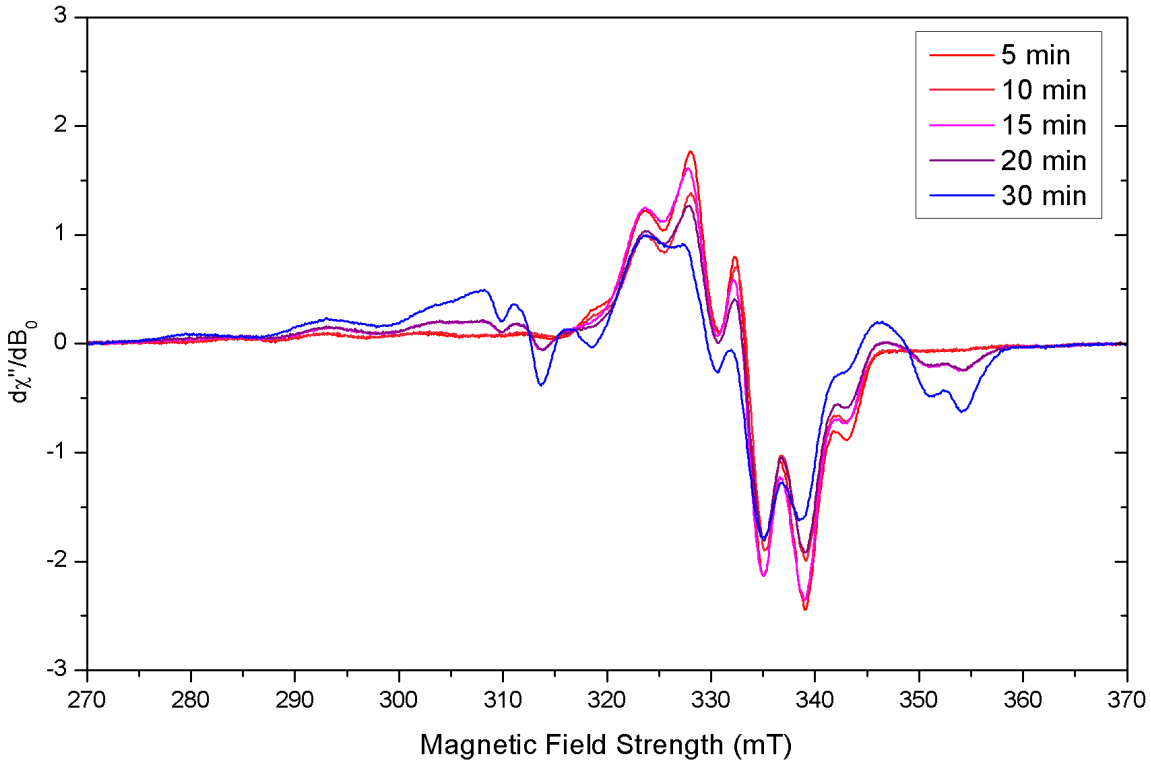

Figure 2.35. Time-course X-band EPR spectra of the catalytic reaction. Acquisition parameters: MW frequency = 9.372-9.374 GHz; temperature = 77 K; MW power = 140 μW; modulation amplitude = 0.4 mT; conversion time = 5.0 ms.

Table 2.5. Concentration of the paramagnet, conversion of the electrophile, and yield of the coupling product from the EPR study of the catalytic reaction.

Reaction time	[Cu(II)]/[Cu_A]$_0$ (%)	Conversion (%)	Product Yield (%)	Product ee (%)
10 min	10	32	22	
20 min	12	53	40	
30 min	16	82	66	90

2.4.10.12. In Situ preparation and decomposition of Cu_C

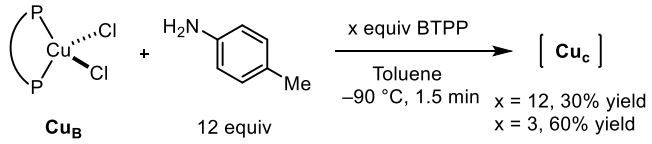

In-situ preparation (GP-9). Due to the temperature sensitivity of **Cu**C, the synthesis of **Cu**C was performed on an EPR-tube scale for immediate freeze-quenching. In a glovebox, a solution was prepared in a 4 mL vial of *p*-toluidine (13 mg, 0.12 mmol), BTPP (9.5 μL, 0.030 mmol or 38 μL, 0.12 mmol), and 1 mL of toluene. The vial was capped with a PTFE-lined open-top cap. An ~10 mM solution of **Cu**B in toluene was separately prepared according to **GP-8**. An EPR tube was charged with a magnetic stir bar and 150 μL of the **Cu**B solution. The tube was sealed with a rubber stopper and removed from the glovebox. A nitrogen-filled balloon was attached to the top of the tube, and the solution was cooled for 2 min in a low-form hemispherical Dewar flask filled with pre-cooled methanol (–90 °C). The solution of *p*-toluidine/BTPP (150 μL) was carefully layered over the solution of **Cu**B, and the tube was incubated for an additional 1 min so that both layers reached the bath temperature. Mixing of the two layers was performed by vigorously moving the internal magnetic stir bar up and down using an external magnet for 90 seconds, at which time the dark-purple color of the solution had changed to dark-green. The magnetic stir bar inside the EPR tube was held above the solution using the external magnet, and the solution was freeze-quenched at 77 K. The magnetic stir bar was removed, and the sample was analyzed by X-band EPR spectroscopy (**Figure 2.11**). The yield of **Cu**C was determined to be ~60% (with 3 equiv of BTPP) or ~30% (with 12 equiv of BTPP) by quantitative X-band EPR spectroscopy, using a solution of $CuSO_4 \bullet 5H_2O$ in deionized water/glycerol (4:1, v/v) as an external standard.

Decomposition. Following the same procedure, the dark-green solution after 90 seconds was further incubated at –78 °C for 30 min, at which point the solution became bright-yellow. The solution was subjected to X-band EPR spectroscopy at 77 K, following the above procedure. No significant amount of a paramagnet was detected. The sample was carefully warmed to room temperature, concentrated in vacuo, and analyzed by preparative TLC and ^{1}H NMR.

2.4.10.13. Synthesis of Cu_C from different CuX_2 and bases

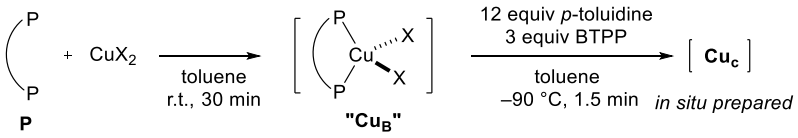

A solution of "Cu_B" prepared in situ according to **GP-8** from $CuCl_2$ and $CuBr_2$ (**Figure 2.36**) showed distinctly different EPR spectra, due to the different halide ligands. **GP-9** was followed with these solutions, to synthesize Cu_C. Analysis of the first and second derivatives (**Figures 2.37** and **2.38**) of the X-band EPR spectra indicates that an identical species was formed from the different "Cu_B" intermediates.

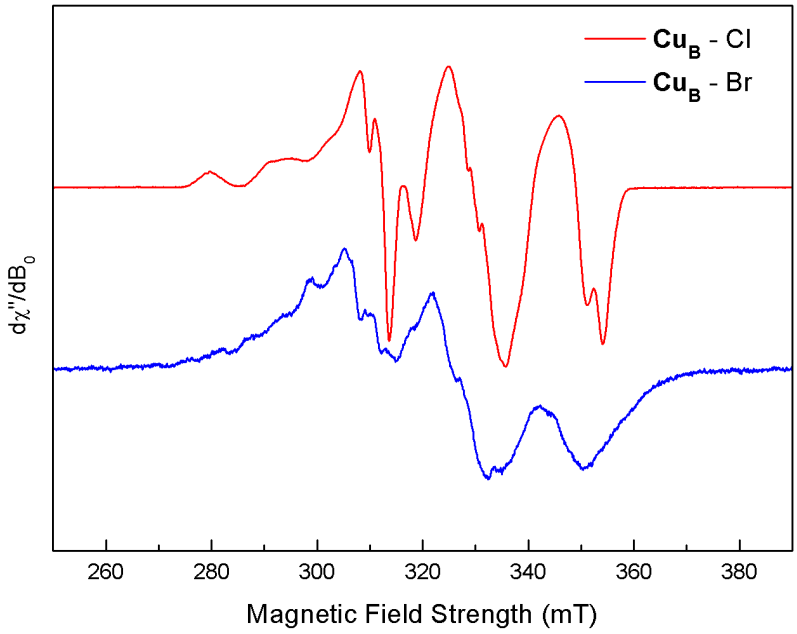

Figure 2.36. X-band EPR spectra of "Cu_B" (**P**CuX_2) prepared from $CuCl_2$ (red trace) and $CuBr_2$ (blue trace). Acquisition parameters: MW frequency = 9.37 GHz; temperature = 77 K; MW power = 140 µW; modulation amplitude = 0.4 mT; conversion time = 5.0 ms.

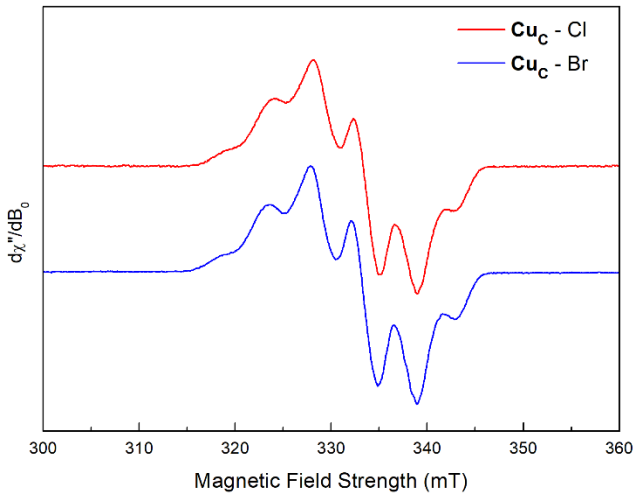

Figure 2.37. X-band EPR spectra of **Cu**c prepared from $CuCl_2$ (red trace) and $CuBr_2$ (blue trace). Acquisition parameters: MW frequency = 9.37 GHz; temperature = 77 K; MW power = 140 µW; modulation amplitude = 0.4 mT; conversion time = 5.0 ms.

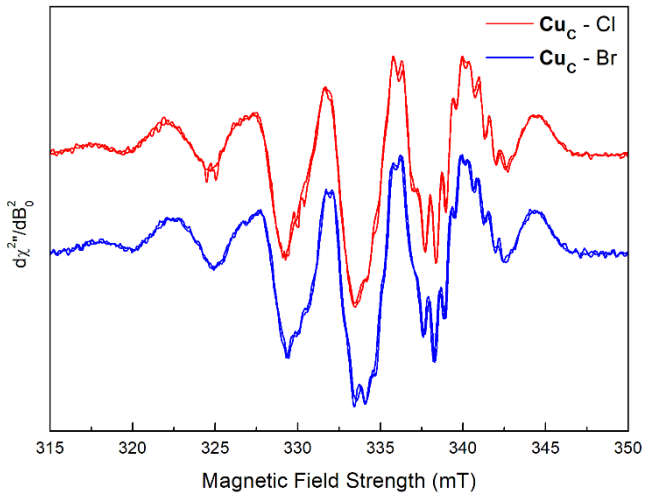

Figure 2.38. 2nd Derivative X-band EPR spectra of **Cu**c prepared from $CuCl_2$ (red trace) and $CuBr_2$ (blue trace). Overlapping spectra from two independent sets of syntheses are provided. Acquisition parameters: MW frequency = 9.37 GHz; temperature = 77 K; MW power = 140 µW; modulation amplitude = 0.1 mT; conversion time = 5.0 ms.

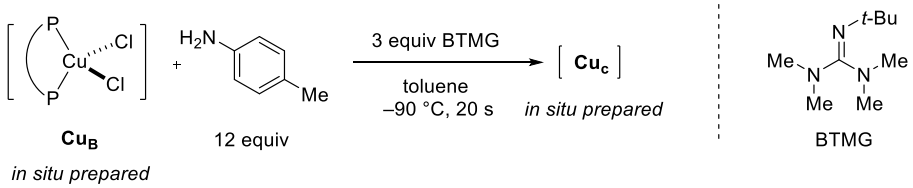

A solution of **Cu$_B$** prepared in situ according to **GP-8** was followed with **GP-9**, using BTMG instead of BTPP to synthesize **Cu$_C$**. The mixing time of the two layers was shortened to 20 seconds, as the consumption of **Cu$_B$** and the decomposition of **Cu$_C$** were more rapid. Analysis of the first and second derivatives (**Figure 2.39**) of the X-band EPR spectra indicated that an identical species was formed from the two reactions.

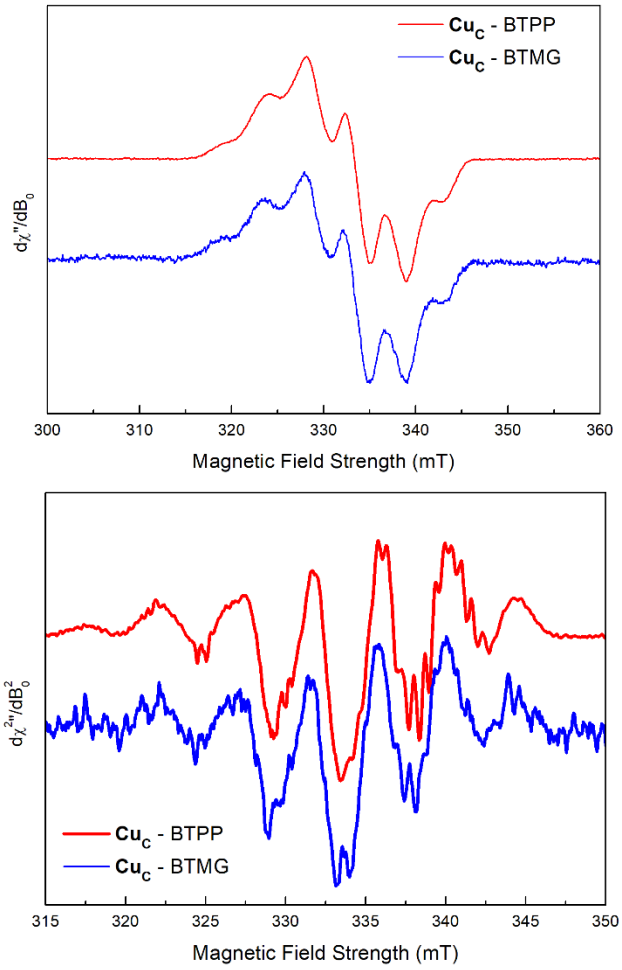

Figure 2.39. 1st and 2nd derivative X-band EPR spectra of **Cu$_C$** prepared from BTPP (red trace) and BTMG (blue trace). Acquisition parameters: MW frequency = 9.37 GHz; temperature = 77 K; MW power = 140 µW; modulation amplitude = 0.1-0.4 mT; conversion time = 5.0 ms.

2.4.10.14. Isotopologues of Cu$_C$ and Q-band pulse EPR experiments

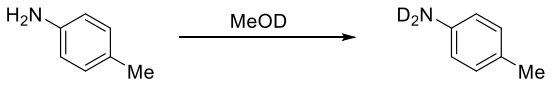

98% D incorporation

Preparation of *d*$_2$-labeled *p*-toluidine. *p*-Toluidine-*ND*$_2$ was synthesized by hydrogen-deuterium exchange in MeOD (three cycles). An oven-dried 20 mL vial was charged with *p*-toluidine (500 mg, 4.67 mmol) and a magnetic stir bar. MeOD (5 mL) was added, and the vial was purged with nitrogen. The solution was stirred for 12 h, and then the solvents were evaporated. This process was repeated three times, providing a white solid (503 mg, 99% yield). The deuterium incorporation was determined to be 98% via ^{1}H NMR spectroscopic analysis. The product was further purified by sublimation before use.

^{1}H NMR (400 MHz, C_6D_6) δ 6.94 – 6.85 (m, 2H), 6.40 – 6.27 (m, 2H), 2.15 (s, 3H).

^{2}H NMR (61 MHz, C_6D_6) δ 2.68.

^{13}C NMR (101 MHz, C_6D_6) δ 144.7, 130.0, 127.1, 115.2, 20.6.

HRMS (ESI+) *m/z* $[M(D_2)+H]^+$ calcd for $C_7H_8D_2N^+$: 110.0933, found: 110.0880.

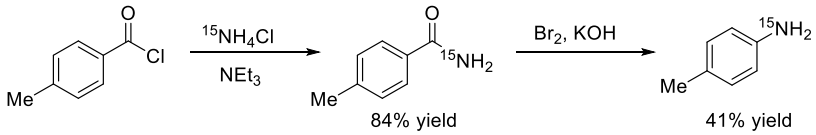

84% yield 41% yield

Preparation of ^{15}N-labeled *p*-toluidine. 4-Methylbenzoyl chloride (1.35 g, 8.74 mmol), a magnetic stir bar, dichloromethane (80 mL), and $^{15}NH_4Cl$ (500 mg, 9.2 mmol) were added sequentially to an oven-dried, nitrogen-filled 250 mL round-bottom flask. The flask was sealed with a rubber stopper, and a nitrogen-filled balloon was attached. The reaction mixture was cooled to 0 °C, and then triethylamine (3.65 mL, 26.2 mmol) was added dropwise. The reaction mixture was warmed to room temperature and stirred for 2 h. The reaction mixture was then acidified with 10 mL of 0.2 N HCl, and the organic layer was separated. The aqueous layer was extracted with 40 mL of dichloromethane, and the combined organic layer was dried over Na_2SO_4, filtered, and concentrated in vacuo. 4-Methylbenzamide-^{15}*N* was purified by flash column chromatography on silica gel (hexanes/EtOAc = 3/1→1/1). White solid (993 mg, 84% yield).

To a 50 mL round-bottom flask was added a magnetic stir bar, KOH (750 mg, 13.3 mmol), and deionized water (5 mL). The solution was cooled to 0 °C, and Br_2 (3.23 mmol, 170 μL) was added dropwise. 4-Methylbenzamide-^{15}N was slowly added to the resulting solution, and the reaction mixture was stirred for 2 h. The flask was fitted with a reflux condenser, heated to 90 °C, and stirred for 2 h. The solution was then cooled to room temperature, diluted with 5 mL of water, and extracted with Et_2O (25 mL). The solvent was removed in vacuo, and the product was purified by column chromatography (hexanes/EtOAc = 10/1). Pale-orange solid (129 mg, 41%). The product was further purified by sublimation to obtain a white crystalline solid.

^{1}H NMR (400MHz, C_6D_6) δ 6.90 (dd, *J* = 7.8, 0.7 Hz, 1H), 6.37 – 6.30 (m, 2H), 2.74 (d, *J* = 77.4 Hz, 2H), 2.15 (s, 3H).

^{13}C NMR (101 MHz, C_6D_6) δ 144.8 (d, *J* = 11.0 Hz), 130.0 (d, *J* = 1.2 Hz), 127.1, 115.3 (d, *J* = 2.8 Hz), 20.6.

^{15}N NMR (41MHz, C_6D_6) δ 52.9 (t, *J* = 77.7 Hz).

HRMS (ESI+) *m/z* $[M+H]^+$ calcd for $C_7H_{10}{}^{15}N^+$: 109.0778, found: 109.0785.

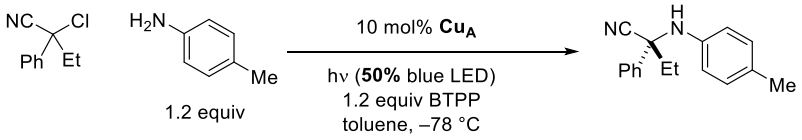

Preparation of Q-band EPR samples of isotopologues of Cu$_C$. In a glovebox under a nitrogen atmosphere, a 4 mL vial equipped with a PTFE stir bar was sequentially charged with **Cu$_A$** (13 mg, 0.010 mmol), toluene-d_8 (2 mL), *p*-toluidine (13 mg, 0.12 mmol), BTPP (38 μL, 0.12 mmol), 1,3,5-trimethoxybenzene (17 mg, 0.10 mmol), and 2-chloro-2-phenylbutanenitrile (18 mg, 0.10 mmol), and the resulting mixture was stirred for 3 min. This mixture was transferred using a microsyringe (30 μL per tube) to Q-band EPR tubes. The top of each tube was sealed with vacuum grease. Meanwhile, ~20 mL of methanol was charged into a 40 mL vial, and the vial was placed in a low-form hemispherical Dewar flask filled with pre-cooled methanol so that the temperature of the methanol inside the vial was maintained at –78 °C. The sealed EPR tubes were placed inside the 40 mL vial. Vacuum grease was maintained on the top of the tubes while the tubes were cooled, to ensure sealing of the tubes. Two Kessil® PR160-440 nm lamps were set at 50% intensity and placed 5 cm above the reactions. The reaction mixtures were irradiated for the given

times and then immediately frozen at 77 K. X-band EPR spectra were taken to determine the sample that contained the strongest and cleanest EPR signal. The sample that was irradiated for 5 min (**Figures 2.40** and **2.41**) was chosen for pulse EPR analysis (**Figures 2.42** – **2.55**).

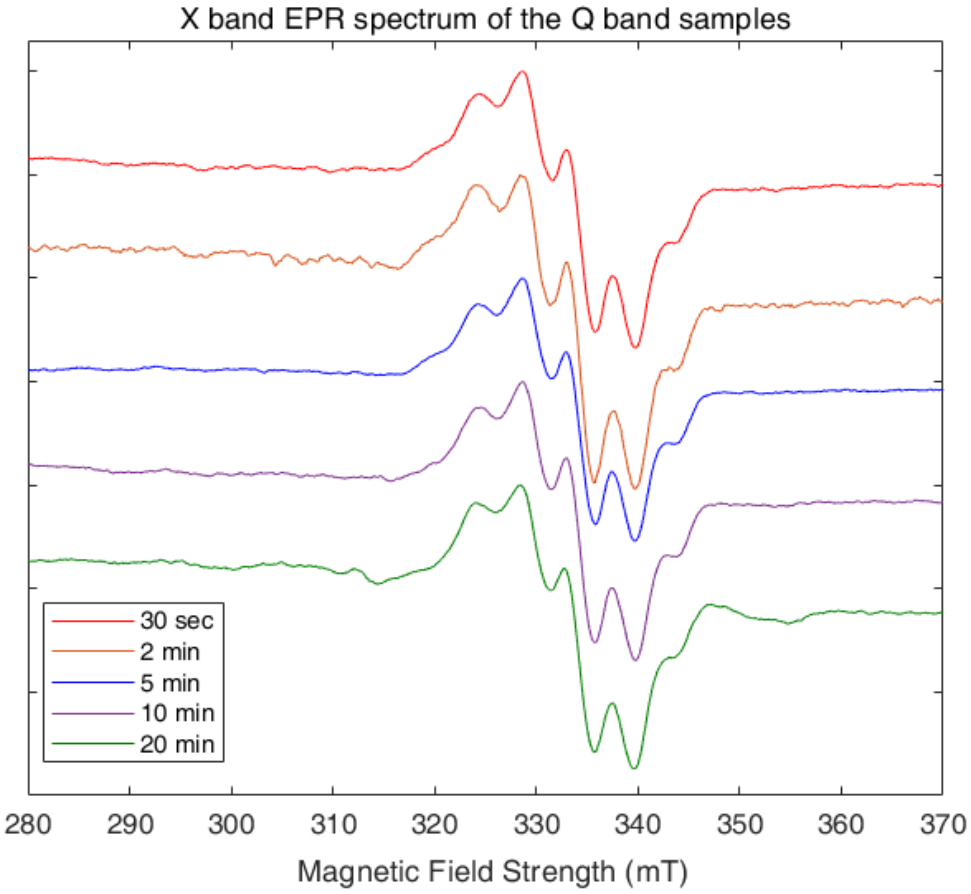

Figure 2.40. X-band EPR spectra of catalytic reactions charged in Q-band EPR tubes and irradiated for the given times. Acquisition parameters: MW frequency = 9.39 GHz; temperature = 77 K; MW power = 2180 µW; modulation amplitude = 0.4 mT; conversion time = 5.0 ms. The baseline was not corrected.

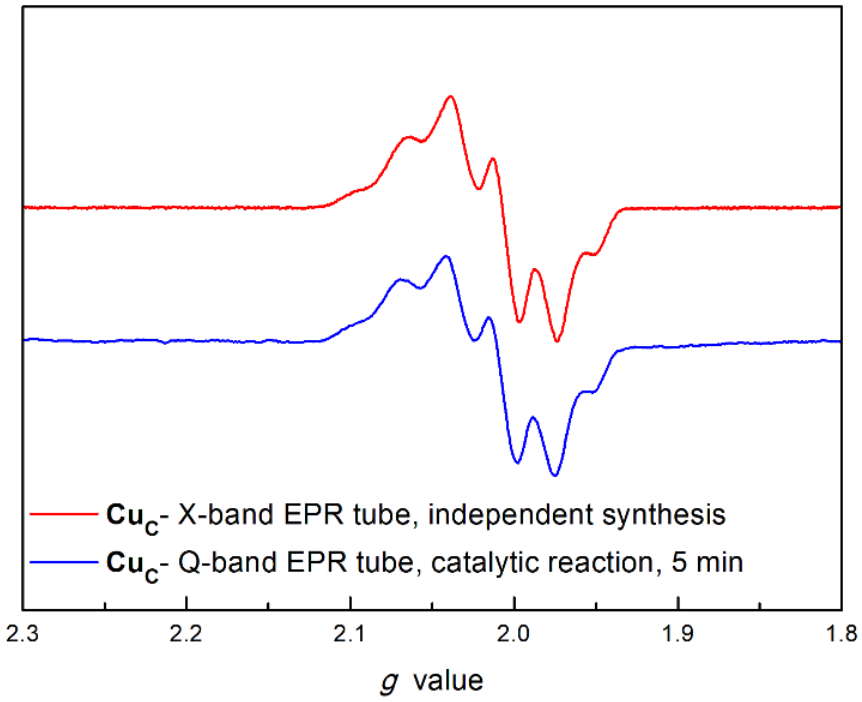

Figure 2.41. X-band EPR spectra of **Cu**$_C$ generated in an X-band EPR tube from $CuCl_2$ (red trace, section **L** of this mechanism section) and from the catalytic reaction charged in a Q-band EPR tube after 5 min of light irradiation (blue trace, **Figure 2.40**). Acquisition parameters: MW frequency = 9.36-9.39 GHz; temperature = 77 K.

EPR Simulation of Cu$_C$ (Figure 2.12, 2.13, 2.14 and Table 2.6).

Simulation parameters of the *g*-values and the hyperfine tensors of ^{31}P and $^{63/65}Cu$ nuclei were obtained by a global fit of the Q-band (~34 GHz) ENDOR (which primarily provided constraints on the ^{31}P couplings) and X- and Q-band field-swept EPR spectra (the higher fields associated with the Q-band spectra provided more robust constraints on simulated *g*-values) (**Figures 2.42** and **2.43**).

A single set of elongated correlation ridges in the (-,+) quadrant in the field dependent Q-band HYSCORE of ^{15}N labeled **Cu**$_C$ (**Figures 2.44** – **2.47**) were simulated by a single class of highly anisotropic ^{15}N hyperfine tensor, with $A(^{15}N) = \pm[6, 90, 6]$ MHz ($a_{iso}(^{15}N) = \pm 24.3$ MHz), with a Euler rotation of the hyperfine tensor relative to the g tensor of $(\alpha,\beta,\gamma) = (-11, 84, 0)°$.

The ^{14}N signals from the Q-band HYSCORE of natural abundance **Cu**$_C$ (**Figures 2.44**, **2.48** – **2.50**) also fall into the strong coupling regime but are additionally complicated by

the influence of ^{14}N nuclear quadrupole interaction which further splits the nuclear spin sublevels due to the electric interaction of the ^{14}N nucleus (I = 1) with the inhomogeneous electric field induced by electron density in p orbitals at the nucleus. These spectra were simulated by scaling the ^{15}N hyperfine tensor determined from ^{15}N HYSCORE by the proportion of ^{15}N/^{14}N gyromagnetic ratios ($|\gamma^{15}N|/|\gamma^{14}N| = 1.403$), with $A(^{14}N) = \pm[4.3, 64.2, 4.3]$ MHz. ^{14}N nuclear quadrupole parameters were then varied independently, with the best match between data and simulations achieved with ^{14}N quadrupole parameters of e^2qQ/h = 1.7 MHz and η = 1. These parameters provide a point-specific measurement of the magnitude of the electric field gradient (EFG, parametrized by e^2qQ/h) and its symmetry, with the asymmetry parameter η ranging from η = 0 for pure axial symmetry to η = 1 for fully rhombic symmetry.

Intense ^{2}H cross-peaks in the (+,+) quadrant of Q-band HYSCORE of ^{2}H-labeled **Cu$_C$** (**Figures 2.44, 2.51** – **2.53**) were simulated by a single class of relatively anisotropic ^{2}H hyperfine tensor with $A(^2H) = \pm[8.9, 4.3, 1.5]$ MHz ($a_{iso}(^2H) = \pm 4.9$ MHz).

The presence of multiple equivalent -NHAr ligands could be ruled out by simulations that showed that the equivalent $^{14/15}$N nuclei would generate combination peaks that are completely absent in the observed spectra (**Figure 2.54**).

Overall, the simulated EPR spectra from the parameters described in **Table 2.6** match with the observed CW-EPR spectra of **Cu$_C$** and its isotopologues (**Figure 2.55**).

Table 2.6. EPR simulation parameters for **Cu**C. All hyperfine and nuclear quadrupole coupling values are reported in MHz.[α]

g-value	2.012	2.014	2.023				
Nucleus	$\lvert A_1 \rvert$	$\lvert A_2 \rvert$	$\lvert A_3 \rvert$	$\lvert a_{iso} \rvert$	T	e^2qQ/h	η
^{1}H$_{(amide)}$	58	28	10	32	[26, -4, -22]		
^{2}H$_{(amide)}$	8.9	4.3	1.5	4.9	[4.0, -0.6, -3.4]	< 0.4	≈ 0
^{15}N$_{(amide)}$	6	90	6	34	[-28, 56, -28]		
^{14}N$_{(amide)}$	4.3	64.2	4.3	24.3	[-20, 40, -20]	1.7	≈ 1.0
$^{63/65}$Cu	18	26	146	63			
^{31}P$_a$	130	100	100	110			
^{31}P$_b$	110	100	130	113			

[α] A(^{1}H$_{(amide)}$) is rotated relative to g-tensor by (α, β, γ) = (-10, 54, 50)°, while A($^{15/14}$N$_{(amide)}$) and the ^{14}N$_{(amide)}$ nuclear quadrupole tensors are both rotated relative to the g-tensor by (α, β, γ) = (-11, 84, 0)°. All other hyperfine tensors are collinear with g-tensor. $^{1/2}$H and $^{14/15}$N parameters primarily determined from simulations of Q-band HYSCORE, while ^{31}P$_{a,b}$ primarily determined from fixing all other parameters and optimizing simulations of Q-band ENDOR and field-swept EPR spectra.

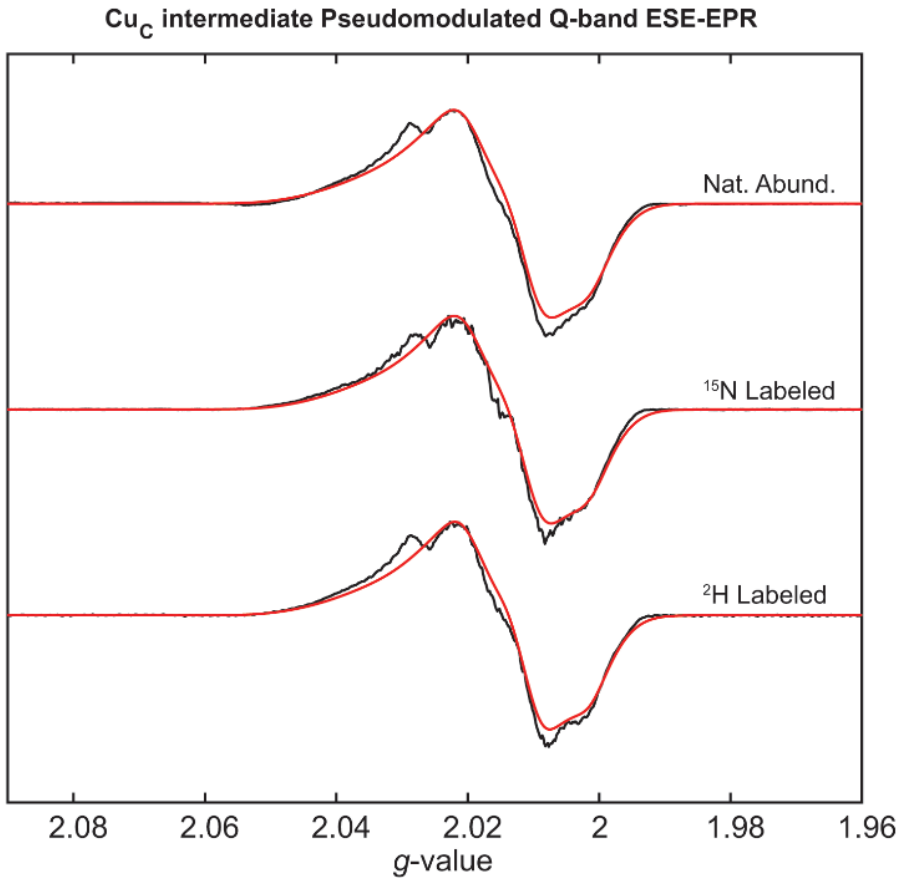

Figure 2.42. Q-band pseudomodulated ESE-EPR spectra of **Cu**c in toluene formed using isotopologues of *p*-toluidine (black traces) with simulations using parameters in **Table 2.6** overlaid (red traces). Acquisition parameters: MW frequency = 34.005 GHz; temperature = 20 K; MW power = 140 μW; modulation amplitude = 0.1 mT; conversion time = 5.3 ms. Acquisition parameters: MW frequency = 34.011 GHz (Nat. Abund.), 34.072 GHz (^{15}N labeled), 34.048 GHz (^{2}H labeled); temperature = 30 K; π pulse length = 160 ns; τ = 300 ns; shot rep time (srt) = 1 ms.

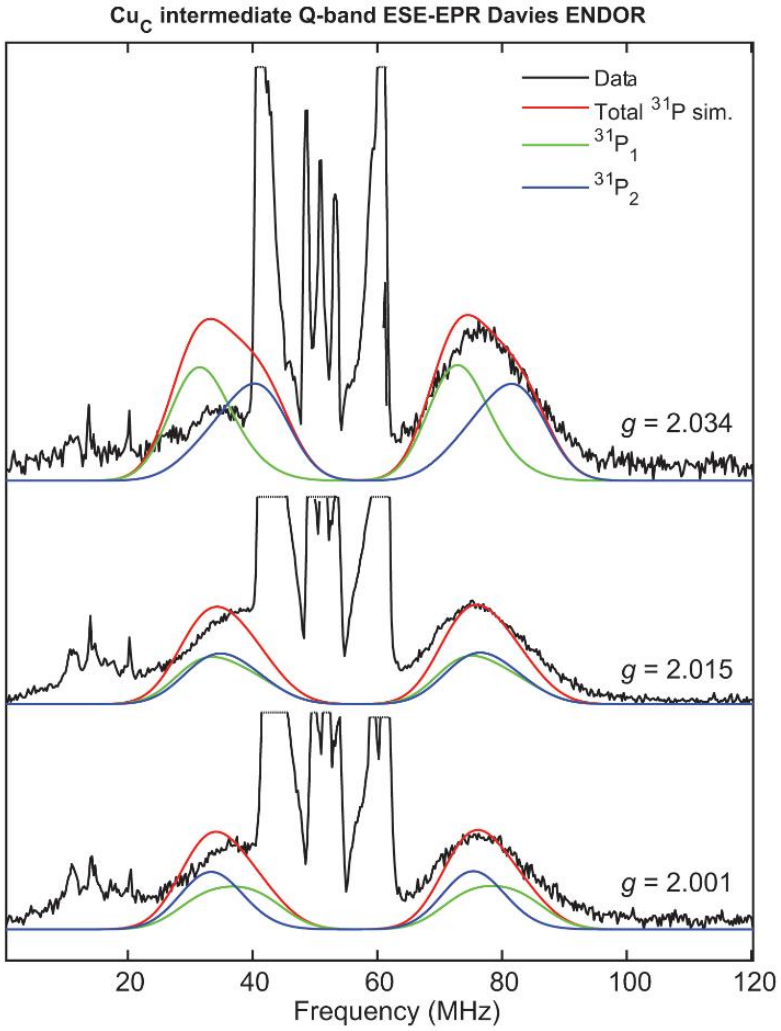

Figure 2.43. Field-dependent Q-band Davies ENDOR of **Cu**C in toluene formed using ^{2}H *p*-toluidine (black) with simulations of total ENDOR contributions from the two ^{31}P nuclei simulated in red, and individual contributions from $^{31}P_1$ and $^{31}P_2$ in green and blue, respectively, using values in **Table 2.6**. Intense ENDOR signals from ligand ^{1}H nuclei in the range from 40 to 60 MHz have been truncated for ease of evaluation of the ^{31}P signals. Experimental conditions: microwave frequency = 34.050 GHz; temperature = 20 K; MW π pulse length = 80 ns; interpulse delay τ = 200 ns; π_{RF} pulse length = 15 μs; T_{RF} delay = 2 μs; shot repetition time (srt) = 5 ms.

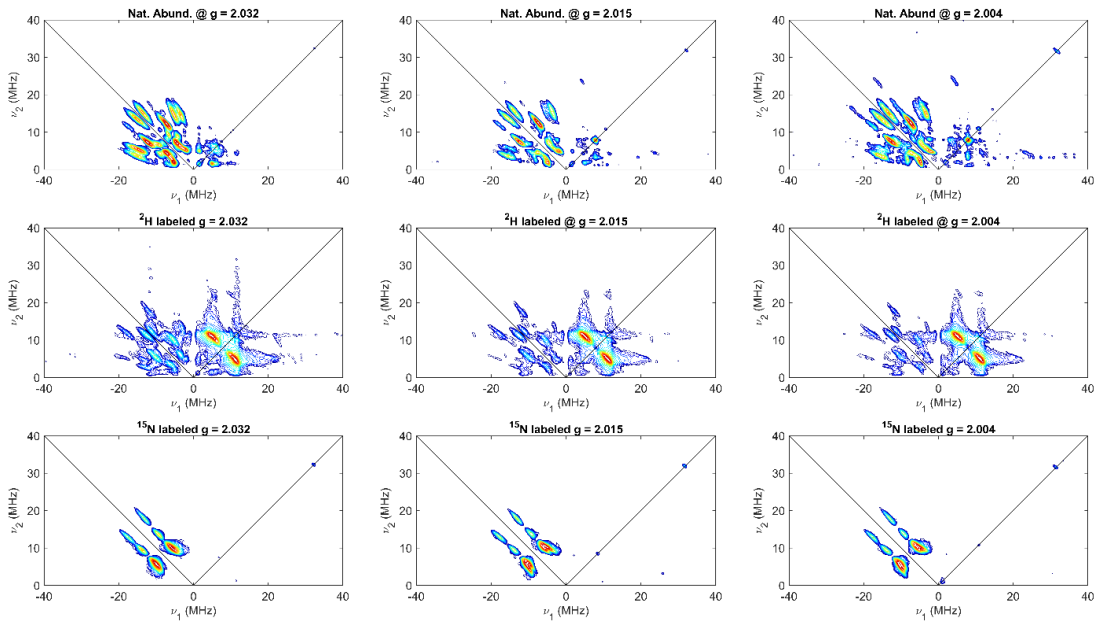

Figure 2.44. Q-band HYSCORE of the **Cu**C intermediate in toluene formed using isotopologues of *p*-toluidine with natural abundance (top), ^{2}H (middle), and ^{15}N (bottom) measured at magnetic fields corresponding to g = 2.032, g = 2.015, and g = 2.004 from left to right. Spectra of ^{2}H isotopologues have been plotted to 2 orders of magnitude further from the intensity maximum compared to Figures in which comparison to the ^{2}H simulations are made in order to show that the ^{14}N signals in the (-,+) quadrant observed the natural abundance HYSCORE are still present. Experimental conditions: MW frequency = 34.005 GHz (Nat. Abund), 34.072 (^{2}H and ^{15}N); temperature = 30 K; τ = 128 ns, $t_1 = t_2$ = 100 ns; $\Delta t_1 = \Delta t_2$ = 12 ns; shot repetition time (srt) = 1.5 ms.

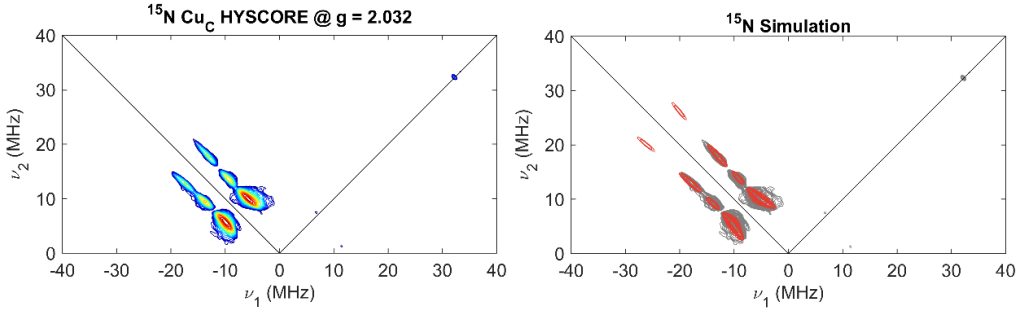

Figure 2.45. Q-band HYSCORE of the **Cu**C intermediate in toluene formed using ^{15}N labeled *p*-toluidine (left) measured at 1198.2 mT (*g* = 2.032) with overlay of ^{15}N simulation contours (right, red) with experimental contours (right, gray). Experimental conditions: MW frequency = 34.072 GHz; temperature = 30 K; τ = 128 ns, $t_1 = t_2$ = 100 ns; $\Delta t_1 = \Delta t_2$ = 12 ns; shot repetition time (srt) = 1.5 ms.

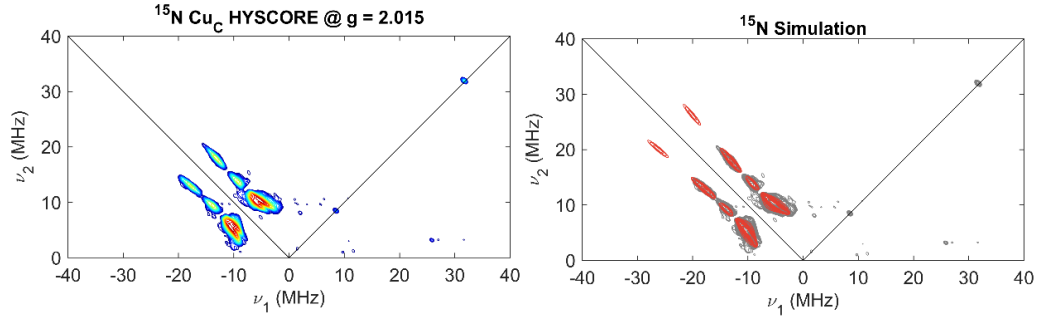

Figure 2.46. Q-band HYSCORE of the **Cu**C intermediate in toluene formed using ^{15}N labeled *p*-toluidine (left) measured at 1208.1 mT (*g* = 2.015) with overlay of ^{15}N simulation contours (right, red) with experimental contours (right, gray). Experimental conditions: MW frequency = 34.072 GHz; temperature = 30 K; τ = 128 ns, $t_1 = t_2$ = 100 ns; $\Delta t_1 = \Delta t_2$ = 12 ns; shot repetition time (srt) = 1.5 ms.

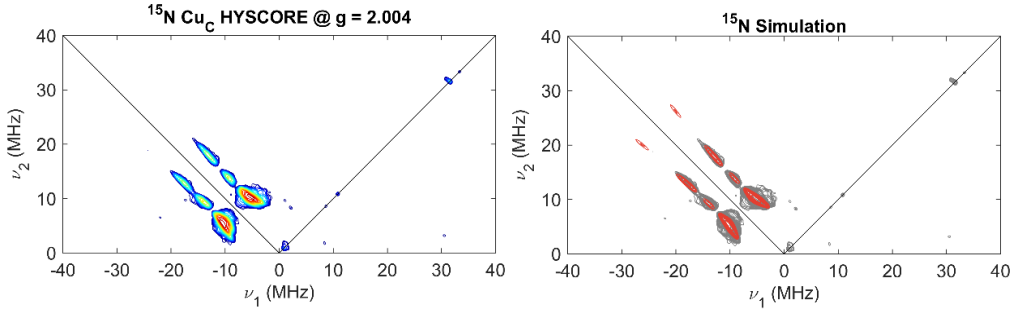

Figure 2.47. Q-band HYSCORE of the **Cu**C intermediate in toluene formed using ^{15}N labeled *p*-toluidine (left) measured at 1214.7 mT (g = 2.004) with overlay of ^{15}N simulation contours (right, red) with experimental contours (right, gray). Experimental conditions: MW frequency = 34.072 GHz; temperature = 30 K; τ = 128 ns, $t_1 = t_2$ = 100 ns; $\Delta t_1 = \Delta t_2$ = 12 ns; shot repetition time (srt) = 1.5 ms.

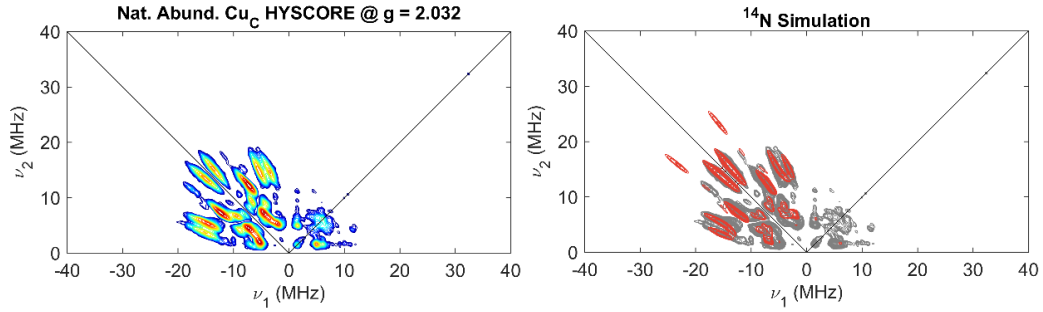

Figure 2.48. Q-band HYSCORE of the **Cu**C intermediate in toluene formed using natural abundance *p*-toluidine (left) measured at 1196 mT (g = 2.032) with overlay of ^{14}N simulation contours (right, red) with experimental contours (right, gray). Experimental conditions: MW frequency = 34.005 GHz; temperature = 30 K; τ = 128 ns, $t_1 = t_2$ = 100 ns; $\Delta t_1 = \Delta t_2$ = 12 ns; shot repetition time (srt) = 1.5 ms.

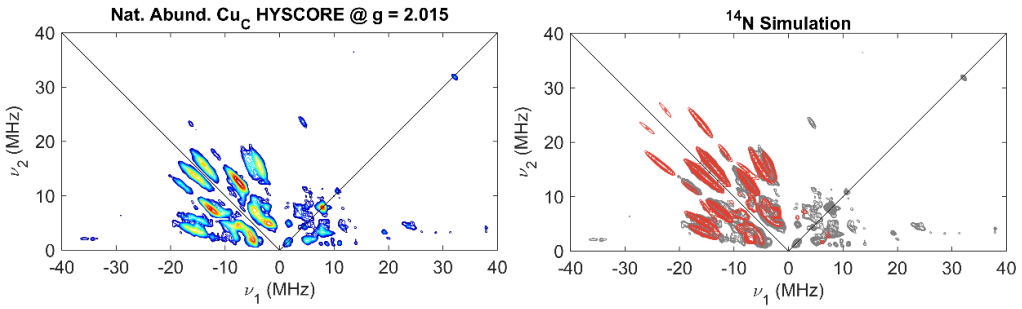

Figure 2.49. Q-band HYSCORE of the **Cu**C intermediate in toluene formed using natural abundance *p*-toluidine (left) measured at 1206 mT (g = 2.015) with overlay of ^{14}N simulation contours (right, red) with experimental contours (right, gray). Experimental conditions: MW frequency = 34.005 GHz; temperature = 30 K; τ = 128 ns, $t_1 = t_2$ = 100 ns; $\Delta t_1 = \Delta t_2$ = 12 ns; shot repetition time (srt) = 1.5 ms.

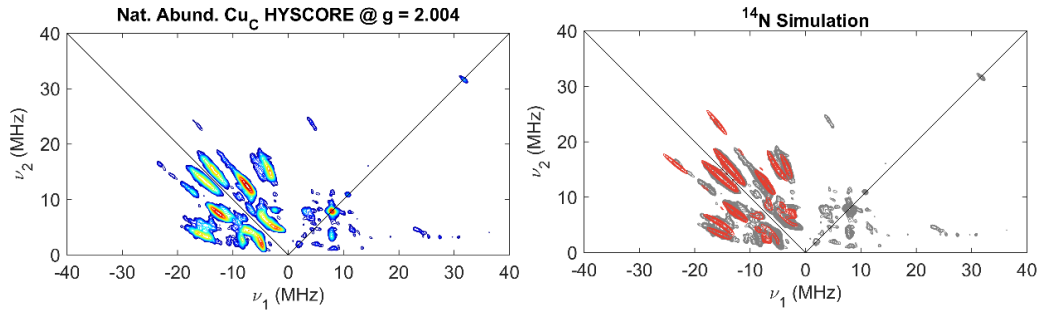

Figure 2.50. Q-band HYSCORE of the **Cu**C intermediate in toluene formed using natural abundance *p*-toluidine (left) measured at 1212.5 mT (g = 2.004) with overlay of ^{14}N simulation contours (right, red) with experimental contours (right, gray). Experimental conditions: MW frequency = 34.005 GHz; temperature = 30 K; τ = 128 ns, $t_1 = t_2$ = 100 ns; $\Delta t_1 = \Delta t_2$ = 12 ns; shot repetition time (srt) = 1.5 ms.

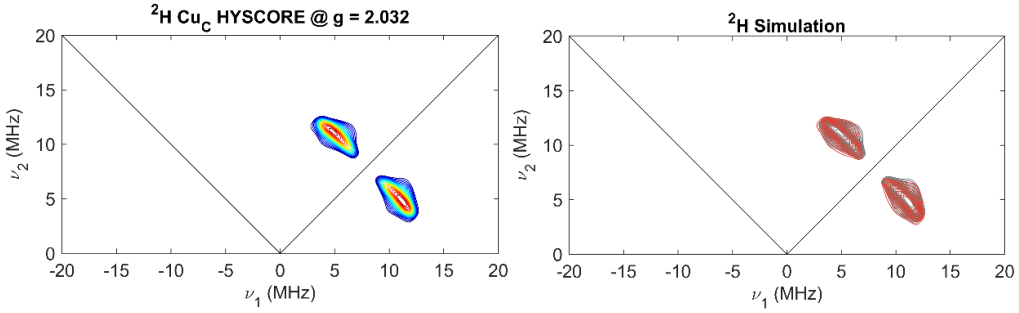

Figure 2.51. Q-band HYSCORE of the **Cu**C intermediate in toluene formed using ^{2}H labeled *p*-toluidine (left) measured at 1198.2 mT (g = 2.032) with overlay of ^{2}H simulation contours (right, red) with experimental contours (right, gray). Experimental conditions: MW frequency = 34.072 GHz; temperature = 30 K; τ = 128 ns, $t_1 = t_2$ = 100 ns; $\Delta t_1 = \Delta t_2$ = 12 ns; shot repetition time (srt) = 1.5 ms.

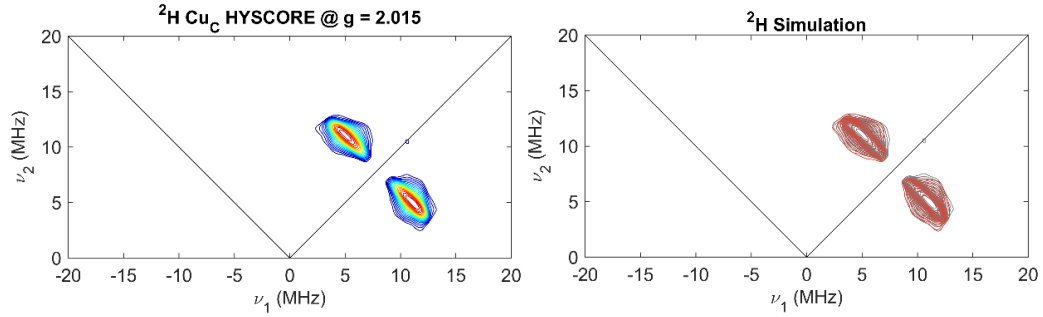

Figure 2.52. Q-band HYSCORE of the **Cu**C intermediate in toluene formed using ^{2}H labeled *p*-toluidine (left) measured at 1208.1 mT (g = 2.015) with overlay of ^{2}H simulation contours (right, red) with experimental contours (right, gray). Experimental conditions: MW frequency = 34.072 GHz; temperature = 30 K; τ = 128 ns, $t_1 = t_2$ = 100 ns; $\Delta t_1 = \Delta t_2$ = 12 ns; shot repetition time (srt) = 1.5 ms.

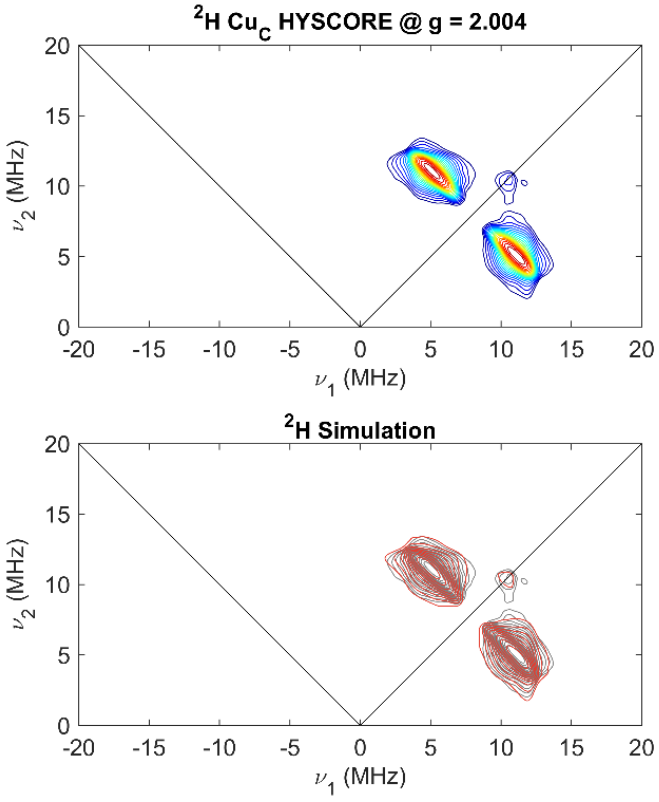

Figure 2.53. Q-band HYSCORE of the **Cu**C intermediate in toluene formed using ^{2}H labeled *p*-toluidine (top) measured at 1214.7 mT (g = 2.004) with overlay of ^{2}H simulation contours (bottom, red) with experimental contours (bottom, gray). Experimental conditions: MW frequency = 34.072 GHz; temperature = 30 K; τ = 128 ns, $t_1 = t_2$ = 100 ns; $\Delta t_1 = \Delta t_2$ = 12 ns; shot repetition time (srt) = 1.5 ms.

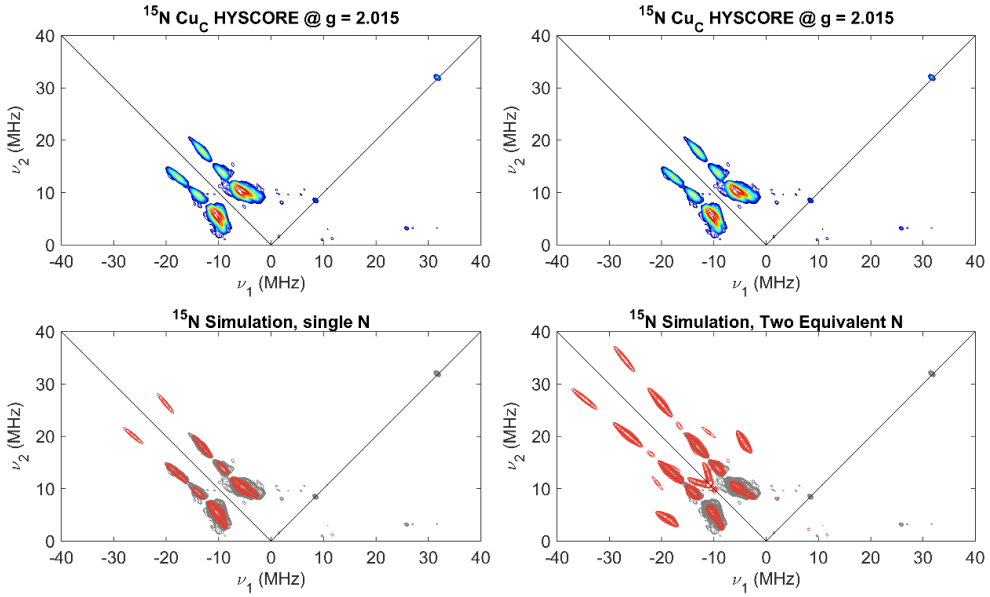

Figure 2.54. Q-band HYSCORE of the **Cu$_C$** intermediate in toluene formed using ^{15}N labeled *p*-toluidine (top) measured at 1208.1 mT (*g* = 2.015) with comparison of ^{15}N simulations using a single nitrogen (left) and two equivalent nitrogen couplings (right), the latter of which produces combination frequency cross-peaks at (-18, 4) and (-4, 18) MHz that are completely absent in the experimental data. Experimental conditions: MW frequency = 34.072 GHz; tem-perature = 30 K; τ = 128 ns, $t_1 = t_2$ = 100 ns; $\Delta t_1 = \Delta t_2$ = 12 ns; shot repetition time (srt) = 1.5 ms.

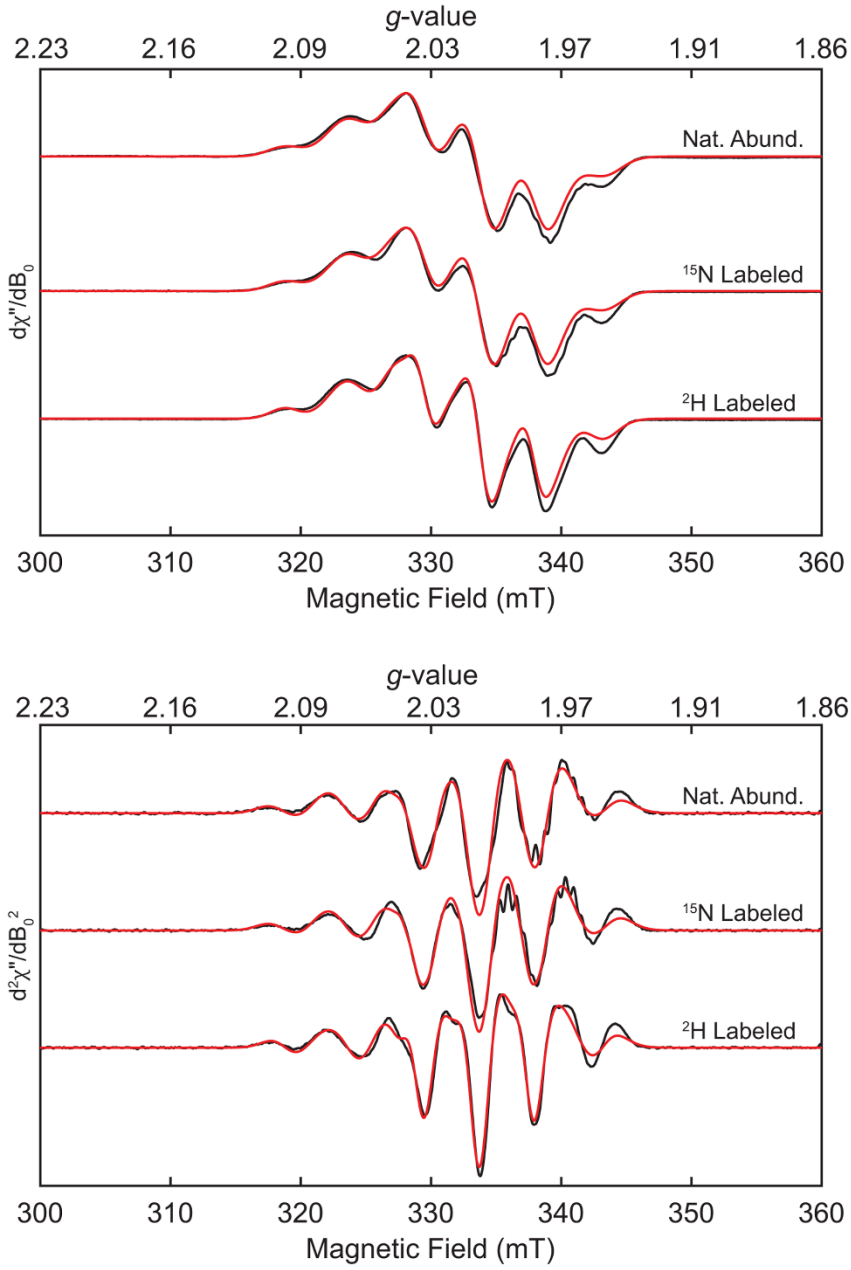

Figure 2.55. X-band CW-EPR spectra (top panel) and 2nd derivative (bottom panel) of **Cu**c in toluene and isotopologues of *p*-toluidine (black traces) with simulations overlaid (red traces); acquisition parameters: MW frequency = 9.372–9.374 GHz, MW power = 140 μW, modulation amplitude = 0.1 mT, conversion time = 5.3 ms, and temperature = 77 K.

2.4.10.15. Reaction of Cu_C with an organic radical

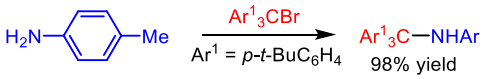

Synthesis of authentic coupling product. In a glovebox, an oven-dried 4 mL vial was charged with a magnetic stir bar, tris(4-(*tert*-butyl)phenyl)methyl bromide (98 mg, 0.20 mmol), and toluene (2 mL). *p*-Toluidine (43 mg, 0.40 mmol) was added, and the reaction mixture was stirred for 24 h, at which time a yellow precipitate was observed. The precipitate was removed via filtration with a PTFE syringe filter, and the solution was concentrated in vacuo. Pentane (2 mL) was added to the residue, and the resulting solution was filtered through a PTFE syringe filter. The solution was concentrated in vacuo to afford the desired product. White solid, 101 mg (0.20 mmol, 98% yield).

^{1}H NMR (500 MHz, $CDCl_3$) δ 7.28 – 7.17 (m, 12H), 6.71 (d, J = 8.2 Hz, 2H), 6.23 (d, J = 8.3 Hz, 2H), 4.88 (s, 1H), 2.13 (s, 3H), 1.29 (s, 27H).

^{13}C NMR (126 MHz, $CDCl_3$) δ 149.3, 144.4, 142.9, 129.0, 128.8, 125.6, 124.7, 115.9, 70.4, 34.5, 31.5, 20.5.

HRMS (ESI+) *m/z* $[M - (NHp\text{-tol})]^+$ calcd for $C_{31}H_{39}^+$: 411.3046, found: 411.3064.

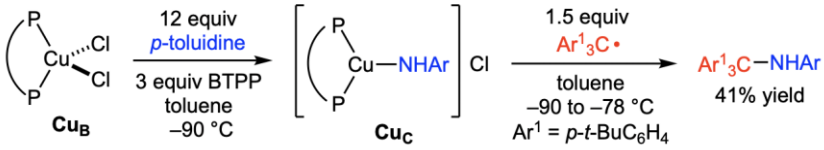

Reaction of Cu_C with an Organic Radical. A solution of tris-(4-*tert*-butyl phenyl)methyl radical (15 mM in toluene) was prepared according to the literature,[55] from tris(4-(tert-butyl)phenyl)methyl bromide (46.4 mg, 0.094 mmol), activated copper powder (90 mg, 1.41 mmol), and toluene (6.3 mL). A solution of *p*-toluidine/BTPP was prepared in a 4 mL vial with *p*-toluidine (13 mg, 0.12 mmol), BTPP (10 µL, 0.030 mmol or 38 µL, 0.12 mmol) and 1.0 mL of toluene.

In a glovebox, an NMR tube was charged with a magnetic stir bar and a solution of **Cu_B** in toluene (10 mM, 200 µL), prepared in situ according to **GP-8**. The tube was sealed with a rubber stopper and removed from the glovebox. A nitrogen-filled balloon was

attached to the top of the tube, and the solution was cooled for 2 min in a low-form hemispherical Dewar flask filled with pre-cooled methanol (–90 °C). The solution of *p*-toluidine/BTPP (200 μL) was carefully layered over the solution of **Cu$_B$**, and the tube was incubated for an additional 1 min so that both layers reached the bath temperature. Mixing of the two layers was performed by moving the internal magnetic stir bar up and down using an external magnet for 90 seconds (at which time the dark-purple color of the solution changed to dark-green), at which point the solution of tris-(4-*tert*-butyl phenyl)methyl radical (200 μL) was carefully layered above the solution of **Cu$_C$**. Mixing of the two layers was performed by moving an external magnet for 5 min. The tube was quickly moved to another hemispherical Dewar flask filled with a dry ice/acetone bath (–78 °C) and incubated for 30 min. The dark color of the solution turned bright yellow. The solution was warmed and transferred to a 20 mL vial using 3 mL of dichloromethane. The solvent was then concentrated, and the residue was dissolved in a solution of internal standard (1,3,5-trimethoxybenzene in $CDCl_3$) and analyzed via ^{1}H NMR spectroscopy (**Table 2.7**). Control experiments with decomposed **Cu$_C$** were performed by warming the dark-green solution of **Cu$_C$** to room temperature (at which point it turned yellow) and cooling it back to –90 °C before layering the solution of tris-(4-*tert*-butyl phenyl)methyl radical.

Table 2.7. Stoichiometric reaction between **Cu$_C$** and tris-(4-*tert*-butyl phenyl)methyl radical, including control experiments.

Entry	Variations	Yield of the C–N coupling
1[a]	-	41%
2	Decomposed **Cu$_C$**	7%
3	**Cu$_B$** was omitted	9%

a. The yields are an average of two runs.

2.4.11. DFT calculations

General information. All geometry optimizations were performed using ORCA 4.2.1 with the BP86 functional, the def2-TZVP basis set for all atoms, dispersion correction with Becke-Johnson damping (D3BJ), and the RIJCOSX approximation to speed up optimizations. A solvation model (CPCM (toluene)) was applied. Structures, molecular orbitals, and spin densities were visualized using Chemcraft 1.8 software.

MO visualization of the ground and the excited triplet state of Cu_A. Cartesian coordinates from the crystal structure of **Cu_A** (**CCDC 1579920**) was used as the input for the geometry optimization. Molecular orbitals of the ground and excited triplet structures of **Cu_A** propose ^{3}MLCT from copper 3*d* orbital to the aryl rings of the SEGPHOS backbone (**Figure 2.56**).

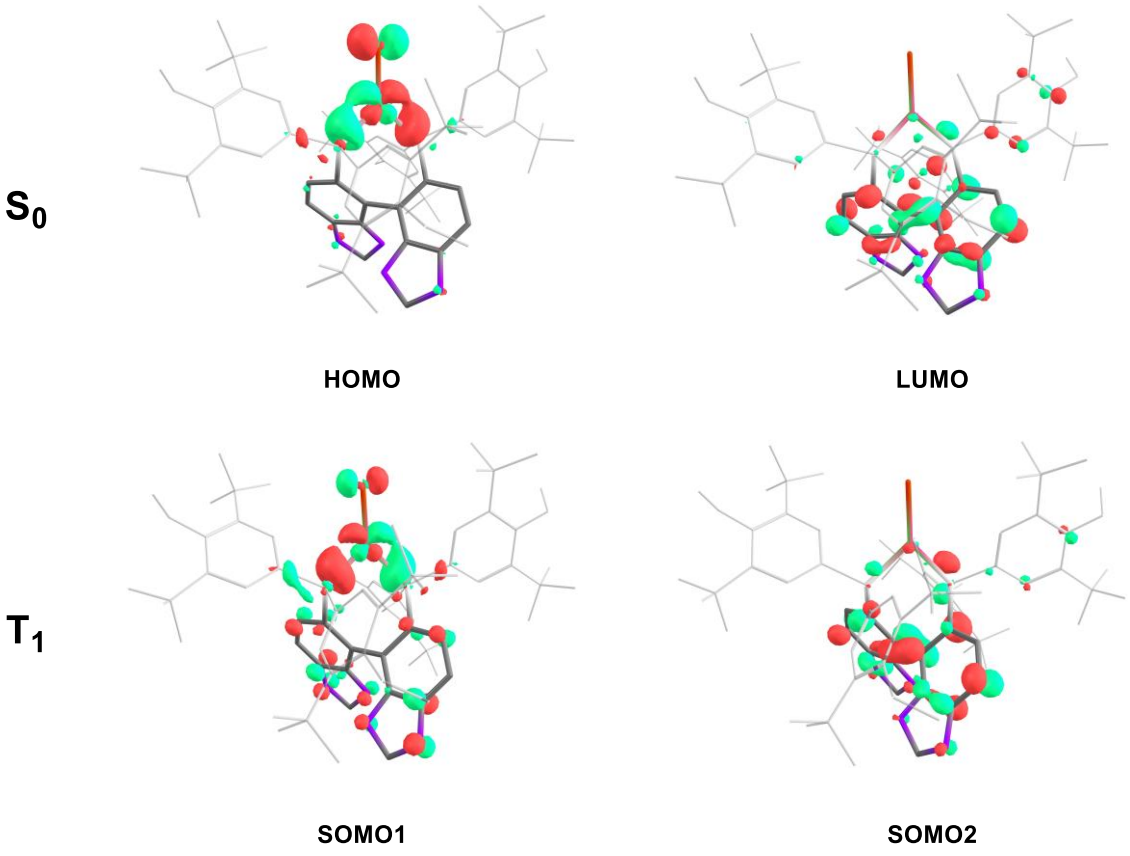

Figure 2.56. Calculated plots of HOMO and LUMO of the ground state of **Cu_A** (top) and corresponding SOMOs of the triplet excited state of **Cu_A*** (bottom). Hydrogen atoms were omitted for clarity. Contour value = 0.05.

Geometry optimization of Cu$_C$. Given the C_2-symmetric structure of the DTBM-SEGPHOS ligand, the structures shown below were chosen for calculation (**Figure 2.57**). Due to limited resources, a frequency calculation was only performed for **Cu$_{C1}$**$^+$ (the proposed structure of **Cu$_C$** from the EPR analysis), to ensure that the structure is a local minimum. Although **Cu$_{C2A}$** has a single point energy that is 2.11 kcal/mol lower than **Cu$_{C2B}$**, and **Cu$_{C3A}$** has a single point energy that is 2.5 kcal/mol lower than **Cu$_{C3B}$**, all structures were considered for the DFT-EPR calculations.

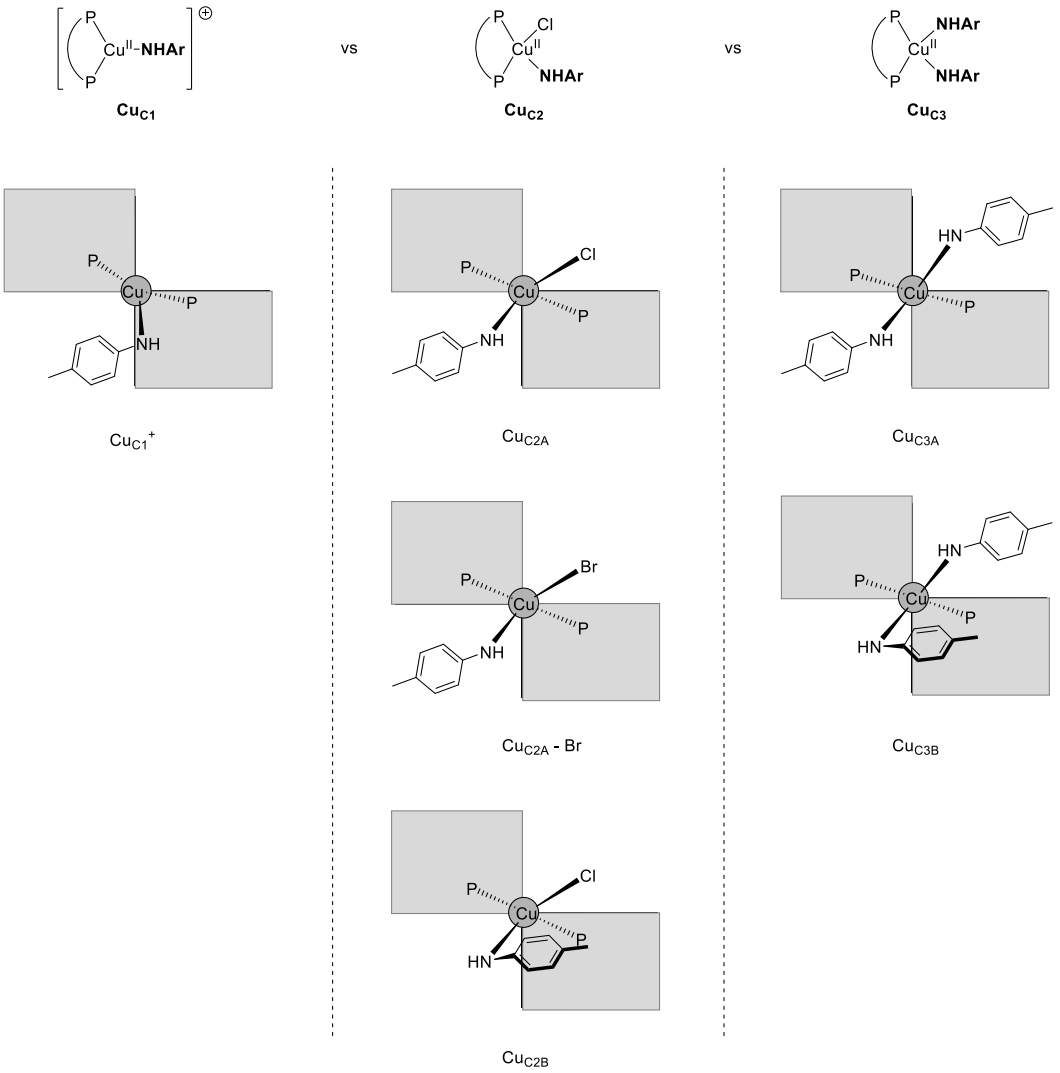

Figure 2.57. Candidate structures considered for **Cu$_C$**.

DFT-EPR calculations. Calculations of EPR parameters were performed using ORCA 4.2.1 with the TPSS functional. For basis sets: core-property basis set CP(PPP) for Cu atom; def2-TZVP for -NH*p*-Tol, -N(*p*-Tol)$_2$, phosphorus, chlorine, and bromine. For the remaining ligand fragments, essentially the same EPR parameters were predicted when def2-SVP and def2-TZVP were both tested for $\mathbf{Cu_{C1}}^+$. Therefore, def2-TZVP was used for $\mathbf{Cu_{C2}}$**,** and def2-SVP was used for $\mathbf{Cu_{C3}}$ (due to limited resources), assuming that the basis set of the remaining ligand fragments does not have a significant effect on the predicted EPR parameters. An expanded grid was used (IntAccX 4.34,4.34,4.67 and GridX 2,2,2) to improve the accuracy of the calculations; dispersion correction with Becke-Johnson damping (D3BJ), and the RIJCOSX approximation to speed up optimizations. A solvation model (CPCM(toluene)) was used. The choice of the TPSS functional was based on the best reproduction of the reported EPR parameters of the formal bisphosphine Cu(II) amido complex[40] (**Figure 2.58** and **Table 2.8**) among other basis sets tested (BP86, TPSS, OLYP, revTPSS, BHandHLYP, B3LYP, B3PW91, PBE0, TPSSH).

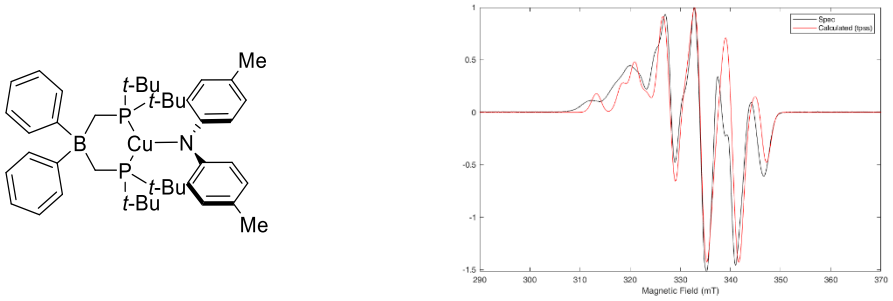

Figure 2.58. Structure of the reference compound (left); reported EPR spectrum (right, black trace) and EasySpin simulation obtained from DFT-predicted EPR parameters (right, red trace). Acquisition parameters: MW frequency = 9.38 GHz; temperature = 77 K; modulation amplitude = 0.2 mT.

Table 2.8. Reported and calculated EPR parameters of the reference compound. A in MHz.

Reported	g_x	g_y	g_z	g_{iso}	**Calculated**	g_x	g_y	g_z	g_{iso}
***g*-value**	2.008	2.008	2.030	2.015	*g*-value	2.013	2.014	2.031	2.019
	$\lvert A_x \rvert$	$\lvert A_y \rvert$	$\lvert A_z \rvert$	a_{iso}		A_x	A_y	A_z	a_{iso}
Cu	34	34	170	79.3	**Cu**	-27.1	7.85	-215	78.3
P1	148	148	173	156.3	**P1**	230	141	139	170
P2	148	148	173	156.3	**P2**	155	254	153	187
N	24	100	24	49	**N**	-6.8	37	-7.1	17

Predicted EPR parameters of the optimized structures (**Figures 2.59** – **2.64**; A in MHz).

Simulated	g_x	g_y	g_z	g_{iso}
***g*-value**	2.012	2.014	2.023	**2.016**
	A_x	A_y	A_z	a_{iso}
Cu	18	26	146	**63**
P1	130	100	100	**110**
P2	110	100	100	**113**
N	4.3	64.2	4.3	**24.3**
H	58	28	10	**32**
Cu_{C1}^+	g_x	g_y	g_z	g_{iso}
***g*-value**	2.010	2.013	2.027	**2.017**
	A_x	A_y	A_z	a_{iso}
Cu	-3	21.3	175	**66.4**
P1	132	192	130	**151**
P2	182	120	121	**141**
N	-8.2	42.5	-8.5	**19.8**
H	-39.4	-24.4	3.4	**22.4**

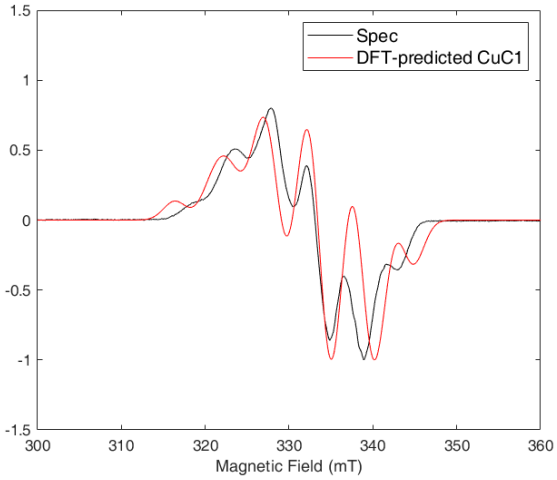

Figure 2.59. Predicted EPR parameters of **Cu_{C1}^+** compared to the simulation (left) and overlay of the predicted EPR spectrum (right, red trace) and the observed spectrum (right, black trace). Simulation line width = 3.

Simulated	g_x	g_y	g_z	g_{iso}
***g*-value**	2.012	2.014	2.023	**2.016**
	A_x	A_y	A_z	a_{iso}
Cu	18	26	146	**63**
P1	130	100	100	**110**
P2	110	100	100	**113**
N	4.3	64.2	4.3	**24.3**
H	58	28	10	**32**
Cu_{C2A}	g_x	g_y	g_z	g_{iso}
***g*-value**	2.006	2.020	2.040	**2.022**
	A_x	A_y	A_z	a_{iso}
Cu	89.3	-6.9	-130	**75.3**
P1	164	122	120	**151**
P2	169	235	169	**191**
N	-6.7	-6.9	-38.8	**17.5**
H	-35	2.1	-22.2	**19.8**

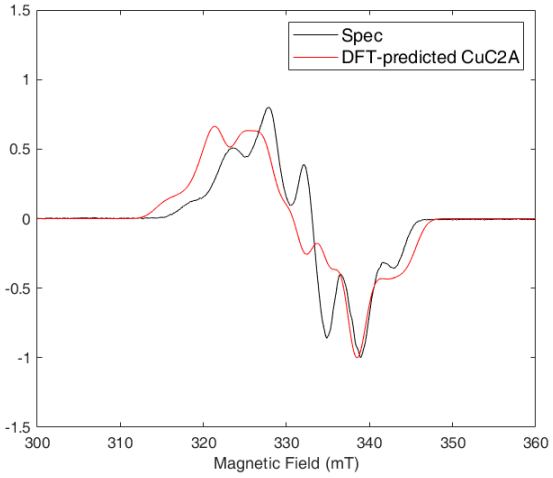

Figure 2.60. Predicted EPR parameters of **Cu_{C2A}** compared to the simulation (left) and overlay of the predicted EPR spectrum (right, red trace) and the observed spectrum (right, black trace). Simulation line width = 2.5.

Simulated	g_x	g_y	g_z	g_{iso}
***g*-value**	2.012	2.014	2.023	**2.016**
	A_x	A_y	A_z	a_{iso}
Cu	18	26	146	**63**
P1	130	100	100	**110**
P2	110	100	100	**113**
N	4.3	64.2	4.3	**24.3**
H	58	28	10	**32**
Cu_{C2A-Br}	g_x	g_y	g_z	g_{iso}
***g*-value**	2.019	2.022	2.036	**2.026**
	A_x	A_y	A_z	a_{iso}
Cu	91	-12	120	**74**
P1	157	116	115	**130**
P2	156	218	156	**177**
N	-7.1	-7.3	39	**18**
H	-36	2.4	-23	**20**

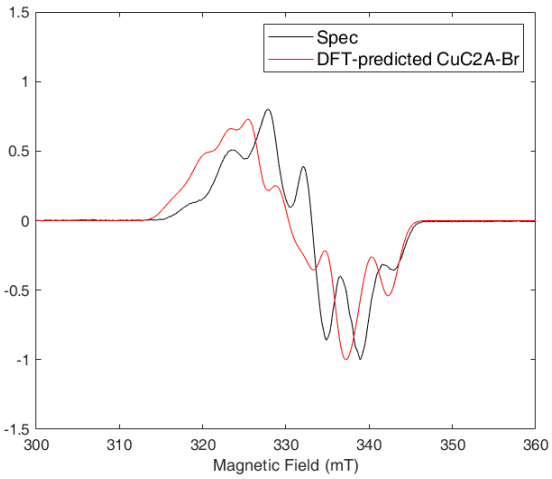

Figure 2.61. Predicted EPR parameters of **Cu_{C2A}-Br** compared to the simulation (left) and overlay of the predicted EPR spectrum (right, red trace) and the observed spectrum (right, black trace). Simulation line width = 2.5.

Simulated	g_x	g_y	g_z	g_{iso}
***g*-value**	2.012	2.014	2.023	**2.016**
	A_x	A_y	A_z	a_{iso}
Cu	18	26	146	**63**
P1	130	100	100	**110**
P2	110	100	100	**113**
N	4.3	64.2	4.3	**24.3**
H	58	28	10	**32**
Cu_{C2B}	g_x	g_y	g_z	g_{iso}
***g*-value**	2.010	2.015	2.045	**2.023**
	A_x	A_y	A_z	a_{iso}
Cu	30	48	-152	**77**
P1	137	136	180	**151**
P2	369	497	372	**413**
N	35.3	-7.1	-7.0	**16**

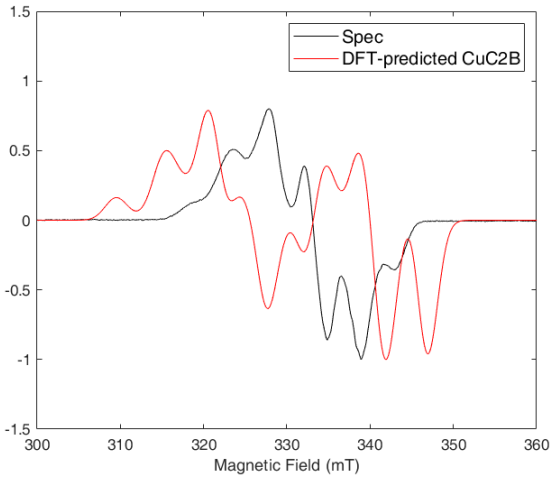

Figure 2.62. Predicted EPR parameters of **Cu_{C2B}** compared to the simulation (left) and overlay of the predicted EPR spectrum (right, red trace) and the observed spectrum (right, black trace). Simulation line width = 3.

Simulated	g_x	g_y	g_z	g_{iso}
***g*-value**	2.012	2.014	2.023	**2.016**
	A_x	A_y	A_z	a_{iso}
Cu	18	26	146	**63**
P1	130	100	100	**110**
P2	110	100	100	**113**
N	4.3	64.2	4.3	**24.3**
H	58	28	10	**32**
Cu_{C3A}	g_x	g_y	g_z	g_{iso}
***g*-value**	2.008	2.011	2.040	**2.019**
	A_x	A_y	A_z	a_{iso}
Cu	-7.1	-15.1	-144	**56**
P1	63	46	45	**51**
P2	84	117	84	**95**
N1	3.7	4.0	33.8	**14**
N2	-4.0	-4.1	34.6	**14**
H1	2.6	-17.0	-14.9	**11**
H2	-11.4	-21.6	3.5	**12**

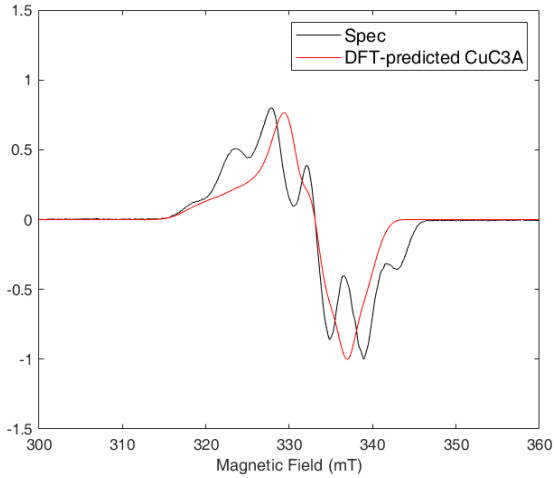

Figure 2.63. Predicted EPR parameters of **Cu_{C3A}** compared to the simulation (left) and overlay of the predicted EPR spectrum (right, red trace) and the observed spectrum (right, black trace). Simulation line width = 2.

Simulated	g_x	g_y	g_z	g_{iso}
***g*-value**	2.012	2.014	2.023	**2.016**
	A_x	A_y	A_z	a_{iso}
Cu	18	26	146	**63**
P1	130	100	100	**110**
P2	110	100	100	**113**
N	4.3	64.2	4.3	**24.3**
H	58	28	10	**32**
Cu_{C3B}	g_x	g_y	g_z	g_{iso}
***g*-value**	2.007	2.011	2.041	**2.020**
	A_x	A_y	A_z	a_{iso}
Cu	18.3	-19.1	-184	**56**
P1	103	136	103	**114**
P2	379	286	288	**318**
N1	-1.9	-2.3	19.7	**8.0**
N2	-1.5	-1.4	29.2	**10.7**
H1	2.4	-24.2	-14.2	**13.6**
H2	-16.3	2.2	-8.8	**9.1**

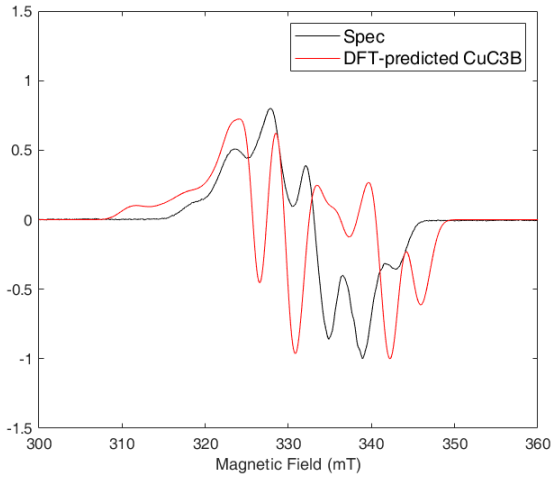

Figure 2.64. Predicted EPR parameters of **Cu_{C3B}** compared to the simulation (left) and overlay of the predicted EPR spectrum (right, red trace) and the observed spectrum (right, black trace). Simulation line width = 2.

Calculated spin densities of Cu_C. Spin densities of the proposed structure of **Cu_C** (three coordinate [**P**Cu(NHAr)]$^+$; **Cu_{C1+}**) were calculated with five different functionals with the def2-TZVP basis set for all atoms, dispersion correction with Becke-Johnson damping (D3BJ), the RIJCOSX approximation, and the solvation model (CPCM (toluene)). All functionals tested support significant spin density on the -NHAr group (**Table 2.9**).

Table 2.9. Calculated spin densities of **Cu_C** with five different functionals.

Functional	BP86	B3LYP	B3PW91	TPSS	PBE0
Spin density					
Cu	0.15 e^-	0.13 e^-	0.13 e^-	0.15 e^-	0.12 e^-
P1	0.08 e^-	0.06 e^-	0.07 e^-	0.08 e^-	0.07 e^-
P2	0.08 e^-	0.06 e^-	0.07 e^-	0.08 e^-	0.06 e^-
NH	0.33 e^-	0.40 e^-	0.41 e^-	0.35 e^-	0.43 e^-
Ar	0.32 e^-	0.32 e^-	0.31 e^-	0.31 e^-	0.31 e^-

Cartesian coordinates of the optimized structures.

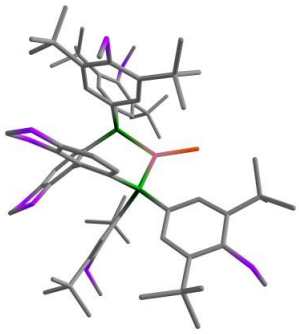

Cu_A (ground)

Cu	6.003193000	12.949017000	21.937938000
P	7.597347000	14.122194000	22.962010000
C	1.101794000	11.680750000	22.160897000
P	5.124284000	14.537650000	20.647169000
Cl	5.600150000	10.792537000	21.987735000
C	5.335191000	16.225987000	28.920117000
O	7.667410000	18.596613000	20.127160000
O	4.751448000	19.533392000	23.860134000
C	1.599101000	17.183334000	17.579235000
O	-0.220582000	13.326793000	18.272658000
O	9.841361000	18.316320000	19.367803000

O	9.243220000	15.091941000	16.345793000
C	9.507870000	17.277987000	20.215331000
O	6.872105000	18.851654000	23.195821000
O	11.908153000	10.701938000	25.286186000
C	1.732071000	14.776472000	18.274223000
C	10.257812000	16.173592000	20.567536000
C	8.197258000	13.771576000	18.092674000
C	7.220127000	13.742955000	19.095534000
C	9.647134000	15.255160000	21.438128000
C	7.541913000	16.005958000	25.089284000
O	4.996780000	16.792447000	27.644825000
C	3.010766000	14.997002000	18.806104000
C	6.302677000	14.772290000	19.282322000
C	8.795952000	19.294399000	19.570019000
C	7.254713000	15.959763000	17.379858000
C	9.090782000	12.514184000	17.980564000
C	6.318310000	15.867597000	18.413195000
C	0.442132000	12.133542000	20.843511000
C	8.190572000	11.256684000	18.089697000
C	8.203972000	17.451482000	20.680036000
C	8.814847000	8.738550000	23.870544000
C	0.969459000	13.733001000	18.857750000
C	9.002168000	13.171855000	23.615595000
C	3.485653000	14.285321000	19.903486000
C	8.239180000	14.933865000	17.289544000
C	3.716484000	16.586520000	21.884830000
C	9.017927000	11.814808000	23.305893000
C	6.958234000	16.643959000	26.192750000
C	6.867022000	15.031128000	24.358921000
C	5.983127000	18.045404000	16.667754000
C	6.122654000	19.962143000	23.731979000
C	2.805477000	14.191727000	24.829287000
C	1.370787000	13.076185000	20.052754000
C	8.341587000	15.422828000	21.920135000
C	10.052649000	13.717776000	24.362373000
C	8.846397000	18.335624000	25.991797000
C	5.539173000	14.739252000	24.672755000
C	3.380938000	15.062957000	25.965178000
C	10.483765000	15.551052000	16.907432000
C	4.876691000	15.358266000	25.733864000
C	4.654305000	18.409864000	23.068046000
C	12.133494000	15.094982000	25.645586000
C	11.350320000	9.983713000	26.399457000
C	8.395140000	17.897539000	16.096341000
C	6.160320000	16.855239000	21.916236000
C	2.577325000	16.381350000	25.976684000
C	3.518516000	17.727530000	22.679753000
C	9.988304000	9.503901000	23.220955000
C	10.029380000	10.952368000	23.760954000
C	3.155147000	14.294058000	27.283548000
C	4.990988000	16.144256000	21.500120000
C	7.559164000	16.546736000	21.511649000
C	-0.849849000	12.899956000	21.206029000
C	2.650508000	13.360230000	20.537013000
C	12.253628000	13.559576000	25.627563000

C	10.086359000	12.494404000	19.158773000
C	5.926936000	17.992390000	22.678270000
C	0.087399000	10.857721000	20.050551000
C	5.634386000	16.254508000	26.536603000
C	9.857653000	12.365607000	16.652767000
C	7.114207000	17.063303000	16.310685000
C	2.091145000	15.421031000	15.859629000
C	11.066611000	12.914840000	24.883880000
C	1.286069000	15.729940000	17.139714000
C	7.807289000	17.695988000	26.943735000
C	11.294995000	8.704681000	23.392383000
C	10.985809000	11.511531000	24.639174000
C	9.730570000	9.567384000	21.693621000
C	8.609901000	17.004882000	28.069516000
C	-0.023104000	12.483045000	17.125484000
C	6.736898000	16.371156000	14.979285000
C	12.347028000	13.097851000	27.097566000
C	6.967068000	18.858994000	27.510101000
C	-0.219862000	15.714738000	16.813959000
C	13.561945000	13.204713000	24.884924000
H	1.361836000	12.532033000	22.805768000
H	2.012538000	11.088716000	21.987930000
H	0.390941000	11.047478000	22.711046000
H	4.429424000	16.264672000	29.539870000
H	6.126395000	16.810197000	29.413481000
H	5.667344000	15.183297000	28.816858000
H	2.669619000	17.358227000	17.743188000
H	1.070290000	17.430765000	18.511160000
H	1.266221000	17.882052000	16.797902000
H	11.273191000	16.024935000	20.204164000
H	7.172141000	12.885877000	19.772597000
H	10.217884000	14.385030000	21.757749000
H	8.540427000	16.295451000	24.773547000
H	3.651105000	15.752679000	18.355922000
H	9.148666000	20.053851000	20.289676000
H	8.514356000	19.733841000	18.606736000
H	5.601321000	16.670561000	18.565795000
H	7.415434000	11.261869000	17.309670000
H	7.693219000	11.164701000	19.062796000
H	8.810548000	10.358696000	17.955303000
H	8.935130000	8.655639000	24.959804000
H	8.759693000	7.720867000	23.455421000
H	7.857240000	9.239557000	23.667857000
H	2.843750000	16.030358000	21.545858000
H	8.198506000	11.421737000	22.699817000
H	6.167802000	18.560371000	17.622287000
H	5.006552000	17.545474000	16.733117000
H	5.908413000	18.807249000	15.879149000
H	6.517403000	20.223199000	24.721066000
H	6.176289000	20.810082000	23.027275000
H	3.257241000	13.190009000	24.799835000
H	2.940441000	14.661217000	23.843676000
H	1.726514000	14.063740000	24.995502000
H	10.075262000	14.789907000	24.536090000
H	9.636029000	17.630697000	25.699192000

H	9.338742000	19.168925000	26.511901000
H	8.381102000	18.718751000	25.074441000
H	5.015627000	14.015831000	24.047065000
H	10.360085000	16.531900000	17.389603000
H	11.190198000	15.633816000	16.072714000
H	10.874653000	14.837248000	17.647817000
H	11.244173000	15.432273000	26.199278000
H	12.092371000	15.522067000	24.633303000
H	13.014752000	15.515209000	26.150016000
H	10.913055000	10.677914000	27.133133000
H	12.179868000	9.432243000	26.858142000
H	10.573624000	9.275819000	26.076319000
H	8.154266000	18.790959000	15.501424000
H	9.160095000	17.330925000	15.558085000
H	8.824830000	18.227711000	17.050372000
H	1.505723000	16.158092000	26.092800000
H	2.715173000	16.914033000	25.026182000
H	2.890279000	17.040571000	26.793685000
H	2.521689000	18.060503000	22.962057000
H	2.099478000	13.992639000	27.355733000
H	3.386086000	14.907284000	28.159443000
H	3.771496000	13.384333000	27.317279000
H	-1.512755000	12.253904000	21.801759000
H	-1.390081000	13.217089000	20.306016000
H	-0.613526000	13.791061000	21.806089000
H	3.036203000	12.842960000	21.414733000
H	10.671185000	11.562592000	19.139922000
H	9.565580000	12.551299000	20.125363000
H	10.790491000	13.337615000	19.111679000
H	-0.441534000	10.153963000	20.711362000
H	0.995143000	10.357427000	19.683710000
H	-0.567303000	11.075257000	19.201044000
H	9.185136000	12.457329000	15.789854000
H	10.310628000	11.363183000	16.629063000
H	10.666934000	13.092593000	16.532654000
H	3.171971000	15.515131000	16.035686000
H	1.810662000	16.121390000	15.058334000
H	1.899433000	14.399834000	15.501173000
H	12.159776000	9.263217000	23.009972000
H	11.207314000	7.774203000	22.812132000
H	11.501621000	8.423599000	24.429397000
H	8.753790000	10.000251000	21.446271000
H	9.750207000	8.548448000	21.280246000
H	10.509629000	10.157501000	21.190767000
H	9.248589000	16.212943000	27.651892000
H	7.964088000	16.546876000	28.827060000
H	9.259344000	17.737152000	28.574252000
H	0.508135000	13.013562000	16.322101000
H	-1.022009000	12.196139000	16.777058000
H	0.549907000	11.582803000	17.394675000
H	6.591852000	17.124698000	14.189802000
H	5.801449000	15.803532000	15.089413000
H	7.528459000	15.681438000	14.660937000
H	11.386224000	13.232777000	27.616425000
H	13.101616000	13.701975000	27.622578000

H	12.644841000	12.048014000	27.175369000
H	6.321871000	19.289662000	26.731326000
H	7.643171000	19.648756000	27.869099000
H	6.318754000	18.566319000	28.340506000
H	-0.429517000	16.549427000	16.127717000
H	-0.827720000	15.853585000	17.717333000
H	-0.548068000	14.796161000	16.318761000
H	14.419282000	13.671536000	25.393118000
H	13.531506000	13.579353000	23.851847000
H	13.720567000	12.120457000	24.858891000

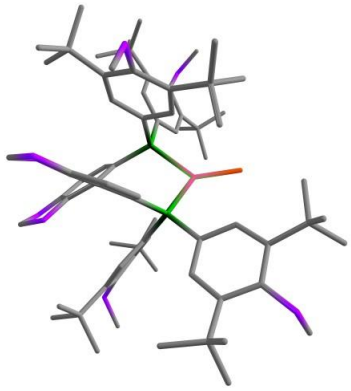

Cu$_A$* (triplet)

Cu	9.119101000	13.629657000	19.830253000
P	9.838184000	14.528298000	21.739395000
C	5.535591000	13.963916000	16.494160000
P	10.142471000	15.193562000	18.606490000
Cl	8.037095000	11.903148000	19.141764000
C	5.032208000	18.357629000	24.459859000
O	13.391802000	18.315377000	20.768798000
O	9.297692000	20.671910000	20.665820000
C	11.348962000	17.481749000	13.998551000
O	8.161091000	14.665531000	13.011661000
O	15.085816000	17.276519000	21.954890000
O	15.972909000	13.979950000	18.937339000
C	13.931273000	16.516108000	22.028699000
O	10.798224000	19.338802000	21.825060000
O	9.711530000	10.173990000	25.815701000
C	9.876706000	15.510408000	14.517106000
C	13.783379000	15.243295000	22.583725000
C	13.676348000	13.206168000	19.061361000
C	12.325392000	13.569947000	18.981971000
C	12.520150000	14.664396000	22.438471000
C	8.978605000	16.687102000	23.321306000
O	5.907163000	18.731070000	23.383869000
C	10.333131000	15.550726000	15.842813000
C	11.920656000	14.845745000	18.607672000
C	14.623168000	18.555864000	21.465433000
C	14.237976000	15.502216000	18.274966000

C	13.969064000	11.739394000	19.456969000
C	12.873368000	15.797746000	18.236154000
C	6.263084000	14.163484000	15.151038000
C	13.011896000	10.809186000	18.670032000
C	12.905766000	17.146980000	21.336974000
C	9.083922000	8.384314000	23.371583000
C	8.605772000	14.922871000	14.298823000
C	9.881121000	13.228007000	22.991682000
C	9.538912000	15.127542000	16.906666000
C	14.618475000	14.221376000	18.771373000
C	9.032130000	17.705150000	18.495597000
C	9.874318000	11.892325000	22.578151000
C	8.082484000	17.674055000	23.747533000
C	8.707903000	15.871081000	22.223901000
C	14.565714000	17.817503000	17.274151000
C	10.374792000	20.696675000	21.627436000
C	5.554148000	16.532015000	19.575014000
C	7.730184000	14.581705000	15.369778000
C	11.455427000	15.309863000	21.781232000
C	10.005000000	13.528374000	24.353835000
C	10.021029000	18.583999000	25.117927000
C	7.551793000	16.083288000	21.475751000
C	5.432232000	17.345655000	20.879778000
C	16.407092000	14.122440000	20.301023000
C	6.631977000	17.078268000	21.812231000
C	9.445667000	19.464355000	20.017718000
C	10.704022000	14.386735000	26.920209000
C	8.319847000	9.930202000	26.114964000
C	16.417616000	16.864006000	18.617246000
C	10.636395000	17.333709000	20.368847000
C	5.387779000	18.836644000	20.481619000
C	8.761449000	19.020363000	18.884112000
C	10.176473000	9.402398000	22.987050000
C	9.916837000	10.837381000	23.493671000
C	4.103557000	16.935334000	21.548389000
C	9.938162000	16.875178000	19.185187000
C	11.638948000	16.591258000	21.134450000
C	5.530877000	15.288487000	14.385911000
C	8.235517000	14.682194000	16.666329000
C	10.405691000	12.881446000	26.780117000
C	13.681321000	11.557044000	20.963460000
C	10.345601000	18.661576000	20.706796000
C	6.143387000	12.835749000	14.371829000
C	6.875288000	17.812370000	23.006433000
C	15.391752000	11.239723000	19.141221000
C	15.252111000	16.497987000	17.673726000
C	12.002685000	15.209372000	13.182483000
C	10.038876000	12.520075000	25.323801000
C	10.800080000	16.140100000	13.447296000
C	8.482259000	18.529715000	24.970242000
C	11.528656000	8.938727000	23.579422000
C	9.875337000	11.183939000	24.873258000
C	10.299464000	9.371665000	21.452166000
C	7.934433000	17.882730000	26.262595000
C	8.767213000	13.502758000	12.421391000

C	15.831296000	15.851319000	16.393381000
C	9.303201000	12.542776000	27.803730000
C	8.008683000	19.993621000	24.853705000
C	10.102822000	16.492282000	12.117889000
C	11.697375000	12.114669000	27.145803000
H	5.541996000	14.877125000	17.105459000
H	5.974714000	13.147879000	17.086166000
H	4.485605000	13.707256000	16.292567000
H	4.032274000	18.738586000	24.212673000
H	5.358674000	18.814831000	25.406084000
H	4.989602000	17.265875000	24.577485000
H	11.992731000	17.347820000	14.877715000
H	10.528910000	18.159699000	14.275446000
H	11.956221000	17.970480000	13.222852000
H	14.587183000	14.748195000	23.124091000
H	11.552801000	12.845124000	19.248251000
H	12.336757000	13.688750000	22.884659000
H	9.935578000	16.573655000	23.826239000
H	11.330031000	15.931748000	16.053870000
H	14.433134000	19.218971000	22.329170000
H	15.362855000	18.974086000	20.773512000
H	12.533904000	16.787376000	17.938009000
H	13.139420000	10.941449000	17.585531000
H	11.953843000	10.973954000	18.909827000
H	13.241836000	9.763389000	18.921492000
H	9.097052000	8.160072000	24.443449000
H	9.264368000	7.442431000	22.833229000
H	8.083825000	8.744293000	23.090413000
H	8.544075000	17.311194000	17.604715000
H	9.836513000	11.680260000	21.510200000
H	14.105126000	18.315060000	18.140130000
H	13.790903000	17.667407000	16.508614000
H	15.319409000	18.496007000	16.850038000
H	10.009772000	21.109428000	22.575097000
H	11.212417000	21.285972000	21.212427000
H	5.490535000	15.448192000	19.750786000
H	6.494551000	16.743604000	19.046620000
H	4.723428000	16.808603000	18.910572000
H	10.104034000	14.567039000	24.655910000
H	10.448962000	17.617923000	25.418630000
H	10.273492000	19.305747000	25.907551000
H	10.506480000	18.900254000	24.184835000
H	7.392760000	15.463241000	20.592632000
H	16.195406000	15.134426000	20.674906000
H	17.488835000	13.942334000	20.302297000
H	15.909881000	13.392436000	20.955387000
H	9.816813000	15.004774000	26.714173000
H	11.515362000	14.711054000	26.252764000
H	11.016507000	14.592052000	27.953572000
H	7.833412000	10.840190000	26.492206000
H	8.302978000	9.151577000	26.887566000
H	7.779491000	9.581930000	25.224201000
H	16.976691000	17.707756000	18.185778000
H	17.110539000	16.028311000	18.747679000
H	16.052359000	17.167725000	19.606093000

H	4.565926000	19.002824000	19.768033000
H	6.327604000	19.127619000	19.991980000
H	5.235985000	19.481260000	21.353325000
H	8.078704000	19.660129000	18.329431000
H	3.281521000	17.024646000	20.821265000
H	3.861092000	17.572596000	22.404429000
H	4.144468000	15.890839000	21.889528000
H	4.476644000	15.010882000	14.236163000
H	5.985691000	15.468251000	13.404870000
H	5.558717000	16.225149000	14.962047000
H	7.621841000	14.384766000	17.514217000
H	13.812929000	10.501294000	21.245571000
H	12.651644000	11.853679000	21.210983000
H	14.355692000	12.164499000	21.582200000
H	5.090828000	12.515409000	14.361112000
H	6.731960000	12.043637000	14.856443000
H	6.471017000	12.938254000	13.333138000
H	15.659025000	11.425867000	18.092804000
H	15.421295000	10.152686000	19.312767000
H	16.159527000	11.692353000	19.775149000
H	12.552988000	15.004803000	14.112295000
H	12.695960000	15.682433000	12.470416000
H	11.689333000	14.244213000	12.762435000
H	12.336818000	9.619951000	23.275914000
H	11.770273000	7.930274000	23.210334000
H	11.488716000	8.910483000	24.675594000
H	9.370506000	9.681812000	20.951306000
H	10.524973000	8.343340000	21.135853000
H	11.112661000	10.014544000	21.089757000
H	8.329062000	16.862186000	26.374386000
H	6.840885000	17.820263000	26.270020000
H	8.250923000	18.468995000	27.138969000
H	9.837388000	13.660981000	12.225592000
H	8.244693000	13.329184000	11.473532000
H	8.651374000	12.627008000	13.077543000
H	16.547115000	16.538365000	15.915301000
H	15.030385000	15.631358000	15.672135000
H	16.355197000	14.915701000	16.629047000
H	8.332923000	12.961873000	27.500452000
H	9.567641000	12.978583000	28.778740000
H	9.195478000	11.462438000	27.943324000
H	8.306598000	20.420939000	23.885748000
H	8.479389000	20.588028000	25.649772000
H	6.924249000	20.106489000	24.938285000
H	10.799629000	17.090082000	11.510942000
H	9.200550000	17.093915000	12.290835000
H	9.818373000	15.615970000	11.528403000
H	12.009621000	12.371093000	28.169697000
H	12.512254000	12.386697000	26.459512000
H	11.540938000	11.030528000	27.090657000

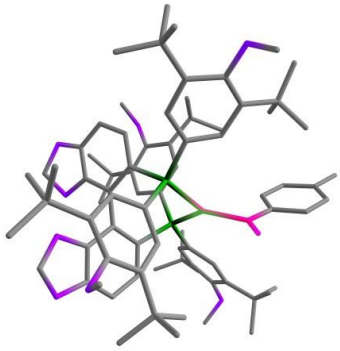

Cu_{C1}^{+}

Cu	5.677199	13.313616	21.953704
P	7.401883	14.408466	22.893360
P	5.053462	14.853729	20.466568
N	5.009167	11.611150	22.352253
C	1.311302	11.319596	21.262409
C	5.985952	16.183505	29.155756
O	7.309825	19.111026	20.519268
O	4.107369	19.388026	24.148325
C	1.714754	16.799963	16.288500
O	-0.118255	13.606271	17.765516
O	9.526797	19.035402	19.828373
O	9.392867	15.823663	16.488285
C	9.220214	17.894002	20.525396
O	6.311065	18.904143	23.614414
O	11.641513	10.482724	24.383448
C	2.047900	14.693326	17.636784
C	10.013561	16.788420	20.756818
C	8.312226	14.337616	18.072825
C	7.298641	14.209139	19.032374
C	9.424760	15.735684	21.478050
C	7.668777	16.107712	25.123842
O	5.494946	16.877335	27.995548
C	5.184955	8.315417	19.743742
C	5.431481	9.629034	19.288898
C	5.355725	10.711497	20.144678
C	5.033559	10.534552	21.519591
C	4.753866	9.216403	21.968730
C	4.837667	8.141003	21.096831
C	3.217051	15.025293	18.334769
C	6.332429	15.190387	19.232287
C	8.404517	19.922748	20.047179
C	7.323607	16.539491	17.463682
C	9.252670	13.122100	17.893627
C	6.340197	16.340289	18.434998
C	0.630298	11.974038	20.046911
C	8.393106	11.834534	17.875068
C	7.890306	17.945154	20.955813
C	8.274558	8.854868	23.243768
C	1.138476	13.826480	18.293343

C	8.771753	13.283997	23.280033
C	3.529943	14.455142	19.565604
C	8.352811	15.558920	17.358347
C	3.420220	16.685779	21.735708
C	8.643030	11.958809	22.870324
C	7.251994	16.729678	26.309484
C	6.854471	15.218134	24.426720
C	6.013755	18.626782	16.835626
C	5.468334	19.516259	24.613787
C	2.802799	14.649572	25.306935
C	1.484946	13.126370	19.482268
C	8.103701	15.786194	21.936078
C	9.946097	13.687066	23.929230
C	9.033544	18.479250	25.869878
C	5.546570	15.000474	24.864232
C	3.564111	15.427788	26.397143
C	10.594793	16.265408	17.140479
C	5.051552	15.597989	26.024578
C	4.146342	18.357501	23.245482
C	12.296747	14.800745	24.988660
C	11.173858	9.711107	25.502941
C	8.464607	18.629396	16.463508
C	5.839780	17.076611	22.016368
C	2.902849	16.819062	26.509099
C	3.088672	17.698183	22.651560
C	9.406429	9.592172	22.498569
C	9.624636	10.989858	23.128814
C	3.386372	14.655806	27.721061
C	4.748273	16.369006	21.416682
C	7.273794	16.913944	21.647152
C	-0.764773	12.448449	20.503690
C	2.690700	13.468413	20.097993
C	12.270749	13.266232	24.874449
C	10.220185	13.044514	19.093182
C	5.476620	18.059616	22.924681
C	0.481945	10.886419	18.959392
C	5.955840	16.393087	26.785867
C	10.061820	13.106535	16.582783
C	7.212757	17.726880	16.484848
C	3.236492	14.985603	15.454978
C	10.950086	12.773464	24.249652
C	1.912083	15.272638	16.207850
C	8.249454	17.715723	26.967590
C	10.661245	8.700018	22.442308
C	10.723177	11.403524	23.920564
C	8.965494	9.784634	21.025905
C	9.282552	16.916134	27.790656
C	-1.032474	14.687844	18.012623
C	6.978327	17.157473	15.067243
C	12.487270	12.701705	26.294059
C	7.599514	18.799314	27.849712
C	0.798886	14.657279	15.339950
C	13.446420	12.851122	23.962066
H	1.410574	12.014395	22.110050
H	2.307691	10.928301	21.015825

H	0.699377	10.471630	21.601399
H	5.328737	16.465335	29.987604
H	7.015320	16.479774	29.401570
H	5.953819	15.093610	29.009921
H	2.539839	17.284105	16.831532
H	0.779203	17.063331	16.803429
H	1.676959	17.233796	15.278373
H	11.044300	16.734995	20.411654
H	7.265788	13.315530	19.657376
H	10.027903	14.857232	21.696654
H	8.648185	16.351225	24.719193
H	3.915819	15.732197	17.890682
H	8.674377	20.660267	20.821863
H	8.124556	20.402850	19.102253
H	5.570686	17.093065	18.590434
H	7.640248	11.875857	17.074201
H	7.872562	11.652308	18.822441
H	9.040683	10.965577	17.691389
H	8.522112	8.683007	24.300139
H	8.088526	7.876311	22.776512
H	7.335471	9.424470	23.208171
H	2.615791	16.120860	21.265433
H	7.734075	11.670427	22.342034
H	6.110001	19.083457	17.831965
H	5.056910	18.084389	16.802237
H	5.947960	19.441038	16.100645
H	5.570681	18.960258	25.561246
H	5.726371	20.576144	24.713958
H	3.152911	13.611102	25.209190
H	2.874583	15.135559	24.322412
H	1.738055	14.610422	25.576384
H	10.074536	14.735312	24.183741
H	9.760962	17.845767	25.345508
H	9.607009	19.289789	26.340211
H	8.366117	18.920733	25.118216
H	4.896541	14.365951	24.261225
H	10.419804	17.192545	17.706047
H	11.328288	16.454421	16.347441
H	10.991123	15.498433	17.822656
H	11.525873	15.179229	25.675988
H	12.172137	15.298472	24.015686
H	13.270270	15.111377	25.392762
H	10.897235	10.364587	26.344591
H	12.003739	9.058269	25.798234
H	10.303839	9.091953	25.239247
H	8.228485	19.565632	15.935652
H	9.301319	18.158827	15.938840
H	8.797431	18.886787	17.477137
H	1.836227	16.707030	26.756753
H	2.971470	17.356523	25.553943
H	3.375699	17.428863	27.287239
H	2.053301	17.944166	22.881426
H	2.319966	14.434611	27.877917
H	3.731334	15.235120	28.583197
H	3.927264	13.698443	27.700949

H	-1.280182	11.622729	21.017687
H	-1.393439	12.754473	19.661720
H	-0.686496	13.286215	21.212469
H	3.000546	12.964931	21.012836
H	10.880501	12.170274	18.991062
H	9.680671	12.952146	20.046329
H	10.858325	13.937495	19.157325
H	-0.103598	10.042197	19.353388
H	1.467151	10.501959	18.655395
H	-0.029268	11.274354	18.070849
H	9.417953	13.253238	15.705896
H	10.545794	12.123053	16.487349
H	10.855358	13.859804	16.551005
H	4.110130	15.440762	15.939174
H	3.177936	15.393479	14.436206
H	3.421371	13.904322	15.380883
H	11.515695	9.229767	22.001219
H	10.440541	7.831439	21.803751
H	10.969868	8.312515	23.417834
H	8.023112	10.337632	20.923778
H	8.805998	8.800277	20.563777
H	9.738488	10.310387	20.449918
H	9.798113	16.183674	27.152175
H	8.825645	16.364852	28.622239
H	10.040363	17.594937	28.210337
H	-1.987901	14.399346	17.558642
H	-0.682263	15.628721	17.562998
H	-1.171554	14.847289	19.093243
H	6.883985	17.981574	14.343437
H	6.052955	16.564632	15.027438
H	7.812369	16.518266	14.752228
H	11.617007	12.897415	26.938577
H	13.358083	13.191828	26.754498
H	12.684287	11.625249	26.279366
H	6.851412	19.380164	27.291651
H	8.383653	19.499424	28.173794
H	7.113378	18.410429	28.747121
H	0.929996	15.016766	14.307963
H	-0.209236	14.945732	15.652837
H	0.853073	13.561071	15.323907
H	14.392965	13.225086	24.380333
H	13.331236	13.279513	22.955534
H	13.519029	11.761251	23.868657
H	4.678288	11.361452	23.287707
C	5.281170	7.150618	18.802920
H	5.678333	9.792794	18.238274
H	5.512652	11.726723	19.772856
H	4.490933	9.059428	23.016895
H	4.629710	7.135193	21.466662
H	5.009794	6.208907	19.296748
H	4.619379	7.284200	17.933172
H	6.303408	7.044629	18.406542

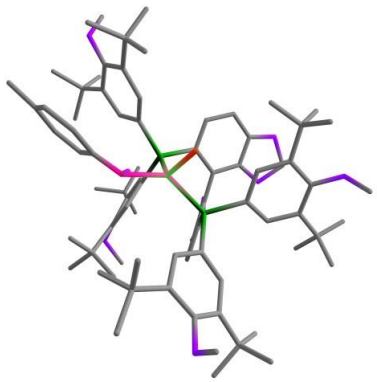

Cu_{C2A}

Cu	5.461036	12.935320	22.139247
Cl	5.024754	11.541074	23.941042
N	5.608579	11.365200	20.954673
P	6.849020	14.509696	23.068793
P	4.173695	14.458097	21.098993
C	1.900166	9.512581	17.007599
C	1.324101	10.405653	22.481060
C	6.357306	15.784588	29.581006
O	5.304156	19.212988	21.253089
O	2.791423	18.396077	25.323715
C	-0.545239	15.259003	17.420739
O	-0.837350	11.977111	18.978773
O	7.353085	19.772683	20.318766
O	7.388673	16.985224	16.736623
C	7.435712	18.525541	20.903923
O	4.886484	18.587079	24.344723
O	12.098642	11.710943	23.654814
C	0.941579	13.618296	18.653113
C	8.498352	17.645149	20.914272
C	7.015218	15.125461	18.251097
C	6.241148	14.631691	19.309475
C	8.289143	16.418575	21.569304
C	7.152150	16.174362	25.310374
O	5.504960	16.395013	28.598497
C	2.947512	9.959852	17.987493
C	3.504179	11.250174	17.917579
C	4.397008	11.712243	18.870144
C	4.781062	10.900177	19.971591
C	4.253653	9.578749	20.010218
C	3.367561	9.128048	19.041935
C	2.071432	14.231657	19.210860
C	5.074151	15.256480	19.739118
C	6.109388	20.322478	20.814438
C	5.363363	16.970664	18.031152
C	8.210092	14.242789	17.818762
C	4.633275	16.410722	19.083336
C	0.343549	10.872811	21.387202

C	7.710021	12.779994	17.704826
C	6.208422	18.196026	21.482515
C	9.044604	9.445263	22.676831
C	0.332618	12.581061	19.409960
C	8.516978	13.782202	23.176807
C	2.635037	13.790249	20.403657
C	6.598000	16.351038	17.684216
C	2.410158	15.680132	22.848251
C	8.676001	12.524009	22.604233
C	6.866181	16.669290	26.589724
C	6.417548	15.143432	24.727542
C	3.421081	18.597212	17.804158
C	4.129791	18.895392	25.534260
C	2.829807	13.720964	26.321762
C	0.925160	12.060292	20.593299
C	7.072420	16.088076	22.175083
C	9.631219	14.409966	23.748048
C	8.169239	18.742151	25.930119
C	5.287852	14.653818	25.383579
C	3.639580	14.578566	27.313995
C	8.492115	17.699338	17.317754
C	4.930396	15.109076	26.656798
C	2.931708	17.444543	24.337008
C	11.777072	16.025011	24.565525
C	11.940263	10.790880	24.749050
C	5.689134	19.386356	17.181769
C	4.623780	16.746446	22.707139
C	2.736452	15.751581	27.753147
C	2.006048	16.517988	23.899806
C	9.912093	10.463560	21.904738
C	9.886179	11.815643	22.653043
C	3.961531	13.684928	28.531166
C	3.678367	15.772027	22.255026
C	5.965391	16.988241	22.116431
C	-0.964626	11.303488	22.085600
C	2.087464	12.681120	21.056119
C	12.098877	14.533788	24.351076
C	9.305387	14.295446	18.904333
C	4.192442	17.557888	23.747893
C	0.079344	9.653480	20.479280
C	5.789335	16.054877	27.282121
C	8.825311	14.585109	16.448720
C	4.773299	18.144155	17.222071
C	1.671303	14.675154	16.462165
C	10.865291	13.766021	23.835851
C	0.474390	14.109443	17.263523
C	7.759566	17.822301	27.108437
C	11.313591	9.873383	21.658220
C	10.938826	12.418821	23.375361
C	9.290504	10.673235	20.500091
C	9.057341	17.232699	27.704417
C	-2.062087	12.703816	19.157724
C	4.527170	17.652979	15.776840
C	12.610852	13.976898	25.696301
C	7.081158	18.741456	28.143002

C	-0.107724	12.978787	16.390403
C	13.222168	14.460822	23.291905
H	1.500792	11.168272	23.252714
H	2.297299	10.122505	22.056975
H	0.900321	9.521853	22.978971
H	5.796765	15.781927	30.524458
H	7.286155	16.358353	29.718305
H	6.608919	14.752895	29.296772
H	-0.093098	16.098173	17.969415
H	-1.444421	14.948986	17.963970
H	-0.855302	15.624604	16.429986
H	9.454726	17.889217	20.454951
H	6.558612	13.725122	19.825913
H	9.112630	15.709755	21.618624
H	7.956825	16.627880	24.737198
H	2.558961	15.041080	18.675204
H	6.325503	20.981570	21.673340
H	5.594771	20.849888	20.003570
H	3.716526	16.886527	19.423336
H	6.892318	12.702412	16.974155
H	7.352176	12.373612	18.658439
H	8.536871	12.139166	17.364170
H	9.462500	9.233559	23.671487
H	8.988494	8.497719	22.120980
H	8.021717	9.823266	22.819663
H	1.714457	14.923486	22.486279
H	7.812383	12.074946	22.111873
H	3.521716	18.965339	18.835776
H	2.677164	17.787171	17.798738
H	3.024762	19.415747	17.186909
H	4.579563	18.361844	26.389160
H	4.098004	19.980819	25.676912
H	3.366446	12.812978	26.012304
H	2.571852	14.286186	25.415500
H	1.893194	13.413126	26.808059
H	9.532183	15.422998	24.125198
H	8.858604	18.253676	25.229465
H	8.690271	19.622040	26.332149
H	7.292013	19.081493	25.363029
H	4.696431	13.889359	24.885649
H	8.135012	18.506778	17.973888
H	9.062749	18.123702	16.482902
H	9.138258	17.029644	17.904824
H	11.044403	16.181962	25.370877
H	11.391182	16.498231	23.651577
H	12.698571	16.550775	24.853403
H	11.601306	11.316947	25.654538
H	12.926760	10.345629	24.924003
H	11.216113	9.999052	24.508779
H	5.124065	20.241980	16.782586
H	6.558927	19.229098	16.537662
H	6.048040	19.650560	18.184326
H	1.812194	15.353355	28.198245
H	2.458646	16.373508	26.892433
H	3.233720	16.386975	28.494154

H	1.017109	16.436047	24.347766
H	3.035267	13.211265	28.891231
H	4.385759	14.258015	29.361901
H	4.665811	12.887231	28.254242
H	-1.330211	10.483078	22.721637
H	-1.753340	11.545967	21.365361
H	-0.794732	12.182710	22.724040
H	2.604352	12.296680	21.934500
H	10.141748	13.637193	18.626814
H	8.920041	13.962319	19.878062
H	9.699108	15.313734	19.028599
H	-0.309141	8.823737	21.089041
H	1.016884	9.323801	20.011994
H	-0.643954	9.880906	19.691252
H	8.057623	14.623257	15.664500
H	9.542658	13.792722	16.188619
H	9.368123	15.535006	16.439679
H	2.060634	15.611623	16.882380
H	1.339745	14.898258	15.438827
H	2.499733	13.955046	16.404964
H	11.978196	10.605601	21.180623
H	11.208055	9.013599	20.979359
H	11.800723	9.512108	22.568631
H	8.242616	10.999247	20.534310
H	9.322525	9.723133	19.948049
H	9.862393	11.419186	19.931400
H	9.570629	16.604918	26.961454
H	8.862905	16.609029	28.585985
H	9.740958	18.043436	27.999558
H	-2.817651	11.991904	19.517938
H	-2.403238	13.126198	18.200841
H	-1.940812	13.512706	19.892169
H	4.092639	18.464619	15.172665
H	3.825587	16.805773	15.767627
H	5.465193	17.334585	15.305955
H	11.805053	13.963171	26.444975
H	13.417897	14.621811	26.076215
H	13.012850	12.964529	25.592705
H	6.150168	19.168750	27.744956
H	7.760486	19.576680	28.367749
H	6.838850	18.240408	29.083192
H	-0.302358	13.371928	15.381903
H	-1.040977	12.564332	16.778018
H	0.612025	12.152907	16.299231
H	14.100104	15.021865	23.645299
H	12.889973	14.910555	22.344629
H	13.525011	13.425983	23.099513
H	5.732561	10.616949	21.649168
H	3.213258	11.912319	17.099433
H	4.798429	12.719520	18.790003
H	4.540934	8.926859	20.838796
H	2.970018	8.112872	19.110822
H	1.836453	8.416937	16.954624
H	0.906344	9.886857	17.306082
H	2.100551	9.898892	15.997692

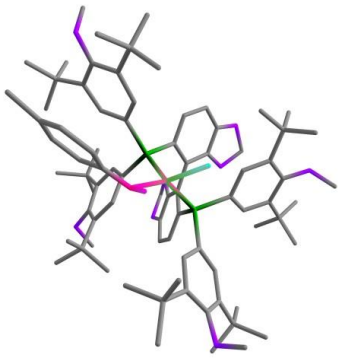

Cu_{C2A} – Br

Cu	5.497803	12.928573	22.094169
Br	5.073490	11.381223	23.962396
N	5.671635	11.394857	20.861681
P	6.858643	14.501879	23.065959
P	4.175681	14.455315	21.092935
C	1.865786	9.540332	17.008295
C	1.339198	10.387547	22.469134
C	6.352960	15.796732	29.580754
O	5.304775	19.197474	21.234469
O	2.800986	18.394453	25.319613
C	-0.584207	15.279569	17.467424
O	-0.849057	11.981553	18.994735
O	7.350177	19.752951	20.290061
O	7.381248	16.978035	16.719051
C	7.435893	18.509700	20.883028
O	4.895004	18.584067	24.337054
O	12.106643	11.711219	23.698545
C	0.920803	13.633756	18.671609
C	8.500089	17.631314	20.897839
C	7.012778	15.126804	18.244779
C	6.240334	14.638738	19.306425
C	8.294247	16.409069	21.562070
C	7.152170	16.167279	25.304954
O	5.502366	16.397171	28.590553
C	2.931989	9.991433	17.965770
C	3.472640	11.288279	17.891155
C	4.386023	11.752658	18.822661
C	4.812875	10.933330	19.902183
C	4.300273	9.606804	19.945659
C	3.388624	9.155721	19.001645
C	2.054738	14.242960	19.225301
C	5.069418	15.260127	19.730915
C	6.107911	20.304933	20.786889
C	5.354028	16.963587	18.011395
C	8.206623	14.240306	17.817134
C	4.623997	16.407542	19.066037
C	0.353644	10.858131	21.381624
C	7.702989	12.778043	17.709637

C	6.210621	18.182876	21.467548
C	9.048862	9.453161	22.685190
C	0.321528	12.586508	19.422640
C	8.529620	13.782040	23.184691
C	2.632234	13.788836	20.406527
C	6.591907	16.347120	17.669892
C	2.418198	15.670859	22.853423
C	8.695944	12.524596	22.613151
C	6.865532	16.665857	26.582642
C	6.416190	15.137061	24.722097
C	3.408457	18.584214	17.772475
C	4.137882	18.899721	25.524552
C	2.826744	13.718893	26.324809
C	0.926159	12.055062	20.595224
C	7.079018	16.080649	22.171830
C	9.639012	14.411256	23.764012
C	8.191592	18.725805	25.924120
C	5.283799	14.653261	25.377614
C	3.639075	14.579076	27.312241
C	8.484209	17.695890	17.296668
C	4.927797	15.109115	26.651101
C	2.941047	17.439972	24.336005
C	11.779402	16.027859	24.595381
C	11.932903	10.792540	24.791945
C	5.675719	19.373311	17.145976
C	4.630429	16.739086	22.704805
C	2.736201	15.751617	27.753015
C	2.015766	16.510676	23.904103
C	9.935693	10.464421	21.925787
C	9.905722	11.816925	22.672923
C	3.968531	13.686363	28.528216
C	3.684639	15.763465	22.256928
C	5.970630	16.979014	22.109912
C	-0.954969	11.275323	22.087420
C	2.092681	12.672243	21.052834
C	12.101736	14.535786	24.388841
C	9.300625	14.294795	18.903746
C	4.200764	17.552738	23.744494
C	0.094594	9.645016	20.463938
C	5.787980	16.054163	27.275670
C	8.823644	14.576019	16.446436
C	4.761648	18.129918	17.193893
C	1.629141	14.720228	16.488231
C	10.872745	13.768029	23.863005
C	0.441262	14.137994	17.290970
C	7.760744	17.816327	27.102662
C	11.336335	9.864144	21.701140
C	10.950981	12.420218	23.405271
C	9.337885	10.679324	20.511403
C	9.046010	17.220808	27.719524
C	-2.076132	12.701883	19.183147
C	4.516909	17.629017	15.751676
C	12.598610	13.981723	25.740894
C	7.075444	18.748994	28.120591
C	-0.139464	13.012782	16.409822

C	13.236582	14.458575	23.342281
H	1.517366	11.146646	23.243998
H	2.312100	10.108317	22.041955
H	0.919189	9.500444	22.964381
H	5.759112	15.712098	30.499991
H	7.234016	16.424680	29.782967
H	6.685450	14.798774	29.262371
H	-0.132797	16.116080	18.020774
H	-1.476803	14.958396	18.014619
H	-0.903916	15.652700	16.482550
H	9.455623	17.874234	20.436176
H	6.560322	13.735892	19.827770
H	9.118559	15.701316	21.614006
H	7.958623	16.618099	24.732379
H	2.535411	15.058938	18.693827
H	6.326666	20.968868	21.641375
H	5.590307	20.827615	19.974922
H	3.703540	16.881162	19.399084
H	6.890697	12.698335	16.973139
H	7.335437	12.379377	18.663099
H	8.530337	12.132434	17.379347
H	9.453204	9.236500	23.684369
H	8.990808	8.506793	22.127588
H	8.027895	9.840312	22.818434
H	1.721817	14.913921	22.493438
H	7.837935	12.073820	22.113482
H	3.507983	18.959717	18.801536
H	2.666371	17.772596	17.772299
H	3.010477	19.397623	17.149534
H	4.589782	18.375268	26.383805
H	4.102813	19.986276	25.658149
H	3.362508	12.808774	26.019616
H	2.567090	14.280337	25.416692
H	1.891068	13.412889	26.813923
H	9.536624	15.424623	24.139184
H	8.883149	18.228413	25.232032
H	8.717324	19.602211	26.327682
H	7.323232	19.071915	25.347516
H	4.683486	13.896464	24.878918
H	8.126234	18.505904	17.949187
H	9.054127	18.117031	16.459723
H	9.131260	17.029538	17.886502
H	11.040590	16.187881	25.394408
H	11.401021	16.497686	23.676579
H	12.698901	16.554122	24.888661
H	11.592004	11.321792	25.694846
H	12.914371	10.339000	24.973747
H	11.203496	10.007135	24.546451
H	5.108818	20.226528	16.744277
H	6.544368	19.214099	16.500793
H	6.036711	19.642199	18.146567
H	1.812121	15.353050	28.198103
H	2.458393	16.374258	26.892771
H	3.233640	16.386594	28.494165
H	1.028033	16.428968	24.354715

H	3.044538	13.213380	28.894847
H	4.399345	14.259441	29.355350
H	4.670795	12.888440	28.247008
H	-1.312292	10.448444	22.719703
H	-1.748185	11.516619	21.371926
H	-0.788802	12.151581	22.730895
H	2.618121	12.279486	21.922579
H	10.135269	13.632595	18.630655
H	8.912737	13.966875	19.878194
H	9.697059	15.312503	19.024293
H	-0.288277	8.808055	21.067312
H	1.033379	9.324459	19.992735
H	-0.631290	9.874952	19.678994
H	8.056465	14.614111	15.661708
H	9.538643	13.780601	16.189100
H	9.369532	15.524200	16.434631
H	2.017205	15.652635	16.918657
H	1.288252	14.955683	15.470794
H	2.460156	14.004572	16.414817
H	12.012389	10.590064	21.230027
H	11.234307	9.002490	21.024055
H	11.808261	9.502761	22.619476
H	8.294387	11.019765	20.529934
H	9.365628	9.728023	19.961252
H	9.927639	11.417027	19.949847
H	9.562943	16.583773	26.987046
H	8.836165	16.604807	28.602965
H	9.732382	18.028332	28.016956
H	-2.826676	11.984482	19.542850
H	-2.423686	13.127776	18.230162
H	-1.955370	13.507221	19.921532
H	4.081750	18.436309	15.142147
H	3.816596	16.780776	15.747098
H	5.455676	17.309130	15.283325
H	11.784787	13.970280	26.480850
H	13.402015	14.626846	26.128037
H	13.000724	12.968692	25.643928
H	6.156673	19.184644	27.703659
H	7.760246	19.577850	28.352137
H	6.810745	18.256601	29.059124
H	-0.345147	13.415082	15.407183
H	-1.066378	12.587077	16.800589
H	0.585512	12.193199	16.304310
H	14.111186	15.019334	23.704300
H	12.915806	14.906488	22.390207
H	13.540254	13.422905	23.155889
H	5.847353	10.626254	21.521549
H	3.153266	11.953003	17.085901
H	4.777069	12.763645	18.738316
H	4.619170	8.951623	20.759956
H	3.001310	8.136927	19.074727
H	1.797585	8.444646	16.965275
H	0.879012	9.920968	17.320991
H	2.049895	9.917979	15.991938

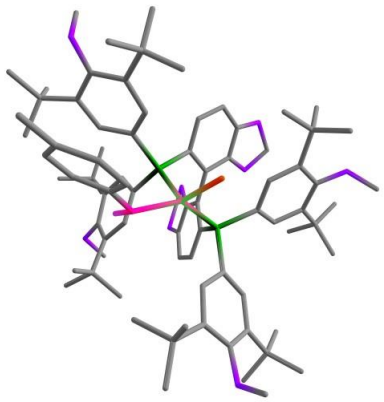

Cu_{C2B}

Cu	5.773249	13.028899	22.383281
Cl	4.522364	12.244255	24.144458
N	5.719245	11.641894	20.976106
P	7.370064	14.344965	23.340685
P	5.081074	14.598679	20.934458
C	1.498191	8.021003	19.608881
C	0.876371	12.341693	22.916708
C	6.338590	16.976987	29.335408
O	7.376436	18.738166	20.413486
O	4.287797	19.559034	24.086466
C	1.953916	14.956640	16.106784
O	-0.195129	12.970779	18.674551
O	9.568933	18.517345	19.690539
O	9.040674	15.548854	16.556181
C	9.255341	17.476582	20.541179
O	6.462082	18.984684	23.514840
O	11.573398	10.411788	24.962406
C	2.111475	13.608861	18.236147
C	10.033193	16.400827	20.918479
C	8.245039	14.159396	18.376328
C	7.341187	14.056194	19.443454
C	9.436566	15.469604	21.788101
C	7.822751	16.291511	25.320997
O	5.836298	17.587966	28.136347
C	2.587630	8.993709	19.970313
C	3.057339	9.102274	21.296083
C	4.065237	9.987255	21.648441
C	4.674412	10.812211	20.665784
C	4.180792	10.719498	19.337294
C	3.165563	9.834624	19.004332
C	3.309019	14.077105	18.798474
C	6.252517	14.912173	19.583567
C	8.493844	19.466730	19.872613
C	6.942040	16.121726	17.582472
C	9.251373	12.995151	18.217524
C	6.045344	15.921526	18.634826

C	0.282075	12.502185	21.504710
C	8.440011	11.674123	18.261376
C	7.938798	17.616827	20.986042
C	8.238123	8.829132	23.709209
C	1.084657	13.242294	19.137908
C	8.740976	13.243792	23.813062
C	3.525570	14.077102	20.172103
C	8.082402	15.270140	17.517784
C	3.473603	16.550306	22.103996
C	8.633548	11.928998	23.366992
C	7.494363	17.104545	26.414473
C	6.921367	15.376891	24.777639
C	5.314213	17.907425	16.781124
C	5.672015	19.746820	24.450513
C	2.873235	15.278397	25.819224
C	1.318500	13.105769	20.535026
C	8.121340	15.602857	22.246215
C	9.887898	13.630175	24.516854
C	9.320800	18.680610	25.659874
C	5.612795	15.331676	25.262470
C	3.736769	16.096284	26.798766
C	10.217204	16.168785	17.107468
C	5.211310	16.118874	26.345837
C	4.280311	18.406034	23.333943
C	12.211555	14.717673	25.664898
C	11.059959	9.634291	26.057557
C	7.719970	18.199597	16.275532
C	5.901780	16.954261	22.211202
C	3.172453	17.533486	26.822555
C	3.192985	17.676648	22.894283
C	9.385762	9.568604	22.987848
C	9.600344	10.951869	23.644448
C	3.581671	15.451841	28.192816
C	4.782676	16.185524	21.758301
C	7.315550	16.703944	21.821752
C	-0.961856	13.406350	21.635015
C	2.562392	13.510599	21.020246
C	12.182049	13.184606	25.528324
C	10.249660	12.996746	19.389851
C	5.589587	18.057425	22.991647
C	-0.135451	11.099154	21.018227
C	6.199356	16.929894	26.968421
C	10.029347	12.963838	16.888494
C	6.614518	17.142312	16.473272
C	3.379777	12.902483	16.177977
C	10.882037	12.707853	24.850040
C	2.059893	13.531713	16.691649
C	8.575395	18.105744	26.891830
C	10.641812	8.678273	22.934860
C	10.669747	11.346791	24.480847
C	8.954504	9.788811	21.514395
C	9.620398	17.365975	27.755102
C	-0.947847	14.149008	18.349992
C	6.407375	16.360141	15.156178
C	12.345411	12.598159	26.946172

C	8.029452	19.322416	27.665603
C	0.933688	12.644804	16.125719
C	13.388340	12.779212	24.651024
H	1.121390	13.311189	23.373492
H	1.788686	11.729141	22.923153
H	0.130049	11.852041	23.558904
H	5.784605	17.426899	30.167935
H	7.412871	17.170880	29.469498
H	6.169825	15.889411	29.321704
H	2.820283	15.567703	16.401653
H	1.048467	15.472262	16.455622
H	1.924874	14.916074	15.007286
H	11.059097	16.282181	20.573362
H	7.508366	13.297387	20.208188
H	10.026757	14.619055	22.124046
H	8.800864	16.400265	24.857042
H	4.100400	14.432549	18.142495
H	8.812638	20.237361	20.596039
H	8.216215	19.896602	18.904275
H	5.173551	16.562524	18.740538
H	7.664771	11.667083	17.481419
H	7.954935	11.503469	19.230198
H	9.115943	10.825177	18.084421
H	8.478280	8.631477	24.762408
H	8.041575	7.865597	23.215095
H	7.312212	9.421338	23.680688
H	2.645739	15.936880	21.751855
H	7.750957	11.656189	22.783990
H	5.392086	18.482309	17.715114
H	4.444395	17.239319	16.860397
H	5.115051	18.614576	15.963773
H	5.833061	19.346373	25.466702
H	5.931412	20.808174	24.368528
H	3.160209	14.218064	25.789005
H	2.938790	15.674013	24.795457
H	1.822858	15.338774	26.139073
H	10.003579	14.670550	24.807017
H	9.933241	17.926776	25.148266
H	10.002885	19.477055	25.990064
H	8.619925	19.097305	24.924794
H	4.911371	14.651756	24.781542
H	9.974553	17.149357	17.543023
H	10.921366	16.291177	16.276018
H	10.672849	15.540139	17.887618
H	11.419495	15.087546	26.331713
H	12.113981	15.222869	24.693141
H	13.174568	15.016628	26.102050
H	10.669836	10.288358	26.852209
H	11.902587	9.046042	26.440400
H	10.258985	8.954157	25.732240
H	7.368604	18.965334	15.568015
H	8.638190	17.762192	15.874849
H	7.954794	18.699054	17.225131
H	2.108601	17.504790	27.103388
H	3.247215	17.995823	25.828764

H	3.706301	18.166203	27.540426
H	2.172198	17.954702	23.150812
H	2.512392	15.334986	28.424394
H	4.028870	16.066277	28.981232
H	4.043620	14.454549	28.214644
H	-1.613837	13.015398	22.431668
H	-1.546936	13.438045	20.710467
H	-0.675353	14.432804	21.909359
H	2.810336	13.380922	22.073598
H	10.940140	12.144860	19.297951
H	9.735717	12.911685	20.357461
H	10.844468	13.920564	19.407263
H	-0.858278	10.661533	21.724269
H	0.746048	10.447730	20.972815
H	-0.596686	11.135036	20.024735
H	9.354766	13.021128	16.024946
H	10.574321	12.009368	16.836111
H	10.768264	13.766497	16.799677
H	4.267495	13.487795	16.448391
H	3.347498	12.842030	15.080750
H	3.506970	11.884382	16.571081
H	11.494973	9.218293	22.502566
H	10.426619	7.812517	22.291020
H	10.945823	8.292243	23.912428
H	7.979384	10.286795	21.423869
H	8.868960	8.812659	21.016237
H	9.700663	10.386638	20.972660
H	10.045782	16.519587	27.197721
H	9.190756	16.970595	28.684002
H	10.440718	18.048718	28.022432
H	-1.972942	13.816530	18.147082
H	-0.546633	14.654529	17.458810
H	-0.947283	14.858602	19.191091
H	6.142950	17.054661	14.344283
H	5.590121	15.631797	15.265163
H	7.318352	15.821351	14.867262
H	11.454805	12.798608	27.560201
H	13.209008	13.068617	27.439931
H	12.522028	11.518640	26.918159
H	7.244989	19.840170	27.096243
H	8.852962	20.034490	27.827077
H	7.616239	19.067189	28.644515
H	1.113900	12.498410	15.050020
H	-0.062405	13.083987	16.234023
H	0.927195	11.659198	16.608540
H	14.319919	13.147253	25.106952
H	13.302332	13.223144	23.648726
H	13.457916	11.690559	24.546159
H	6.042940	12.050965	20.093288
H	2.612458	8.470396	22.068935
H	4.406315	10.074191	22.679055
H	4.612513	11.372224	18.576197
H	2.806804	9.789273	17.972982
H	1.322868	8.005607	18.524667
H	1.750747	6.998170	19.929158

H 0.545988 8.282378 20.097821

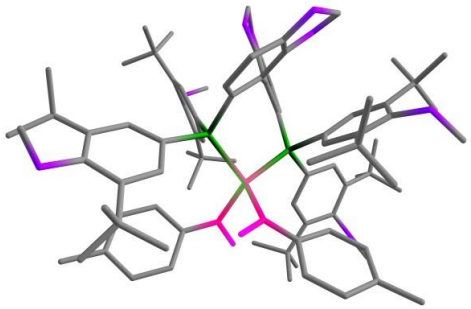

Cu$_{C3A}$

Cu	5.367816000	12.705254000	21.863013000
N	6.655493000	14.176125000	21.689165000
N	6.792435000	11.601180000	22.778085000
P	4.250401000	12.288252000	19.908910000
P	3.494595000	12.708587000	23.118446000
C	7.592205000	11.630367000	28.466300000
C	7.003782000	15.834439000	25.210266000
C	4.513382000	17.502094000	15.887255000
O	-0.845586000	11.845117000	21.167624000
O	0.077099000	16.600785000	20.211723000
C	1.048192000	12.886997000	28.401095000
O	4.353656000	14.886891000	28.620412000
O	-1.108871000	9.715750000	20.280040000
O	1.211624000	7.180818000	23.229188000
C	0.184215000	10.151118000	20.066465000
O	0.177629000	14.438358000	19.371792000
O	8.120490000	9.439766000	16.366004000
C	3.269185000	13.203406000	27.232974000
C	1.239272000	9.474055000	19.488537000
C	3.100419000	8.665719000	22.882160000
C	3.532592000	9.997568000	22.829502000
C	2.468546000	10.154751000	19.435791000
C	3.163522000	13.825504000	17.786547000
O	3.473757000	17.381527000	16.870945000
C	7.413215000	11.601789000	26.972553000
C	6.218727000	11.128644000	26.399406000
C	6.016109000	11.120587000	25.029967000
C	7.008717000	11.600025000	24.133678000
C	8.220046000	12.062446000	24.715826000
C	8.410949000	12.056797000	26.094604000
C	3.011246000	12.777688000	25.921550000
C	2.727300000	11.063047000	23.219815000
C	-1.825697000	10.899893000	20.698476000
C	0.940375000	9.505489000	23.782127000
C	4.154415000	7.595864000	22.511690000
C	1.442488000	10.807966000	23.711056000
C	6.162283000	15.727744000	26.498422000
C	5.476772000	7.938596000	23.243315000

C	0.339228000	11.434908000	20.590628000
C	9.533845000	10.739742000	19.770027000
C	4.193151000	14.266464000	27.388973000
C	5.277584000	11.269106000	18.797993000
C	3.703280000	13.289269000	24.830202000
C	1.763395000	8.453693000	23.285370000
C	2.160268000	15.136119000	22.893305000
C	6.448566000	10.764082000	19.356389000
C	2.957640000	15.001066000	17.050630000
C	3.844035000	13.823304000	19.001719000
C	-1.070033000	10.547149000	24.940680000
C	-0.076202000	15.811718000	19.011857000
C	4.839374000	17.315283000	21.070235000
C	5.003578000	14.727126000	26.314749000
C	2.632516000	11.446187000	19.949702000
C	4.986659000	10.978121000	17.460179000
C	1.098988000	13.790856000	15.831776000
C	4.223931000	15.038389000	19.574392000
C	4.437293000	17.565936000	19.603865000
C	0.791172000	6.811936000	21.905655000
C	4.042118000	16.249967000	18.906180000
C	0.838507000	15.811787000	21.047220000
C	4.015069000	10.222730000	14.932351000
C	9.113783000	10.420817000	16.020975000
C	-1.426828000	8.480382000	23.619580000
C	1.596950000	13.484928000	21.163400000
C	3.234188000	18.533207000	19.612921000
C	1.440470000	16.152062000	22.242454000
C	8.635309000	9.544549000	19.382475000
C	7.407166000	10.069087000	18.603864000
C	5.650626000	18.228819000	18.916956000
C	2.261127000	13.833740000	22.381292000
C	1.542308000	12.121057000	20.573670000
C	5.628801000	17.137356000	26.828763000
C	4.732431000	14.211948000	25.047238000
C	5.485758000	9.869646000	15.222689000
C	4.414935000	7.649965000	20.991568000
C	0.903441000	14.512947000	20.541021000
C	7.117379000	15.251311000	27.613446000
C	3.494190000	16.196842000	17.596768000
C	3.807212000	6.151867000	22.922536000
C	-0.401440000	9.234402000	24.492698000
C	2.566508000	10.932203000	28.068900000
C	5.889763000	10.288253000	16.650949000
C	2.528950000	12.452132000	28.365612000
C	2.199090000	14.873459000	15.708831000
C	9.471599000	8.479086000	18.650160000
C	7.147436000	9.936953000	17.221951000
C	8.134531000	8.872184000	20.685311000
C	3.184625000	14.413137000	14.612107000
C	3.303564000	15.813844000	28.936979000
C	-0.106413000	8.395903000	25.757973000
C	6.344624000	10.561255000	14.143977000
C	1.478478000	16.160763000	15.260436000
C	3.155533000	12.613116000	29.764859000

C	5.621974000	8.335562000	15.094537000
H	6.436043000	16.256649000	24.367933000
H	7.399470000	14.851154000	24.915372000
H	7.859179000	16.498358000	25.397811000
H	4.687965000	18.575039000	15.739519000
H	4.211141000	17.055397000	14.927568000
H	5.439601000	17.021832000	16.233810000
H	0.558858000	12.700547000	27.434095000
H	0.940557000	13.956905000	28.626505000
H	0.507142000	12.319207000	29.172445000
H	1.126596000	8.469594000	19.084809000
H	4.535204000	10.229126000	22.467763000
H	3.319335000	9.658692000	18.973636000
H	2.772144000	12.885259000	17.404445000
H	2.276165000	11.993949000	25.748602000
H	-2.357243000	11.324969000	19.828886000
H	-2.508438000	10.644093000	21.517183000
H	0.823275000	11.645588000	24.025756000
H	5.327791000	7.959149000	24.332577000
H	5.898599000	8.904350000	22.940334000
H	6.225298000	7.167243000	23.011147000
H	9.945384000	11.242481000	18.883976000
H	10.373977000	10.394228000	20.391039000
H	8.970762000	11.492639000	20.339208000
H	2.676258000	15.377453000	23.821913000
H	6.621974000	10.944970000	20.418598000
H	-1.305489000	11.200526000	24.087647000
H	-0.440707000	11.112537000	25.643721000
H	-2.010655000	10.310005000	25.457554000
H	0.679571000	16.131224000	18.272490000
H	-1.101586000	15.908812000	18.638404000
H	5.762532000	16.725347000	21.145429000
H	4.050451000	16.794418000	21.628210000
H	5.018094000	18.285628000	21.555752000
H	4.034433000	11.296409000	17.046908000
H	1.508002000	12.777702000	15.938223000
H	0.486507000	13.793743000	14.918669000
H	0.444447000	13.982320000	16.692400000
H	4.692423000	15.016586000	20.556773000
H	0.030827000	7.511247000	21.525874000
H	0.363579000	5.805155000	21.984727000
H	1.639991000	6.796125000	21.205273000
H	3.843345000	11.309683000	14.933953000
H	3.327987000	9.762224000	15.656602000
H	3.750659000	9.849690000	13.933059000
H	8.646372000	11.308300000	15.567597000
H	9.783601000	9.942103000	15.296320000
H	9.691841000	10.737269000	16.901699000
H	-2.407785000	8.496428000	24.118326000
H	-1.143046000	7.434785000	23.471754000
H	-1.535362000	8.949849000	22.633772000
H	3.508047000	19.462638000	20.134682000
H	2.384610000	18.084001000	20.146494000
H	2.912275000	18.786756000	18.596655000
H	1.374573000	17.158221000	22.653626000

H	5.992838000	19.079361000	19.526784000
H	5.402931000	18.612847000	17.922695000
H	6.484372000	17.517584000	18.828786000
H	6.458740000	17.860207000	26.811436000
H	5.175423000	17.174438000	27.824870000
H	4.880995000	17.458796000	26.088682000
H	5.327444000	14.520480000	24.190191000
H	5.176236000	6.905322000	20.714651000
H	4.780008000	8.639749000	20.683222000
H	3.501449000	7.435387000	20.419894000
H	7.950551000	15.963038000	27.714273000
H	7.533723000	14.269226000	27.354736000
H	6.605130000	15.172681000	28.577684000
H	3.537478000	6.090655000	23.984720000
H	4.698639000	5.527176000	22.760015000
H	2.992356000	5.716342000	22.336141000
H	2.085086000	10.665526000	27.120261000
H	2.037993000	10.394527000	28.868873000
H	3.601003000	10.564509000	28.036522000
H	8.840918000	7.657145000	18.285918000
H	10.198486000	8.059235000	19.362190000
H	10.036465000	8.875306000	17.801278000
H	7.598879000	9.563853000	21.349222000
H	8.997996000	8.481824000	21.243903000
H	7.464449000	8.032061000	20.456970000
H	3.647058000	13.455809000	14.893979000
H	3.993820000	15.135954000	14.453901000
H	2.656212000	14.271476000	13.657293000
H	3.645361000	16.382468000	29.810678000
H	2.365192000	15.296001000	29.185585000
H	3.116572000	16.499584000	28.096821000
H	-1.039931000	8.198231000	26.306759000
H	0.578724000	8.933503000	26.429396000
H	0.349162000	7.433864000	25.492962000
H	6.336312000	11.653515000	14.274952000
H	5.934536000	10.336218000	13.147663000
H	7.380660000	10.210914000	14.167102000
H	0.817762000	16.542079000	16.051741000
H	0.855276000	15.929313000	14.384167000
H	2.162607000	16.966981000	14.984849000
H	2.676730000	11.892104000	30.444229000
H	3.019657000	13.610375000	30.193888000
H	4.232219000	12.397299000	29.743143000
H	5.307884000	8.016533000	14.089008000
H	4.979398000	7.828099000	15.828885000
H	6.657080000	8.013218000	15.254144000
H	7.648665000	11.942149000	22.324822000
H	5.421987000	10.766850000	27.051788000
H	5.079378000	10.744684000	24.624081000
H	9.006170000	12.440183000	24.056630000
H	9.352401000	12.430812000	26.505499000
H	8.576417000	12.031306000	28.744605000
H	6.825826000	12.261172000	28.945351000
H	7.500288000	10.624396000	28.905771000
H	7.016993000	14.483305000	22.596443000

C	8.847043000	15.955404000	18.534433000
C	7.953092000	14.895166000	18.302546000
C	7.267508000	14.273042000	19.336544000
C	7.422434000	14.690230000	20.685502000
C	8.379221000	15.719538000	20.920314000
C	9.053593000	16.336084000	19.872917000
H	7.791065000	14.546898000	17.278985000
H	6.604176000	13.439932000	19.118525000
H	8.553746000	16.047332000	21.949017000
H	9.759576000	17.141239000	20.095361000
C	9.530623000	16.670989000	17.399267000
H	10.517625000	17.051621000	17.697904000
H	9.666324000	16.008647000	16.532174000
H	8.939473000	17.537595000	17.057137000

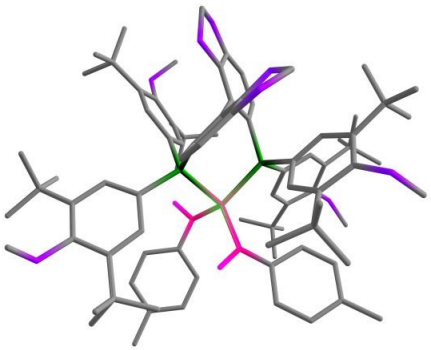

Cu$_{C3B}$

Cu	5.383487000	12.437317000	21.659662000
N	6.751162000	13.792192000	21.470377000
N	6.255834000	11.073544000	22.858834000
P	4.166049000	12.176019000	19.729121000
P	3.532174000	12.513694000	22.925008000
C	10.575273000	12.273348000	26.454559000
C	7.343049000	15.402714000	24.904964000
C	4.730603000	17.372977000	15.776715000
O	-0.898865000	12.063231000	21.157023000
O	0.386371000	16.800070000	20.322159000
C	1.673117000	12.097625000	28.333103000
O	4.922578000	14.306632000	28.445233000
O	-1.333271000	9.963098000	20.267513000
O	0.729087000	7.233200000	23.114123000
C	-0.027658000	10.320795000	19.995769000
O	0.275697000	14.677886000	19.389371000
O	7.896406000	9.175019000	16.178236000
C	3.773898000	12.675445000	27.055258000
C	0.956694000	9.585450000	19.366235000
C	2.728919000	8.519864000	22.635166000
C	3.287734000	9.801945000	22.541748000
C	2.224500000	10.186020000	19.268479000
C	3.145725000	13.819131000	17.662915000
O	3.704642000	17.350318000	16.782206000

C	9.447039000	11.939207000	25.515208000
C	9.552901000	12.183369000	24.132058000
C	8.506824000	11.920015000	23.257552000
C	7.275695000	11.386988000	23.726511000
C	7.170745000	11.153906000	25.123282000
C	8.232875000	11.412118000	25.983924000
C	3.388823000	12.339851000	25.748627000
C	2.636488000	10.937009000	23.013259000
C	-1.955898000	11.184402000	20.727077000
C	0.737651000	9.567387000	23.692908000
C	3.655751000	7.349840000	22.223655000
C	1.373725000	10.807818000	23.601913000
C	6.570788000	15.270761000	26.233114000
C	5.025275000	7.560152000	22.920989000
C	0.230447000	11.586968000	20.523759000
C	9.366048000	10.471137000	19.553129000
C	4.683916000	13.750560000	27.196441000
C	5.124551000	11.105169000	18.612058000
C	3.949149000	12.955387000	24.635238000
C	1.410236000	8.441678000	23.136394000
C	2.394582000	15.049489000	22.884998000
C	6.281505000	10.565936000	19.167879000
C	3.001665000	15.019031000	16.952260000
C	3.857367000	13.749225000	18.857723000
C	-1.088151000	10.814796000	24.947657000
C	0.144999000	16.083357000	19.091573000
C	5.144903000	17.124674000	20.953690000
C	5.393871000	14.285919000	26.086477000
C	2.493445000	11.455165000	19.792376000
C	4.818048000	10.823000000	17.276187000
C	0.965711000	14.021909000	15.834439000
C	4.338055000	14.923307000	19.439809000
C	4.731018000	17.428385000	19.500846000
C	0.204604000	6.918917000	21.812502000
C	4.226905000	16.155160000	18.793904000
C	1.093446000	15.912631000	21.103522000
C	3.825219000	10.113409000	14.742734000
C	8.928571000	10.114658000	15.831165000
C	-1.721507000	8.766992000	23.698087000
C	1.651974000	13.527937000	21.097417000
C	3.597629000	18.475647000	19.553014000
C	1.746992000	16.148693000	22.297518000
C	8.431329000	9.293536000	19.197810000
C	7.214828000	9.839312000	18.416113000
C	5.970533000	18.020022000	18.795771000
C	2.369726000	13.768464000	22.312811000
C	1.474927000	12.192116000	20.467182000
C	6.060056000	16.672376000	26.626273000
C	4.999574000	13.864842000	24.816369000
C	5.282193000	9.707162000	15.035047000
C	3.885103000	7.381802000	20.698138000
C	1.033799000	14.636233000	20.538998000
C	7.581820000	14.766144000	27.284356000
C	3.642941000	16.161805000	17.499207000
C	3.178290000	5.945284000	22.639635000

C	-0.577085000	9.436444000	24.488403000
C	3.355358000	10.318207000	27.789893000
C	5.697965000	10.103591000	16.466281000
C	3.181543000	11.806034000	28.188347000
C	2.171313000	14.975633000	15.647766000
C	9.224912000	8.185817000	18.481033000
C	6.944733000	9.709406000	17.035549000
C	7.922109000	8.673195000	20.524445000
C	3.038016000	14.405351000	14.504039000
C	3.861896000	15.167223000	28.888187000
C	-0.277045000	8.594432000	25.750148000
C	6.166357000	10.378231000	13.963504000
C	1.575479000	16.334153000	15.226748000
C	3.870413000	11.954415000	29.558338000
C	5.366115000	8.170421000	14.895865000
H	6.742343000	15.868978000	24.110623000
H	7.702900000	14.423623000	24.553883000
H	8.222534000	16.041435000	25.068100000
H	4.925676000	18.428267000	15.550637000
H	4.404908000	16.862036000	14.858014000
H	5.650268000	16.897001000	16.145740000
H	1.140786000	11.913629000	27.388860000
H	1.491567000	13.142994000	28.620140000
H	1.232628000	11.449534000	29.105437000
H	0.762846000	8.593569000	18.961725000
H	4.263126000	9.922581000	22.072357000
H	3.023818000	9.639620000	18.771083000
H	2.677621000	12.914584000	17.280393000
H	2.642473000	11.562751000	25.594187000
H	-2.499736000	11.650107000	19.886426000
H	-2.614268000	10.962953000	21.575126000
H	0.878324000	11.701196000	23.976990000
H	4.904647000	7.601627000	24.013089000
H	5.531723000	8.476959000	22.596316000
H	5.688433000	6.717109000	22.677415000
H	9.782951000	10.947796000	18.655594000
H	10.201172000	10.113761000	20.174082000
H	8.825831000	11.245187000	20.115248000
H	2.953848000	15.203121000	23.806951000
H	6.473692000	10.754277000	20.226411000
H	-1.304270000	11.474896000	24.094672000
H	-0.368571000	11.325969000	25.604483000
H	-2.016890000	10.679632000	25.519876000
H	0.918282000	16.364738000	18.354330000
H	-0.871718000	16.290518000	18.740634000
H	6.025736000	16.470082000	21.002776000
H	4.330210000	16.652554000	21.517617000
H	5.400624000	18.071789000	21.450853000
H	3.877218000	11.175663000	16.863053000
H	1.265752000	12.970172000	15.932092000
H	0.315310000	14.087315000	14.950237000
H	0.374630000	14.285562000	16.722240000
H	4.827495000	14.853011000	20.409760000
H	-0.529934000	7.673884000	21.494843000
H	-0.279468000	5.938935000	21.899240000

H	1.007970000	6.869313000	21.061792000
H	3.689961000	11.205864000	14.755354000
H	3.119629000	9.668458000	15.458916000
H	3.553229000	9.759521000	13.738578000
H	8.496584000	11.020822000	15.380008000
H	9.575645000	9.609101000	15.104098000
H	9.521119000	10.406252000	16.710248000
H	-2.661666000	8.880958000	24.258640000
H	-1.542092000	7.697952000	23.555010000
H	-1.854677000	9.229380000	22.711560000
H	3.948461000	19.375563000	20.080091000
H	2.732116000	18.077899000	20.101671000
H	3.270676000	18.766303000	18.548139000
H	1.775313000	17.138037000	22.751713000
H	6.379135000	18.837183000	19.410425000
H	5.724951000	18.435187000	17.813294000
H	6.754008000	17.257786000	18.678978000
H	6.897471000	17.386852000	26.620275000
H	5.624083000	16.675466000	27.631272000
H	5.301958000	17.028310000	25.912653000
H	5.506525000	14.242507000	23.929857000
H	4.595909000	6.592582000	20.410398000
H	4.304202000	8.345713000	20.377038000
H	2.949250000	7.217906000	20.145323000
H	8.424490000	15.471088000	27.348809000
H	7.978008000	13.787895000	26.983824000
H	7.125839000	14.674287000	28.275134000
H	2.945270000	5.900770000	23.710989000
H	3.993861000	5.235280000	22.435934000
H	2.300040000	5.602121000	22.083680000
H	2.826771000	10.057092000	26.863637000
H	2.956471000	9.677378000	28.589388000
H	4.418686000	10.075083000	27.651642000
H	8.563998000	7.376789000	18.141744000
H	9.946612000	7.758520000	19.193977000
H	9.792513000	8.545427000	17.617747000
H	7.445254000	9.407845000	21.188339000
H	8.776667000	8.247267000	21.070297000
H	7.202477000	7.866276000	20.326906000
H	3.412170000	13.405558000	14.768935000
H	3.907499000	15.038501000	14.289303000
H	2.442089000	14.315375000	13.583211000
H	4.186251000	15.589323000	29.846543000
H	2.922501000	14.612306000	29.029848000
H	3.686029000	15.977356000	28.163980000
H	-1.189497000	8.479802000	26.355460000
H	0.485898000	9.087165000	26.370521000
H	0.085221000	7.594945000	25.478497000
H	6.195362000	11.468823000	14.104977000
H	5.749940000	10.176922000	12.964675000
H	7.189479000	9.992408000	13.984000000
H	0.995545000	16.783979000	16.045473000
H	0.893070000	16.169364000	14.380024000
H	2.329305000	17.063120000	14.917665000
H	3.499000000	11.156579000	30.219488000

H	3.662292000	12.909904000	30.050291000
H	4.959162000	11.845262000	29.469979000
H	5.044268000	7.869004000	13.887319000
H	4.704757000	7.680282000	15.625310000
H	6.389200000	7.812600000	15.056029000
H	5.523687000	10.621286000	23.416629000
H	10.486233000	12.590547000	23.733776000
H	8.618021000	12.115899000	22.192136000
H	6.227057000	10.770162000	25.519525000
H	8.113828000	11.214811000	27.052505000
H	10.444954000	11.778227000	27.426288000
H	11.548593000	11.968244000	26.041948000
H	10.631459000	13.358476000	26.643842000
H	7.169449000	14.028973000	22.374126000
C	8.973734000	15.590454000	18.344879000
C	8.003494000	14.605774000	18.085662000
C	7.295548000	13.983130000	19.104094000
C	7.503882000	14.323690000	20.468630000
C	8.529915000	15.278623000	20.726779000
C	9.228749000	15.893975000	19.694081000
H	7.801046000	14.315542000	17.050962000
H	6.579501000	13.202035000	18.860663000
H	8.743609000	15.546018000	21.765645000
H	9.993301000	16.637162000	19.938015000
C	9.685038000	16.307093000	17.227178000
H	10.673934000	16.666623000	17.544550000
H	9.822516000	15.652872000	16.353779000
H	9.114190000	17.187359000	16.885176000

2.5. Notes and references.

1. *Amino Group Chemistry: From Synthesis to the Life Sciences*; Ricci, A., Ed.; Wiley–VCH: Weinheim, Germany, 2008.
2. Lawrence, S. A. *Amines: Synthesis, Properties, and Applications*; Cambridge University Press: Cambridge, U.K., 2004.
3. *The Alkaloids: Volume 84*. 1st ed.; Knölker, H.-J., Series Ed.; Academic Press: San Diego, 2020.
4. *The Chemistry of Anilines*; Rappoport, Z., Ed.; John Wiley & Sons: Chichester, U.K., 2007.
5. Marvin, C. C. 6.02. Synthesis of Amines and Ammonium Salts. In *Comprehensive Organic Synthesis*. 2nd. Ed.; Knochel, P., Molander, G. A., Eds.; Elsevier: Amsterdam, 2014; Vol. 6, pp 34–99.
6. Shi, F.; Cui, X. *Catalytic Amination for N-Alkyl Amine Synthesis*, 1st Ed. Academic Press: San Diego, 2018.
7. For representative examples that utilize unactivated alkyl halides and are not enantioselec tive, see: Bissember, A. C.; Lundgren, R. J.; Creutz, S. E.; Peters, J. C.; Fu, G. C. Transit ion-Metal-Catalyzed Alkylations of Amines with Alkyl Halides: Photoinduced, Copper-Catalyzed Couplings of Carbazoles. *Angew. Chem. Int. Ed*. **2013**, *52*, 5129–5133.
8. Do, H.-Q.; Bachman, S.; Bissember, A. C.; Peters, J. C.; Fu, G. C. Photoinduced, Copper-Catalyzed Alkylation of Amides with Unactivated Secondary Alkyl Halides at Room Temperature. *J. Am. Chem. Soc*. **2014**, *136*, 2162–2167.
9. Peacock, D. M.; Roos, C. B.; Hartwig, J. F. Palladium-Catalyzed Cross Coupling of Secondary and Tertiary Alkyl Bromides with a Nitrogen Nucleophile. *ACS Cent. Sci*. **2016**, *2*, 647–652.
10. Matier, C. D.; Schwaben, J.; Peters, J. C.; Fu, G. C. Copper-Catalyzed Alkylation of Aliphatic Amines Induced by Visible Light. *J. Am. Chem. Soc*. **2017**, *139*, 17707–17710.
11. Ahn, J. M.; Peters, J. C.; Fu, G. C. Design of a Photoredox Catalyst that Enables the Direct Synthesis of Carbamate-Protected Primary Amines via Photoinduced, Copper-Catalyzed *N*-Alkylation Reactions of Unactivated Secondary Halides. *J. Am. Chem. Soc*. **2017**, *139*, 18101–18106.

12. Dow, N. W.; Cabré, A.; MacMillan, D. W. C. A general *N*-alkylation platform via copper metallaphotoredox and silyl radical activation of alkyl halides. *Chem* **2021**, *7*, 1827–1842.
13. Gorski, B.; Barthelemy, A.-L.; Douglas, J. J.; Julia, F.; Leonori, D. Copper-catalysed amination of alkyl iodides enabled by halogen-atom transfer. *Nat. Catal.* **2021**, *4*, 623–630.
14. Grange, R. L.; Clizbe, E. A.; Evans, P. A. Recent Developments in Asymmetric Allylic Amination Reactions. *Synthesis* **2016**, *48*, 2911–2968.
15. Zhang, H.; Kang, H.; Hong, L.; Dong, W.; Li, G.; Zheng, X.; Wang, R. Construction of the N1−C3 Linkage Stereogenic Centers by Catalytic Asymmetric Amination Reaction of 3-Bromooxindoles with Indolines. *Org. Lett.* **2014**, *16*, 2394−2397.
16. Kainz, Q. M.; Matier, C. M.; Bartoszewicz, A.; Zultanski, S. L.; Peters, J. C.; Fu, G. C. Asymmetric copper-catalyzed C–N cross-couplings induced by visible light. *Science* **2016**, *351*, 681–684.
17. Bartoszewicz, A.; Matier, C. D.; Fu, G. C. Enantioconvergent Alkylations of Amines by Alkyl Electrophiles: Copper-Catalyzed Nucleophilic Substitutions of Racemic α-Halolactams by Indoles. *J. Am. Chem. Soc.* **2019**, *141*, 14864–14869.
18. Zhang, Y.-F.; Dong, X.-Y.; Cheng, J.-T; Yang, N.-Y.; Wang, L.-L.; Wang, F.-L.; Luan, C.; Liu, J.; Li, Z.-L.; Gu, Q.-S.; Liu, X.-Y. Enantioconvergent Cu-Catalyzed Radical C–N Coupling of Racemic Secondary Alkyl Halides to Access α-Chiral Primary Amines. *J. Am. Chem. Soc.* **2021**, *143*, 15413–15419.
19. Zhang, X.; Ren, J.; Tan, S. M.; Tan, D.; Lee, R.; Tan, C.-H. An enantioconvergent halogenophilic nucleophilic substitution (S_N2X) reaction. *Science* **2019**, *363*, 400–404 (organocatalytic).
20. See also: Wang, Y.; Wang, S.; Shan, W.; Shao, Z. Direct asymmetric N-propargylation of indoles and carbazoles catalyzed by lithium SPINOL phosphate. *Nat. Commun.* **2020**, *11*, 226 (organocatalytic).
21. Chen, C.; Peters, J. C.; Fu, G. C. Photoinduced copper-catalysed asymmetric amidation via ligand cooperativity. *Nature* **2021**, *596*, 250–256.

22. Colburn, R. W.; Dax, S. L.; Flores, C. M.; Ludovici, D. W.; Matthews, J. M.; Xia, M.; Xu, X; Youngman, M. A.; Zhu. B. Cold Menthol Receptor Antagonists. US Patent 0048589 A1, 2010.

23. Cotter, T. G.; Jensen, D. M. Glecaprevir/pibrentasvir for the treatment of chronic hepatitis C: design, development, and place in therapy. *Drug Design, Development and Therapy* **2019**, *13*, 2565–2577.

24. Guo, W.; Zuo, L.; Cui, M.; Yan, B.; Ni, S. Propargylic Amination Enabled the Access to Enantioenriched Acyclic α-Quaternary α Amino Ketones. *J. Am. Chem. Soc.* **2021**, *143*, 7629–7634.

25. Yang, W.; Dong, P.; Xu, J.; Yang, J.; Liu, X.; Feng, X. Enantioselective Synthesis of 3-substituted 3-amino-2-oxindoles by Amination with Anilines. *Chem. - Eur. J.* **2021**, *27*, 9272−9275.

26. For leading references, see: Kouznetsov, V. V.; Galvis, C. E. P. Strecker reaction and α-amino nitriles: Recent advances in their chemistry, synthesis, and biological properties. *Tetrahedron* **2018**, *74*, 773–810.

27. Wang, J.; Liu, X.; Feng, X. Asymmetric Strecker Reactions. *Chem. Rev.* **2011**, *111*, 6947–6983.

28. For leading references to catalytic asymmetric methods for the synthesis of α-disubstituted α-aminonitriles, see: Lupidi, G.; Palmieri, A.; Petrini, M. Enantioselective Catalyzed Synthesis of Amino Derivatives Using Electrophilic Open-Chain *N*-Activated Ketimines. *Adv. Synth. Catal.* **2021**, *363*, 3655–3692.

29. Vachal, P.; Jacobsen, E. N. Enantioselective Catalytic Addition of HCN to Ketoimines. Catalytic Synthesis of Quaternary Amino Acids. *Org. Lett.* **2000**, *2*, 867–870.

30. Ohmatsu, K.; Ando, Y.; Nakashima, T.; Ooi, T. A Modular Strategy for the Direct Catalytic Asymmetric α-Amination of Carbonyl Compounds. *Chem* **2016**, *1*, 802–810.

31. Zhang, J.; Fu, K.; Lin, L.; Lu, Y.; Liu, X.; Feng, X. Efficient Catalytic Enantioselective Hydroxyamination of α-Aryl- α-Cyanoacetates with 2-Nitrosopyridines. *Chem. Eur. J.* **2018**, *24*, 4289–4293.

32. Saaby, S.; Bella, M.; Jørgensen, K. A. Asymmetric Construction of Quaternary Stereocenters by Direct Organocatalytic Amination of α-Substituted α-Cyanoacetates and b-Dicarbonyl Compounds. *J. Am. Chem. Soc.* **2004**, *126*, 8120–8121.

33. Friis, S. D.; Pirnot, M. T.; Dupuis, L. N.; Buchwald, S. L. A Dual Palladium and Copper Hydride Catalyzed Approach for Alkyl–Aryl Cross-Coupling of Aryl Halides and Olefins. *Angew. Chem. Int. Ed.* **2017**, *56*, 7242–7246.

34. Xi, Y.; Hartwig, J. F. Mechanistic Studies of Copper-Catalyzed Asymmetric Hydroboration of Alkenes. *J. Am. Chem. Soc.* **2017**, *139*, 12758–12772.

35. We were unable to carry out the ^{31}P NMR spectroscopic studies at –78 °C, due to overlap of the low-temperature spectrum of **Cu$_A$** (see also Reference 33**Error! Bookmark not defined.**) with the resonance of BTPP.

36. *EPR Spectroscopy: Fundamentals and Methods*; Goldfarb, D., Stoll, S., Eds.; Wiley: New York, 2018.

37. Gu, N. X.; Oyala, P. H.; Peters, J. C. Hydrazine Formation via Coupling of a Nickel (III)–NH2 Radical. *Angew. Chem. Int. Ed.* **2021**, *60*, 4009–4013.

38. Taguchi, A. T.; Baldansuren, A.; Dikanov, S. A. Basic and Combination Cross-Features in X- and Q-band HYSCORE of the 15N Labeled Bacteriochlorophyll α Cation Radical. *Z. Phys. Chem. (München, Ger.).* **2017**, *231*, 725–743.

39. Mims, W.; Peisach, J. The nuclear modulation effect in electron spin echoes for complexes of Cu2+ and imidazole with 14N and 15N. *J. Chem. Phys.* **1978**, *69*, 4921–4930.

40. Mankad, N. P.; Antholine, W. E.; Szilagyi, R. K.; Peters, J. C. Three-Coordinate Copper(I) Amido and Aminyl Radical Complexes. *J. Am. Chem. Soc.* **2009**, *131*, 3878–3880.

41. Jang, E. S.; McMullin, C. L.; Ka¨ß, M.; Meyer, K.; Cundari, T. R.; Warren, T. H. Copper (II) Anilides in sp3 C–H Amination. *J. Am. Chem. Soc.* **2014,** *136*, 10930–10940.

42. Kimura, T.; Lee, J. C.; Gray, H. B.; Winkler, J. R. Folding energy landscape of cytochrome cb_{562}. *Proc. Natl. Acad. Sci. U. S. A.* **2009**, *106*, 7834–7839.

43. Yamada, S.; Ford, N. D. B.; Keller, G. E.; Ford, W. C.; Gray, H. B. Winkler, J. R. Snapshots of a protein folding intermediate. *Proc. Natl. Acad. Sci. U. S. A.* **2013**, *110*, 1606–1610.

44. Stoll, S.; Schweiger, A. EasySpin, a comprehensive software package for spectral simulation and analysis in EPR. *J. Magn. Reson.* **2006**, *178*, 42–55.

45. Schultz, K.; Hesse, M. Total synthesis of the spermidine alkaloid (+)-(9*S*,13*S*)-isocyclocelabenzine. *Tetrahedron* **1996**, *52*, 14189–14198.

46. Kischkewitz, M.; Daniliuc, C.-G.; Studer, A. 3-Alkylperoxy-3-cyano-oxindoles from 2-Cyano-2-diazo-*N*-phenyl-acetamides via Cyclizing Carbene Insertion and Subsequent Radical Oxidation. *Org. Lett.* **2016**, *18*, 1206–1209.

47. Iorga, B.; Ricard, L.; Savignac, P. Carbanionic displacement reactions at phosphorus. Part III. Cyanomethylphosphonate *vs.* cyanomethylenediphosphonate. Synthesis and solid-state structures. *J. Chem. Soc., Perkin Trans. 1* **2000**, 3311–3316.

48. Murata, Y.; Takeuchi, K.; Nishikata, T. The synthetic protocol for α-bromocarbonyl compounds via brominations. *Tetrahedron* **2019**, *75*, 2726–2736.

49. McNeill, E.; Barder, T. E.; Buchwald, S. L. Palladium-Catalyzed Silylation of Aryl Chlorides with Hexamethyldisilane. *Org. Lett.* **2007**, *9*, 3785–3788.

50. Friis, S. D.; Pirnot, M. T.; Dupuis, L. N.; Buchwald, S. L. A Dual Palladium and Copper Hydride Catalyzed Approach for Alkyl–Aryl Cross-Coupling of Aryl Halides and Olefins. *Angew. Chem. Int. Ed.* **2017**, 56, 7242–7246.

51. Werry, J.; Stamm, H.; Sommer, A. Arenhydride, 8. Konkurrenz zwischen SET und nucleophilem Angriff bei Reaktionen von α-Bromisobutyrophenon mit Carbanionen. Fragmentierung des Anions von Tetrahydrobianthracen. *Chem. Ber.* **1990**, *123*, 1553–1562.

52. Liu, X.; Li, H.-Q.; Ye, S.; Liu, Y.-M.; He, H.-Y.; Cao, Y. Gold-Catalyzed Direct Hydrogenative Coupling of Nitroarenes to Synthesize Aromatic Azo Compounds. *Angew. Chem. Int. Ed.* **2014**, *53*, 7624–7628.

53. Uoyama, H.; Goushi, K.; Shizu, K.; Nomura, H.; Adachi, C. Highly efficient organic light-emitting diodes from delayed fluorescence. *Nature* **2012**, *492*, 234–238.

54. Leitl, M. J.; Zink, D. M.; Schinabeck, A.; Baumann, T.; Volz, D.; Yersin, H. Copper(I) Complexes for Thermally Activated Delayed Fluorescence: From Photophysical to Device Properties. *Top. Curr. Chem.* **2016**, *374*, 1–34.

55. Eisenberg, D. C.; Lawrie, C. J.; Moody, A. E.; Norton, J. R. Relative Rates of Hydrogen Atom Transfer from Transition-Metal Hydrides to Trityl Radicals. *J. Am. Chem. Soc.* **1991**, *113*, 4888–4895.

C h a p t e r 3

SYNTHESIS OF TERTIARY ALKYL AMINES VIA PHOTOINDUCED, COPPER-CATALYZED NUCLEOPHILIC SUBSTITUTION OF UNACTIVATED ALKYL HALIDES BY SECONDARY ALKYL AMINES

Adapted in part from:

Cho, H.; Tong, X.; Zuccarello, G.; Anderson, R. L.; Fu, G. C. Synthesis of Tertiary Alkyl Amines via Photoinduced, Copper-Catalyzed Nucleophilic Substitution of Unactivated Alkyl Halides by Secondary Alkyl Amines. *Submitted*.

[Chapter 3 Intentionally Redacted: pp. 190-365]